Isolation of physiological binding partners of Bcl-2, a survival protein in lymphomagenesis

Dissertation

Zur Erlangung der Doktorwürde
der Fakultät für Biologie
der Albert-Ludwigs-Universität Freiburg i.Br.

vorgelegt von

Thomas Kiefer

Dezember 2010

Dekan der Fakultät für Biologie:	Prof. Dr. Gunther Neuhaus
Promotionsvorsitzender:	Prof. Dr. Samuel Rossel
Betreuer der Arbeit:	Prof. Dr. Christoph Borner
Betreuer an der Fakultät für Biologie:	Prof. Dr. Gunther Neuhaus
Koreferent:	Prof. Dr. Bernd Fakler
Drittprüfer:	Prof. Dr. Rudolf Grosschedl

Tag der Verkündigung des Ergebnisses: 18.03.2011

Progress is impossible without change, and those who cannot change their minds cannot change anything.

G.B. Shaw

Acknowledgements

First of all, I wish to express my deep and sincere gratitude to my supervisor, Prof. Dr. Christoph Borner, for introducing me to the field of apoptosis research. I thank him for giving me the opportunity to conduct my PhD research in his lab at the Institute of Molecular Medicine and Cell Research. I deeply thank him for his support and guidance to the projects he suggested. I also appreciated the possibility to participate in international meetings on apoptosis research, this was an unforgettable experience. Thank you!

Many thanks to Prof. Dr. Gunther Neuhaus for taking over supervision and representing this thesis at the Faculty of Biology at Albert Ludwigs University Freiburg, I thank him also for his time and great efforts.

In particular I would like to thank Dr. Ulrich Maurer for his technical advices und suggestions throughout my research work at the institute.

I'm very grateful to Dr. Martin Biniossek for his great collaboration, his ideas and enthusiasm during all Mass Spectrometry Analysis arrangements.

For my colleagues and friends Dr. Robert Pick and Dr. Jisen Huai, my warmest and sincere thanks. You made the lab a wonderful place to work and learn in. Thank you for your support and your exceptional advice. I must also thank Dr. Marie Follow who introduced me in confocal laser scanning microscopy.

I also owe the entire former and present lab crew the same amount of thanks for their support and the positive working environment. Thank you, Nina, Lars, Kai, Silke, Anand, Andreas, Martin, Florian, Daniel, Katja, Britta, Dorothea, Christin, Souhayla, Karen, Sandra, Céline, Stefan, Yvonne, Karine, Angela, Prisca, Sabine.

My warmest thanks also to Paula who came from Argentina to achieve her Master's degree. By the way, gratulation and all the best for your PhD! Thank you for having inspiring discussions and a good time.
Very special thanks to Karin Neubert, Manuela Wissler, Aneta Kovacs, Mirela Tataru, Angelika Haber, Katrin Wieland, Bettina Kind, Walter, Achim Gramel und Herrn Bach.

And finally I thank Claudia for her love, time, support and her inspiration.

Abstract

Bcl-2 is found on mitochondrial membranes connected to the endoplasmatic reticulum via mitochondria-ER-associated membranes and the nuclear membrane. It belongs to the group of anti-apoptotic proteins that rather enhance survival than proliferation. Bcl-2α is always inserted into membranes by its transmembrane domain to prevent apoptosis by sequestration of pro-apoptotic proteins. So called BH3-only proteins are practically able to bind to Bcl-2 shown by co-immunoprecipitations using samples with over expressed bait and target proteins. Aside of BH3-only proteins other interactors have been found to bind to Bcl-2 but only one binding protein is found in immunoprecipitations using endogenous cell extracts of healthy cells.

In this dissertation different protein biochemical methods were used: Protein expression analysis, subcellular fractionation, blue native gel electrophoresis and co-immunoprecipitation, to (I) examine if reported Bcl-2 binding proteins are real binders under endogenous conditions, and (II) to employ a proteomic approach using co-immunoprecipitations and mass spectrometric amino acid sequencing to isolate, identify and verify new "physiological" binding partners of endogenous expressed Bcl-2.

In our basic experiments we used wild type Bcl-2 and Bcl-2 $^{-/-}$ factor dependent monocytes (FDMs) and FDC-P1 cells. To immunoprecipitate endogenous Bcl-2 we have taken digitonin to solubilize heavy membrane fractions of wild type FDMs and FDC-P1 combined with extracts from Bcl-2 $^{-/-}$ cells as controls as well as an isotype control antibody. To verify and investigate the role of a new Bcl-2 interaction partner we used subcellular fractionations, confocal microscopy and protein co-expression combined with co-IPs. In these experiments we used mouse embryonal fibroblasts, rat-6 cells, HeLa and HEK293T cells.

Our results can be summarized as following: We are able to show that Bcl-2, Bax and Bak are equally expressed but rather localized to distinct cellular fractions and degraded than translocated to other compartments. Endogenous expressed Bcl-2 is consistently found on mitochondria and ER and does not bind any of the BH3-only proteins as reported in the literature. In our proteomic approach, using a combination of two independent co-immunoprecipitation strategies and mass spectrometric analysis we found several potential binding partners of Bcl-2 in healthy FDM and FDC-P1 cells.
First, our focus was on IQGAP2 as a possible Bcl-2 binding partner, which was found in the mass spectrometric data analysis of specific ABT-737 IP assay samples and in yeast-two hybrid screens. Using up scaled protein amounts of FDM cells, we were able to validate IQGAP2 as an endogenous binding partner in immunoprecipitates of Bcl-2.

By analysing Bcl-2 IPs we always found that cells deficient in Bcl-2 display less or very weak amounts of IQGAP2 on mitochondria. In order to examine the distribution of IQGAP2 in healthy and stressed cells, we detected a specific subset of IQGAP2 that is stabilized and recruited by Bcl-2 and translocates during apoptosis from the ER to mitochondria. Moreover, the indicated IQGAP2 stabilization pattern in subcellular fractions differ between FDMs, mouse embryonic fibroblasts and HeLa cells pointing to a cell type specific regulation of the Bcl-2/IQGAP2 interaction. In order to test the inverse situation in IQGAP2 deficient MEFs, examining the abundance, distribution and stability of Bcl-2, we found that a distinct subset of Bcl-2 and IQGAP2 cooperates with each other on intracellular membranes that possibly depend on cytoskeletal filaments. This was indicative to verify a possible impact of Bcl-2 on IQGAP2 on the mitochondrial morphology using confocal microscopy. While healthy and stressed wild type MEFs display a different structural morphology, cells deficient in Bcl-2 or IQGAP2 show in both cases mitochondria with a similar punctated and clustered mitochondrial pattern. These findings support the interdependence of Bcl-2 and IQGAP2 with changes in mitochondrial morphology. Co-localization studies confirm that a part of Bcl-2 and IQGAP2 are stabilized in protein complexes.

However, co-expressed Bcl-2 and IQGAP2 could not be immunoprecipitated, possibly because of the expression of a GFP-tagged form of IQGAP2. Furthermore, we detected two specific splicing forms of IQGAP2 in our immunoprecipitates of endogenous Bcl-2 whereas the lower form is more specifically bound to Bcl-2. Future studies have to be undertaken with untagged IQGAP2 and si/shRNA knock-down to elucidate the Bcl-2/IQGAP2 interaction and to examine that all bands detected with our IQGAP2 antibody belong to various protein bands of IQGAP2.

Table of contents

1. Introduction

1.1 Cell death

Multicellular organisms have to maintain tissue homeostasis during embryonic development, in the adult and during diseases. Eukaryotic cells developed a set of specific cellular adaptations to promote cell death of damaged or harmful cells. Deregulation of the death process may lead to the development of cancer, autoimmune and neurodegenerative diseases. The major types of cellular adaptations to extrinsic or intrinsic cell death stimuli are described as "apoptosis" and "necrosis" (Fig. 1-1).

1.1.1 Apoptosis

The term "apoptosis" or "programmed cell death" is defined as a sequence of specific morphological changes, which are regulated through a genetic program (Lockshin et al., 1964, Kerr et al., 1972). Characteristic morphological changes of the apoptotic process are the retraction of pseudopods followed by membrane blebbing, cellular shrinkage and chromatin condensation. In parallel so called apoptotic bodies are formed, which are membrane-enclosed vesicles containing cellular material such as cytosol, chromatin and organelles. These structural manifestations are the consequence of cleavages of numerous cellular filaments and signaling proteins, mainly mediated by a set of cysteine-aspartate proteases called caspases. The activation of caspases starts with the release of cytosolic cytochrome c from the mitochondrial intermembrane space and the binding to apoptotic protease activating factor 1 (Apaf-1). Upon binding to Apaf-1, cytochrome c induces the exchange of dATP/dADP supporting the oligomerization of this adapter protein into a wheel-like structure, called apoptosome. Pro-caspase-9, an initiator caspase is processed and activated upon binding to the central ring of the apoptosome. Executioner caspases-3 and -7 are then processed by caspase-9 into the active state and in turn cleave hundreds of cellular substrates in all parts of the cell, leading to morphological changes associated with apoptosis. One substrate is ICAD, an inhibitor of the caspase-activated DNase (CAD), which after cleavage releases CAD to move into the nucleus to degrade genomic DNA into 50 up to 200 kbs DNA fragments (Galluzi L, et al., 2007, Danial NN., et al 2004). In most cases, the appearance of fragmented DNA is a late apoptotic event that may even occur independently of apoptosis. The best characterized signal appearing early in the apoptotic process is the exposure of phosphatidylserine (PS) on the outer side of the plasma membrane. This process attracts macrophages, exposing PS receptors on their surface and subsequently

engulfs apoptotic cells, thereby avoiding an inflammatory reaction in the surrounding tissue (Fadok et al., 1992, Savill et al., 2000, Krieser et al., 2002).

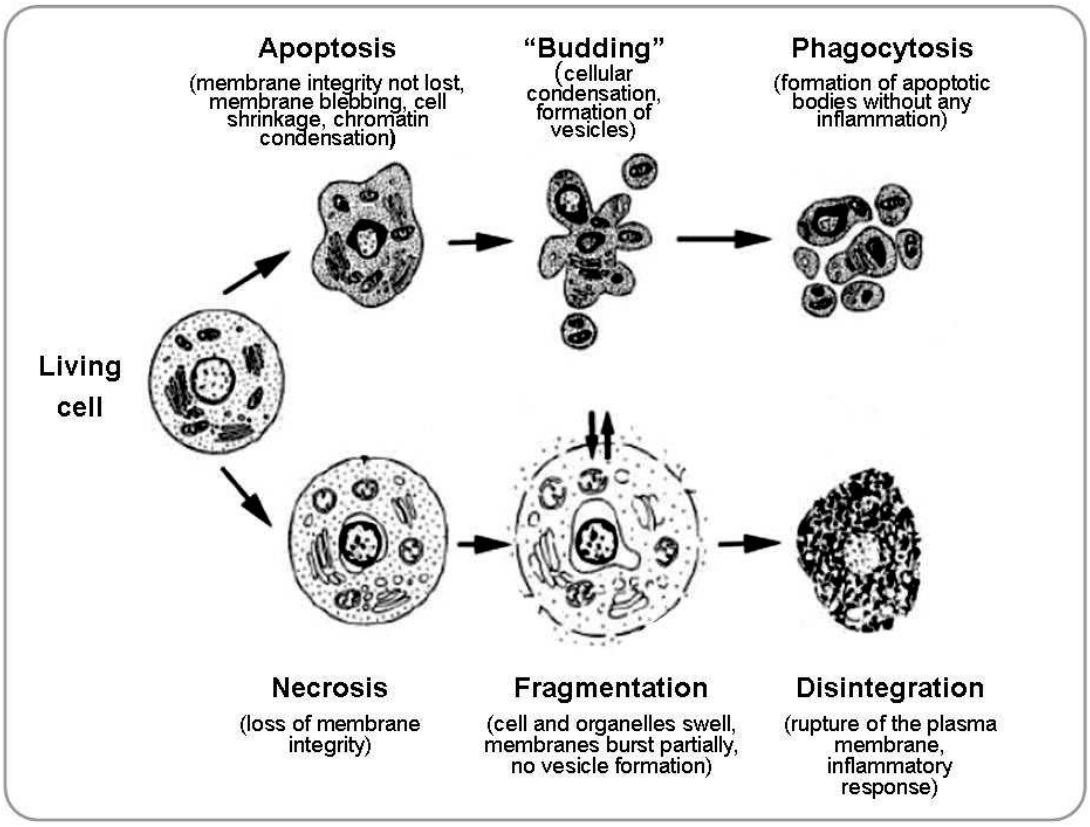

Figure 1-1: Morphological features of apoptosis and necrosis. Apoptotic cells exhibit a deformed shape, the plasma membrane ruffles and starts to bleb. Subsequently chromatin condensates followed by fragmentation of the nuclei. Finally apoptotic bodies are formed and engulfed by phagocytic cells. Apoptotic cell death is characterized without any form of inflammatory reaction. During necrosis, the cell loses plasma membrane integrity leading to an increase of the cell volume and rupture of the cell membrane. The cell dismantles and cellular contents are released. In tissues these microsomes are spilled into the intracellular membrane space of surrounding cells resulting in a strong inflammatory response. The decision which particular mode of cell death will be initiated depends on stimuli and cell type. (Adapted and modified from Van Cruchten, 2002)

1.1.2 Necrosis

In contrast to apoptosis, necrosis is described as a non-programmed, accidental form of cell death (Fig.1-1). It is caused by mechanical stress, such as pressure, high tensions, burns, toxins and infections. Necrosis is characterized by an early loss of the integrity of plasma membrane which disturbs ion homeostasis. As a consequence, the volume of the cell and its organelles increases and the plasma membrane perforates partially. In contrast to apoptosis, there is no membrane blebbing or formation of membrane vesicles. The membrane of the cell and its organelles disintegrates and the cellular content is released into the intercellular space in an uncontrolled way. Inflammation is induced by damage-associated molecular

pattern molecules (DAMPs) such as high-mobility group box 1 proteins (HMGB1) leading to the activation of phagocytes and attraction of leukocytes (Lotze et al., 2005).

1.1.3 Autophagy

Autophagy is an evolutionarily conserved process regulated by autophagy-related genes (ATGs). In mammals, autophagy is important for embryonic development and cell differentiation during erythropoiesis, lymphopoiesis and adipogenesis (Mizushima and Levine, 2010). Autophagy is thought to function primarily as a cytoprotective mechanism to maintain nutrient and energy homeostasis, or to recycle up misfolded proteins, damaged organelles and invasive pathogens. However, deregulation of autophagy in cancer may play a role in the cell resistance to chemotherapy, and excessive autophagy may cause cell death, muscular diseases and neurodegenerative disorders (Yang and Klionsky, 2010). Deletion of the crucial autophagy genes (ATGs) often accelerates cell death confirming that autophagy normally protects cells from apoptosis (Lum et al., 2005, Ferraro et al., 2007, Hotchkiss et al., 2009).

The process of autophagy can be divided into microautophagy and macroautophagy. The two modes differ in the pathway by which cytoplasmic material is delivered to the lysosomes but share in common the final steps for degrading and recycling proteins. Microautophagy describes the engulfment of cytoplasmic material directly at the surface at the lysosomes. Macroautophagy, referred to as autophagy is the primary mechanism for degrading and recycling of long-lived proteins and organelles within double-membrane vesicles.
Autophagy occurs in response to extracellular stress like temperature, hypoxia and starvation. The origin of autophagic vesicles are most likely the membrane of the endoplasmatic reticulum (ER), the mitochondria and the lysosomes, although this has not yet been clearly dissected (Lum et al., 2005, Levine et al., 2004, 2005, Hoyer-Hanson et al., 2007). A recent publication demonstrates that distinct membrane structures are created by an ER-associated membrane called the "omegasome", which increase in size to build up autophagosomes (Tooze and Yoshimori, 2010). This membrane fuses later in the process with lysosomes creating "autophagolysosomes", where the contents are degraded.

1.1.4 Cell death during development

During development apoptosis is already a part of sculpturing tissues and organs (Meier et al., 2000, Hotchkiss et al., 2009). During embryogenesis various "ancestral" stages are formed up and removed to create new organs and tissues. As an example, the developing vertebrate limb constitutes a classical model of programmed cell death responsible for morphogenesis. In this embryonic model large cell populations are eliminated by apoptosis. These areas of cell death, formerly termed necrotic areas, are known as interdigital necrotic zones (INZs) located between the developing digits and cause the freeing of the digits from the hand or foot plate. Some reports show that INZ occurs through a caspase-dependent apoptotic process and active caspase-3 has been identified in the apoptotic interdigits (Mirkes et al., 2001, Huang et al., 2002). Cell death in interdigital necrotic zones represent a new model of cell death induced by anoikis (cell death is induced by the loss of cell contact to its extracellular matrix). It was shown that apoptotic interdigital cells do not express paxillin (connected to integrins) which is a survival factor for adherent cells. These cells display a disorganization of actin microfilaments and the loss of cell anchorage to extracellular matrix. (Chay et al., 2002).
Similar processes are detected during insect and amphibian development. Tissues and organs are eliminated which do have no further function like muscles, neurons, or the degeneration of the tadpol tail. Cells of the immune system like T and B lymphocytes undergo positive and negative selection by programmed cell death in many instances during their development, homeostasis and activation (Rathmell and Tompson, 2002).

1.2 Survival and apoptosis pathways in metazoans

Since apoptosis is a crucial process to maintain the proper functioning of a multicellular organism, the signalling pathways leading from stimulus to cell death are evolutionary conserved from lower (*C. elegans, D. melanogaster*) to higher eukaryotes (mouse, man). Figure 1-2 depicts these pathways.

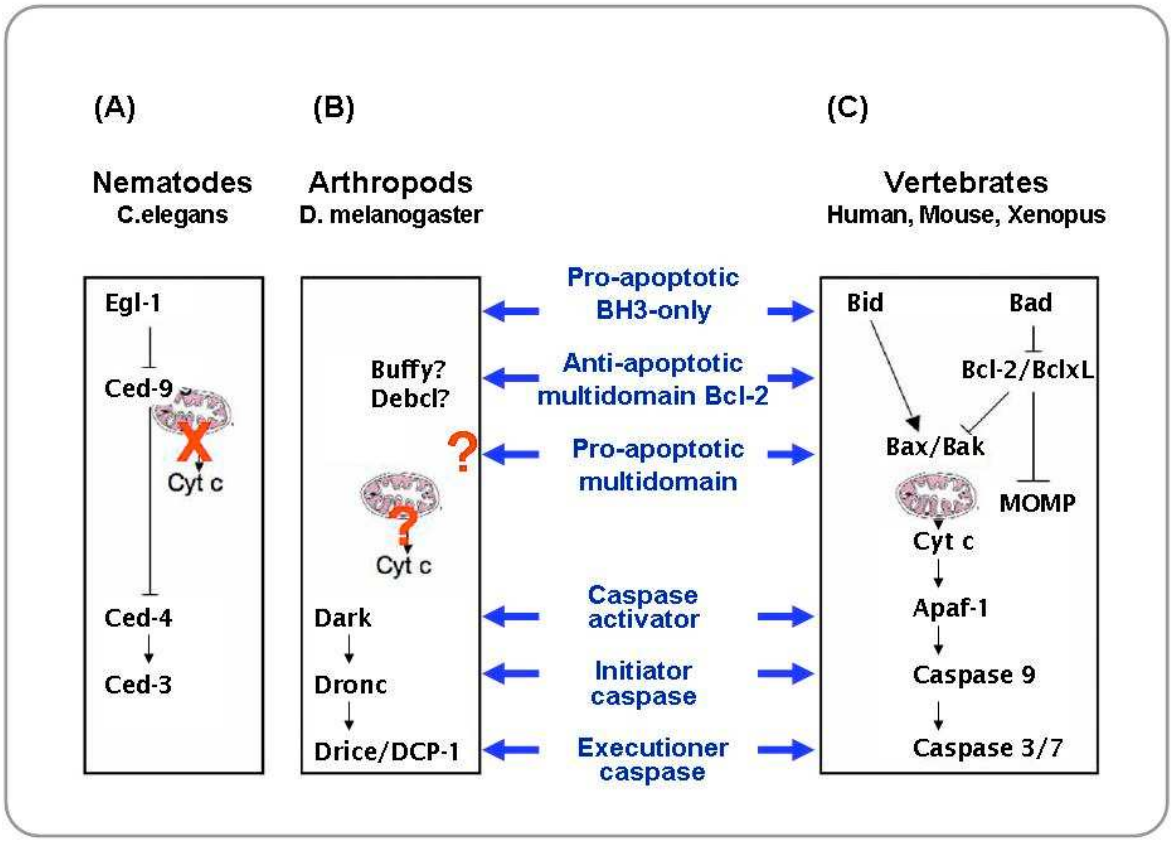

Figure 1-2: Pathways of apoptosis in different taxa: (A) In nematodes**:** *C. elegans* represents a simple basic regulation system of programmed cell death. Apoptotic signaling becomes finer tuned through convergent evolution into a set of specific interactors. BH3-only proteins derived from Egl-1, Bcl-2 survival proteins from CED-9, Apaf-1 from CED-4 and multiple initiator- and executioner caspases from CED-3. Most importantly: Apoptosis in *C. elegans* does not require mitochondrial outer membrane permeability (MOMP) and/or cytochrome c release. **(B)** Homologs of these proteins found in *D. melanogaster*. Cytochrome c does not appear to be required for Dark activation (Apaf-1 in mammals) **(C)** In mammals: cytochrome c binds to Apaf-1 to activate caspases. (Adapted and modified from Oberst, 2008)

1.2.1 Apoptosis in the nematode Caenorhabditis elegans

The study of apoptosis in the nematode *C. elegans* revealed that cell death is a genetically controlled process. The analyses by inhibitory RNA identified several genes responsible for the regulation of nematodal programmed cell death, described as cell death defective (CED) phenotypes. Proteins with pro-apoptotic functions in *C. elegans* are CED-4, CED-3 and egg laying defective 1 (EGL-1), with anti-apoptotic function, the survival factor CED-9 (Oberst et al., 2008). Under healthy conditions CED-4, the mammalian homolog of Apaf-1 is sequestered by CED-9 (the mammalian homolog of Bcl-2) on the mitochondrial membrane, thereby inhibiting apoptosis induction. Upon developmental cues or stress EGL-1, a BH3-only protein is upregulated and binds with high affinity to CED-9. The interaction of EGL-1 and CED-9 "displaces" CED-4, which then oligomerizes into a tretrameric protein complex that recruits CED-3, a caspase with an N-terminal CARD-domain, most closely homologous

to mammalian caspase-3. The high molecular protein complex is also known as the apoptosome, able to activate CED-3. In nematodes CED-3 is the only caspase expressed, acting at as initiator- and executioner caspase. During embryonic development 131 of the 1090 somatic cells die by programmed cell death which is solely dependent on the direct activation of CED-3 (Hengartner et al., 1992, 1994, Lettre et al., 2006, Lamkanti et al., 2002). In contrast to mammals apoptosis is initiated without MOMP and cytochrome c release (Fig. 1-2). Investigations on the mitochondrial morphology indicate an additional function of CED-9 for fission and fusion dynamics of this organelle (described in chapter 1.5.2). This is probably the reason why CED-9 localizes to mitochondria in *C. elegans*.

1.2.2 Apoptosis in the fly Drosophila melanogaster

In Drosophila, the cell death regulating system becomes more complex (Figure 1-2). In Drosophila, Buffy and Debcl, the fly homologues of mammalian Bcl-2 proteins do not appear to play a major role in the core apoptotic pathway. Drosophila Apaf-1 related killer (Dark), the fly homolog of Apaf-1 and CED-4 activates Drosophila caspases. Seven caspases are found which can be grouped into initiator and executioner caspases. Initiator caspases like Drosophila nedd2-like caspases (Dronc) act like the mammalian caspases 2 and 9 or CED-3 in C. elegans. Activated Dronc cleaves the executioner caspases Drice and DCP-1 (homolog to mammalian caspase-3). The Apaf-1 homolog Dark does not appear to require cytochrome c to activate Dronc.

Cell death in Drosophila is regulated by the Drosophila Inhibitor of Apoptosis Protein 1 (DIAP-1), the homolog of mammalian IAP proteins. HID, Grim and Reaper are IAP antagonists and act on DIAP1 by inducing its autoubiquitination and proteasome-dependent degradation (Vaux et al., 2005, Kumar et al., 2000 and 2007). HID, Grim and Reaper are also termed as RHG proteins which are upregulated under apoptotic conditions.

Spontaneous apoptosis is observed in DIAP1-deficient cells whereas ablation of IAP does not cause any apoptosis in mammals. Upon induction of apoptosis mitochondrial fragmentation, release of cytochrome c and caspase activation is caused by Reaper and HID (IAP antagonists) in cultured cells and in the developing fly embryo. DIAP1 knock down alone did not induce mitochondrial changes despite of caspase activation. HID or Reaper upregulation and treatment with the pancaspase inhibitor zVAD-fmk inhibited fragmentation of mitochondria. HID and Reaper seem to function similar to pro-apoptotic Bcl-2 family members. A mutant form of Reaper that does not block DIAP-1 function was still able to cause mitochondrial fragmentation, indicating that apoptosis induction and mitochondrial disruption represent two distinct functions of Reaper (Abdelwahid et al., 2007).

1.3 Extrinsic and intrinsic apoptotic pathways in mammals

In mammals the regulation of cell death evolved into a much more complex system consisting of two main apoptotic pathways (Fig. 1-3).

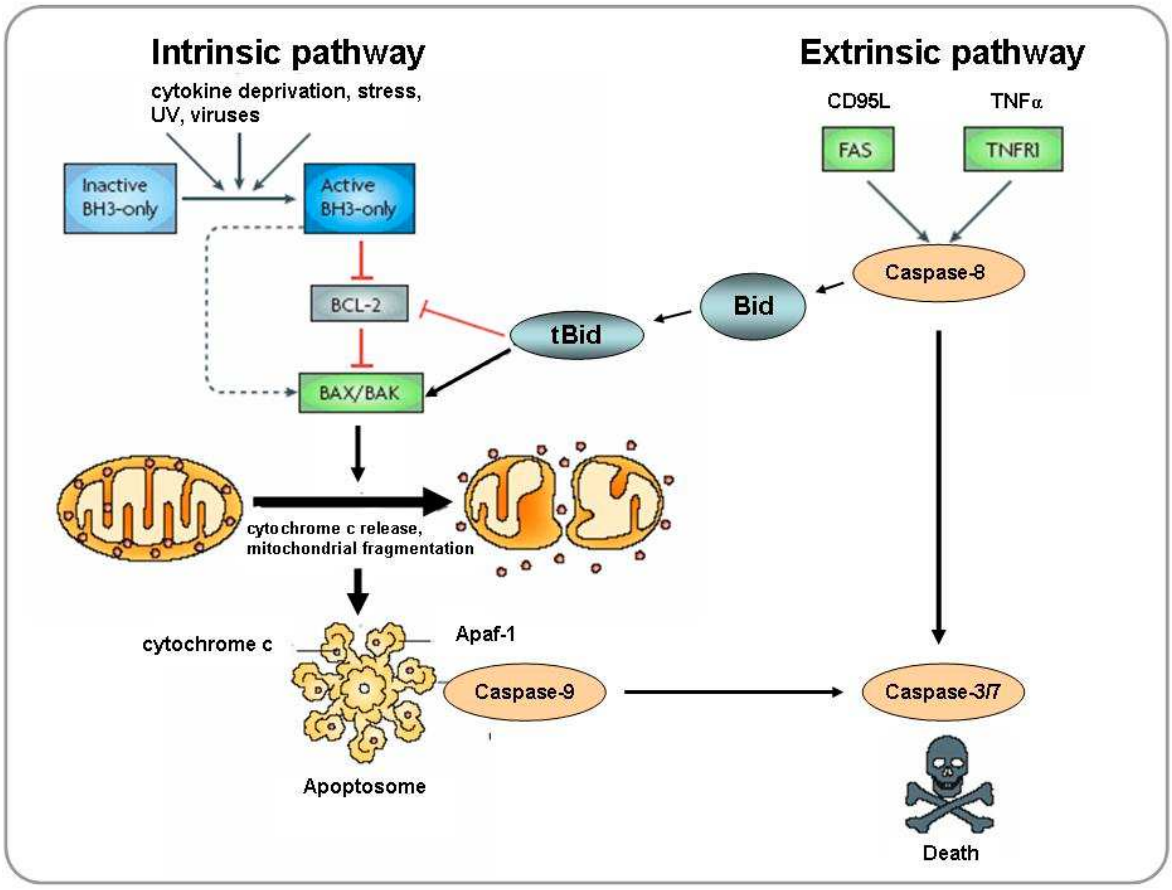

Figure 1-3: The intrinsic- and extrinsic pathways of apoptosis. "**Intrinsic pathway":** The intrinsic pathway is induced by various forms of stress and is regulated by Bcl-2 family members on mitochondria. It provokes the release of cytochrome c and the IAP antagonists. Cytochrome c binds to Apaf-1 and triggers the assembly of the apoptosome. Caspase-9 is recruited to the apoptosome, gets activated and cleaves and activates pro-caspase-3 and 7. Active caspases cleave cellular substrates in a concerted mechanism culminating in fulminant apoptosis. "**Extrinsic pathway":** The extrinsic pathway is regulated by death receptors, such as Fas and tumour necrosis factor receptor-1 (TNFR1). This pathway bypasses the mitochondrial step and directly activates caspase-8 which induces caspase-3 and 7 activation and cell death. Caspase-8 cleaves Bid thereby producing truncated tBid which translocates to the mitochondrial membrane connecting the extrinsic- and intrinsic pathway. (Adapted and modified from Youle and Strasser, 2008)

1.3.1 The extrinsic or death-receptor mediated apoptotic pathway

This pathway (Fig. 1-3) is induced by trimerization of the death-receptors (DR) upon binding of their specific death-ligands, such as FasL/CD95L or TNF α. The intracellularly located trimerized death domains (DD) of the death receptors further recruit non-enzymatic adaptor proteins such as the Fas-associated death domain (FADD; also known as MORT1) or TRADD. Together they constitute the death inducing signaling complex (DISC) which

subsequently recruits initiator pro-caspase-8, causing its autoproteolytic cleavage and activation. Active caspase-8 cleaves and activates effector caspases-3 and -7. The two pathways intersect through cleavage of Bid by caspase-8 into the p15 fragment tBid which is able to translocate to the mitochondrial outer membrane. tBid is able to interact with Bcl-2 family members at the MOM provoking mitochondrial outer membrane permeabilization (MOMP).

1.3.2 The mitochondrial or intrinsic pathway of apoptosis

In this apoptotic pathway death is induced through various developmental cues, cytotoxic stress, ionizing radiation, viral infection, DNA-damage or growth factor deprivation. Thereby BH3-only proteins get activated and interact with anti-apoptotic Bcl-2 family proteins at the mitochondrial outer membrane. Anti-apoptotic Bcl-2, Bcl-xL, Bcl-w, Mcl-1, (A1) and pro-apoptotic BH3-only proteins are able to interact differentially to activate pro-apoptotic pore forming proteins like Bax and/or Bak. Pore formation by Bax and/Bak induces mitochondrial outer membrane permeabilization (MOMP). Mitochondrial fragmentation releases cytochrome c, endoG, AIF, Smac/DIABLO and Omi/HtrA2 (serine protease) from the inner mitochondrial space. Released cytochrome c stimulates the assembly of the "apoptosome", an ATP dependent oligomerization of seven Apaf-1 monomers (Hu et al., 1999, Acehan et al., 2002, Rodriguez et al., 1999, Hedge et al., 2002, Martins et al., 2002) followed by the recruitment and activation of caspase-9. The apoptosome then activates executioner caspases-3 and -7. In viable cells, the activation of caspase-9 and -3 is inhibited by the inhibitor of apoptosis proteins (IAPs) like e.g. XIAP. In apoptotic cells, this inhibition is relieved by the release of Smac/Diablo and Omi/HtrA2 which bind XIAP and thereby sequester it away from caspase-3 and -9.

1.4 Bcl-2 family proteins and programmed cell death

In this chapter the mammalian Bcl-2 family proteins are described and categorized more in general. In mammals members of the Bcl-2 family interact with each other to support or suppress apoptosis induction via the mitochondrial pathway. The members of the family are divided into anti-apoptotic proteins which promote survival and pro-apoptotic proteins that support cell death (Fig. 1-4). Nine Bcl-2 homologues and eight "pure" BH3-only proteins have so far been found.

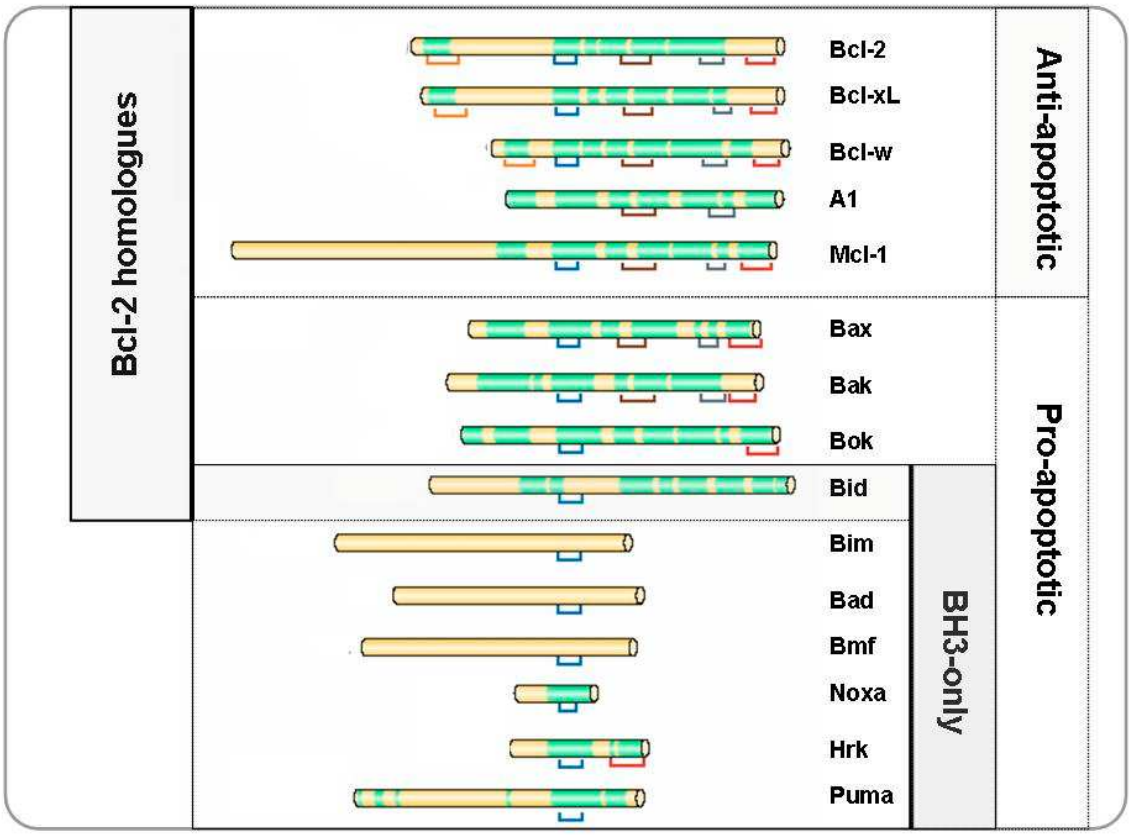

Figure 1-4: Bcl-2 family proteins. Anti-apoptotic proteins: Bcl-2, Bcl-xL, Bcl-w, A1 and Mcl-1. Pro-apoptotic proteins are subdivided into BH3-only proteins and pore forming proteins like Bax and Bak. Bid is a BH3-only protein which connects the extrinsic and the intrinsic apoptotic pathway. Members of the Bcl-2 homologues contain anti-apoptotic and pro-apoptotic proteins that display sequence and predicted structural homologies. (**Green bars**) α-helical segments, **Red lines**: regions of predicted transmembrane (TM) domains. **Brown lines**: BH1 sequence homologies; **Grey lines**: BH2 sequence homologies; **Blue lines**: BH3 sequence homologies. **Orange lines**: BH4 sequence homologies. (Adapted and modified from Youle and Strasser, 2008)

Bcl-2 homologues share conserved regions of sequence- and structural homologies in spite of divergent physiological functions. The anti-apoptotic proteins Bcl-2, Bcl-xL and Bcl-w are described as multi Bcl-2 homology domain proteins which contain three or four Bcl-2 homology domains (BH1-4). Anti-apoptotic Mcl-1 and A1 do not contain the BH4 domain. The pro-apoptotic proteins Bax and Bak contain only three BH domains (BH1-3).

During evolution several viral homologues with anti-apoptotic functions co-evolved. Karposi-sarcoma-associated herpes virus (KSHV) expresses a viral homologue of Bcl-2, as well as two other viral proteins, M11L39,40 and N1L41, which do not show a sequence similarity to Bcl-2 family proteins (Huang et al., Q, 2002). However, the 3D structure and the function of all three viral proteins are similar to that of Bcl-x_L. This indicates that the anti-apoptotic structure of Bcl-2 proteins co-evolved independent of each other to counteract host defence. At least eight viral anti-apoptotic homologues and the bacterial pore forming toxins colicin and diphtheria exert structural homology to Bcl-x_L (Muchmore et al., 1996, Polster et al., 2004).

1.4.1 Anti-apoptotic or survival proteins of the Bcl-2 family

The mammalian anti-apoptotic proteins Bcl-2, Bcl-xL, Bcl-w, Mcl-1 and A1 are mostly inserted to membranes via their C-terminal transmembrane domain. In general, they are localized on the mitochondrial outer membrane (MOM) and on mitochondria associated membranes (MAM). Bcl-2 survival proteins form a hydrophobic pocket with their BH1, BH2 and BH3 domains which perfectly fits to the amphiphatic α-helix (BH3 domain) of pro-apoptotic proteins in a high affinity manner. It is described that anti-apoptotic proteins sequester activated BH3-only proteins until all Bcl-2 survival proteins are saturated. The imbalance between pro-apoptotic and anti-apoptotic forces shifts then towards the pro-apoptotic side, inducing apoptotic signaling (Cory et al., 2003, Chipuk et al., 2010). Over expression of survival proteins Bcl-2, Bcl-xL and Bcl-w protects cells from cell death induced by a variety of stress stimuli, UV- and gamma irradiation, and cytokine withdrawal (Huang et al., 1997).

The name giving protein of the anti-apoptotic members Bcl-2 is constitutively bound on membranes and often upregulated in cancer cells. Overexpressed Bcl-2 is thought to bind activated Bax and/or Bak as well as pro-apoptotic BH3-only proteins thereby inhibiting cell death (Hanada *et al.*, 1995; Yin *et al.*, 1994).
The specific focus on Bcl-2 is summarized in chapter 1.7 (p. 29) and chapter 1.8 (p. 34).

Bcl-xL is found in the cytosol and on mitochondrial outer membranes. An additional function of Bcl-xL, independent of its anti-apoptotic activity of Bcl-xL has been described for its effect on of the cell cycle by delaying entry into S-phase (Borner et al., 1996, Chattopadhyay et al., 2001, Mazel et al., 1996, O'Reilly et al., 1996). Mice deficient in Bcl-xL die around embryonic day 14 with 100% mortality, caused by death of erythroid and neuronal progenitors (Boise et al., 1993, Gombert *et al.*, 1996).

Mcl-1 is a high turn-over protein found on membranes in the cytosol and on mitochondrial membranes (Yang et al., 1995, Chen et al., 1996). Expression of Mcl-1 is induced upon stimulation by various growth factors, such as stem cell factor, IL-5, IL-6, VEGF, GM-CSF, and IL-3, as well as through B cell receptor stimulation (Wang et al., 1999, Huang et al., 2000, Jourdan et al., 2003, Le Gouill et al., 2004, Petlickovski et al., 2005). The stability of Mcl-1 is regulated by phosphorylation through glycogen synthase kinase-3 (Gsk-3) dependent ubiquitination and its degradation by the proteasome (Maurer et al., 2006).

1.4.2 Pro-apoptotic proteins of the Bcl-2 family

This group of proteins is divided into Bcl-2 homologues such as Bax, Bak and Bok which are defined by their structural and sequence homology as pore-forming pro-apoptotic proteins and the BH3-only proteins encompassing only one single BH3 domain (Huang and Strasser, 2000, Puthalakath and Strasser, 2002). Recent sequence analyses indicate that the predicted secondary structures of BH3 domains from BH3-only proteins are unrelated to core BH3 domains of Bcl-2 homologues. The BH3-only proteins acquired the BH3-motif by co-evolution (Aouacheria et al., 2005). In contrast, the BH3 domain of Bid exhibits a unique secondary structure that is comparable to the BH3 domain of Bcl-2 homologues (Youle and Strasser, 2008).

1.4.2.1 Pro-apoptotic BH3-only proteins

In mammals, this subclass contains to date around 11 characterized members, Bim, Bid, Bad, Bmf, Noxa, Hrk, Puma, Bik, Mule, Bnip3 and Beclin1. Each BH3-only protein is activated by different stress stimuli and translocates thereafter to the mitochondrial outer membrane to interact with Bcl-2 survival proteins and/or Bax/Bak. The overall common functional relationship is the ability to fit into the hydrophobic pocket of anti-apoptotic Bcl-2 proteins. Most of the BH3-only proteins are found in the cytosol and exhibit a specific binding to anti-apoptotic proteins thereby promoting the activation of Bax and/or Bak. Pro-apoptotic Bid, Bim and Puma are able to bind to all anti-apoptotic proteins, Bad binds selectively to Bcl-2, Bcl-xL and Bcl-w, Harakiri (Hrk) binds to Bcl-w and Noxa binds to A1 and Mcl-1 (Huang and Strasser, 2000, Puthalakath
and Strasser, 2002, Letai et al., 2002; Willis and Adams, 2005, Youle and Strasser, 2008). Below I describe BH3-only proteins Puma, Bad, Bid, Bim and Bmf in greater detail.

Puma, p53 upregulated modulator of apoptosis is transcriptionally activated in response to DNA damage (ionization radiation) by the tumor suppressor protein 53 (TP53, p53) (Nakano et al., 2001, Chipuk et al., 2005). Puma is also upregulated by p53 independent mechanisms i.e. by withdrawal of cytokines and treatment with glucocorticoids (Villunger et al., 2003, Jeffers et al., 2003, Jabbour et al., 2010). Gene knock out mutants of Puma and Bim show protection against apoptosis thereby facilitating spontaneous tumor genesis, causing the malignancies observed in Bcl-2 transgenic mice (Erlacher et al., 2006).

Bcl-2 associated agonist of cell death (Bad) is post-translationally phosphorylated at several serine residues and sequestered by 14-3-3 scaffold proteins in the presence of growth factors. Withdrawal of IL-3 turns protein kinase B (PKB)/AKT into the inactive state thereby Bad is dephosphorylated and released from the scaffold protein 14-3-3 to interact with Bcl-2 family proteins (Zha et al., 1996b).

BH3 interacting domain death agonist (Bid) is proteolytically cleaved by activated caspase-8 into its active truncated form tBid (Li et al., 1998). The interaction of the p15 fragment tBid with the mitochondrial membrane is facilitated by N-myristoylation and its high affinity to cardiolipin a mitochondrial specific lipid (Lutter et al., 2000, 2001). Several investigations indicate that membrane targeted tBid activates Bax to permeabilize artificial liposomes thereby releasing dextran from liposomes which depends on cardiolipin, a particular membrane phospholipid of mitochondria (Kuwana et al., 2002, Oh et al., 2006, Lovell et al., 2008, Ott et al., 2007).

The pro-apoptotic Bcl-2 interacting mediator of cell death (Bim) is activated upon physiological forms of stress (cytokine withdrawal) and binds to pro-survival proteins to exert its pro-apoptotic function. Additionally, Bim is *de novo* expressed after withdrawal of survival factors in hematopoietic cell lines, primary sympathetic neurons, osteoclasts and fibroblasts. Phosphorylation of Bim by MAPK/ERK leads to its degradation by the ubiquitin/proteasome system thereby reducing the induction of apoptosis (Adachi et al., 2005, Ley et al., 2005). Bim exists in 18 various isoforms which differ in size and exhibit variable apoptotic functions. These splice variants have not all been physiologically defined. Bim is able to bind to dynein light-chain 1 (DCL1) proteins which are components of the dynein and myosin V motor complexes. Some of these Bim isoforms act as decoys in the pro-apoptotic signaling because they do not contain a BH3 domain or lack the DLC domain (Adachi et al., 2005).

Bcl-2-modifying factor (Bmf) is activated by anoikis, treatment with histone deacetylase (HDAC) inhibitors, transforming growth factor β (TGFβ) and MEK inhibition (Schmelzle et al., 2007, Zhang et al., 2006, Ramjaun et al., 2007, Vanbrocklin et al., 2009).

Bmf is able to bind to DLC2 and is sequestered to the actin-linked myosin V motor complex in healthy cells from which it is released after induction of apoptosis (Puthalakath et al., 2001).

1.4.2.2 Pro-apoptotic Bcl-2 homologues Bax, Bak and Bok

Bax, Bak and Bok belong to the Bcl-2 homologues containing only three Bcl-2 homology domains BH1-3 (Fig. 1-4). Bak is integrated into the mitochondrial outer membrane via its transmembrane domain. Bax is a cytosolic protein and its hydrophobic C-terminal membrane anchor is bound to its own hydrophobic pocket. A minor fraction of Bax is loosely attached to the mitochondrial outer membrane (Hsu, et al., 1997b; Suzuki et al., 2000; Schinzel, et al., 2004). The subcellular localization of Bok is less clear, as is its function. In mice, Bok expression is found in the brain, liver, lymphoid tissue, testis, ovary and the uterus (Hsu, et al., 1997a; Inohara, et al., 1998; Gao, et al., 2005).

The BH1-3 of Bax and Bak form a hydrophobic pocket like the anti-apoptotic survival factors Bcl-2, Bcl-xL, Bcl-w and Mcl-1. The most important function of Bax and Bak is to promote cell death via oligomerization and pore formation to support mitochondrial outer membrane permeabilization (MOMP). Bax/Bak double knockout cells (DKO) are resistant against most forms of stress-induced apoptosis *in vitro* and show no signs of MOMP, no release of cytochrome c or any other proteins from the mitochondria inner membrane space (Wei et al., 2001). Mice deficient of Bax show mild phenotypes such as aberrancies in brain, ovary and testis development. By contrast Bak knockout mice show no obvious defects. However, mice deficient in Bax and Bak are embryonically lethal and show severe defects during embryogenesis and development indicating functional redundance of the two proteins (Knudson et al., 1995, Lindsten et al., 2000).

1.4.2.3 Bax and Bak dynamics during apoptosis

Upon apoptosis induction, Bax (19 kDa) translocates from the cytosolic compartment to mitochondrial outer membranes. Activated Bax releases its C-terminal transmembrane domain (TM) from the hydrophobic pocket and inserts into the mitochondrial outer membrane (Goping, et al., 1998; Antonsson, et al., 2001; Schinzel et al., 2004). This leads a conformational change upon which the N-terminal alpha helix 1 gets exposed (accessible for a specific anti-N antibody). The BH3 domain of membrane bound Bax is now more flexible to rotate around the axis to expose it to Bcl-2 survival proteins (Sattler et al., 1997). Swapping this region from Bax to Bcl-2
converted Bcl-2 into a death agonist (Hunter and Parslow, 1996). However, it is still a matter of debate how the process of MOMP is regulated by the anti-apoptotic and the pore-forming proteins Bax and Bak. The biochemical properties of Bax and Bak pores are still not clear (Chipuk et al., 2006). At the mitochondrial outer membrane both Bax and Bak assemble into high molecular weight complexes, to create either protein-protein, protein-lipid or lipid pores to facilitate cytochrome c release from the mitochondrial inner membrane space (Mikhailov et al., 2003, Green and Kroemer 2004). How many Bax or Bak monomers are needed to form up these pores is still unknown and it seems that these oligomers are distributed over a wide range of molecular weights (Youle and Strasser, 2008). At present, oligomerized Bak complexes of 400 kDa were found to disintegrate into smaller complexes at the size of 70 kDa after apoptosis induction (own data and by communication Michael Ryan 2010).

1.4.2.4 Binding affinities between pro-apoptotic BH3-only and survival proteins

BH3-only proteins or peptides specifically bind to anti-apoptotic proteins. The specificity in binding has been determined by yeast-two hybrid analysis, plasmon resonance binding

assays (Biacore) and by cell free mitochondria and liposome permeabilization experiments as shown in Fig. 1-5 (Youle and Strasser, 2008).

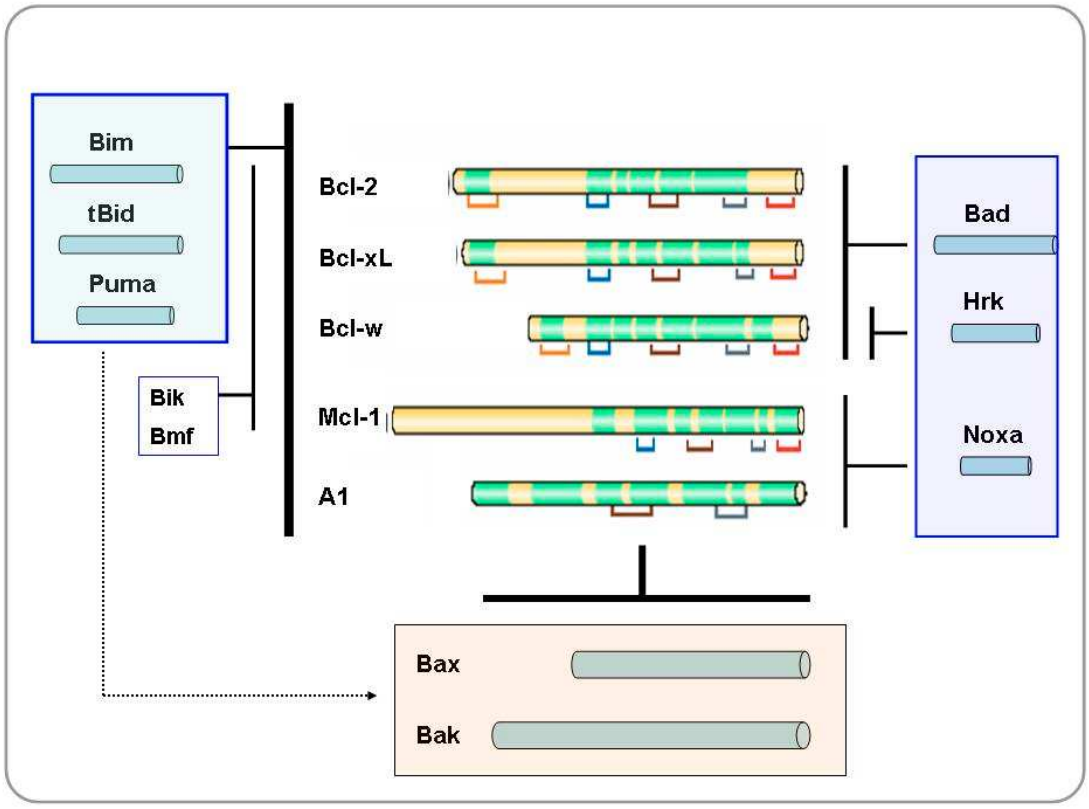

Figure 1-5: Binding specificity of BH3-only proteins to core Bcl-2 homologues. Bim and Puma strongly bind to all anti-apoptotic proteins whereas tBid associates only weakly to Bcl-2 but with increased affinities to the other survival proteins. Bad interacts selectively with Bcl-2, Bcl-xL and Bcl-w. Noxa binds to Mcl-1 and A1, Hrk solely to Bcl-w, Bik and Bmf to Bcl-2, Bcl-xL, Bcl-w and Mcl-1. BH3-only proteins Bim, tBid and Puma may induce apoptosis by direct binding to Bax or Bak. (Adapted and modified from Youle and Strasser, 2008, Chipuk 2010)

1.4.2.3 Activated BH3-only proteins and models of Bax/Bak activation

The question is still open how exactly BH3-only proteins activate Bax and Bak and thereby lead to MOMP. Peptide specific binding experiments led to the development of models how this might occur (Wang et al., 1996, Kuwana et al., 2002, 2005, Cartron et al., 2004, Kim et al., 2006, Letai et al., 2002, Certo et al., 2006).

The models discussed are called: "derepressor", "hierarchy", "neutralization" or "sensitizer" models, which try to explain how BH3-only proteins promote cell death. They can be simply summarized as "direct" and "displacement" models. Figure 1-6 A-C depicts the basic mode of interaction between BH3-only proteins, Bcl-2 survival proteins and pore forming proteins Bax and Bak. BH3-only proteins are divided into "activators" (Bim, Bid, Puma) and "sensitizers" (Bmf, Bad, Hrk, Bik, Noxa, BNIP3).

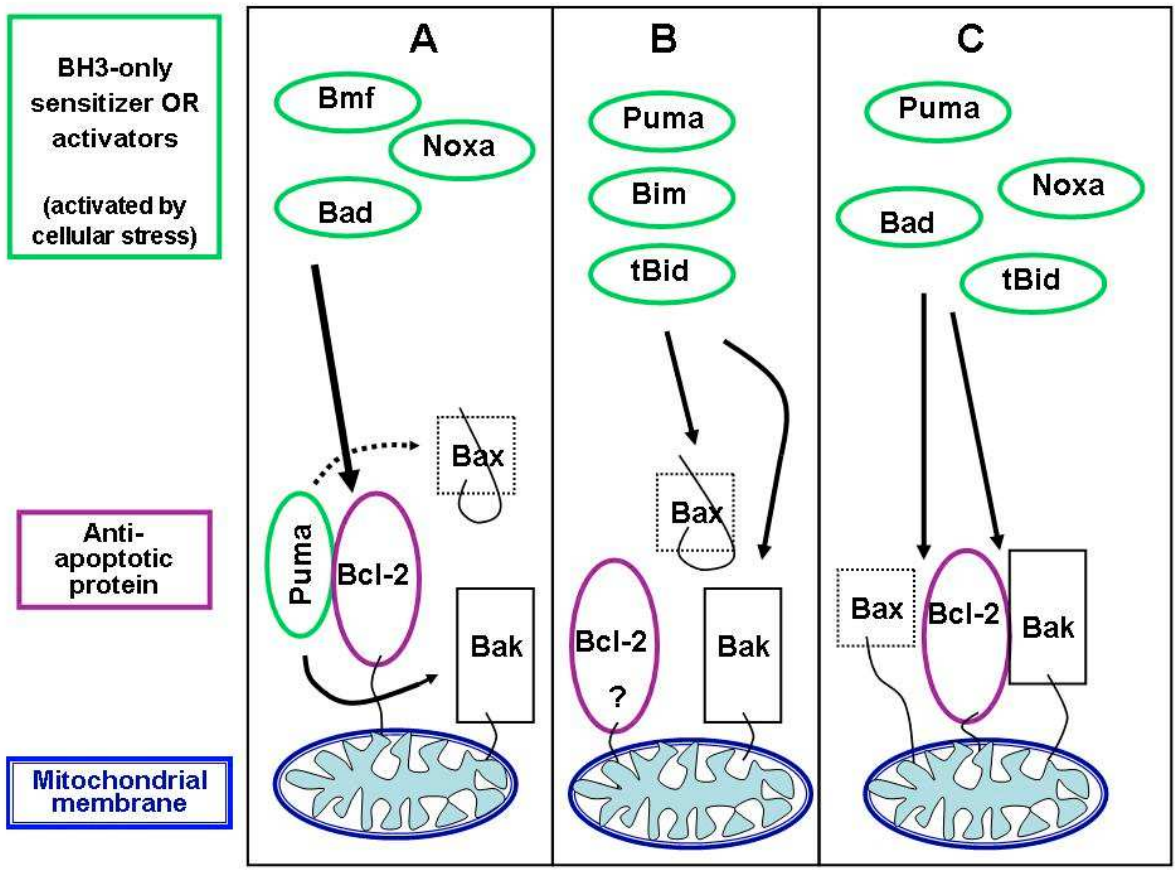

Figure 1-6: Bax-Bak activation and mitochondrial outer membrane permeabilization. (A, B) "direct" activation model**; (A)** sensitizer BH3-only protein Bad translocates to anti-apoptotic Bcl-2. Thereby Puma is released and induces Bak and/or Bax activation, oligomerization and induction of MOMP. **(B)** Bax or Bak are directly activated by the activator proteins Bim, tBid or Puma. **(C) "displacement"** model: activated Bax and Bak are bound to survival factors and displaced by either activator or sensitizer BH3-only proteins. Released Bax and Bak oligomerize to induce MOMP (Own scheme).

1.4.2.4 The "direct" activation model

In this model the “activator” BH3-only proteins Bim, Puma and tBid are bound to the Bcl-2 survival proteins. Upon apoptotic stimuli the “sensitizer” BH3-onlies cause the release of the “activators” (Fig. 1-6 A), thereby allowing them to directly activate Bax and Bak. This model also implies that the “activator” BH3 only proteins can directly activate Bax and Bak after being induced by apoptotic stimuli without the need of a prior binding to Bcl-2 (Fig. 1-6 B).

Difficulties of the direct activation model:

Endogenous interactions of Bid, Bim and Puma with Bax and/or Bak seem to be difficult to detect because of the fast and transient interaction. While some reports detect such an interaction (Gallenne et al., 2009), Galvathiotis et al., 2008) other fail to see any endogenous interaction of the BH3-only proteins Bim, Puma or Bid with Bax or Bak (Bouillet et al., 1999, Willis et al., 2007). In contrast, Bim was found to bind to Bcl-2 and Mcl-1 in healthy and apoptotic thymocytes. Moreover, mutants of tBid and Bim which are able to bind Bax and

Bak are neither able to bind to anti-apoptotic proteins nor inducing cell death very efficiently. A recent publication shows that the combined loss of Bim, Bid and Puma still leads to cell death indicating that there are still other factors able to induce apoptosis (Willis et al., 2007). Additionally, there is now good evidence, that tBid at first directly interacts with the membrane and then interacts with Bax to cause membrane insertion and oligomerization. Furthermore, Bcl-xL inhibits membrane-bound tBid to bind Bax and addition of Bad releases again tBid from Bcl-xL (Lovell et al., 2008). Kim et al. (2006) proposes that activator BH3-only proteins (tBid, Bim, Puma) directly interact with Bax and Bak and remain bound to the N-terminally exposed Bax to drive the homo-oligomerization in vitro.

1.4.2.5 The "displacement" or "derepressor" model

In this model Bax and Bak are sequestered by anti-apoptotic Bcl-2 proteins until displaced by the binding of BH3-only proteins (both activators and/or sensitizer) to the hydrophobic pocket of Bcl-2 anti-apoptotic proteins (Fig. 1-6 C).

Difficulties of the displacement model:
Most of these experiments are done with overexpressed proteins and not really under endogenous conditions. Two publications support the displacement model, (i) the interaction of Bak with Bcl-xL and Mcl-1 but not Bcl-2, Bcl-w and A1 (Willis et al., 2005), and (ii) the controversial result of Bak binding to Bcl-xL and Bcl-2 in FDC-P1 cells (Ekert et al., 2006).

1.5 Mitochondria: Structure and functional dynamics

1.5.1 Morphology, structure and function of mitochondria

Mitochondria are not de-novo synthesized. They grow during the interphase period of the cell cycle and new mitochondria are formed by division of pre-excisting mitochondria. Mitochondria excist as single units of different sizes, stay in contact with membranes of the endoplasmatic reticulum (ER), and are able to create an elongated tubular interconnected network (Fig. 1-7).

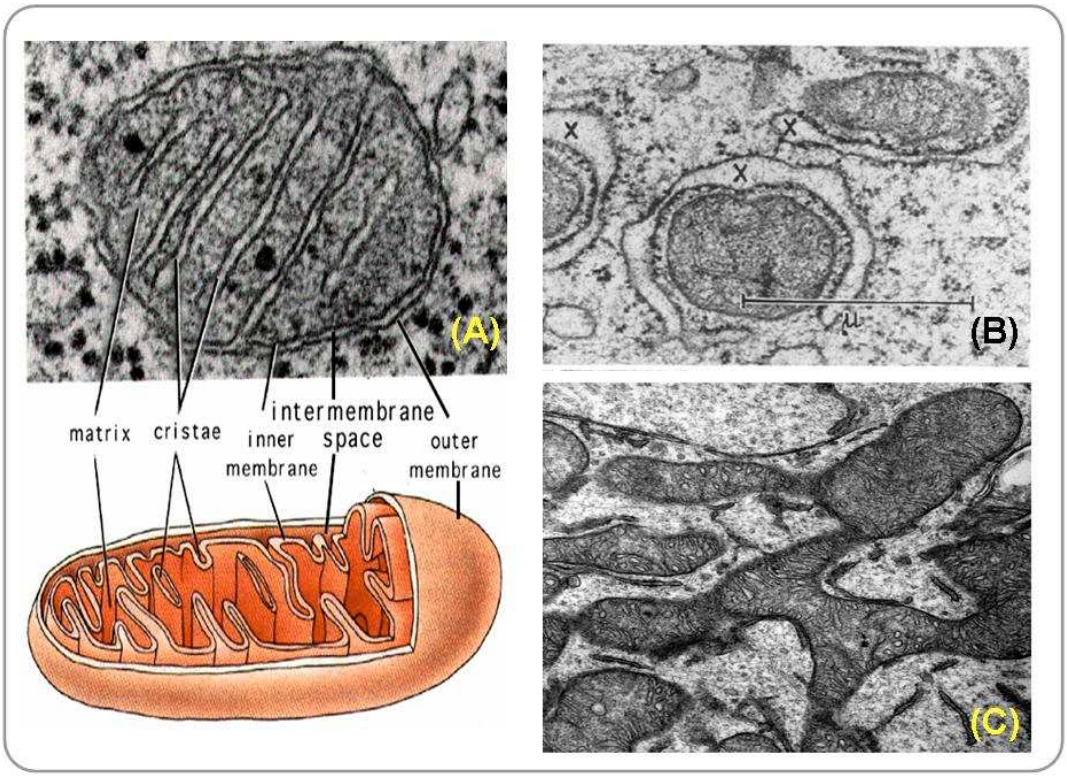

Figure 1-7: Mitochondrial membranes and morphology. Transmission electron microscopy (TEM), (**A**) Scheme of a mitochondrion (www-microbewiki.kenyon.edu/index.php/Mitochondria). (**B**) Membranes of the endoplasmatic reticulum (ER) in close contact to mitochondria, X lumen of the ER (Adopted and modified: Merker et al., 1968). (**C**) Fused mitochondria form up an elongated intracellular network (Dissertation: Kukat, 2007).

The outer membrane encompasses the complete mitochondrion, whereas the mitochondrial inner membrane is compartmentalized into numerous cristae which expand until the outer mitochondrial membrane. At the inner membrane ATP is produced by the process of oxidative phosphorylation. The core aqueous matrix space houses the citric acid cycle (Krebs cycle), ß-oxidation, biosynthesis of phospholipids, amino acids, and nucleotides. The aqueous intermembrane space (IMS) lies in between the structurally and functionally distinct outer and inner membrane.

1.5.1.1 Protein complexes of the outer and inner mitochondrial membrane

Voltage dependent anion channel:

The most abundant transmembrane protein, the voltage-dependent anion channel (VDAC) exists in three isoforms, VDAC1, VDAC2 and VDAC3. The voltage-dependent anion channel 1 is a ß-barrel protein which is in functional and physical connection with the adenine nucleotide translocator (ANT) at the inner mitochondrial membrane (IMM). These two main protein complexes create a channel of high and low conductivity thereby regulating the flow of small molecules (< 5 kDa) and selective proteins of bigger molecular size (< 1.5 kDa,

ADT/ATP-translocator). The channel is regulated by a tetrameric complex of hexokinase that associates to VDAC at the cytosolic side, and four dimers of creatinine kinase which are able to bind at the side of the inter membrane space. This channel is referred as the main component of the permeability transition pore (PTP, Kroemer et al., 2007). VDAC2 sequesters Bak thereby regulating Bak oligomerization (Cheng et al., 2003). In contrast, Baines et al. 2007 indicates that VDAC1-3 proteins are dispensable during programmed cell death.

Mitochondrial protein import complexes:

Most of the mitochondrial proteins (99%) are synthesized on cytosolic ribosomes and subsequently transported to mitochondria post-translationally, known as mitochondrial precursor proteins. These new synthesised proteins are recognized by receptors of the mitochondrial membrane and imported by a multiprotein complex the pre-protein translocase of the outer mitochondrial membrane (TOM). This general import gate is associated with different import machineries that are connected to mitochondrial morphology, redox regulation and energy metabolism. At present four classes of precursor proteins exist that are directed to four distinct mitochondrial import pathways. One of them, the presequence pathway to matrix and inner membrane is driven by the electrochemical proton gradient and ATP generated during the process of oxidative phosphorylation (Bolender et al., 2008). The most abundant mitochondria-specific phospholipid in the matrix membrane is cardiolipin (CL), representing 25% of the total phospholipids of the mitochondrial inner membrane and 4% of the MOM. Cardiolipin is required to restore enzymatic functionality of the respiratory chain complexes (Hoffmann et al., 1994, Jiang F, et al., 2000, Koshkin V, et al., 2000, Choi et al., 2007).

1.5.1.2 Cardiolipin and its function in mitochondria

Cardiolipin or diphosphatidylglycerol is only found in bioenergetic membranes those of bacteria and mitochondria. CL consists of one molecule which exhibits a dimeric structure that distinguishes it from other glycerophospholipids (Fig. 1-8).

Most of the cardiolipin associates with cytochrome c at the outer leaflet of the mitochondrial inner membrane and contributes to the regulation of cytochrome c release during apoptosis. ROS generation causes peroxidation of cardiolipin thereby reducing the activities of complexes I and IV. Peroxidation of cardiolipin was also demonstrated by a variety of apoptotic stimuli such as nitric oxide, Fas receptor stimulation, NGF deprivation, staurosporine and actinomycin D (Kagan VE, et al., 2005). Cytochrome c interacts with cardiolipin at two different binding sites, (I) an electrostatic interaction site (A), and (II) a hydrophobic binding site (C). Cytochrome c bound via the A-site participates in the electron

transfer and ROS scavenging. A cytochrome-c-cardiolipin complex with hydrogen peroxide peroxidase activity is able to oxidize cardiolipin to peroxi-cardiolipin (Fig. 1-9 A)

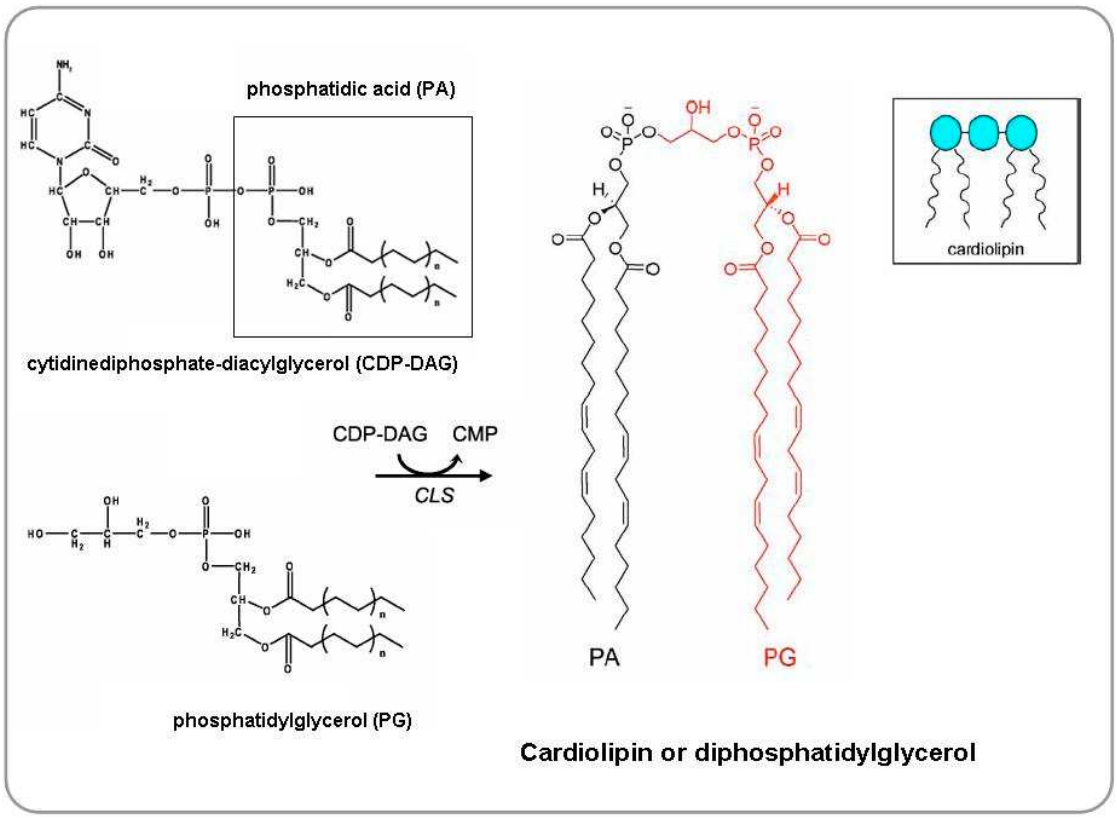

Figure 1-8: Cardiolipin synthesis in eukaryotes. The condensation of one monomer phosphatidylglycerol (PG) and one monomer cytidinediphosphate-diacylglycerol (CDP-DAG) at the mitochondrial inner membrane is catalysed by the enzyme cardioplin synthase (CLS). The resulting cardiolipin consists of four acyl chains, three glycerols and two phosphate groups per molecule (Adapted and modified from Gonzalvez, 2007 and Houtkooper, 2008).

Peroxidized cardiolipin is thought to be the trigger to redistribute to both mitochondrial membranes, thereby supporting the formation of non-bilayer hexagonal structures shown in figure 1-9 B (Ardail et al., 1990, Van Venetie et al., 1982). The redistribution of cardiolipin within the inner and outer mitochondrial membrane was also observed after death receptor induced apoptosis, before PS exposure at the same time of ROS production (Garcia Fernandez et al., 2002). Moreover, peroxidized cardiolipin has an active role in inducing apoptosis when added to isolated mitochondria. It alone induces release of cytochrome *c* and smac/diablo release (Kagan et al., 2005).

1.5.1.3 Cardiolipin interacts with Bcl-2 family proteins

Cardiolipin is predominantly found in the matrix membrane but also at sites of contact between the mitochondrial outer and inner membrane. Lutter M, et al. (2000) showed that pro-apoptotic tBid interacts exclusively with liposomes that contain at least physiological

levels of cardiolipin (Fig. 1-9 C, D). Further results from Garcia-Saez et al. (2004) indicate that tBid interacts specifically at "docking" sites of the inner and outer mitochondrial membrane by a specific hairpin structure (helix 6) which is required for lipid binding. The treatment of isolated mitochondria with tBid resulted immediately in ANT inhibition, the loss of the ADP-driven respiration and oxidative phosphorylation (Gonzalvez F, et al., 2005). The mechanism on how tBid may work might be either BH3-domain-dependent or independent. Recently, it has been found that these "docking" sites or micro domains form a procaspase-8 activation platform to generate tBid at the mitochondria. Bcl-xL survival protein prevents membrane bound tBid from binding of Bax but Bad is able to displace tBid. Interaction of Bax and tBid induce Bax oligomerization depicted in figure 1-9 A (Gonzalvez et al., 2008).

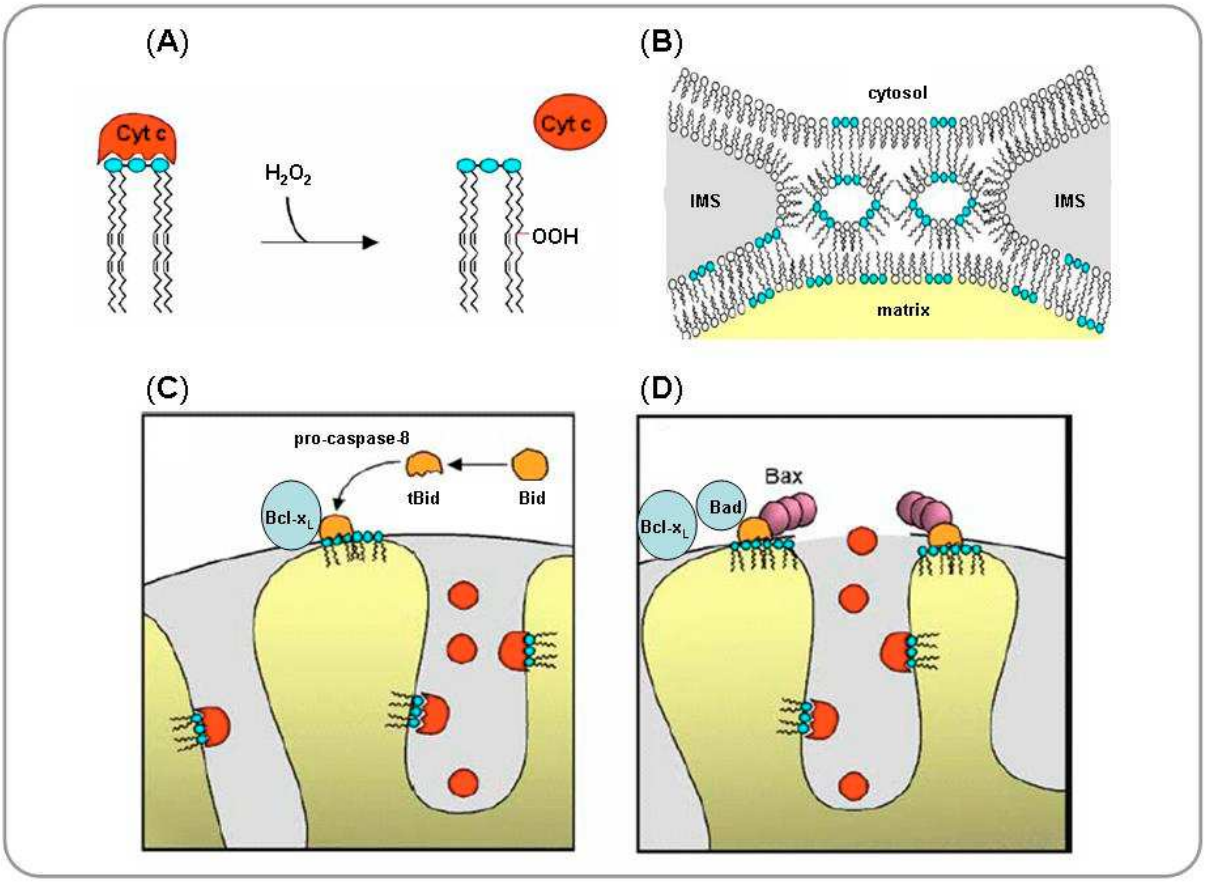

Figure 1-9: Cardiolipin, cytochrome c and Bcl-2 family proteins. Cardiolipin executes apoptosis-supporting roles at "docking" sites of the mitochondrial outer and inner membranes. (**A**) Peroxidation of cardiolipin acyl-groups by a cytochrome-c-cardiolipin complex to peroxidated CL. (**B**) Peroxi-cardiolipin supports formation of non-bilayer hexagonal structures. Fused membranes redistribute cardiolipin to the cytosolic face of the mitochondria. (**C**) Cardiolipin "docking" sites or micro domains serve as scaffolds for pro-caspase-8 and Bid to generate tBid. Its interaction with Bax is inhibited by Bcl-xL. (**D**) Cardiolipin facilitates perforation of the mitochondrial outer membrane by supporting of a Bad dependent tBid Bax oligomerization. The mechanism is still elusive (Adapted and modified: Gonzalvez et al., 2008).

The structure and function of mitochondrial membranes is affected by tBid in concert with the distribution of cardiolipin but the significance of this mechanism is still unclear. Cardiolipin

dependent binding of tBid to mitochondria induces a transient opening of the permeability transition pore (PTP) which is mediated by specific membrane proteins (Scorrano L., 2002). In contrast, anti-apoptotic proteins like Bcl-2, Bcl-xL and Mcl-1 are anchored via their transmembrane domain in the MOM to support membrane integrity, so that the cell survives. Moreover, other membrane proteins are integrated in this dynamic process with increasing complexities. How these protein interactions might take place in healthy and apoptotic cells is depicted in the next chapters.

1.5.2 Morphological changes of mitochondria and Bcl-2 family proteins

1.5.2.1 Mitochondrial fusion, fission and hyperfusion machineries

Mitochondria continually form elongated tubules that fuse and divide important for normal homeostasis and during apoptosis. Fusion and fission processes are necessary to maintain mitochondrial integrity, by exchanging mitochondrial DNA (mtDNA) or protein quality control. Most of the genes or proteins involved in mediating fusion and fission have been identified in yeast and most of them are conserved in mammals.

1.5.1.2 Fusion of mitochondrial outer and inner membranes

In mammals and yeast three large GTPases of the dynamin family, mitofusin-1, mitofusin-2 (Mfn1, Mfn2), optic atrophy-1 (OPA-1) and mitochondrial phospholipase D (mitoPLD) mediate fusion of mitochondrial membranes (Fig. 1-10). The mitofusins Mfn1 and Mfn2 are integrated into the mitochondrial outer membrane (MOM) through two transmembrane domains which face the intermembrane space. Their N-terminal GTPase domain and C-terminal coiled-coil regions point toward the cytosol and support the fusion of the MOM (Santel and Fuller, 2001).

Mitochondrial phospholipase D is located on the outer mitochondrial membrane and links cardiolipin directly to mitochondrial fusion. Downregulation of mitoPLD by RNAi results in reduced fusogenic activity and increases thereby the amount of fragmentised mitochondria which is a hallmark of mitochondrial apoptosis (Choi et al., 2007).

OPA1 regulates fusion of the matrix membrane (Meeusen et al. 2004, 2006, Olichon et al. 2002). In mammals OPA1 is encoded by a single gene that exhibits eight transcript variants by alternative splicing (Delettre et al. 2001). The splice variants of OPA1 are differentially proteolysed into short and long forms, S-OPA1 and L-OPA1. The long forms are inserted into the matrix membrane by a hydrophobic domain and the short forms of OPA1 (S-OPA1) are more loosely attached to the inner mitochondrial membrane (Fig. 1-10). OPA1 is crucial for inhibition of apoptosis. OPA1 expression rescues cells from cell death in type II cells but not of that one occurring in type I cells (Frezza et al. 2006). Moreover, OPA1 is expressed in

eight RNA transcript variants that regulate fusion and cytochrome c release (Delettre et al. 2001, Olichon et al. 2007). Knock down of OPA1 by RNAi induces spontaneous cell death and co-expression of Bcl-2 inhibits apoptosis pointing to a regulation of mitochondrial fusion upstream of mitochondrial outer membrane permeabilization (Olichon et al. 2003).

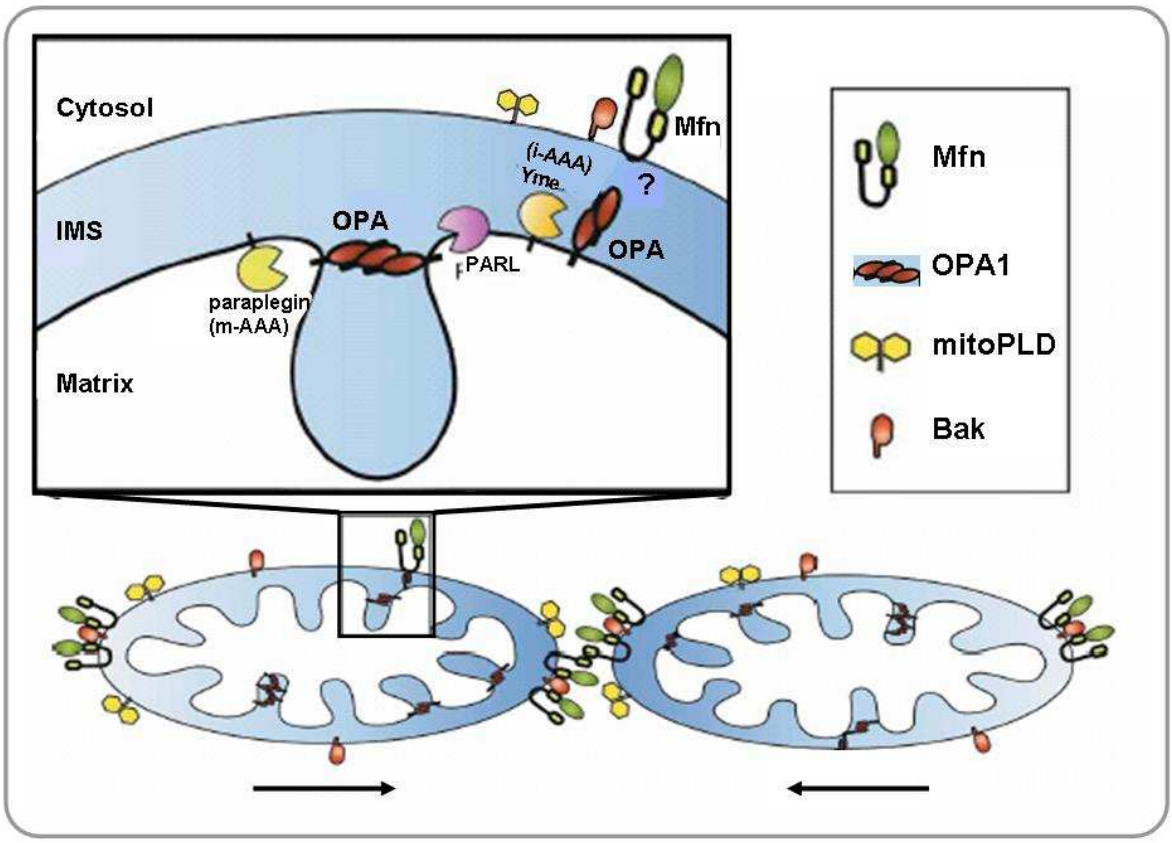

Figure 1-10: Sheme of the mitochondrial fusion machinery. Submitochondrial localization of mammalian proteins involved in mitochondrial fusion in healthy cells, including the mitofusins, L-OPA1 and S-OPA1, mitoPLD, and Bak. The box above shows the localization of proteases proposed to function in OPA1 cleavage. Presenilin-associated rhomboid-like (PARL) is one member of the rhomboid family. (Adapted and modified: Der-Fen Suen, 2008)

1.5.2.3 Fission and fragmentation of mitochondria

Mitochondrial fission is mediated by the dynamin-related protein 1 (Drp1) and Fis1. Drp1 is a large GTPase usually located in the cytosol. The functional mechanism of Drp1 is homolog to dynamin that assembles in spirals around endosomes to mediate scission of lipid tubules (Roux et al. 2006). In analogy to the Drp1 homolog Dnm1 in yeast, Drp1 would act in the same way moving between cytosol and mitochondria to constrict membranes of mitochondria either due to the assembly of the spiral or to subsequent changes in helical diameter as depicted in figure 1-11 (Smirnova et al. 2001; Wasiak et al. 2007). In yeast, Fis1 a mitochondrial membrane protein is required to recruit and assemble Dnm1 to mitochondria, but orthologs in mammals have not been found (Mozdy et al. 2000; Tieu and Nunnari 2000; Griffin et al. 2005, Lee et al. 2004).

Mitochondrial fission, mediated by Drp1 is an early event during apoptosis followed by MOMP (Martinou and Youle, 2006). In response to apoptotic stress Drp1 translocates to mitochondria and co-localizes with Bax and Mfn2 at fission sites (Figure 1-11, Karbowski et al., 2002).
In mammals, the recruitment and assembly of Drp1 to mitochondria seems to depend on actin and microtubules (Varadi et al. 2004; De Vos et al. 2005). Moreover, mitochondrial Rho-1 (Miro-1), a Rho-like protein seems also to be involved in the transport of mitochondria especially in the motility of neuronal mitochondria (Fransson et al., 2006, Saotome et al., 2008, Macaskill et al., 2009, Wang et al., 2009).

The inhibition of apoptosis by expression of a dominant-negative Drp1 K38A mutant or RNAi down-regulation displays a delay in mitochondrial fission. Inhibition of cytochrome c release and apoptosis is shown in some publications in others not and therefore controversial (Frank et al., 2001, Neuspiel et al., 2005, Arnoult et al., 2005, Parone et al., 2006, Brooks et al., 2007, Estaquier et al., 2007).
Recently, results from Cassidy-Stone et al. (2008) demonstrate that mitochondrial fission, cytochrome c release and apoptosis is inhibited by adding a chemical mitochondrial division inhibitor-1 (midivi-1) that blocks polymerization activity of Drp1. Inhibition of mitochondrial outer membrane permeabilization facilitated by midivi-1 does not block tBid/Bax-Bak dependent oligomerization but it rather inhibits self assembly of Drp1 thereby inhibiting cytochrome c release and apoptosis. This may indicate that apoptosis is regulated by Drp1 in a complex of Bax and Bak before oligomerization of Drp1 either by conformational changes via cardiolipin or by maintenance of a Bax/Bak dependent normal fusion activity controlling the activity of the fusion protein Mfn2 (Karbowski et al., 2006).

The process of mitochondrial fragmentation is normally associated with apoptosis, but fission is also seen in the absence of apoptosis. As an example: The reversible uncoupling agent dinitrophenol, CCCP or FCCP that abolish the obligatory linkage between the respiratory chain and the phosphorylation system induce reversible mitochondrial fragmentation which is not linked to apoptosis. Further, the expression of viral mitochondria-localized inhibitor of apoptosis (vMIA) induces fragmentation of the mitochondrial network but simultaneously cell death is inhibited (McCormick et al. 2003).

Mitochondrial fission and/or fusion seem to be an intermediate state during the decision to release cytochrome c to induce apoptosis or to regulate transcription of mitochondrial genes and energy status during growth and proliferation.

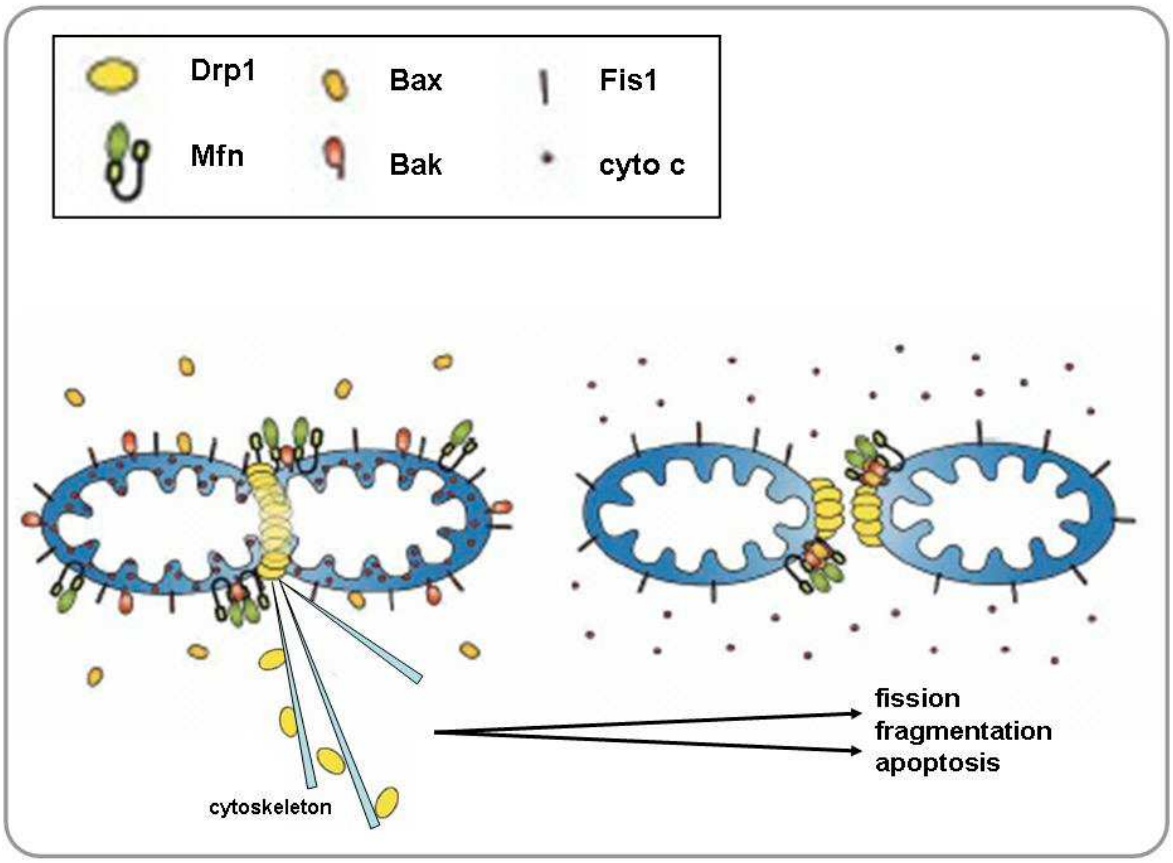

Figure 1-11: Sheme of the mitochondrial fission machinery. Submitochondrial localization of mammalian proteins involved in mitochondrial fission or fragmentation including Drp1, Mfn, Bax, Bak, Fis1, cytochrome c and cytoskeletal filaments. Possible crosstalk of morphological machineries with pro-apoptotic progression (Adapted and modified: Der-Fen Suen, 2008)

1.5.2.4 Hyperfusion of mitochondria

Tondera et al. (2009) showed that stress-induced mitochondrial hyperfusion (SIMH) is accompanied by an increase of mitochondrial ATP production representing a novel adaptive pro-survival response against stress. The results indicate a requirement of Mfn1 and long-OPA1 (L-OPA1) for SIMH under low stress conditions but not Mfn2 and short-OPA1 (S-OPA1). Extended stress levels commit cells to induce apoptosis via Drp1-mediated fission/fragmentation of the mitochondria outer membrane to promote cytochrome c release and apoptosis (Fig. 1-12).

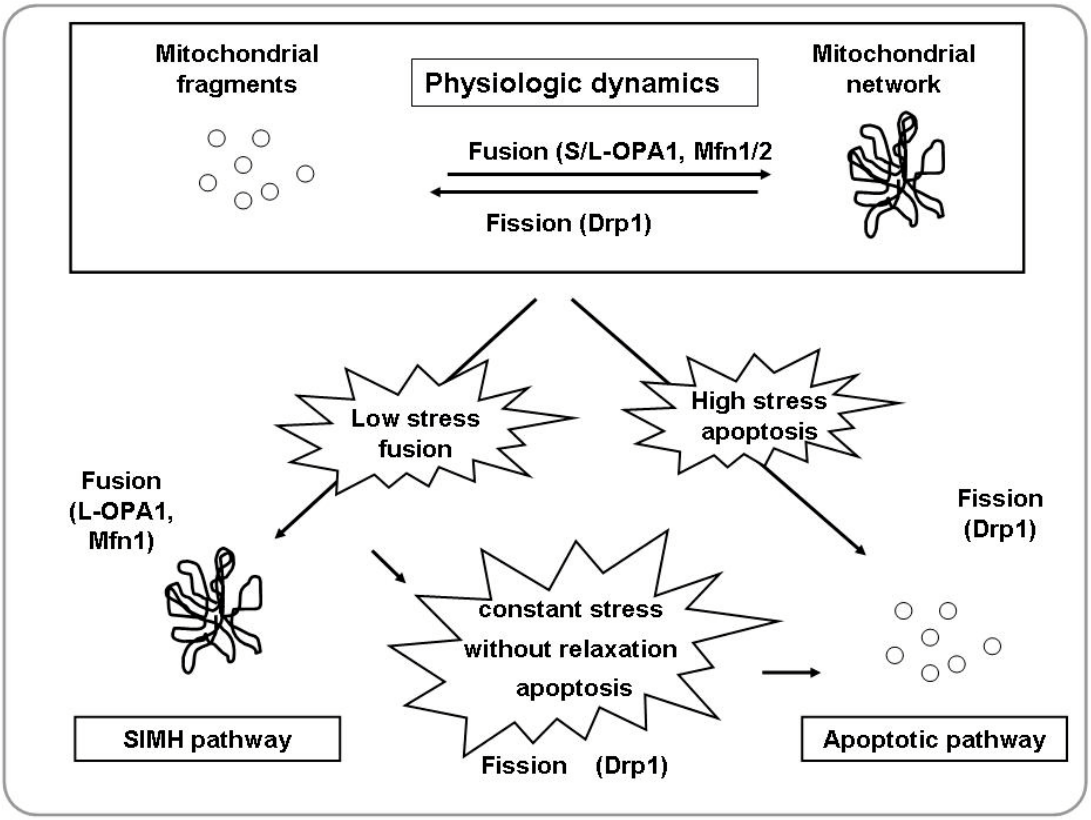

Figure 1-12: A model of the steady-state of mitochondria fission and fusion. Different forms of cellular stress induce mitochondria to fragment or form up a stress resistant network of elongated mitochondria. But mitochondrial fission or fragmentation is not necessarily related to apoptosis. (Adapted from Bliek, 2009)

1.6 Bcl-2 family proteins and mitochondrial membrane dynamics

In C.elegans mitochondrial fission is induced upon interaction of CED-9/EGL-1 indicating that mitochondrial fragmentation does have an essential role in apoptosis but incompletely understood (Jagasia et al., 2005).

Sheridan et al. (2008) and others show that overexpressed Bax and/or Bak induce mitochondrial fission, cytochrome c release and apoptosis. Co-expression of Bcl-xL or Mcl-1 inhibited cytochrome c release and apoptosis but did not affect mitochondrial fragmentation. Further. Bax and Bak were shown to interact with Mfn1 and Mfn2 in healthy cells pointing to a direct regulation of mitofusins by these proteins (Brooks et al., 2007).

HeLa cells expressing CED-9 exhibit an increased amount of cells with a fused mitochondrial network independent of the induction of apoptosis by actinomycin or daunorubicin treatment (Delivani et al., 2006). Expression of EGL-1 alone in HeLa cells did not affect mitochondrial fragmentation but co-expression of CED-9 rendered fused mitochondria into a fragmented pattern. Moreover, they were able to demonstrate that Ced-9, Bcl-xL and Bcl-2 interact with mammalian mitofusin 2 (Mfn2) but not with Mfn1 in co-immunoprecipitation experiments.

However, the mitochondrial phenotype of those cells expressing Bcl-xL and Mfn2 or Bcl-2 and Mfn2 were distinct. 50 % of Bcl-xL/Mfn2 expressing cells displayed fused mitochondria whereas Bcl-2/Mfn2 expressing cells show fragmentated mitochondria.

As already mentioned before mitochondrial fission and fusion dynamics may have an additional function that is not necessarily linked to cytochrome c or apoptosis. Alternatively, some proteins involved in fission/fusion maybe required for particular processes in apoptosis. Consistent with this notion, the group of Martinou J.C. recently published and confirmed that Drp-1 is required for Bax oligomerization dependent on tBid and cardiolipin. The ability of Drp1 to induce Bax polymerisation strongly depends on cardiolipin in membranes and liposome experiments (Montessuit et al., 2010). Most of these results were obtained through artificial expressed proteins and peptides, representing a non-physiological experimental state to understand step by step endogenous signaling.
However, it is still unclear how members of the Bcl-2 family fit into this process regulating survival or apoptosis possibly seen by fission and fusion dynamics. It is likely that the Bcl-2 family members possess multiple functions of still unknown and conserved roles.
Anti-apoptotic Bcl-2 proteins may therefore integrated in a series of events that lead to the axonal movement of mitochondria by interaction with filaments of the cytoskeleton, because mitochondria of Bax/Bak double knockout (DKO) cells show a reduced mitochondrial motility (Boldogh and Pon, 2007).
A second role might be the ability to modify the properties of membrane lipids thereby altering the structure, the size of subcompartments of membranes and therefore the movement and activity of proteins within membranes. Bcl-2 anti-apoptotic factors may therefore regulate the activity of pro-apoptotic Bh3-only proteins by altering the membrane lipid properties and regulating thereby the structure of membrane proteins (Hannun et al., 2008, Montessuit et al., 2010).

1.6.1 Alteration of lipid composition of the MOM: a regulator of apoptosis?

Eukaryotic membranes consist of glycerophospholipids, sphingolipids and glycolipids. Glycerophospholipids consist of a hydrophobic portion diacylglycerol (DAG) and various polar heads groups created by phosphatidylcholine (PtdCho), phosphatidylethanolamine (PtdEtn), phosphatidylserine (PtdSer), phosphatidylinositol (PtdIns) and phosphatidic acid (PA).
Sphingolipids contain ceramide as hydrophobic backbone which is synthesized by sphingosine and a fatty acid. The endoplasmatic reticulum (ER) is the main site of lipid and ceramide synthesis beside the ER derived mitochondria associated membranes (MAM)

which contain specific enzymes for lipid synthesis. Mitochondria can also synthesize phosphatidylethanolamine (mt PtdEtn), phosphatic acid (PA) and phosphatidylglycerol (PtdGro) which is used for cardiolipin (CL) synthesis. The major sphingolipids in mammalian cells are sphingomyelin (SM) and the glycosphingolipids (GSLs), containing mono-, di- or oligosaccharides linked to glucosylceramide (GlcCer) and galactosylceramide (GalCer).
Figure 1-13 depicts how sphingomyelins, ceramides, sphingosines and sphingosine-1-phosphate regulate the actin cytoskeleton, the cell cycle, apoptosis, endocytosis and other processes. The sphingolipid ceramide is implicated in the regulation of apoptosis and senescence. Sphingosine-1-phosphate (SIP) is crucial for cell survival, cell migration and inflammation (Smith et al., 2000, Obeid et al., 1993, Venable et al., 1995, Hla et al., 2004). Interestingly, protein phosphatase 1 (PP1) and PP2A belong to the family of ceramide-activated serine-threonine phosphatases (CAPPs), indicating protein-ceramide interactions (Chalfant et al., 2004).

1.6.1.1 The sphingolipid ceramide and Bcl-2 family proteins

Ceramide channels are formed by self-assembly and generate pore sizes of 6-10 nm which are capable to pass proteins (Siskind et al., 2005). Ceramide-induced mitochondrial permeabilization of isolated mitochondria from rat liver and yeast were inhibited by expression of Bcl-xL and CED-9. Siskind et al. (2008) showed that ceramide channels were not assembled by Bcl-xL in a defined system of solvent-free planar phospholipid membranes. However N-terminally truncated forms of Bcl-xL failed to disassemble ceramide channels. At present, a publication from Siskind et al. (2010) indicates a second function for Bak in long chain ceramide synthesis in different cell types during the induction of apoptosis. The function is described independent of MOMP and caspase activation. Bax/Bak double knock-out cells (DKO) show no increase of long chain ceramide synthesis and blocking of long chain ceramide synthesis inhibits caspase activation and cell death. They define a model of a Bak mediated increase in ceramides that supports MOMP induction via mitochondrial fragmentation, pore formation and the release of cytochrome c. These processes, which are under control of the Bcl-2 family proteins, may act in parallel or successively after each other.

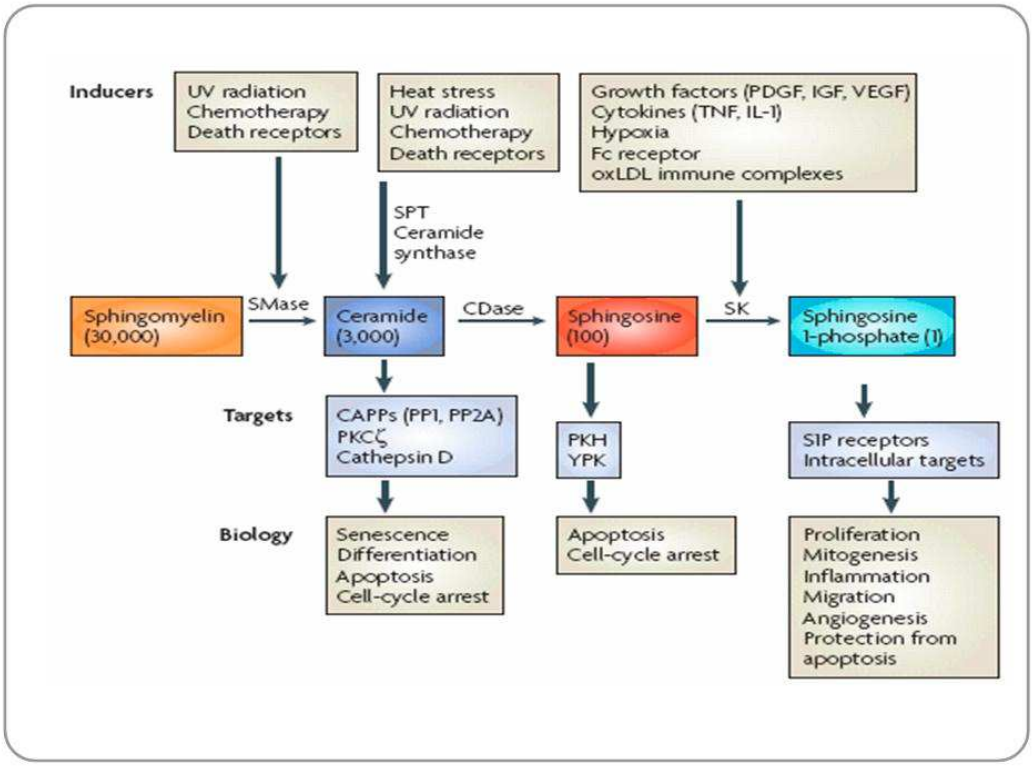

Figure 1-13: Overview scheme of sphingolipids in biology. Ceramide, sphingosine and sphingosine-1-phosphate (S1P) in cell biological responses. Ceramide is also generated by the breakdown of sphingomyelin by sphingomyelinases (SMases) or synthesized de novo by serine palmitoyl transferase (SPT) and ceramide synthase. Both processes can be induced by diverse stimuli (upper boxes). Sphingosine and S1P can be generated by ceramidases (CDases) and sphingosine kinases (SKs). These interconnected metabolites interact with specific proteins such as phosphatases, kinases and G protein-coupled receptors (S1P receptors), which in turn mediate the effects of these lipids and, at least in part, also mediate the effects of the inducers on specific cell responses. The numbers in brackets indicate the relative levels of these sphingolipids. CAPP, ceramide-activated Ser–Thr phosphatase; IGF; insulin-like growth factor; IL-1, interleukin-1; oxLDL, oxidized low-density lipoprotein; PDGF; platelet-derived growth factor; PKC, protein kinase C; PKH, PKB homologue; TNFa, tumour necrosis factor-a; VEGF, vascular endothelial growth factor; YPK, yeast protein kinase. (Adapted from Hannun Y, 2008)

1.7 B-cell lymphoma 2 (Bcl-2): an anti-apoptotic protein

The bcl-2 gene was first identified by Yoshide Tsujimoto (1986) when looking for chromosomal translocations in follicular lymphoma. Systematically, several genes were found at the breakpoints these translocations, called ‘Bcl-1’, ‘Bcl-2’, ‘Bcl-3’, etc. for B-cell leukaemia/lymphoma gene number 1, 2, 3, and so on.

The high expression rate of Bcl-2 in follicular lymphoma associated with the t (14:18) translocation lead them conclude that Bcl-2 might be an oncogene. Similar associations were found with Abl, which is involved in the t(9:22) translocation that generates the Philadelphia chromosome in chronic myeloid leukaemia, or c-myc, which is involved in the t(8:14) translocations of Burkitt’s lymphoma. Vaux et al. (1988) showed that lymphoid and myeloid cells transfected with Bcl-2 did not show enhanced proliferation, but enhanced survival after IL-3 withdrawal. They concluded that Bcl-2 might be an oncogene that is not affecting the cell cycle, but the apoptotic machinery. That this effect could lead to cancer formation was later shown with bone marrow cells infected with Eμ-myc and Bcl-2. This combination triggered the enhanced growth of colonies in soft agar and lymphoma formation in mice after cell transfer.

1.7.1 The biological role of endogenous Bcl-2

Bcl-2 is found in the nucleus/nuclear membrane fraction, on membranes of the intracellular network of the endoplasmatic reticulum (ER), on the mitochondrial outer membrane (MOM) and on the mitochondria associated membranes (MAM) which are connected to the ER. Bcl-2 protects cells from apoptosis by sequestering and inhibiting the action of BH3-only proteins. Bcl-2 knockout cells show an increased sensitivity against stress-induced apoptosis. In newborn mammals Bcl-2 is expressed in all tissues, in the adult phase only at high levels in thymus, spleen and kidneys, in liver, heart and brain at low levels (Negrini et al., 1987). Bcl-2 deficient mice are born, but develop growth retardation and greying and exhibit 100% mortality by 4-8 weeks through the development of polycystic kidney disease. Lymphoid and myeloid differentiation is initially normal but spleen and thymus undergo a massive involution. Mice develop grey hair with the second hair follicle cycle, implicating a defect in redox-regulated melanin synthesis. The abnormalities in these loss in function mice point out that Bcl-2 is a death repressor molecule functioning in a common antioxidant pathway. It acts after the generation of superoxide (ROS) and peroxides to prevent cellular damage including lipid peroxidation and DNA degradation (Hockenbery et al., 1993, Veis et al., 1993).

1.7.1.1 Sequence and structure of Bcl-2

After transcription, two alternatively spliced forms of Bcl-2 can be generated known as Bcl-2α or Bcl-2β, which only differ in their carboxyl termini. Bcl-2α is membrane bound and Bcl-2β is cytosolic. The mouse Bcl-2 (mBcl-2) gene consists of two exons separated by a sequence of 15 kb. Two species of mRNA produce two isoforms of different length. The 7.5 kb transcript codes for a protein of 236 amino acids (mBcl-2α, 26.47 kDa) and the 2.4 kb transcript codes for a protein of 199 amino acids (mBcl-2β, 22.25 kDa). The mouse 2.4 kb transcript is homologous to the human 3.5 kb transcript (hBcl-2β, 22.9 kDa) coding for a protein of 205 aa. The mouse 7.5 kb transcript is homologous to the 8.0 kb and the 6.0 kb splice variant of human Bcl-2α with 26.8 kDa coding for a protein of 239 aa. Sequence alignments of Bcl-2, Bcl-xL and the homolog from Kaposi sarcoma-associated herpes virus (v-Bcl-2-KSHV) reveal homolog sequences containing four Bcl-2 homology domains, BH1, BH2, BH3 and BH4 (Fig. 1-14)

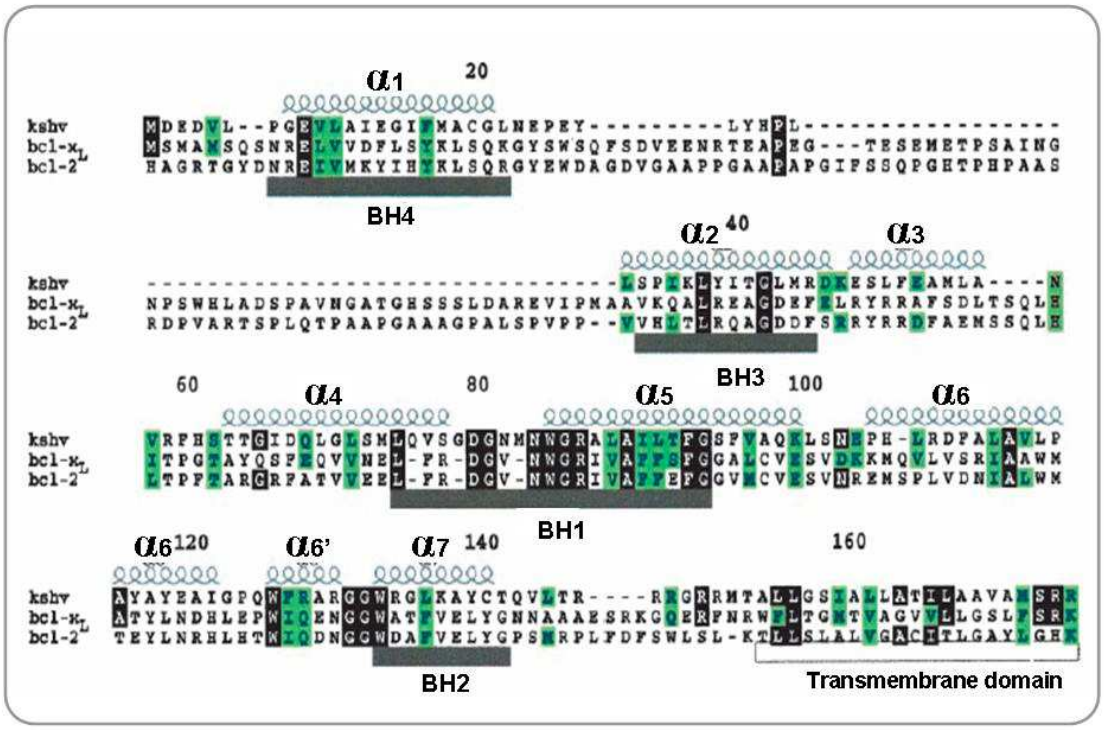

Figure 1-14: Sequence alignments of KSHV Bcl-2, hBcl-xL and hBcl-2. Alignments were done based on the observed secondary structure. α-helices are shown above and the BH 1-4 domain regions are shown below the sequence. The transmembrane domain (TM) is indicated below the sequence. (Adapted from Huang et al., 2002).

The solution structure of Bcl-2 displays three Bcl-2 homology domains (BH1, BH2 and BH3) that fold up a hydrophobic pocket shown in figure 1-15 and 1-16. These three domains create one of the anti-apoptotic regions of survival proteins which were investigated using

mutant forms of the BH1 and BH2 domain (Yin et al., 1994) but no other domains (Cheng EHY, 1997). The second area with an anti-apoptotic function is the BH4 domain at the N-terminal end. This domain represents the amphiphatic α-helix 1 that is partially exposed to the outer surface of the protein. The inner surface of the helix forms hydrophobic interactions with the helices α2, α5 and α6 thereby stabilizing the hydrophobic pocket from the backside (Muchmore et al., 1996). The structural stabilization of this pocket by the BH4 domain (α-helix 1; Fig. 1-15) from the backside determines the inability of Bcl-2 to form homodimers (Conus et al., 2000).

At D-34 and A-35 Bcl-2 can be cleaved by caspase-3. This converts it into a pro-apoptotic protein indicating that endogenous Bcl-2 may contribute to an amplification of cell death downstream of caspases. Mutations within the Bcl-2 homology domains exert the anti-apoptotic function suggesting that the hydrophobic pocket is one of the functional parts of Bcl-2 and related family members (Huang et al., 2002, Petros et al., 2001).

The three dimensional structure of Bcl-2 has been solved by nuclear magnetic resonance (NMR) spectroscopy. At the N-terminal end Bcl-2 contains a long flexible unstructured loop between a-helix 1 and a-helix 2 that increases its solubility. Therefore Bcl-2/Bcl-xL chimeras were created to reveal the structure of Bcl-2. In the center of Bcl-2 the hydrophobic helices α5 and α6 are packed against four amphiphatic helices (Fig. 1-15). The α-helix 1 (residues 11-24) is connected to α-helix 2 (residues 93-108) via the chimeric shortened loop from Bcl-xL (because of the solubility of natural Bcl-2). A long loop containing α-helix 3 (residues 111-119) connects α-helix 2 to α-helix 4 (residues 127-136). Helix 4, helix 5 (residues 144-163) and α-helix 6 (residues 167-192) are orientated in nearly antiparallel fashion with a kink at histidine 184, and an irregular turn connects α-helix 6 with α-helix 7 (residues 195-202). The C-terminal transmembrane domain (α-helix 9) is not expressed because of the difficulties to extract synthesized proteins from bacterial membranes. The BH4 domain encompasses α-helix 1, the BH3 domain α-helix 2, the BH1 domain is partially overlapping α-helix 4 and 5 and the BH2 domain α-helix 6/7 (Fig. 1-15, 1-16).

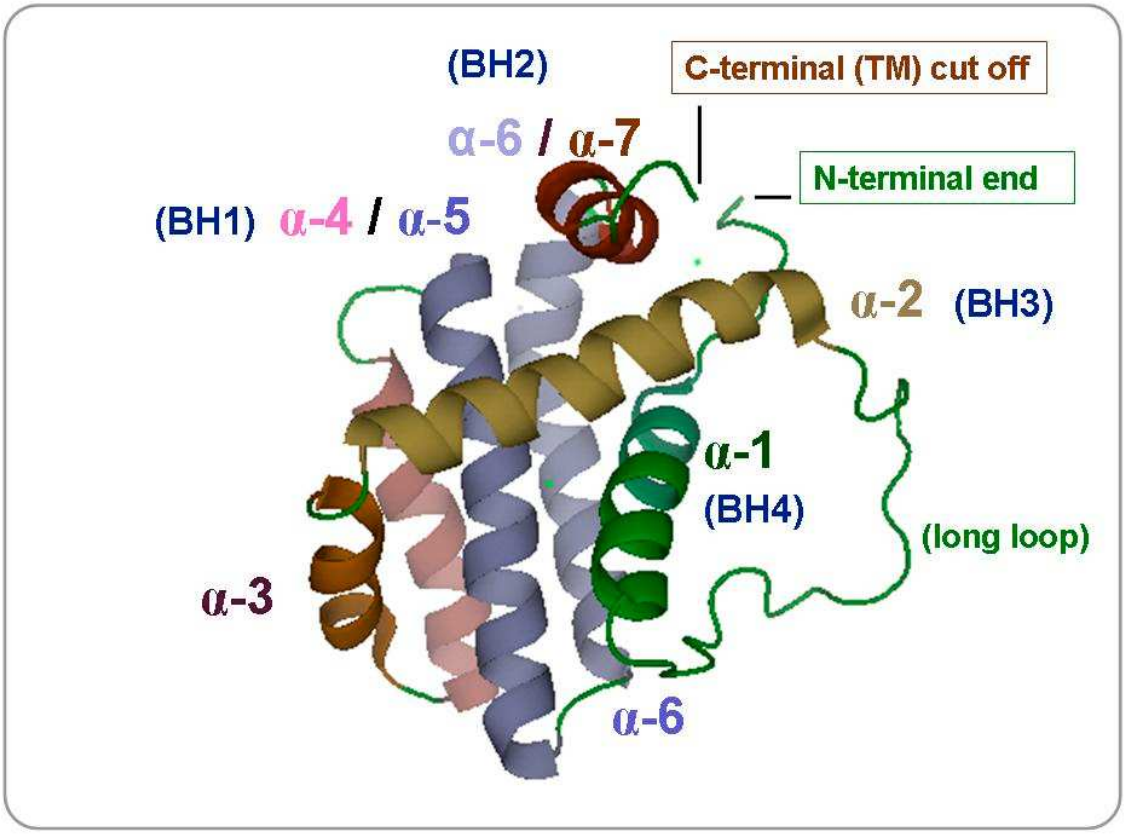

Figure 1-15: NMR 3D structure from Bcl-2. Alpha helices and BH domains are depicted. The hydrophobic pocket is folded up by BH1, BH2 and BH3. (Adapted and modified from PDB, 1YSW)

1.7.1.2 The structure determines the function of anti-apoptotic Bcl-2

Bcl-2 is the founding member of the Bcl-2 family, seven of which, Bcl-2, Bcl-xL, Bcl-w, Mcl-1, BAX, Bak and Bid are characterized by their conserved regions of sequence homology and three-dimensional structural similarities. Three of them, Bax, Bak and Bid, have pro-apoptotic functional activities, because of the missing BH4 domain and the increased flexibility of the BH3 domain. Bcl-2, Bcl-xL and Bcl-w have a similar 3-D structure but they have an anti-apoptotic function. The BH4 domain of Bcl-2 is also described to regulate its pro-survival activity. BH4 deletion mutants of Bcl-2 and Bcl-xL are not able to interact with co-expressed CED4, and further incapable to antagonize the pro-apoptotic function of CED4-CED3 (Yin et al., 1994, Chinnaiyan et al., 1997, Huang et al., 1998). The karposi sarcoma-associated herpes virus (Fig. 1-16) expresses a protein which mimics both sequence and functional homology of human Bcl-2 with decreased homology in the BH4 and BH3 domains. It is believed that the "NWGR" sequence within the BH1 domain is crucial for the anti-apoptotic function and heterodimerization with further Bcl-2 homologues, because KSHV Bcl-2 does not heterodimerize with Bax and Bak (Yin et al., 1994, Cheng et al., 1997).

More recent data from Rong et al. (2009) demonstrate evidence that the BH4 domain acts also as a ligand for the IP3 receptor, inhibiting IP3-dependent Ca^{2+} release from the ER, and Ca^{2+} -mediated apoptosis. Overexpressed Bcl-2 and Bcl-xL is further able to form ion channels on artificial membranes. It was proposed that the hydrophobic α5/α6 helices insert into the membrane, comparable to pores created by Bax and/or Bak (Schendel et al., 1998). But it seems to be unlikely that these pores are sufficient to release cytochrome c because of the non-physiological pH 4.0 during the experiment. Bacterial pore forming toxins (colicin, diphtheria) exhibit similar 3D structures compared to Bcl-xL or Bcl-2 that possibly mimic a part of their function (Muchmore et al., 1996).

The crystal structure of Bcl-2 has never been solved, because of the above described solubilization properties. Instead of that, a chimeric protein consisting of the N-terminal part from Bcl-xL and the rest from Bcl-2 was crystallized to obtain the 3D structure of "Bcl-2" (Figure 1-15; Figure 1-16). The three dimensional interface of the hydrophobic pocket of Bcl-2 which supports the pro-survival activity is seen in better detail by adding ABT-737, a BH3-mimetic of Bad (see below) (Fig. 1-16).

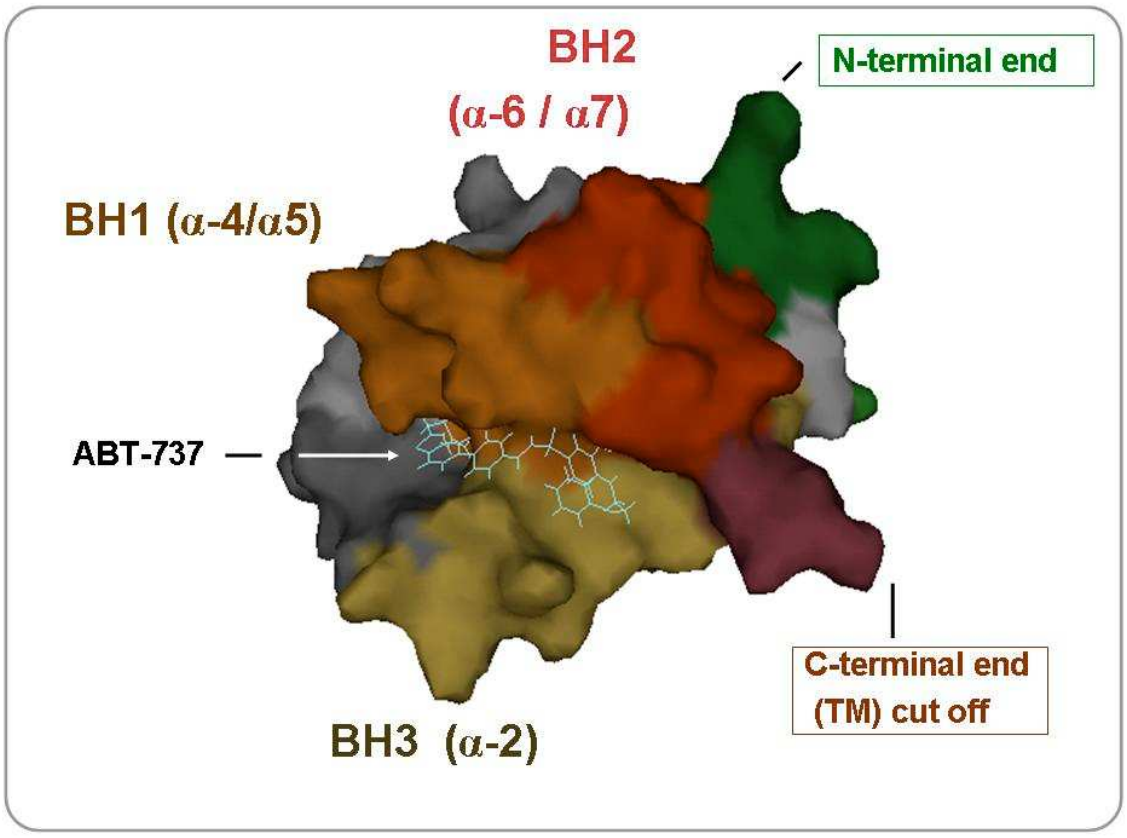

Figure 1-16: Three dimensional structure of Bcl-2. Electron surface density of the 3 dimensional structure of Bcl-2 obtained by NMR, **BH1** domain (Orange area, α4/α5 helices), **BH2** domain (grey area, α6/α7 helices) and **BH3** domain (ochre area, α 2 helix), **N**-terminal end. (green area), **C**-terminal end (light blue area), and the transmembrane domain α 9 helix cut. The hydrophobic pocket is folded up by BH1, BH2 and BH3. The core interface is visualized by the ABT-737 peptide which mimics the binding of a BH3-only protein. (Adapted and modified from PDB, 1YSW)

1.7.1.3 Properties of detergents and protein-lipid complexes

It has been shown that non-ionic detergents such as Triton X-100 and NP-40 can change the conformation of Bcl-2 proteins, in particular Bax and Bak (Antonsson, 2001, Hsu *et al.*, 1997b, Yin et al., 1994, Suzuki et al., 2000). Through this change Bax and Bak exposed their BH3-domain and are able to interact with Bcl-2-like survival factors in an artificial way. This is also how Bax and Bak were initially identified, as Bcl-2 binding partners in anti-Bcl-2 immunoprecipitations using Triton X-100 as solubilizing agent. To isolate and identify novel Bcl-2 binding partners it is therefore critical to use ionic detergents such as CHAPS, a sulfobetaine-type zwitterionic detergent, which does not provoke conformational changes in Bcl-2-like proteins. However, data from Valentijn et al. (2008) show that the properties of native Bax complexes may be perturbed by CHAPS. We therefore decided to use digitonin because this detergent has been successfully used by Schägger et al. (2000) to isolate the mitochondrial respiratory complexes in their native form. Membranes solubilized by digitonin are more or less cutted in big pieces thereby supporting the integrity of the extracted membrane-protein-lipid complexes.

1.8 Bcl-2 and its binding partners

1.8.1 Post-translational modifications that control the structure and binding of Bcl-2

Bcl-2 is shown to be phosphorylated on residues within an unstructured loop in response to diverse stimuli like chemotherapeutics, cytokine deprivation and protein kinase C (PKC) activation (Haldar et al, 1998; Ling et al, 1998; Scatena et al, 1998, May et al, 1994; Poommipanit et al, 1999, Ruvolo et al, 1998). Phosphorylation of Bcl-2 has been associated with its inactivation (Chang et al, 1997; Haldar et al, 1998; Srivastava et al, 1999; Yamamoto et al, 1999). Contradictory results where reported that reduce the activity of Bcl-2 to bryostatin-1 (May et al, 1994).

Bcl-2 was reported to be transcriptionally induced by cytokines (Akbar *et al.*, 1996; Gombert *et al.*, 1996) and age dependent reduction of Bcl-2 expression in T cells (Tamura et al., 1995). Transcription of Bcl-2 is repressed by phosphorylation with apoptosis signal-regulating kinase 1/Jun N-terminal kinase 1 (ASK1/JNK1) and mitogen-activated protein kinase /extracellular signal-regulated kinase (MAPK/ERK). Dephosphorylation of Bcl-2 by phosphatase 2 A (PP2A) (Haldar et al., 1994; Chen and Faller, 1996; Guan et al., 1996; Yamamoto et al., 1999; Tamura et al., 2004).

But Bcl-2 is also found to regulate the cell cycle by delaying the entry into S-phase (Borner, 1996; Chattopadhyay *et al.*, 2001; Huang *et al.*, 1997). In Jurkat cells, Bcl-2 is

phosphorylated at G_2/M (Yamamoto et al, 1999). Phosphorylated Bcl-2 was also found at the ER to reduce the calcium concentration within the ER and to protect against Ca^{2+} -dependent death stimuli. Furthermore, phosphorylation of Bcl-2 is indicated to regulate the binding ability of BH3-only proteins Bim, Bid and Bax. Additional to the described kinases above there are further reports that indicate binding of Raf-1, R-Ras, PKA and PKCα to Bcl-2 (Bassik et al., 2004, Reed, 2006). Paclitaxel treatment inhibits microtubule dynamics and phosphorylates thereby Bcl-2. One publication from Brichese et al. (2002) claims a phosphorylation dependent inhibition of the degradation by the proteasome-dependent pathway, and a second report claims the opposite (Chadebech et al. 1999). In summary, it is not really clear if Bcl-2 phosphorylation is an important process for apoptosis regulation.

1.8.2 Reported binding partners of Bcl-2

Bak, Bax, Bad, Bid and Bik were all described to interact with full length Bcl-2 in co-IPs when they were co-expressed with Bcl-2 as EE-tagged proteins in cells and the extracts prepared with NP-40 (Huang et al., 1998). Recent experimental data from Bcl-2 family proteins expressed by *in vitro* transcription/translation experiments of reticulocyte lysate show also interactions between Bcl-2, Puma, tBid and $Bim_{L.}$ However, the protein interactions were also solubilized with Triton X-100 or NP-40 (Kim et al., 2006). The artificially induced interactions with Bcl-2 family proteins were shown by repeated experiments expressing Bcl-2 family members.

In general: All BH3-only proteins in apoptotic cells or BH3-peptides are able to interact with Bcl-2 when their BH3-only domains are exposed (Bad, Bid, Bik, Bim). These interactions were also found in yeast-two-hybrid experiments.

The endogenous protein-protein interactions on the other side are hardly to detect in healthy cells. Most of the protein interactions were found after induction of apoptosis or in cancer cells.

Bcl-2 (B-cell CLL/lymphoma 2):

In several reports, Bcl-2 was described to homodimerize (Sedlak et al., 1995, Huang et al., 1998, Zhang et al., 2004). In contrast, results from Conus et al. (2000) indicate that Bcl-2 is a monomeric protein. A contradictory publication claims the existence of Bcl-2 homodimers by the usage of a site specific photocross-linker, postulating acceptor- and donor surfaces to explain the formation of homo- and hetero-oligomers (Zhang et al., 2004).

Bak (Bcl-2 antagonist killer):

Bak consists of 211 amino acids with a molecular size of 28 kDa and exerts its pro-apoptotic function in presence with tBid which is important for pore formation and cytochrome c release (Wei et al., 2000, Ruffolo et al., 2000, 2003). Ectopic expressed Bak was shown to interact with EE-tagged Bcl-2, Bcl-xL, Mcl-1 and A1 in immunoprecipitations and yeast-two hybrid experiments using NP-40 as detergent (Sedlak et al., 1995, Huang et al., 1998). In contrast, endogenous Bak is shown to interact with Flag-tagged survival proteins Mcl-1 and Bcl-xL in lysates of healthy cells solubilized with CHAPS, but Bak does not bind to Bcl-2, Bcl-w and A1 (Willis, et al., 2005). Immunoprecipitations of Bcl-xL and Bcl-2 are described to interact with Bak under healthy conditions and less Bak remained bound to Bcl-xL and Bcl-2 when apoptosis is induced (Ekert et al., 2006). However, the bulk of Bak does not co-IP with Bcl-2, Bcl-xL or Mcl-1 (see Ekert et al., 2006) even under CHAPS conditions, indicating that the major cellular inhibitor of Bak is probably not Bcl-2 or its related proteins, but VDAC-2 (Cheng et al., 2003).

Bax (Bcl-2 associated X protein):

Bax resides inactive in the cytosol by folding its C-terminal mitochondrial targeting and insertion domain into the hydrophobic binding pocket. This prevents Bax from exposing its BH3-domain and interacting with anti-apoptotic Bcl-2 family proteins. In addition Bcl-2 is rarely found in the cytosol so that Bcl-2 cannot be a binding partner and inhibitor of Bax in healthy cells. In response to apoptotic stimuli, Bax unfolds and translocates to mitochondria via the released C-terminal targeting sequence. There it inserts into the MOM and oligomerizes with itself or with Bak. In the active state, Bax has its BH3-domain exposed and can bind and heterodimerize with Bcl-2. It is thought that the homology domains BH1 and BH2 of Bcl-2 are required for heterodimerization and inhibition of apoptosis, thus Bax is likely to bind to Bcl-2 via the hydrophobic pocket (Yin et al., 1994). Bax was also found to interact with Bcl-2 by co-immunoprecipitation of overexpressed HA-tagged Bax and hBcl-2 (Oltvai et al., 1993, Otter et al., 1998) but again this experiment was performed in Triton X-100.

Beclin1:

Beclin1 the mammalian ortholog of yeast autophagy related gene 6 product (Atg6) belongs to a class III phophoinositide 3-kinase (PI3K) complex which takes part in the very early stages of vesicle development in the autophagosomal pathway. It was first found in yeast-two hybrid screens as a Bcl-2 interacting protein (Liang et al., 1998). Mice exhibiting a heterozygous disruption of Beclin1 show a high incidence to develop spontaneous tumors. Decreased levels are found in human breast carcinoma and prostate cancer. Its expression reduces proliferation and tumor genesis in breast carcinoma (Liang et al., 1999, 2001).

Potential anti-apoptotic effects of Beclin1 are, (i) the disruption of Sindbis virus replication, (ii) the inhibition of apoptosis of the infected neurons, and (iii) the expression levels increase upon head trauma (Diskin et al., 2005, Ehrlich et al., 2005). The interaction of Beclin1 with anti-apoptotic proteins Bcl-2, Bcl-xL, Bcl-w and Mcl-1 was inhibited by co-expression of tBid and Bad but not Bax and Bak. Therefore Beclin1 was suggested to be a BH3-only protein. Also, Beclin1 is required for embryonic development in the nematode C. elegans and its deletion results in CED-3 dependent apoptosis which is inhibited by CED-9 (Takacs-Vellai et al., 2005).

Cell growth under nutrient-rich media conditions inhibit autophagy by binding of endogenous Beclin1 to endogenous Bcl-2 and loss of nutrients or conditions of starvation reduce the binding of Beclin1 to Bcl-2, suggesting that the differential binding reflects a physiological mechanism to regulate the induction of autophagy in response of starvation described by Pattingre et al. (2006). Nevertheless the binding of endogenous Beclin1 to endogenous Bcl-2 found from Pattingre is the only physiological interaction described.

VDAC1 (voltage dependent anion channel 1):

VDAC1 is one of the three isoforms found (VDAC1, VDAC2, VDAC3), a β-barrel protein composted of 16 β-barrel strands in the size of 30-35 kDa predominantly found in the MOM. The interaction of the adenine nucleotide translocator (ANT) with VDAC1 changes the structure of the voltage dependent anion channel in artificial or physiologically systems. It is proposed, that the VDAC's are components of the permeabilization transition pore (PTP) acting as a non-selective channel (3nm) to release cytochrome c (Vyssokikh et al., 2002, 2003, 2004, Zalk et al., 2005). VDAC1 was shown to bind to Bcl-2 (Shimizu et al., 1999). A publication from Pavlov et al. (2001) suggested that VDAC is not involved in the Bax-induced pore formation in yeast deficient in VDAC (Shimizu et al., 1999, Baker et al., 2004). As mentioned before in chapter 1.5.1.1 VDAC's seem not to be involved apoptosis signaling (Baines et al., 2007).

G_0-G_1 switch protein (G0S2):

TNF-α induced activation of NF-kB is known to support pro- and antiapoptotic functions. A recent investigation used high-density cDNA micro arrays of TNF-α treated and non-treated human primary foreskin fibroblasts to find new upregulated proteins (Welch et al., 2009). One of the unknown proteins identified was G0G2. Co-localization and co-immunoprecipitation of overexpressed G0G2 with Bcl-2 in H1299 cells was shown indicating binding of Bcl-2 with G0G2. Further, they claim a G0G2 dependent induction of apoptosis by preventing the Bcl-2-Bax heterodimerization in HeLa cells. G0G2 is epigenetically silenced in human cancer cell lines which might indicate that G0G2 is a tumor suppressor gene. Overexpression of G0G2

and treatment with TNF-α in presence or absence of camptothecin (DNA damage), sensitizes primary foreskin fibroblasts to undergo apoptosis. The inhibition or induction of apoptosis by NF-kB depends on the cell type and the amount of activated NF-kB. The mitochondrial and cytosolic fraction were prepared after generating whole cell lysates of TNF-α treated human primary foreskin fibroblasts (PFF), which is quite unusual.

FKBP38:

FKBP38 is a member of the FK506-binding protein immunophilin family proteins. It consists of a peptidylprolyl cis-trans isomerase (PPIase) domain to assist protein folding and serves as a scaffold protein to support protein-protein interactions. It contains also a tripartite tetratricopeptide repeat (TTR) domain, and a calcium calmodulin-binding motif (CaM). FKBP38 is localized on the outer mitochondrial membrane and the endoplasmatic reticulum (ER). It was shown that FKBP38 interacts with the flexible loop of Bcl-2 which supports the possibility that FKBP38 is able to modify the cleavage of Bcl-2 to favour cell survival (Kang et al., 2005). Results from Choi et al. (2010) indicate a stabilization of Bcl-2 by post-translational modifications. Binding of FKBP38 to Bcl-2 blocks caspase mediated cleavage, which leads to an accumulation of Bcl-2 and a potential chemoresistance of cancer cells overexpressing Bcl-2.

Ku70:

Wang et al. (2008) describes that Bcl-2 exhibits an additional function to block non-homologous end-joining (NHEJ). DNA repair by NHEJ involves a core complex of Ku70/Ku80, DNA-PK_{CS}, Cermunnos/XLF and the DNA ligase IV/Xrcc4 complex, which coordinate the rejoining of the broken DNA ends. The ATP-dependent DNA helicase 2 subunit 1 a Ku70 complex component and Ku86 are shown to interact in an increased manner with Bcl-2 in nuclear fractions after ionization radiation (IR). The physiological relevance could be explained by a specific expression pattern of Bcl-2 during B cell development. Pro-B cells express high levels of Bcl-2, but during V (D)J rearrangements Bcl-2 expression disappears until the B cell mature. Bcl-2 was also shown to block mismatch repair indicating a further role in modulating DNA repair (Hou et al., 2007).

IP3 receptor (inositol 1,4,5 triphosphate receptor):

The inositol-1,4,5-trisphosphate receptor is a multi-pass membrane protein located on the endoplasmatic reticulum (ER) in the size of 304.27 kDa protein that contains 2670 amino acids. The IP3-receptor is an IP3-gated calcium channel by regulating calcium release processes like cell proliferation and cell death. Fragments of the IP3-receptor are reported to interact with endogenous Bcl-2 specifically with the BH4 domain in lysates of the T cell line

S49.A2. Rong et al. (2008, 2009) shows by overexpressing of full length Bcl-2 and Bcl-2 deficient in the BH4 domain that GST-IP3-receptor peptides interact only with the non-truncated form of Bcl-2.

Mitofusin 2 (Mfn2):

As described in chapter 1.8.1.1 mitofusins are large GTPases of the outer mitochondrial membrane. CED-9, Bcl-2 and Bcl-xL were shown directly to interact with Mfn2 but not with Mfn1 by co-immunoprecipitation (Delivani et al. 2006).

1.8.3 Endogenous protein-protein interactions with Bcl-2

Endogenous protein-protein interactions of physiological expressed Bcl-2 and further endogenous binding proteins were shown between Beclin1 and Bcl-2 from Pattingre et al. (2006). Until now there are no other proteins known that bind to Bcl-2 under "physiological", endogenous conditions.

1.9 Goal and concept

Bcl-2 is localized on nuclear membranes that are connected with the intracellular network of the endoplasmatic reticulum (ER), mitochondria associated membranes (MAM) and the mitochondrial outer membrane. Bcl-2 is anchored with its C-terminal transmembrane domain to membranes so that the functional part faces the cytosol. In concert with survival proteins like Bcl-xL, Bcl-w, Mcl-1 and A1, it sequestrates activated BH3-only proteins, thereby antagonizing the activation of Bax and Bak to prevent mitochondrial outer membrane permeabilization (MOMP). The physiologic function and the mechanism how Bcl-2 transmits the function of BH3-only proteins to Bax and Bak under apoptotic conditions is still a matter of debate. Does Bcl-2 bind Bax/Bak and releases them upon binding pro-apoptotic BH3-only proteins, or does it initially bind an activator BH3-only protein and releases it in response to the binding of a sensitizer BH3-only protein? Or alternatively, does endogenous Bcl-2 bind yet other unknown proteins, which upon release by BH3-only proteins act as Bax/Bak activators?
The problem with the lack of knowledge of endogenous Bcl-2 regulation is that most of the previous were either performed on tumor cells, by in vitro binding (pull-downs or recombinant proteins) or on cells overexpressing Bcl-2 and its partners. The present study therefore focused on endogenous interactions between Bcl-2 family proteins and unknown proteins. Monocytes dependent on IL-3 die by withdrawal of cytokines via the mitochondrial death signaling pathway. This represents a physiological relevant apoptosis system to detect endogenous protein-protein interactions.

The goal of this work was to isolate and identify endogenous binding proteins of Bcl-2 in mitochondrial enriched fractions of sedimented heavy membranes (HM). Therefore, different approaches were envisaged: (i) to analyse the endogenous distributed Bcl-2 family proteins in fractions of cytosol, HM, ER and separation of natural Bcl-2 complexes by blue native PAGE to find candidates that possibly interact with Bcl-2, (II) examination of specific Bcl-2 binding proteins that were reported and identified by co-expression or yeast-two hybrid experiments, and (iii) isolation and identification of new binding proteins bound to Bcl-2 under endogenous conditions.
Therefore two fractions of Bcl-2 co-immunoprecipitations were analysed by mass spectrometry: (i) co-immunoprecipitates of Bcl-2 were treated with a BH3-only mimetic (ABT-737) to release specifically bound proteins and (ii) co-immunoprecipitates of Bcl-2 were treated with physiological salt concentrations to obtain the whole set of bound proteins to Bcl-2.

2 Materials and Methods

2.1 Materials

Table 2-1: List of materials and chemicals for cell culture.

Materials/Chemicals	*Supplier*
Dulbecco's modified Eagle's medium	Invitrogen/PAA
FCS (fetal calf serum)	PAA, Austria
Hygromycin	PAA, Austria
Gentamycin (G418)	PAA, Austria
Interleukin-3 (IL-3)	Peprotec
Penicillin	Gibco, Invitrogen, Karlsruhe
Puromycin	Sigma-Aldrich GmbH, Taufkirchen
RPMI	PAA, Austria
Streptomycin	Gibco, Invitrogen, Karlsruhe
Flasks and dishes	TPP

2.1.1 Kits

Table 2-2: List of used kits.

DNAzol Reagent	Gibco, Invitrogen, Karlsruhe
ECL Super Signal kit	Perbio Science Deutschland GmbH, Bonn
High molecular weight standard kit for blue native	Amershan/GE Healthcare
Jet star plasmid Maxi prep	Genomed
Mycoplasma Detection Kit VenorGeM	Minerva Biolabs, Berlin
OptiMEM	PAA, Austria
Protein determination assay	Bio-Rad
QIAquick Gel Extraction kit	Qiagen, Hamburg
Silver Quest. Silver stain	Invitrogen
Wizard Plus SV plasmid Miniprep	Promega

2.1.2 Chemicals

Table 2-3: List of the used chemicals and solutions.

Chemicals	Supplier
ABT-737	Servier. Paris
Acetone-nitrile	Sigma-Aldrich GmbH, Taufkirchen
Acrylamide (30%)	AppliChem GmbH, Darmstadt
Ammonuim bicarbonate (NH_4HCO_3)	Sigma-Aldrich GmbH, Taufkirchen
Actinomycin D (ActD)	Alexis Deutschland GmbH, Grünberg
AEBSF	Roche Diagnostics
Agarose	Lonza GmbH, Wuppertal
Ammonium peroxide sulfate (APS)	Carl Roth GmbH & Co, Karlsruhe
Annexin-V-GFP	Produced in the lab
Aprotinin	Sigma-Aldrich GmbH, Taufkirchen
Bis-Tris	Carl Roth GmbH & Co, Karlsruhe
BenchMark Prestain Protein ladder	Gibco, Invitrogen, Karlsruhe
Blotting paper	Merck-VWR International GmbH, Darmstadt
Bromephenol blue	Merck- VWR International GmbH, Darmstadt
Bovine serum albumine (BSA) Fra V	Sigma-Aldrich GmbH, Taufenkirchen
Calcium chloride ($CaCl_2$)	Merck- VWR International GmbH, Darmstadt
Casein hydrolysate	Merck- VWR International GmbH, Darmstadt
CHAPS	Calbiochem, San Diego, USA
Chloroform	Baker, Griesheim
Collagen Type I	BD Biosciences, Heidelberg
Coomassie Blue G250	Carl Roth GmbH & Co, Karlsruhe
Coomassie Blue R250	Carl Roth GmbH & Co, Karlsruhe
Cycloheximide (CHX)	Calbiochem, San Diego, USA
Cypermethrin	Calbiochem, San Diego, USA
Cytochalasin B	Sigma-Aldrich GmbH, Taufenkirchen
Digitonin	Amershan/GE Healthcare
Dithiothreitol (DTT)	AppliChem GmbH, Darmstadt
Dimethyl sulfoxid DMSO	Sigma-Aldrich GmbH, Taufkirchen
DNA gene ruler 1 kb ladder	Fermentas GmbH, St. Leon-Rot
Ethylene diaminetetra acetic acid (EDTA)	Sigma-Aldrich GmbH, Taufkirchen
Ethylene glycol tetra acetic acid (EGTA)	Carl Roth GmbH & Co, Karlsruhe

Ethidium bromide	Merck- VWR International GmbH, Darmstadt
Etoposide	Sigma-Aldrich GmbH, Steinheim
FACS Clean	Becton Dickinson Biosciences, Heidelberg
FACS Flow	Becton Dickinson Biosciences, Heidelberg
FACS Rinse	Becton Dickinson Biosciences, Heidelberg
Gelatine	Sigma-Aldrich GmbH, Taufenkirchen
Glycerol	Amershan/GE Healthcare
Hoechst 33342	Sigma-Aldrich GmbH, Taufkirchen
Hyper film	Fuji film Deutschland, Düsseldorf
Iodacetamide	Sigma-Aldrich GmbH, Taufkirchen
Isotone II	Beckman Coulter, Krefeld
Leupeptin	Alexis Deutschland GmbH, Grünberg
Magnesium chloride ($MgCl_2$)	Merck-VWR International GmbH, Darmstadt
Methanol	Merck-VWR International GmbH, Darmstadt
Milk powder	Carl Roth GmbH & Co, Karlsruhe
Nitrocellulose membrane	Merck-VWR International GmbH, Darmstadt
MG132	Alexis Deutschland GmbH, Grünberg
NP40	Fermentas GmbH, St. Leon-Rot
Paraformaldehyde (PFA)	Sigma-Aldrich GmbH, Taufenkirchen
Penicillin	PAA Laboratories GmbH, Austria
Pepstatin	Sigma-Aldrich GmbH, Taufkirchen
Polymethylsulfonylfluoride (PMSF)	Sigma-Aldrich GmbH, Taufkirchen
Propidiumiodide	Sigma-Aldrich GmbH, Taufkirchen
Potassiumcloride (KCL)	Merck-VWR International GmbH, Darmstadt
Protein G Sepharose beads	Amershan/GE Healthcare
Sodium chloride (NaCl)	Merck-VWR International GmbH, Darmstadt
Sodium dododesyl sulfate (SDS)	Carl Roth GmbH & Co, Karlsruhe
Sodium-ortho-vanadate (Na_3VO_4)	Carl Roth GmbH & Co, Karlsruhe
Streptomycin	PAA Laboratories GmbH, Austria
Sucrose	Sigma-Aldrich GmbH, Taufkirchen
SuperFect	Invitrogen GmbH, Karlsruhe
Trichloroacetic acid (TCA)	Sigma-Aldrich GmbH, Taufkirchen
Tris-HCl	Sigma-Aldrich GmbH, Steinheim
Triton-X-100	Sigma-Aldrich GmbH, Taufkirchen
Trizol Reagent	Invitrogen, Carlsbad, CA
Trypan blue	Sigma-Aldrich GmbH, Taufkirchen
Trypsin	PAA Laboratories GmbH, Pasching

Tunicamycin	Alexis Deutschland GmbH, Grünberg
Tween-20	Merck-VWR International GmbH, Darmstadt

2.1.3 Buffers and reagents

Table 2-4: List of used buffers

Phosphate buffered saline (PBS) (pH 7.4):	0.5 mM Potassium dihydrogen phosphate 135 mM Sodium chloride 3.2 mM Disodium hydrogen phosphate 1.3 mM Potassium chloride
Tris buffered saline tween-20 (TBST) (pH 7.4):	20 mM Tris-HCl, (pH 7.5) 150 mM Sodium chloride, 0.05% Tween-20
H8 buffer:	20 mM TRIS-HCl, pH 7.5, 2 mM EDTA, 2 mM EGTA, 50 mM DTT,
Isotonic homogenization buffer (MSH):	210 mM Sucrose, 70 mM Mannitol 10 mM HEPES, (pH 7.4), 1 mM EDTA
IBC Buffer (IBC):	200 mM Sucrose 10 mM Tris/MOPS (pH 7.4) 1 mM EGTA/Tris
5 x Laemmli buffer/100 ml:	30 ml 1 M Tris-HCl pH 6.8, 10 g SDS, 50 ml glycerol, 0.25 mg bromphenolblue, 250 mM DTT
SDS-PAGE reagents:	**Solution A**: 1.5 M Tris-HCl (pH 8.9), 8 mM EDTA **Solution B**: 0.5 M Tris-HCl (pH 6.8), 8 mM EDTA 30% (37.5:1) mix Acrylamide 4K (ready made; Applichem) 10% (v/v) TEMED, 1.5% (w/v) APS 10% (w/v) SDS
SDS-Electrophoresis buffer:	24.8 mM Tris 192 mM Glycine, 0.1% (w/v) SDS
Semi-dry transfer buffer:	25 mM Tris 190 mM Glycine, 20% (v/v) Methanol
4X Tris/HCL/SDS buffer:	1.5 M Tris-HCL (pH 8.9), 0.4 % SDS
3X Gel buffer:	150 mM BisTris-HCL 1.5 M 6-amino-caproic acid, pH 7.0
Blue native loading buffer:	100 mM Bis-Tris 500 mM 6-amino-n-caproic acid, (pH 7.0) 5% Coomassie Blue G250

2.1.4 Equipments

Table 2-5: List of the employed equipment.

Equipment	*Supplier*
Agarose gel chamber	Produced by the factory of the institute
Balance LP6200S	Sartorius, Göttingen
Blotting system	Semi Dry Transfer Cell, Biorad, München
Cell Counter Z1	Beckman Coulter, Krefeld
Centricons	Millipore, Schwalbach/Ts.
Confocal Microscope	Leica TCS SP2 AOBS
FACS Calibur™	Beckton Dickinson
Film developing machine Curix 60	AGFA-Geveart, Leverkusen
Fluorescence microscope Axiovert	Zeiss, Jena
Fridges	
-80 ℃	Thermo Forma, Marietta OH, USA
-20 ℃	Siemens, München
+ 4 ℃	Liebherr, Biberach a. d. Riß
Ice machine	Scotsman AF-10, Mailand
Incubators	Heraeus Instruments, Stuttgart
Hoefer Gel System	Hoefer
Laminar flow HB-2448K	Heraeus, Hanau
Light microscope (cell culture)	Nikon TMS, Düsseldorf
Liquid nitrogen tank	Messer Griesheim, Krefeld
Lumi Imager™ F1	Roche Diagnostics, Mannheim
Magnetic stirrer K-550 GE	Scientific Industries inc. Bohemia, New York
Microwave DMR-703	Mio-Star, Migros, Zürich
Nitrocellulose membrane	Merck-VWR International GmbH, Darmstadt
PCR machine	MI Research Biozym, Hess, Oldendorf
Photospectrometer (Vis/UV)	Beckman Coulter, Fullerton, California
Pipet boy Acu Classic	Integra Bioscience, Fernwald
Pipettes	Gilson, France and Eppendorf,
PVDF	Millipore GmbH, Schwalbach
Vortex Genie	Bender and Hobein, Zürich
Semi Dry Transfer Cell	Biorad, München
ScanR screening station	Olympus, Hamburg
SpectraMax Gemini XS reader	Molecular Devices, München
Spectra Max Spectrophotometer	Molecular Devices, München

Table top centrifuge	Eppendorf
Tecan Infinite 200	Tecan Group Ltd., Männedorf
Thermal cycler for PCR	MJ Research
Thermo mixer 5436	Eppendorf, Hamburg
Transilluminator	BioDoc Analyse, Biometra, Göttingen
Ultracentrifuge	Becton-Dickinson
Water bath	Produced by the factory of the institute

2.1.5 Materials for polyacryl gel electrophoresis (PAGE)

Table 2-6: List of the used chemicals and solutions for PAGE.

Equipment	*Supplier*
Acrylamide (30%)	Bio-Rad Laboratories Inc., California
Buffer A	Made by the Institute, see chapter 2.1.4
Buffer B	Made by the Institute, see chapter 2.1.4
Ammoniumpersulfate 1.5 % (APS)	Carl Roth GmbH & Co, Karlsruhe
N,N,N´,N´- Tetramethylendiamine (TEMED)	Sigma-Aldrich GmbH, Taufkirchen
Sodium dodecyl sulfate (SDS)	Carl Roth GmbH & Co, Karlsruhe

Table 2-7: List of the used chemicals and solutions for the gradient PAGE.

Equipment	*Supplier*
Acrylamide (30%)	Bio-Rad Laboratories Inc., California
4X Tris/HCL/SDS Buffer	Self-made stuff, see chapter 2.1.4
Sucrose	Sigma-Aldrich GmbH, Taufkirchen
Ammoniumpersulfate 10 % (APS)	Carl Roth GmbH & Co, Karlsruhe
N,N,N´,N´- Tetramethylendiamine (TEMED)	Sigma-Aldrich GmbH, Taufkirchen
Sodium dodecyl sulfate (SDS)	Carl Roth GmbH & Co, Karlsruhe

Table 2-8: List of the used chemicals and solutions for Blue Native PAGE.

Equipment	*Supplier*
Acrylamide (48.0 %)	Amershan,
Bis-tris-acrylamide (1.5 %)	Carl Roth GmbH & Co, Karlsruhe
3x Gel buffer	see chapter 2.1.4
Glycerol (75%)	Amersham/GE Healthcare
Ammoniumpersulfate 10 % (APS)	Carl Roth GmbH & Co, Karlsruhe
N,N,N´,N´- Tetramethylendiamine (TEMED)	Sigma-Aldrich GmbH, Taufkirchen

2.2 Molecular biological methods

2.2.1 Genotyping of mouse embryonal fibroblasts

2.2.1.1 Isolation of genomic DNA

Genomic DNA was obtained from mouse embryonic fibroblasts (MEFs) cultured on 100 mm culture plates. Adherent cells were washed once with 10 ml PBS and lysed in 1 ml of DNAzol reagent by gently agitating the culture plate. The lysate was than gently transferred into an eppendorf tube to sediment the homogenate for 10 min. at 10.000 x g at 4° or RT to minimize RNA carry-over into the DNA. The supernatant was transferred into a new eppendorf tube and 500 µl (100% ethanol) were added, to precipitate DNA from the lysate. After precipitation of DNA the remaining clear liquid was removed and the pellet was shortly washed with 75% ethanol by inverting the tube 4-6 times. After sedimentation DNA was solubilized with 8 mM NaOH, air dried and neutralized by adding of 0.1 M HEPES. DNA concentration was measured using a NanoDrop (Thermo scientific). The PCR results of wild type and IQGAP2 $^{-/-}$ alleles are shown in chapter 3.6.3.4 figure 3-28.

2.2.1.2 Polymerase chain reaction (PCR)

PCR technique was use to amplify genomic DNA. Specific wild type and IQGAP2 knock out primer pairs were combined to produce fragments of wt and IQGAP2 null alleles (Table 2-9, see also Schmidt VA, et al 2008).

Table 2-9: List of primer sequences and their final concentration in the PCR reaction.

IQGAP2 wild type Allele amplified	Primer sequence (5'-3')	Concentration
Forward primer **P3**	AAGGCATGATTCATTCACCTGAGA	20 pM
Reverse primer **P4**	AGGGCAGGAAAGGCACAGCACTT	20 pM
IQGAP2 null Allele amplified		
Forward primer **N2**	GTCAAGAAGGCGATAGAAGG	20 pM
Reverse primer **N3**	TTGAACAAGATGGATTGCACGCA	20 pM

Table 2-10: Amplified fragments for wild type and knock out alleles. The sizes of the amplified fragments are depicted in base pairs (bp) and results are shown in figure 3-28.

Primer combination	Amplified fragment	Fragment size
IQGAP-2: P3 + P4	Wild type	600 bp
IQGAP-2: N2 + N3	Knock out	750 bp

Table 2-11: PCR program for the described genotypes.

PCR program	**IQGAP-2**	
1. Denaturation	15 min.	94.0 ºC
2. Denaturation	1 min.	94.0 ºC
3. Annealing	2 min.	55.0 ºC
4. Elongation	3 min.	72.0 ºC
5. Cycles 2-4	35	35
6. Final elongation	10 min.	72.0 ºC

Table 2-12: PCR composition for wild type and IQGAP2 knock out primer pairs.
PCR reaction conditions had to be optimized for each genotype to obtain distinct wt and IQGAP2 knock out fragments.

PCR-contents	wild type allele: Primer: P3 + P4	IQGAP2 null allele: Primer: N2 + N3
Genomic DNA (0.35µg)	1.0 µl	1.0 µl
10X buffer (15 mM Mg^{2+})	5.0 µl	5.0 µl
dNTP (20 mM)	5.0 µl	5.0 µl
Hot Star DNA Polymerase (5U/µl)	0.5 µl	0.5 µl
Primers (20µM)	1.0 µl + 1.0 µl	1.0 µl + 1.0 µl
ddH_2O final 50 µl)	41.5 µl	41.5 µl
added (25 mM Mg^{2+}) final concentration (Mg^{2+})	2.0 µl 2.46 mM	4.0 µl 3.35 mM

2.2.1.3 Agarose gel electrophoresis

The amplified DNA was separated according to its size by agarose gel electrophoresis. To separate amplified fragments 1-2% concentrated agarose gels were casted. Gels were always freshly prepared before usage. The respective amount of agarose was weighted in 150 ml 1 x TAE buffer and subsequently cooked in a microwave in order to dissolve clumps. The agarose solution was cooled down to less than 60 ℃ before adding 4 µl ethidium bromides (EtBr, 10 mg/ml). After solidification of the agarose DNA samples were mixed with 6 x loading dye to final 1 x concentration and loaded onto the gel slots, together with 10 µl of a DNA marker (vivantis, EcoR1-Hind III) containing defined molecular weights. The gel underwent electrophoresis at 140 mV for 20-30 min. and the DNA bands were detected by a UV transilluminator.

50 x TAE buffer: 242 g Tris, pH 8.5, 57.1 ml glacial acetic acid, 37.2 g $Na_2EDTA \times 2\ H_2O$

2.2.1.4 Expression vectors

pGS5 large T antigen:

To transform 129J1 MEFs the pGS5 large T antigen plasmid was used to transfect wild type mouse embryonic fibroblasts and MEFs deficient in IQGAP2 (Fig. 2-13).

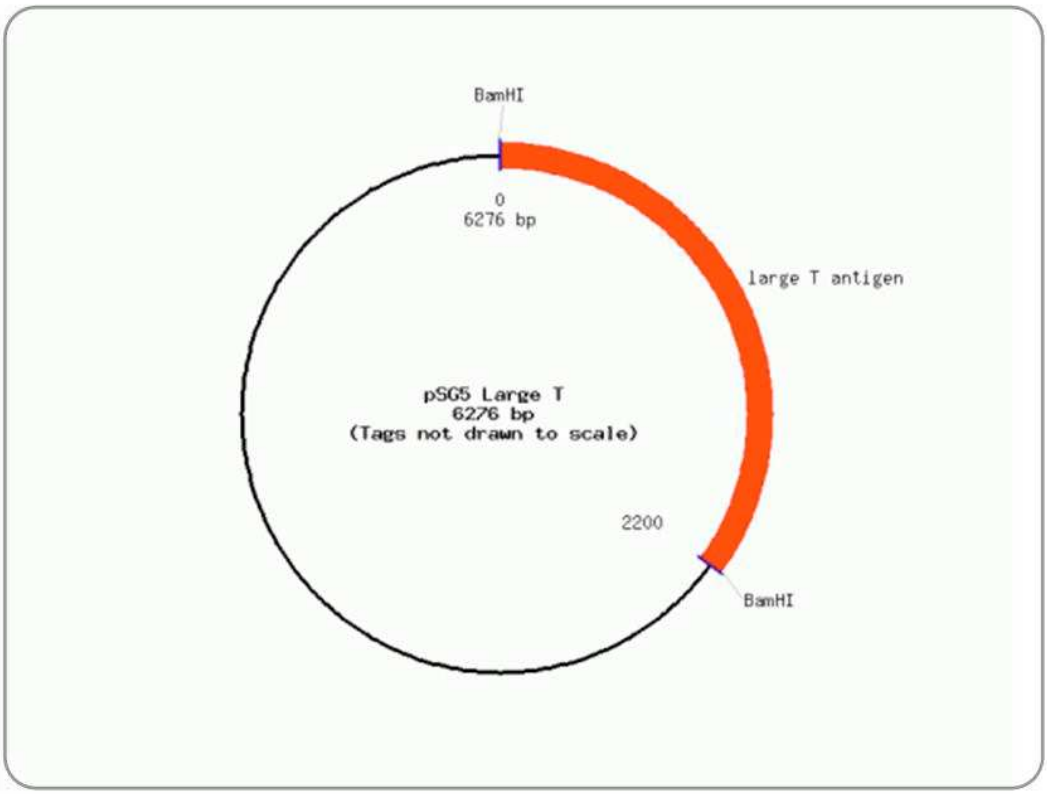

Figure 2-13: pSG5 large T antigen. (Schema adapted from "Addgene vector data base")

pJ3-omega-human-IQGAP2-HA:

To overexpress human IQGAP2 (4500 bp) following vectors were used. We obtained the IQGAP2-HA plasmid from the laboratory of David Sacks, UK. This unusual pJ3-omega vector of 3500 bp contains a human IQGAP2-HA insert (4511bp) under the control of a weak P_{SV40} early promoter. C-terminally, HA was directly linked to the 5'-end of IQGAP2 thereby moving the stop codon to the end of the HA sequence. Figure 2-14 shows a scheme of the pJ3-omega human-IQGAP-HA plasmid.

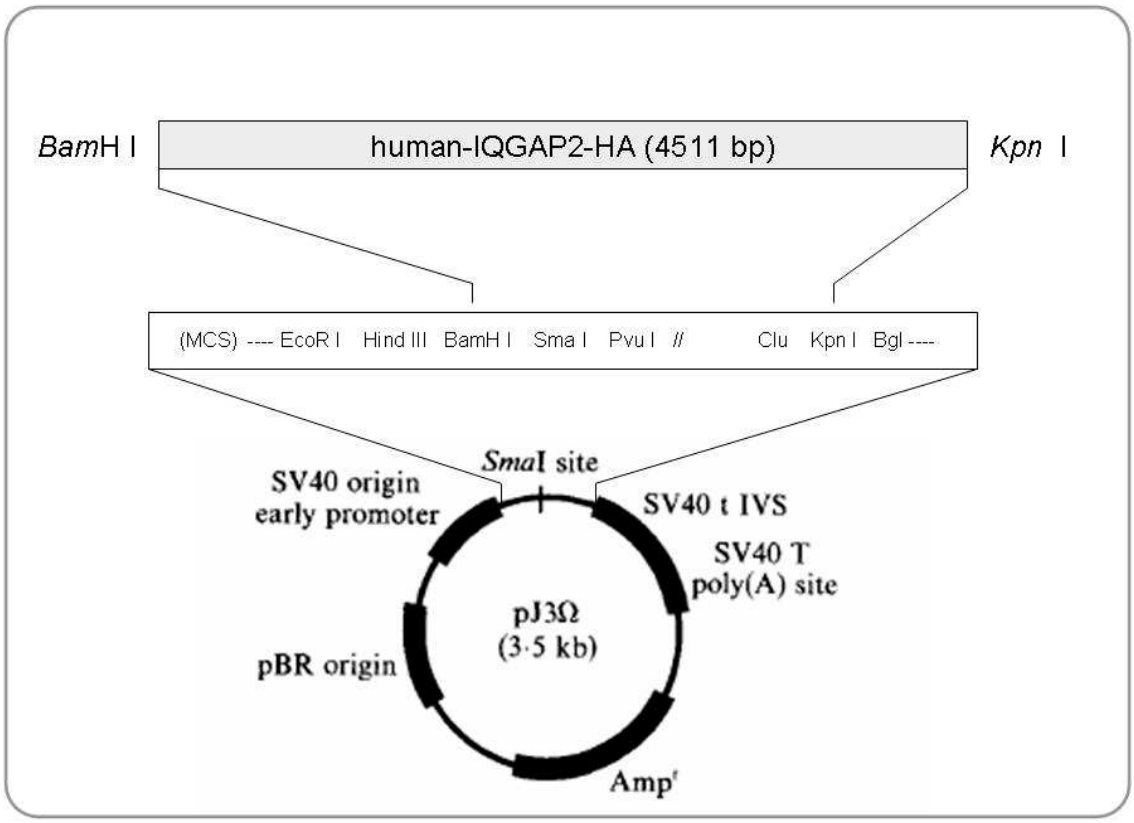

Figure 2-14: Vector map and multiple cloning site (MCS) of pJ3-omega-h-IQGAP2-HA. Human-IQGAP2-HA inserted in frame N-terminally at *Bam*HI and C-terminally at Kpn I. Restriction sites EcoR I, Hind III, BamH I, Sma I represent single cleavage sites. Clu, Kpn I and Bgl are not indicated as single restriction sides (Adapted and modified from Morgenstern and Land, 1990; Kumar et al., 1992; and "Addgene Vector Data Base")

pEGFP-C1-human-IQGAP2:

To overexpress IQGAP2 we obtained a second plasmid from Valentina Schmidt, NY, USA. This plasmid is based on a pEGFP-C1 vector (4700 bp) which additionally expresses GFP (723 bp) and h-IQGAP2 (4500 bp) under control of a strong P_{CMV} promoter as shown in figure 2-15.

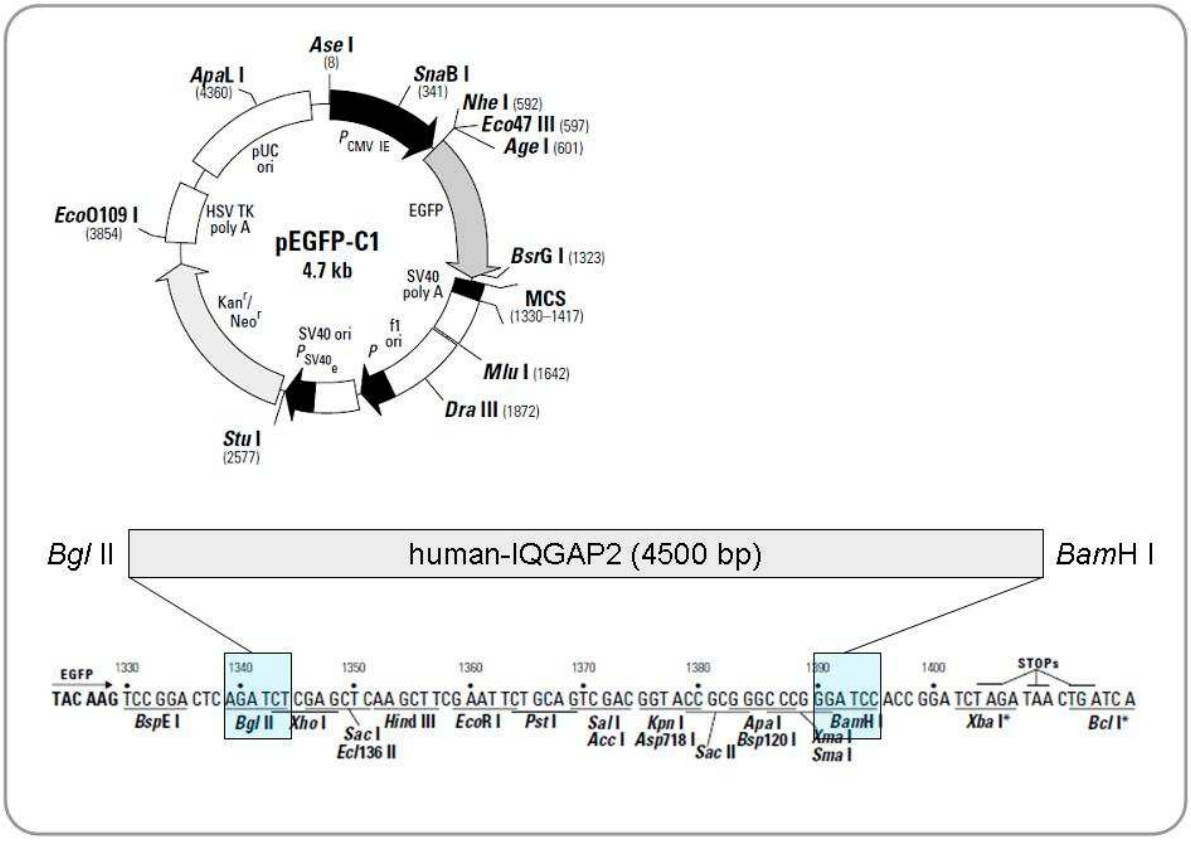

Figure 2-15: Restriction map, multiple cloning site (MCS) of pEGFP-h-IQGAP2. Human-IQGAP2 inserted in frame N-terminally at *Bgl* II and C-terminally at *Bam*H I shortly after EGFP. The full size of the plasmid is 9200 bp (Adapted and modified from Clontech, PT3028-5).

As irrelevant expression controls during transfections pEGFP-C1 (4700 bp) and pcDNA3.1 (5523 bp) were used (Fig. 2-16).

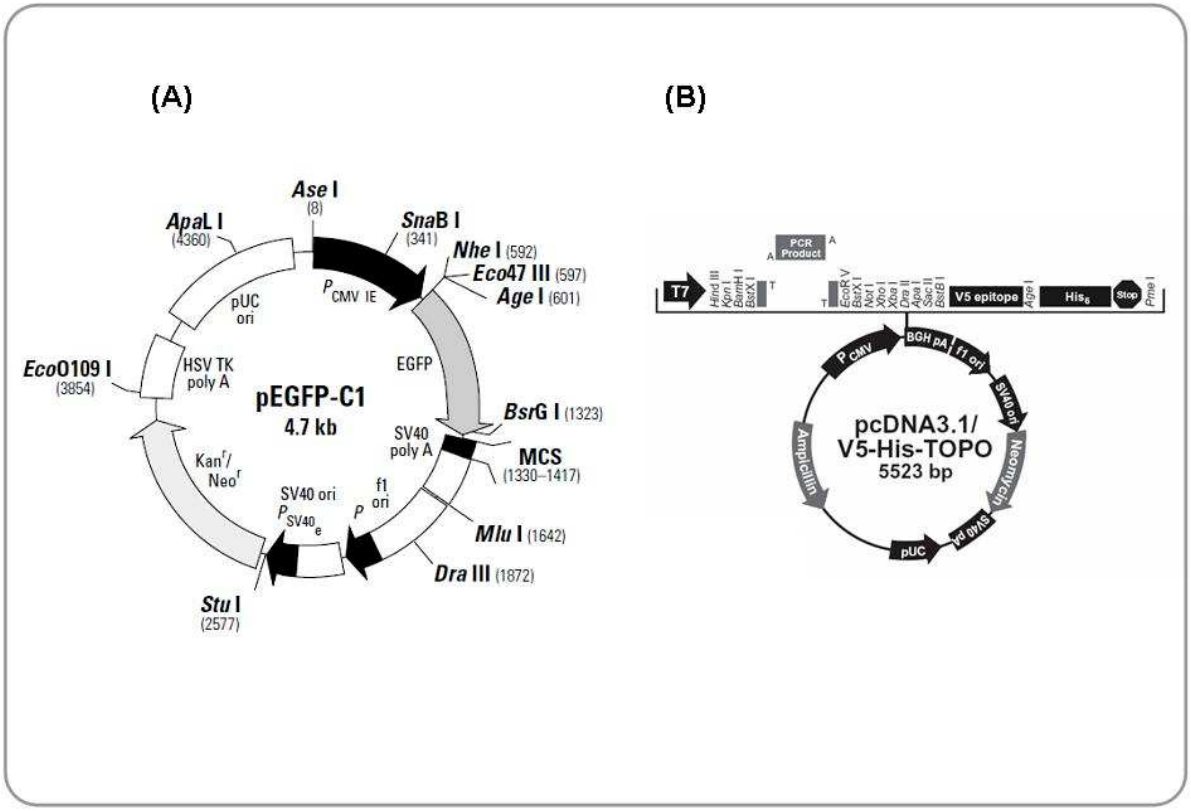

Figure 2-16: Vector maps of pEGFP-C1 and pcDNA3.1 V5-His-TOPO. Vectors without any insert were used as negative expression controls (Clontech).

2.2.1.5 Transfection

Transforming cDNA in Bacteria:

Obtained vectors (pJ3-omega IQGAP2-HA, pEGFP-IQGAP2) were transformed (by heat shock) into chemo-competent E. coli Top 10 F'. Bacteria have been grown in amp-*LB* agar plates overnight (16-24 hr). Resistant colonies were picked and grown in an Ampicillin broth for plasmid Miniprep (Wizard Plus SV, Promega). pEGFP-C1 vector was amplified in the same way but in a Kanamycin resistance background. Purified Miniprep cDNA has been analytically digested using restriction enzymes with a corresponding unique cleavage site. Digested plasmids were verified applying agarose gels to detect the correct size of the cleaved plasmid fragments. Positive clones have been stored as Glycerol stocks at -80℃ for future use.

2.2.1.6 Sequencing of plasmid DNA

As a further control, after amplification, the orientation of the IQGAP2 insert was verified by sequencing the 5' and 3' cloning sites. Therefore cDNA was send to GATC Biotech, Konstanz, Germany and the obtained sequences were compared with vector and IQGAP2 insert sequences.

2.2.1.7 Amplification of plasmid DNA

In order to produce high amounts of plasmid DNA transformed E. coli Top 10 F' have been grown in 250 ml Luria-Bertani-medium (LB-medium) at 37℃ on a shaker plate for 16 hours. To extract high amounts of purified cDNA the Maxi-Preparation kit from Genomed was used in order to the manufacturer's protocol. The appropriate concentration of highly purified cDNA was detected using the NanoDrop (Thermo scientific). The plasmid DNA was than routinely prepared in aliquots at concentrations of 1 µg/µl and stored at -20° C.

2.2.1.8 Transfection of cDNA into mammalian cells

The SuperFect reagent (QIAGEN GmbH, Hamburg) was used to transfect HeLa and HEK293T cells. SuperFect consists of dendrimer molecules that interact with negatively charged phosphate groups of deoxyribonucleotides and assembles cDNA into compact structures. The cDNA bound to SuperFect is taken up by the cell through non-specific endocytosis. Thereby, plasmid DNA can be delivered past the membrane to the nucleus of the cell.
Prior to transfection of plasmid DNA cells have been seeded one day before transfection on 100 mm dishes and 12-well plates containing cover slips. According to the protocol, a cell density of 2 x 10^6 cells per 100 mm dish was improved. Optimized seeding densities of 2 x 10^5 cells per well in a 12-well plate containing cover-slips were applied for fluorescence microscopy (confocal microscope).
HeLa cells seeded on cover slips (12-well plates) were transfected under optimized conditions with 3.0 µg plasmid DNA per well. To co-transfect HEK293T cells with Bcl-2 and IQGAP2 we used 100 mm dishes containing 5.0 µg cDNA of each following plasmid, FLAG-tagged human-Bcl-2 and pJ3-omega HA-IQGAP2 or pEGFP human-IQGAP2. To transmit a single type of plasmid DNA 10.0 µg per 100 mm dish were used for transfections. In order to avoid possible toxic effects of SuperFect reagent upon prolonged incubation on cells, SuperFect was washed off after 4 h using 5 ml PBS. For increased protein synthesis 10 ml of fresh cell culture medium was added to 100 mm dishes. After 24 hours of protein expression HEK293T cells were harvested and whole cell lysates have been prepared. Cell lysates were

either used for analysis of total protein expression or co-IP experiments using the appropriate antibodies.

HeLa cells transfected with h-IQGAP2 were fixed over night at 4℃ after the indicated time points using 4% formaldehyde in PBS followed by immunocytochemistry as described in chapter 5-8.

2.3 Cell biological methods

2.3.1 Cell culture

Table 2-13: Cells and culture media.

Cells	*Cell Type*	*Medium*	*Supplier/Reference*
Factor dependent myeloid progenitors (FDMs)	Fetal liver myeloid progenitor cell line from mouse liver.	DMEM (4 g/L glucose) 10% FCS, 60 µg/ml penicillin, 100 µg/ml streptomycin, Interleukin-3	HoxB8 retroviral co-culture in the presence of high levels of IL-3 Ekert et al (2004) Pardo et al (2006)
Factor dependent cell progenitors (FDC-P1) Mouse lymphoblasts factor dependent cell paterson	Murine non-tumorigenic diploid progenitor cells of granulocytes, monocytes, and macrophages originally obtained from bone marrow cells.	RPMI 1640 (2 g/L glucose), 10% FCS, Penicillin (100 units/ml), Streptomycin (100 µg/ml) and 10% WEHI-3B concentrated conditioned medium as a source of multicolony stimulating factor multi-CSF or Interleukin-3 (IL-3).	Long-term bone marrow culture Dexter et al (1980)
Jurkat E6	Human T lymphocyte Leukaemia cell line	RPMI-1640, (2.0 g/L glucose) 10% FCS, 60 µg/ml penicillin, 100 µg/ml streptomycin	ACC 282 from DSMZ (German resource center for biological material)
3T9 MEF primary MEF	Mouse embryonic fibroblast (3T9 Method transformed)	DMEM (4 g/L glucose) 10% FCS, 60 µg/ml penicillin, 100 µg/ml streptomycin	S. Korsmeyer, USA A. Strasser, WEHI, Australia
3T9 MEF primary MEF Bcl-2 deficient	Mouse embryonic fibroblast (3T9 Method transformed)	DMEM (4 g/L glucose) 10% FCS, 60 µg/ml penicillin, 100 µg/ml streptomycin	
129 J MEF WT	Mouse embryonic fibroblast (Primary cells)	DMEM (4 g/L glucose) 10% FCS, 60 µg/ml penicillin, 100 µg/ml streptomycin	V. Schmidt, NY, USA

129 J MEF IQGAP-2 deficient	Mouse embryonic fibroblast (Primary cells)	DMEM (4 g/L glucose) 10% FCS, 60 µg/ml penicillin, 100 µg/ml streptomycin	V. Schmidt, NY, USA
HeLa-WT		DMEM (4 g/L glucose) 10% FCS, 60 µg/ml penicillin, 100 µg/ml streptomycin	derived from the epithelioid cervix carcinoma of a 31-year-old black human female in 1951 Gey (1952) Scherer *et al.* (1953
HeLa-mBcl-2 over expressing		DMEM (4 g/L glucose) 10% FCS, 60 µg/ml penicillin, 100 µg/ml streptomycin 400 µg/ml Gentamycin	
Rat 6 WT	Embryonic rat cells	DMEM (4 g/L glucose) 10% FCS, 60 µg/ml penicillin, 100 µg/ml streptomycin	Egger *et al.* (2003)
Rat 6 mBcl-2 over expressing	Embryonic rat cells	DMEM (4 g/L glucose) 10% FCS, 60 µg/ml penicillin, 100 µg/ml streptomycin 400 µg/ml Hygromycin	Egger *et al.* (2003)
HEK 293T	Human embryonic kidney cells (SV40 large T antigen transformed)	DMEM, 10% FCS, Penicillin (100 units/ml), Streptomycin (100 µg/ml).	

2.3.2 Generation of IL-3 dependent cell lines

IL-3 dependent factor-dependent myeloid monocytes (FDM) have been generated by co-culturing of E14.5 fetal liver single-cell suspensions with fibroblasts expressing a HoxB8 retrovirus in the presence of high levels IL-3 as previously described (Ekert, et al., 2004).
All mice were derived from C57BL/6 embryonic stem (ES) cells or from 129SV-derived ES cells but have been back-crossed onto a C57BL/6 background for at least 10 generations. Cell lines were tested for IL-3 dependence by determining their ability to proliferate in the absence of IL-3 in liquid culture and soft agar. None of the cell lines developed colonies under these conditions.

2.3.3 Cultivation of mammalian cells

2.3.3.1 Cell counting

The Particle Counter device "Z1 Coulter" was used to count the amount of cells per milliliter (cells/10^{-3} L). This particle counter allows the setting of a lower and upper size threshold and acquires only counts between the set thresholds. A lower threshold of 9 µm and an upper threshold of 27 µm particle size were adjusted for trypsinized adherent and suspension cells. Each mammalian cell sample was prepared as a single cell suspension, diluted in a small container (Accuvette) 1:100 in 10 ml isotone solution and counted.

2.3.3.2 Factor Dependent Myeloid Progenitors (FDMs)

FDMs were cultured in Dulbecco's modified Eagle's medium (DMEM) supplemented with 10% FCS, Penicillin (100 units/ml), Streptomycin (100 µg/ml) and 1 µg/l (1ng/ml) recombinant interleukin-3 (Peprotech) at 37℃ in a 5% CO_2 incubator. Cell densities were kept between 5 x 10^5 to 7 x 10^5 cells/ml. FDMs were controlled every day and 1/3 or ½ of the culture medium was replaced at last every second day during log phases to provide optimal growth conditions.

2.3.3.3 Cultivation of adherent cells

All adherent cells have been cultured in DMEM (Dulbecco´s Modified Eagles Medium, high glucose) at 37° C in a 5 % CO_2 incubator. Every three days after reaching 70-80 % confluency, sub cultivation of MEF was achieved by passaging. Therefore, the medium was discarded and the cells were washed once in PBS. By trypsination for 3 min. at 37° C cells detach from the bottom. Trypsination was excerted by resuspending all cells in fresh cell culture medium. Subsequently, cells were diluted 1:8 on new culture plates.

2.3.3.4 Immortalization of MEFs

To achieve persisting cell lines out of primary cells, the 3T9 immortalization method is used (Todaro GJ, and Green H, 1963). In this process, the cells undergo spontaneous mutations during several culture passages until immortalization is achieved.
Primary wild type and IQGAP2 $^{-/-}$ MEFs from embryonic day 12.5 (E12.5) on a 129J1 background were kindly provided by Dr. Valentina Schmidt, (New York, USA). All cells have been grown at 37° C in a humidified atmosphere of 5 % CO_2 in air. Every three or six days, primary MEFs were transferred onto gelatine-coated culture plates. 129J1 MEFs grow very slowly and they have to be cultured in 60 mm dishes to establish suitable cell densities between 80-90 %. After approximately 18 passages small cell clusters of proliferating cells appear between the flattened residual primary cells. In passages between p27-p32 all wt and

IQGAP2 $^{-/-}$ MEFs displayed a typical fibroblastic morphology with equal cell proliferation. At these passages, aliquots have been taken as soon as a dense cell population was observed and 3T9 MEFs were frozen for storage at -196°C.

2.3.3.5 Immortalization by transfecting pSG5 large T antigen into MEFs (129J1):

SV-40 large T antigen (Simian Vacuolating Virus 40) is a hexamer protein that is a proto-oncogene derived from polyoma virus SV-40. It is able to transform a variety of cell types by binding to the retinoblastoma protein (pRB), p53 and p21. In addition, it binds to several other cellular factors, including the transcriptional co-activators p300 and CBP, which may contribute to its transformation function. T-antigen interactions with p53 and p105 cause the cells to leave G1 phase and enter into S phase, which promotes DNA replication.
To facilitate transformation of primary mouse embryonic fibroblasts, cells were passaged according to the 3T9 immortalization method. In passages p10-p15 small cell clusters of mitotic subpopulations appear which are suitable to be transfected with the pGS5 plasmid (chapter 5.3.1 figure 5-1). To transfect wild type and IQGAP-2 $^{-/-}$ 129J1 MEFs the SuperFect reagent was used according to the instructions of the protocol.

2.3.3.6 Freezing and thawing of cells

Cell lines that are not in use for longer time periods were preserved through freezing. The cryopreservation in liquid nitrogen at -196°C is a common method for the long-term storage of cells. Therefore, after trypsination cells were resuspended in culture medium, counted and a respective cell number of 0.5 x 10^6 cells per ml was adjusted. An appropriate volume of medium containing cells was centrifuged at 1200 rpm for 3 min. (adherent cells) or 5 min. at 400 x g (FDMs). Cells were resuspended in 1 ml ice-cold medium supplemented with 20 % FCS, 10 % and put into special freezing tubes. DMSO avoids granulation which could potentially harm the cells. Cells were frozen at -80°C using a freezing container that contains isopropanol. Long-term storage was archived by transferring frozen vials from -80°C into a liquid nitrogen tank after 3-4 days pre-freezing.

To thaw up cells:
Prior to use, frozen cell vials have been desinfected to avoid any contamination with bacteria. Cells thawed up at RT and were picked up by resuspending with a pipette containing 6 ml culture medium and transferred into 10 ml of prewarmed medium. After centrifugation at 1200 rpm for 2 min. the DMSO-containing medium was replaced by fresh medium and centrifuged again. Cells were resuspended in fresh medium and plated on culture dishes or gelatine-coated plates to facilitate adherence.

2.4 Cell biological detection methods

2.4.1 Flow cytometry analysis

The fundamentals of flow cytometry are the measurement of individual properties, the size, the granularity and fluorescence of cells. Within a flow cytometer particles or cells are focused by a liquid flow system thereby a single file of cells is established to measure one cell at a time. The individual properties of a cell are measured by light scattering in the forward direction known as the forward scatter channel (FSC) and at a 90^{o} angle to the excitation line that is called side scatter channel (SSC). A flow cytometer is also able to detect the emission of different fluorescence light by an appropriate filter system and optical lens. Filter separated fluorescence light is measured by different photomultiplier tubes (PMTs) that are known as Fl-1, Fl-2 and Fl-3 channels.

Detected light in the forward scatter channel corresponds to the particle's size and can be used to distinguish between cellular debris and living cells. Scattered light detected in the side scatter channel displays the granulation within cells. The combination of FSC and SSC displays the unique properties of specific types of cells. Flow cytometry was used to analyse and to distinguish between living, apoptotic and dead (necrotic) cells. A schematic overview of a flow cytometer is shown in figure 2-17.

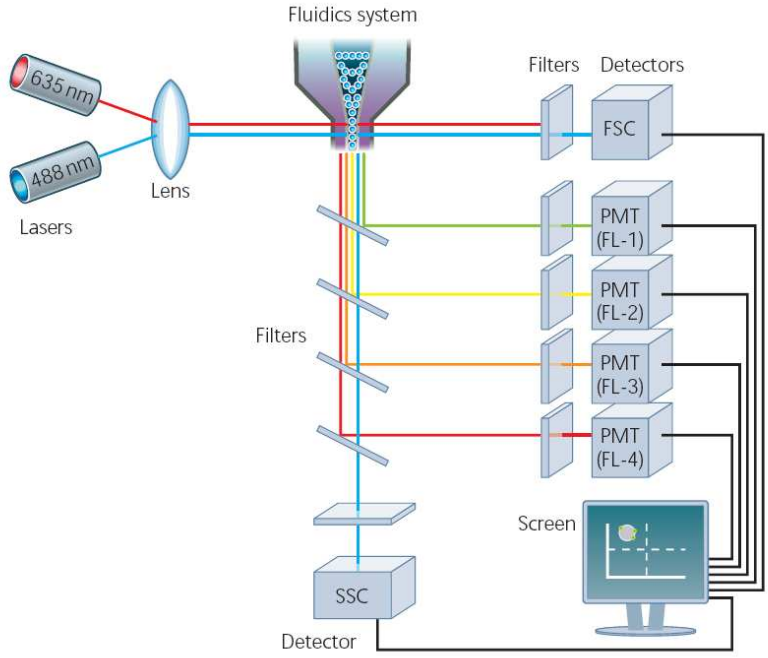

Fig. 2-17: Schematic overview of a typical flow cytometer setup. Depending on the manufactory a FACS unit is comprised of detectors (PMT) in which the cells are characterized due to their diameter (Forward Scatter, FSC), their granularity (Sideward Scatter, SSC) and to their fluorescent intensities (Photomultiplier tube, PMT) due to a particular staining (e.g. green and red-coupled fluorescence antibodies) (Scheme adapted from AbD Serotec, 2006).

2.4.1.1 Annexin V-GFP and propidium iodide (PI) flow cytometry analysis

With this method we are able to distinguish between healthy, early apoptotic and death cells by the usage of two different fluorochromes, know as green fluorescence protein (GFP) and propidiumiodide (PI). Annexin V-GFP has been used to label phosphatidylserine (PS) on the outer leaflet of the plasma membrane during early apoptotic stages. GFP emits green light which is detected by the FL-1 channel. Propidiumiodide the second fluorochrome emits in the red spectrum of light and binds to DNA of necrotic (dead) cells. Healthy cells exhibit normally no phosphatidylserine at the outer surface of the plasma membrane and PI is not able to diffuse through membranes, therefore living cells are annexin V PI negative cells.

Flow cytometry was carried out by preparing a cell suspension containing 1x 10^6 cells per ml. The properties of each cell type were tested before flow cytometry and distinct cell type specific settings have been set up. Samples containing non-treated and treated cells were centrifuged at 1200 – 1400 rpm at 4 °for 3 minutes. The pellets were washed once with 1x Annexin V binding buffer, resuspended in the same buffer containing 1x annexin V (1:2000) and incubated in the dark. Propidiumiodide (1.0 µg/ml) was added after 15-20 min. and flow cytometry was done directly after adding PI.

10x Annexin V binding buffer:	0.1 M HEPES/NaOH, pH 7.4
	1.5 M NaCl
	25 mM $CaCl_2$

2.5 Confocal microscopy

Confocal imaging was invented to improve traditional wide-field fluorescence microscopy. Conventional wide-field fluorescence microscopes detect light from all parts at the same time of the specimen. The resulting picture taken up by a camera is a mix of different detected fluorescence light producing an unfocused background and false positive signals.
In contrast, a confocal microscope (Fig. 4-6) the specimen is illuminated point by point at a distinct level, "Point Spread Function" and a pinhole in front of the detector eliminates out-of-focus signals. Point by point, fluorescence light that is very close to the focal plane can be detected, because of the pinhole. The resulting optical resolution in the sample depth is much better than that of wide-field microscopes. But, the improved resolution is at the cost of decreased signal intensities, therefore long exposures are required.

2.5.1 Confocal laser scanning microscopy

Principle of confocal laser scanning microscopy (CLSM):

During confocal laser scanning microscopy point in-focus images are illuminated and detected at a time. Each visible pixel at the display of a laser scanning microscope represents an illuminated volume element within the object of interest. The whole image is assembled pixel-by-pixel and line-by-line as the laser scans over the area of the specimen. The brightness of an image pixel corresponds to the relative intensity of detected light and the scanning is done through servo controlled oscillating mirrors with low reaction latency. The best signal-to-noise ratio is obtained by slow scans resulting in better contrast and higher resolution.

To obtain 2-dimensional pictures it requires multiple scans over a regular raster in the specimen. Three-dimensional pictures of a specimen are obtained by assembling a stack of these two-dimensional images from successive focal planes (overview projection or z-stacks), a process known as optical sectioning. In figure 2-18 the principle of confocal microscopy is depicted.

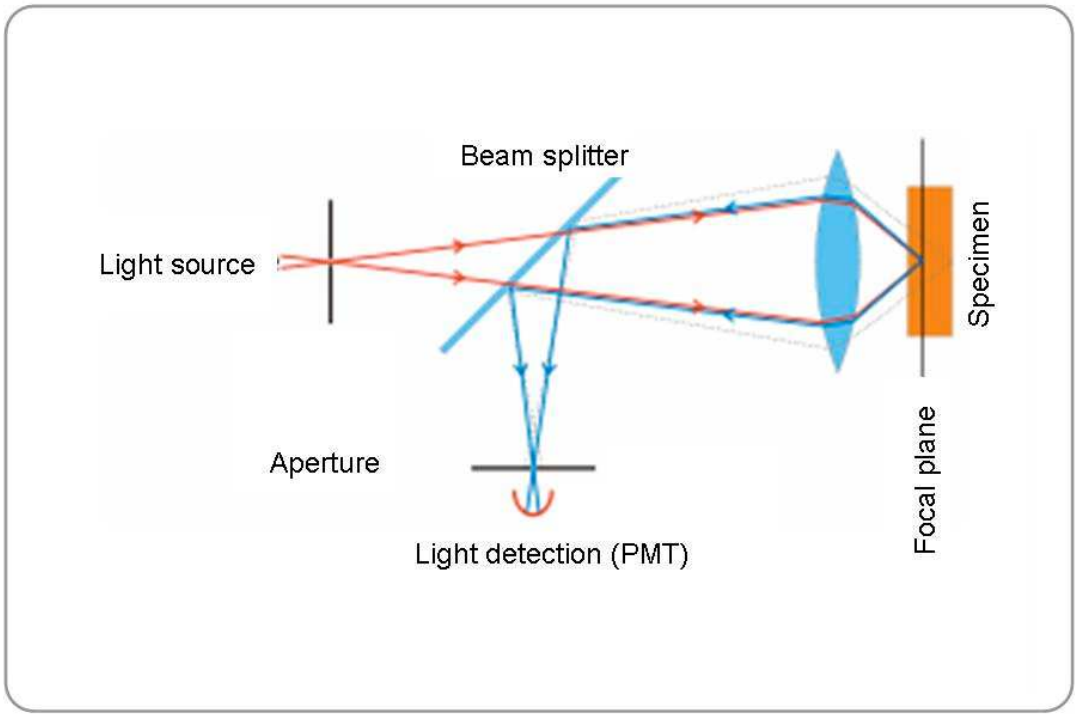

Figure 2-18: Principle of confocal microscopy. Only the light that is very close to the focal plane can be detected, because of the pinhole. Several focal planes are able to adjust by moving up or down the stage of the microscope (sectioning). A parallel a beam splitter separates off some portion of the light into a photomultiplier tube (PMT). Each photon is than transformed into an electrical signal that is displayed at a computer screen.

2.5.1.1 Immunocytochemistry (ICC)

This method uses the specific interaction of antibodies to target proteins within a cell that is not part of a tissue e.g. cells grown on cover slips. It allows further determination and localization of distinct expressed peptides or protein. The specific protein of interest is detected in a fluorescence microscope after incubation with a secondary antibody conjugated to a fluorophore.

Fixation and permeabilization:

The cell culture medium was discarded and the cells were washed with 1 x PBS and fixed with 4 % (PFA in 1 x PBS) at 4° C over night. The n ext day paraformaldehyde was collected and cover slips were washed twice in 1 x PBS. Cells were permeabilized with 0.05 % Tween-20 for 15 min. at RT. Than cells on cover slips were washed twice in 1 x PBS.

Blocking and antibody incubation:

Blocking of non-specific surface areas was done using blocking solution (1 % BSA, 5 % milk (MLK) in 1 x PBS) for 30 min. at RT and washed with 1 x PBS. Primary antibodies incubated over night at 4° C (Table 2-14). The next day cover slips were washed three times with 1 x PBS. Secondary antibodies and Hoechst 33342 (Table 2-15) were incubated for 1.5 hours at RT. Cover slides were washed with 100 % ethanol, double distilled H_2O, dried and labeled. The cover slips were washed three times with 1 x PBS and three times with double distilled H_2O to remove salts. Cover slips were mounted upside down with mounting solution on cover slides and air dried over night at 4° C.

Table 2-14: Primary antibodies and their concentrations used for confocal microscopy. All antibodies were diluted in 1% BSA, 5% MLK blocking solution.

Antigen	Species	Clone	Mass (kDa)	Dilution	Supplier
Bcl-2	mouse	10C4	26	1:200	Zymed
Bcl-2	rabbit	22-6	26	1:200	self-made
IQGAP2	mouse	BB9	60	1:400	upstate
Cytochrome c	mouse	BALB/c	15	1:50	BD Pharmingen
IgG_1	mouse		150	1:200	sigma

Table 2-15: Secondary antibodies and their concentrations used for confocal microscopy. All antibodies were diluted in 1% BSA, 5% MLK blocking solution.

Antigen	Conjugate	Species	Dilution	Supplier
Mouse IgG	Alexa 488	Goat	1:200	Molecular Probes Europe BV, Paisley, UK
Rabbit IgG	Alexa 546	Goat	1:200	Molecular Probes Europe BV, Paisley, UK
Hoechst 33342			1:500	Sigma-Aldrich

2.6 Protein biochemistry

2.6.1 Preparation of whole cell lysate

For total cell lysates, 1 x 10^7 adherent cells have been scraped off from dishes at selected time points and were washed in ice cold PBS before adding an appropriate lysis buffer. Whole cell lysates of FDM suspension cells were prepared with 5 x 10^7 cells due to the size of these cells. Cell pellets were solubilized in H8 lysis buffer containing 1 % SDS by boiling for 5 min. at 95 °C. Thereafter, samples have been sonicated on ice 3 x 10 seconds (sec.) combined with pauses 3 x 10 seconds to avoid thermic degradation of proteins. After that samples were centrifuged and the supernatant was transferred into a new tube. After protein determination an appropriate amount of protein was mixed with 5x loading buffer.

2.6.2 Subcellular fractionation

The distribution of Bcl-2 family members in fractions of cytosol, total membranes, heavy membranes (HM) and light membranes (ER) were studied using the subcellular fractionation method. To get sufficient protein of each fraction, suitable amounts of cells have to be provided. As an example: To examine protein distribution of Bcl-2 in different cellular fractions of healthy and IL-3 depleted FDMs, after 16 and 24 hours, 300 x 10^8 cells at any given time were used (175 cm^2 cell culture flasks with 200 ml of cell suspension contain 100 x 10^8 cells corresponding to 0.5 x 10^6 cells/ml).

2.6.2.1.Start of preparation

Cells were centrifuged in a 200 ml container at 1200 rpm for 5 min. at 4° C. Obtained pellets have been washed in ice-cold PBS and resuspended in 400-600 µl of IBc buffer containing protease inhibitors (see Table: 2-16). The cells were allowed to swell on ice for 45-60 min. prior to homogenization by using a Dounce homogenizer (Kontes Glass, USA). Cell lysis was verified using trypan blue a cell impermeable dye that only enters dead cells. Lysed cells were diluted 1:5 with trypan blue on a cover slide and bright shining cells or dark spheres have been counted under a microscope. Lysates containing 50-60 % of broken cells were used for further preparation. Unbroken cells, debris and nuclei were removed by centrifugation at 500 x *g* for 5 min at 4° C s. This spin cycle was repeated t wice to completely avoid contamination of unbroken cells, debris and nuclei. The post nuclear supernatant (PNS) contains cytosol, heavy- and light membranes.

2.6.2.2 Total membrane fraction (TM)

The post nuclear supernatant was centrifuged at 100,000 x *g* for 45 min at 4° C using an ultra centrifuge (Optima Max, Beckman Coulter). The supernatant (S_{100}) consists of cytosol and the total membrane fraction (heavy- and light membranes) is found at the pellet.

2.6.2.3 Heavy membrane fraction (HM)

The post nuclear supernatant was centrifuged at 20,000 x *g* for 15 min at 4° C using an ultra centrifuge (Optima Max, Beckman Coulter) to pellet the mitochondria-enriched heavy membrane fraction. The pellet was washed twice with the same buffer to exclude contamination of cytosolic and light membrane proteins.

2.6.2.4 Cytosolic fraction (CYTO)

The supernatant was further centrifuged at 100,000 x g for 45 min at 4° C using an ultra centrifuge (Optima Max, Beckman Coulter) to obtain cytosolic fraction at the supernatant.

2.6.2.5 Light membrane fraction (LM)

The remaining pellet (P_{100}) contained the light membranes enriched with the microsomes or membranes of the endoplasmic reticulum (ER). They were washed twice with the same buffer prior solubilization.

2.6.2.6 The nuclear fraction (Nuc):

The nuclear membrane fraction was prepared by using 5 x 10^7 cells. After centrifugation cells were washed in ice cold PBS and incubated on ice for 15 min. with Buffer A (see table below). After that 0.5% NP-40 (final concentration) was added and subsequently vortexed for 10 seconds. Broken cells and nuclei were centrifuged at 14.000 x g for 2 min. at 4℃. The supernatant (SN) contains cytosolic proteins and mitochondria. The pellet was washed twice with Buffer A without NP-40. Thereafter the pellet was resuspended by pipetting and shortly vortexed with buffer B (high salt buffer). Nuclear proteins and DNA are extracted on a rocker plate at 4 °C for 30 min. The resulting lysate was further centrifuged at 16.1 x g for 15 min. at 4 °C using a tabletop centrifuge to separate nuclear proteins (SN) and DNA (pellet). Protein concentration of the SN was determined and aliquots containing 50µg per 20µl were adjusted by adding 5 x loading buffer. Prior to freezing and PAGE samples were heated at 95℃ for 5 min.

Buffer A: 10 mM HEPES, pH 7.9
10 mM KCL, 0.1 mM EDTA
1 mM DTT, + inhibitors

Buffer B: 20 mM HEPES, pH 7.9
400 mM KCL, 1 mM EDTA
1 mM DTT, + inhibitors

2.6.2.7 Solubilization of cellular fractions under denaturing conditions

The total cell lysate obtained was dissolved in H8 lysis buffer as mentioned earlier or in 1 % NP-40 IBC-buffer and loaded on to SDS-gels under reducing (DTT) or non-reducing conditions and immunoblotted for the subcellular distribution analysis of various proteins (see below).

2.6.2.8 Solubilization of cellular fractions under non-denaturing conditions

To obtain TM, HM and LM fractions for subcellular distribution analysis and co-immunoprecipitation (see below), the pellet was resuspended in IBC buffer with protease inhibitors but containing detergents like CHAPS 1% (w/v), Digitonin 1%, and 0.5 % and Triton X-100. An appropriate volume of buffer according to the size of the pellets, approximately 200-800 µl has been added. Pellets were resuspended and solubilized on ice for 45 min. Heavy membranes lysates have been centrifuged at 20,000 x *g* for 15 min at 4° C using an ultra centrifuge (Optima Max, Beckman Coulter). Total- and light membranes were centrifuged at 100.000 x g for 15 min. at 4 ℃ to exclude the non-solubilized materials.

Table 2-16: List of inhibitors used. Two fold concentrations are used to avoid early degradation of inhibitors. Every 4 hours inhibitors were added during prolonged preparations.

Protease Inhibitors	Stock concentration		Dilution	Final concentration
Aprotinin	10 mg/ml	H_2O	1:500	20 µg/ml aprotinin
Leupeptin	50 mg/ml	H_2O	1:500	100 µg/ml leupeptin
AEBSF	300 mM	H_2O	1:500	600 µM AEBSF
Pepstatin A	400 µg/ml	EtOH	1:500	800 ng/ml pepstatin
Cypermethrin	10 mM	DMSO	1:2000	5 µM
MG 132	20 mM	DMSO	1:5000	4 µM
Sodium ortho vanadate	200 mM	H_2O	1:1000	0.2 mM

2.6.2.9 Protein determination assay (BIO-RAD)

The Bio-Rad protein assay is a dye-binding assay in which a differential colour change of a dye occurs in response to various concentrations of protein. The absorbance maximum for an acidic solution of Coomassie Brilliant Blue G-250 dye shifts from 465 nm to 595 nm when binding to protein occurs. The Coomassie Blue dye binds to primarily basic and aromatic amino acid residues, especially arginine. It was found that the extinction coefficient of a dye-albumin complex solution was constant over a 10-fold concentration range (Spector et al. 1978). Thus, Beer's law may be applied for an accurate quantitation of protein by selecting an appropriate ratio of dye volume to sample concentration.

To measure the samples a standard with increasing bovine serum albumine (BSA) amounts was prepared. The different amounts of BSA (0, 1.25, 2.5, 5, 10, 20, 40 µg/ml) were dissolved in 100 µl H_2O bidest. Protein samples have been diluted 1:1000 and 1:2000 in H_2O bidest. The dye reagent was diluted 1:5 in distilled deionised water before usage. The BSA standard and the diluted samples were both pipetted on a 96-well plate and mixed with 100 µl BIO-RAD Protein ASSAY solution up to final volume of 200 µl. The plate was incubated at RT for 5 min and subsequently measured at 562 nm. Obtained values were analysed with the SoftmaxPro Software and determination of the protein amount in each sample was achieved by relating the values of the samples to the values of the standard curve.

2.7 Methods applied to extract endogenous Bcl-2 binding proteins

2.7.1 Blue native poly acryl gel electrophoresis (BN-PAGE)

To analyse the molecular mass, oligomeric state, and homogeneity of native biological membrane protein complexes the blue native method was invented (Riccio, Schägger et al., 1977).The method was originally developed to separate membrane protein complexes in a molecular mass range from 10 kDa up to 10 Mda. In a first dimension blue native PAGE native protein complexes are separated. The subunits of these complexes are separated in a second SDS-PAGE under reducing conditions (Fig. 2-19). Therefore the subunit composition of the separated membrane protein complexes can be analysed.

2.7.1.1 Protein solubilization for BN-PAGE

To solubilize biological membranes mild neutral non-ionic detergents like digitonin, dodecyl-ß-D-maltoside, octyl-ß-D-glucopyranoside are required to isolate mitochondrial membrane complexes. Digitonin, one of the mildest detergents was applied to solubilize and identify multiprotein complexes of the mitochondria enriched heavy membrane fraction.

2.7.1.2 Principles of blue native gel electrophoresis

Coomassie an anionic dye is added to the lysate and binds to solubilized protein complexes due to its hydrophobic property to the surface of membrane proteins. Hydrophobic surface areas of protein complexes are now negatively tagged (charge shift) and repel each other. Aggregations of protein complexes are omitted and the three dimensional structure is still in its native conformation.
Dye associated protein complexes are visible during blue native first dimension gel electrophoresis and migrate as blue bands (coomassie) within the gel. The subunit composition of multi-protein complexes can further be determined by applying a second SDS PAGE. First dimension tracks or lanes are excised and put on top of a second gradient SDS-PAGE. During the second electrophoresis, protein subunits of protein complexes are separated (blue native second dimension, BN-2D SDS-PAGE).

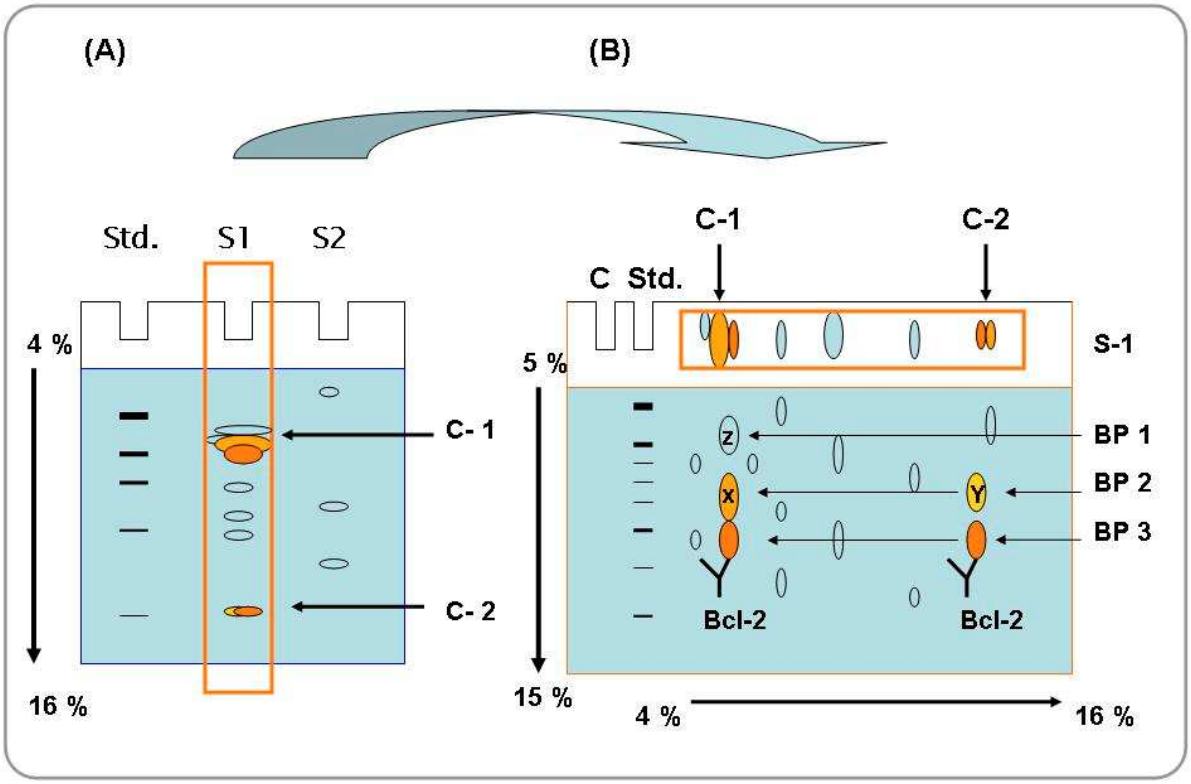

Fig. 2-19: Schematic overview of the blue native method. First dimension blue native gel sample-1 transfer on top of second dimension SDS-PAGE. Protein complexes C-1 and C-2 are separated according to their molecular size during first dimension blue native (**A**). Subunits of these complexes are separated during 2D SDS-PAGE (**B**). Molecular weight Standard (Std.), Sample 1 (S1), Sample 2 (S2), Binding protein 1-3 (BP 1-3) or protein subunits of protein complexes (Own scheme).

Table 2-17: High molecular weight standard for blue native. Each vial of the kit contains the amounts of the listed non-denatured proteins solubilized in blue native loading buffer (Table 2-3).

Molecular mass (kDa)	Native proteins per vial	
670	Thyroglobulin, porcine thyroid,	76 µg
440	Ferritin, equine spleen,	50 µg
232	Catalase, bovine liver,	36 µg
140	Lactate dehydrogenase, bovine heart,	48 µg
66	Albumine, bovine serum,	40 µg

2.7.2 Co-immunoprecipitation (co-IP)

To study endogenous protein-protein interactions conventional co-IPs are an important tool to extract proteins or protein complexes. This technique or method detects protein interactions that do not accept peptide tags or for which biology is altered after addition of tags.

Co-immunoprecipitation is a method by which peptides or proteins that specifically interact with an antibody are removed from cell extracts. After incubation with the bait specific antibody protein A or protein G sepharose beads are added to the lysate that bind to the specific IP-antibody. Antibody-antigen complexes bound to protein A or protein G are "pulled down" by centrifugation. Due to different binding affinities of protein A and protein G to the species and immunoglobulin subtypes of monoclonal and polyclonal antibodies it is advisable to test for the best affinity.

Co-immunoprecipitates of endogenous Bcl-2 where obtained from lysates of the mitochondrial enriched heavy membrane fraction (HM). After protein determination samples were adjusted to specific sample volumes correlating to the amount of protein (Low scale concentration: 100 – 1000 µg protein to 250-500 µl and high scale concentrations 5000 – 20.000 µg protein to 500-1000 µl. Pre-clearing was performed with 50-100 µl 50 % protein A/G sepharose suspension (Protein G Sepharose™ 4 Fast Flow recombinant protein G, GE Healthcare Bio-Sciences AB) on a turning wheel for 1 hr at 4 ℃.

Protein A/G beads are removed by centrifugation (8000 rpm) for 3 min. at 4 ℃ and specific antibodies were added to prepared vials according to the optimized conditions to the supernatant and incubated on a turning wheel at 4 °C for 60 min. The “INPUT” control sample was always kept as a separate sample without any IP antibody.

To "precipitate" the antigen-antibody complexes 50-150 µl of 50 % slurry of protein A/G beads were added and incubated for 60 min at 4 ℃ on a turning wheel. The protein-G – antibody – antigen complexes were pelleted by centrifugation and the supernatant was transferred into a new tube as "SN" control. The protein A/G beads of the IP were washed 3 times in 1 ml solubilization buffer and boiled in 60 µl of 3 x reducing- or non- reducing SDS sample buffer for 5 min. at 97 ℃ to obtain the IP sample fraction. PAGE was done under reducing and non-reducing conditions according to the size of the protein of interest to exclude any interference with broken antibody fragments.

Loading: 5-10 % input, 20 µl IP sample and 5-10 % SN sample. Proteins were separated depending on their molecular size and plotted on a nitro cellulose membrane.

Table 2-18: Antibodies used for co-immunoprecipitation.

Antigen	*epitope*	*Species*	*specificity*	*Dilution*	*Supplier/Reference*
Bcl-2 (10C4)	NS	mouse monoclonal	mouse, rat	0.5 µg/µl	Zymed invitrogen
Bcl-2 (100)	NS	Mouse monoclonal	human	1.0 µg/µl	Zymed
Iqgap-2	AA 319-519	mouse monoclonal	mouse, human	1.0 µg/µl	upstate

Negative immunoprecipitation control samples:

The study of protein-protein interactions involving endogenous proteins frequently relies on the immunoaffinity capture of a protein of interest followed by mass spectrometry based identification of co-purifying interactors. One problem of each co-immunoprecipitation is to distinguish between real physiological interactors and non-specific binders. Therefore a set of strategic IP-controls has to be developed to facilitate the identification of non-specific proteins. To do so, co-IPs were performed in parallel with either a "matrix only" IP, a "mock" IP, an "antibody only" IP, or a "Knock-out" IP. In the "mock" IP the specific antibody of the IP is replaced by a species specific but non-specific isoform of IgG.
The "antibody only" IP control represents the IP-specific antibody incubated without any cell lysate to distinguish between the different heavy- and light chains during Western blot analysis. The "knock-out" IP control is in accordance with the cell type in which the specific protein is knocked out. Protein data obtained after mass-spectrometric analysis have been manually screened for the presence of a protein which is only found in the "positive" IP sample (bait specific antibody Bcl-2).

2.7.3 ABT-737 assay

Oltersdorf and colleagues, (2005) developed by using a nuclear magnetic resonance (NMR) based screening, parallel synthesis and structure-based design, ABT-737 a small molecule inhibitor of the anti-apoptotic proteins Bcl-2, Bcl-xL and Bcl-w. The compound binds with high affinity (K_i < 1 nM) to Bcl-XL, Bcl-2 and Bcl-w but not to the less homologous proteins Bcl-B, Mcl-1 and A1 (K_i = 0.46 +/- 0.11 µM, 1 µM and 1 µM, respectively). The binding of ABT-737 to the hydrophobic pocket of survival proteins like Bcl-xL was further validated. ABT-737

treated cells co-expressing Bcl-xL and the GFP-tagged BH3-only protein Bcl-Gs show a reduced amount of fluorescence on mitochondria (Oltersdorf et al., 2005).

The property of ABT-737 to displace specific proteins bound to the hydrophobic pocket of Bcl-2 was now used to treat co-immunoprecipitates of Bcl-2 with the artificial peptide ABT-737. Figure 6-1 shows the three dimensional structure of Bcl-2 with ABT-737 bound to the hydrophobic pocket detected by nuclear magnetic resonance (NMR) spectroscopy.

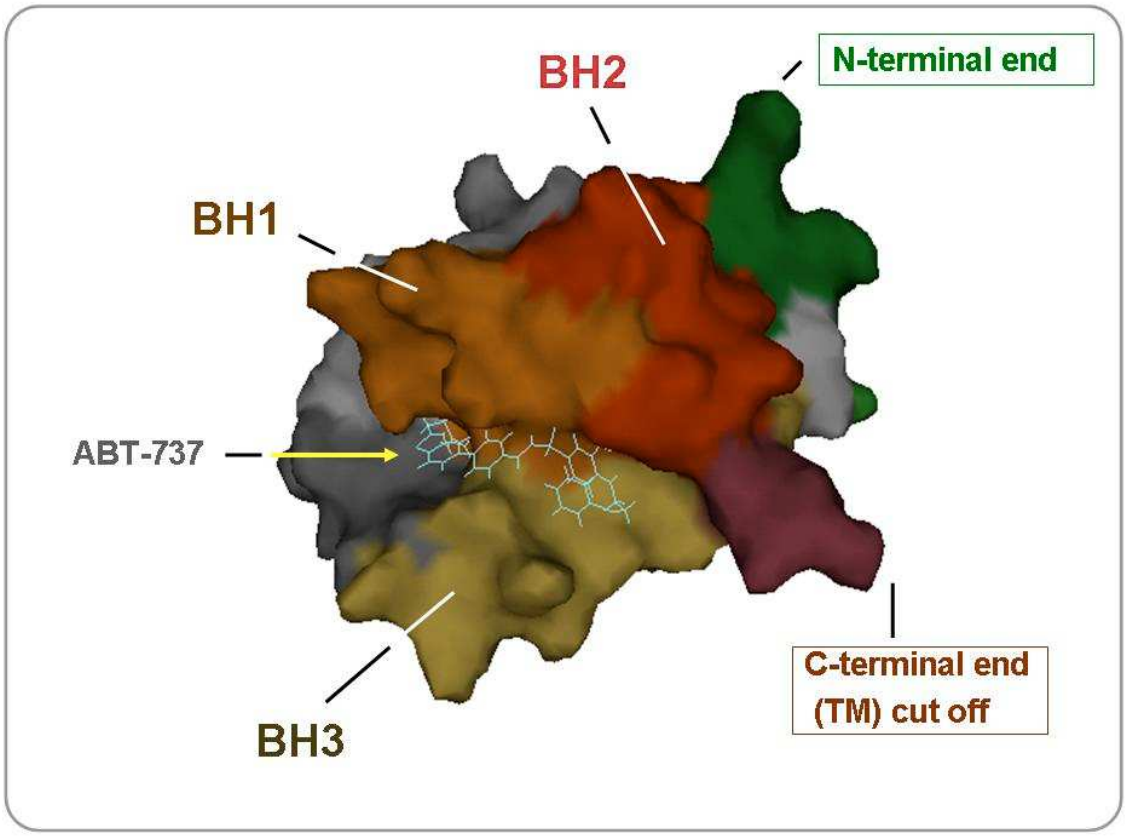

Figure 2-20: ABT-737 binds to the hydrophobic pocket of Bcl-2. NMR derived structure of Bcl-2 complexed with ABT-737. Bcl-2 homology domains 1-3, BH1, BH2 and BH3. (Adapted and modified from PDB, 1YSW)

2.7.4 Denaturing and separation of proteins

2.7.4.1 Western blot analysis

The Western blotting analysis permits detection of specific proteins in a given protein extract. This method is based on the principle of SDS-PAGE to separate proteins according to their molecular weight. Thereafter, separated proteins are electrophoretically transferred on a membrane which can be probed with a specific antibody.

2.7.4.2 Sample preparation for polyacrylamide gel electrophoresis (PAGE)

Appropriate protein amounts of solubilized whole cell lysate, total membranes, heavy/light membranes, cytosolic and nuclear fractions were resuspended with 5 x Laemmli buffers containing 5 % SDS and adjusted to final 1 x SDS concentration. Fractions of immunoprecipitates were mixed with 3 x SDS sample buffer. Proteins were boiled at 95 ℃ for 5 min. and thereby denatured. Depending on the detection of the protein of interest the interference in molecular size with heavy and light chains of the antibody used for co-IP (25 kDa, 50 kDa and 150 kDa) was avoided by specifically chosen non-reducing and reducing conditions.

2.7.4.3 SDS Polyacryl gel electrophoresis (PAGE)

The samples were loaded onto the gels and separated on 8, 12, or 15 % SDS-PAGE mini-gels using the Bio-Rad mini gel (12 slots) system or PeqLab vertical gel system (20 slots). Table 2-18 shows SDS-PAGE composition for 10x mini gels. To increase the resolution in between the proteins gradient PAGE was done using the Hoefer system. According the requirements 3-16 %, 6-18 % up to 12-18 % gradient gels were prepared using a gradient mixer (self-made stuff). Table 2-19 shows the ratio of the gel components used for the preparation of gradient gels of different percentage.
SDS polyacrylamide gels consist of a stacking and a separation part. The separation gel was casted and layered with H_2O containing 0.2 % SDS to guarantee an even border on top of the gel. After polymerization of the separation gel, the surface was washed shortly with dd H_2O and the stacking gel was poured on top of the separation gel. For mini-PAGE combs with 12 or 20 slots were used. The combs were taken out of the polymerized gel and the slots were washed twice with H_2O bidest before loaded with the sample. The principle of SDS-PAGE is that proteins bind to negatively charged SDS and get linearized. The proteins are now able to migrate to the anode (positively charged) and get separated according to their molecular mass through a defined grid size of polyacrylamide.

Table 2-18: SDS-PAGE composition for 10x mini gels.

Separation gel	**8 %**	**15 %**	**Stacking gel**	**4 %**
Solution A	12.5 ml	12.5 ml	Solution B	7.5 ml
30 % acryl amide	12.89 ml	24.74 ml	30 % acryl amide	5.1 ml
H_2O bidest	21,22 ml	9,84 ml	H_2O bidest	15.3 ml
10 % SDS	500 µl	500 µl	10 % SDS	300 µl
10 % TEMED	300 µl	300 µl	10 % TEMED	300 µl
1.5 % APS	2.5 ml	2.5 ml	1.5 % APS	1.5 ml
Total	**49.91 ml**	**50.38 ml**		**30.0 ml**

Solution A: 1.5 M Tris, pH 8.9, 8 mM EDTA
Solution B: 0.5 M Tris, pH 6.8, 8 mM EDTA

Casted gels were put into a gel chamber and filled with 1 x running buffer until gels were fully covered with buffer. Equal amounts of protein (50-150 µg) have been loaded into the slots together with 3 µl of a coloured protein ladder composed of defined molecular weights. Gel electrophoresis started at 40 V until proteins migrated into the separating gel. Voltage was then increased up to 100-120 V until the gel run was completed according the requirements.

Table 2-19: Gradient SDS-PAGE (Hoefer System).

	Heavy gel acryl amid solution		Light gel acryl amid solution	
	18 %	16 %	9 %	6 %
4x Tris/SDS pH 8.8	3.75 ml	3.75 ml	3.75 ml	3.75 ml
Acryl amide 30 %	9.0 ml	8.0 ml	4.5 ml	3.0 ml
H_2O bidest	1.0 ml	2.0 ml	6.75 ml	8.25 ml
Sucrose	2.25 g	2.25 g	----------	----------
100 % TEMED	10 µl	10 µl	10 µl	10 µl
10 % APS	50 µl	50 µl	50 µl	50 µl
Total	16.06 ml	16.06 ml	15.06 ml	15.06 ml

2.7.4.3 Protein transfer

Denatured and separated proteins have been made accessible to antibody detection by transferring them to either nitrocellulose (NC) or PVDF membranes. This was done working with two distinct methods used for protein transfer.

Tank-Blotting:
The preparation and composition of the sandwich was handled in the same way as described for the Semi-Dry Blotting. The sandwich was placed in an ice-containing tank filled with 1 x transfer buffer so that all components were completely immersed. The transfer was carried out at 100 V per gel for 60 min.

Semi-Dry-Blotting:
PVDF membranes had to be activated in 100% methanol. PVDF membranes were equilibrated together with 7 Whatman papers per gel in transfer buffer for 5-10 min. A sandwich of gel, membrane and Whatman papers was assembled in a Semi-Dry-Blotting chamber. The sandwich was placed between the anode and cathode and consists of three Whatman papers, a nitrocellulose membrane, the gel and four Whatman papers. The chamber was closed with a lid and the blotting proceeded at a constant current of 40 mA per gel for 90 min using mini-gels.

5 x Transfer buffer:	125 mM Tris HCl (pH 6.8), (50 mM DTT in reducing gels), 1 mM EDTA, 2 % SDS, 10 % glycerol, 0.025 % bromphenol blue

2.7.5 Detection of protein bands

Analysis of equal protein transfer on membranes:
Protein separation by SDS-PAGE and protein transfer on nitrocellulose membranes was examined for equal transfer by Ponceau S staining (0.5 % Ponceau red in 3% trichloro acetic acid, TCA). Membranes were destained by shaking those 5 min. in TBST.
Proteins left over in poly acryl gels after PAGE have been stained by coomassie (2.5 % phosphoric acid, 625 mM ammonium sulphate, 0.1% w/v Coomassie brilliant blue G-250) overnight by gentle shaking and destained with 10 % Methanol.

Blocking of the membranes:

To avoid non-specific bindings of the antibody and to increase its specificity membranes with blotted proteins were blocked with 3-5 % non-fat dry milk powder in TBST containing 0.05 % Tween-20. Blocking has been performed at room temperature under gentle agitation for 1 h.

2.7.5.1 Detection of the protein

After washing 3 x 5 min. in TBST membranes were incubated with the indicated primary antibodies listed in Table 2-21. The incubation was carried out overnight at 4 ℃. After primary antibody incubation, the membrane was washed three times in 1 x TBST, followed by a 60 min incubation step at room temperature with horseradish peroxidase-conjugated species specific secondary antibodies (Table 2-22). After three additional washing steps in 1 x TBST, proteins have been visualized by enhanced chemiluminescence (ECL) reagents (Super Signal, West Pico, Thermo). Protein bands on membranes were detected by exposing the blots to high performance chemiluminescence films (GE, Amersham) which were visualized using a developing device (AGFA, Curia 60). A second possibility to detect ECL activated proteins was facilitated using a luminescence imager (Lumi Imager™ F1, Roche Diagnostics, Mannheim) to measure protein band intensities.

Table 2-20: Primary antibodies used for Western Blotting.

Antigen	Species	Clone	Mass (kDa)	Dilution	Supplier
Bcl-2	Monoclonal Mouse	10 C 4	25	WB:1:1000 **IF: 1:200**	Invitrogen
Bcl-2	Monoclonal human	100	25	1:1000	Zymed
Bcl-2	Polyclonal rabbit	22-6	25	**IF: 1:200**	(self-made)
Mcl-1	Polyclonal rabbit		35	1:10000	Rockland
IQGAP2	Monoclonal mouse	BB9	180 human lysate	WB:1:5000 **IF: 1:400**	upstate
Beclin-1	Monoclonal mouse	20	60	1:2000	BD-Bioscience
VDAC1	Monoclonal mouse		30	1:1000	Calbiochem
VDAC-2	Mouse monoclonal		30	1:1000	Abcam
Actin	Mouse	C 4	43	1:40.000	MP-Biochemical's
ATPase	Mouse	Ox-Phos-complex V	56	1:3000	Molecular Probes
Bak (NT)	Polyclonal rabbit	O6-499	26	1:5000	Upstate
Bax (NT)	Polyclonal rabbit		21	1:5000	Upstate
Bid	Rat		15+, 17	1:1000	(Australia)
Bad	Polyclonal rabbit		23	1:1000	Cell signaling
Cytochrome c	Monoclonal mouse	BALB/c	15	**IF: 1:50**	BD Pharmingen
Puma	Polyclonal rabbit		(23), 27	1:1000	ProSci

Table 2-21: Secondary antibodies used for Western Blot

Antigen	Species	Tag	Dilution	Supplier
Mouse H+L	Goat	HRP	1:8000 3 % milk	Jackson Laboratories
Mouse H+L Affinity purified	Goat	HRP	1:8000 3 % milk	Jackson Laboratories
Mouse-Fc	Goat	HRP	1:8000 3 % milk	Jackson Laboratories
Rabbit H+L	Goat	HRP	1:8000 3 % milk	Jackson Laboratories
Rabbit H+L Affinity purified	Goat	HRP	1:8000 3 % milk	Jackson Laboratories
Rabbit-Fc	Goat	HRP	1:8000 3 % milk	Jackson Laboratories
Rat	Goat	HRP	1:10000 3 % milk	Dianova

Membrane stripping:

Primary and secondary antibodies bound on PVDF were washed off and reused for a second probing when required. For that purpose, antibodies from the first incubations have been stripped off the membranes with 50 ml Solution A containing 10 % DTT by agitation at 50 ℃ for 30 min. After three additional washing steps in TBST for 15 min, membranes were incubated in the respective blocking reagent overnight at 4 ℃ before a new incubation with primary and secondary antibodies was possible.

2.7.6 Silver staining

To detect protein bands within polyacryl gels we used the silver staining method. With this method we are able to detect between 0.6-1.2 ng of proteins in a gel. In contrast, coomassie needs 36-47 ng protein that is 100 times more as compared to silver staining. Due to the high sensitivity to detect proteins by silver staining it is compelling to work with gloves, hair protection, a mask and a lab coat to avoid protein contaminations. All devices used during this method were cleaned before usage with formic acid (1 %) and cleaned intensely with double distilled water.

First and second dimension gels were stained using the Silver Quest silver staining kit (Invitrogen) according to the protocol provided by the manufacturer. Stained gels were scanned (Cano Scan, Canon) for documentation.

2.7.7 Mass spectrometry

Mass spectrometry determines the masses of particles, for determining the elemental composition of a sample or molecule, such as peptides and other chemical compounds. During mass spectrometry charged molecules or molecule fragments are generated and their mass-to-charge ratios are measured. The obtained mass spectra from proteins are then analysed by the Mascot software that combines several data bases.

Because mass spectrometry detects the elemental compositions of proteins it is useful to take care during preparation and handling of the samples. Therefore, gloves, lab coat, a surgical mask, and cap were worn at all times during sample preparation. All reagents were prepared freshly and filter sterilized. The equipment was thoroughly cleaned with 1% formic acid, 75% EtOH and rinsed with double distilled water (dd H_2O).

Sample preparation and trypsin digestion:

The tryptic in-gel digest of the protein samples was performed according to the protocol obtained from Dr. Martin Biniossek, from the Department of Central Mass Spectrometry. The gel was placed on a transilluminator and sizes of gel segments were organized according to their molecular size before excising them. Each segment was cutted with a new sterile scalpel to avoid any contamination of proteins. The gel slices were transferred to 1.5 ml tubes and cut into small pieces inside of the tubes. Destaining of the gel slices was not necessary (personnel communications, Dr. Martin Biniossek).

Cutted gel pieces were washed in 100 µl ddH_2O for 10 min at RT, the water discarded and 100 µl acetonitril (CH_3CN) was added for 15 min. at RT. Acetonitril an organic solvent dehydrates the gel pieces by displacing water out if the gel so that it shrinks. The CH_3CN was removed and the gel pieces dried in a Vacuum Concentrator (Speed vac) for 10 minutes. Dried gel pieces were reduced in 100 µl of 50 mM ammonium bicarbonate (NH_4HCO_3) supplemented with 10 mM DTT at 56 ℃ for 30 to 60 min. To block the N-termini of proteins DTT was replaced with an equal volume of 50 mM NH_4HCO_3 supplemented with 55 mM iodacetamide and incubated for 30 min. in the dark. The samples were vortexed every 10 min. during incubation. After removing of the alkylating reagent the gel pieces were washed with 100 µl 50 mM NH_4HCO_3 for 15 min. Than the NH_4HCO_3 was removed and again replaced with 100 µl CH_3CN and dehydrated for 10 min. The supernatant was removed and the gel pieces have been completely dried in the vacuum concentrator (10 min).

To digest proteins by trypsin gel pieces were hydrated in 50 µl of 50 mM NH_4HCO_3 buffer supplemented with 12.5 ng/µl trypsin on ice for 60 min. A volume of 10-20 µl 50 mM NH_4HCO_3 was added to gel pieces after 60 min. incubation on ice when cutted pieces were

not completely covered with trypsin-solution. Proteins in gel pieces were than further digested over night at 37 ℃.

The next day, the first supernatant with the digested proteins was transferred to a 0.5 ml microfuge tube from Eppendorf. Acetonitril (50 µl) was added on top of the gel pieces and incubated for 15 min in a sonicator at 4 ℃ thereby all trypsinized peptides were solved out of the gel. This second supernatant was added to the first over night supernatant and the samples were dried again in the vacuum concentrator for 1-2 h. Dry samples were stored at -20 ℃ until Mass spectrometry analysis (MS/MS) of the samples was performed by Dr. Martin Biniossek, from the 'Central Mass Spectrometry Unit of the Medical Faculty' and the 'Center of Biochemistry and Medical Cell Research (ZBMZ)' at the University of Freiburg.

MS/MS measurement and protein identification:

The Nanoflow-HPLC-MS/MS measurements of the digested protein samples were done using a LTQ-FT mass spectrometer (Thermo Scientific, Bremen) or an Orbitrap XL (Thermo Scientific, Bremen) linked to an Ultimate3000 HPLC system (Dionex, Idstein). The HPLC-column tips with 75 µm inner diameter were packed with Reprosil-Pur 120 ODS-3 (Dr. Maisch, Ammerbuch). A gradient of A [0, 5% acetic acid (ACS Reagent, Sigma) in water] and B [0, 5 % acetic acide in 80% ACN (HPLC gradient grade, SDS, Peypin, France)] with increasing organic portion were used. For the protein identification a MASCOT-Software (Matrix science, London, United Kingdom) was used combined with the NCBI_nr data bank (National Center for Biotechnology Information, WA, and USA). The search criteria were: m/z monoisotopisch; mass accuracy for MS ≤ 15 ppm, for MS/MS ≤ 0, 8 Da; up to one „missed cleavage"; variable modifications: Carbamidomethyl (-Cys), Propionamid (-Cys), Oxidation (-Met), Gln -> pyro- Glu (N-term Gln), Glu -> pyro-Glu (N-term Glu)).

3 RESULTS

IL-3 dependent cells have shown to be a physiological working model for understanding the proliferation and survival of cytokine-dependent cells. During inflammation activated T cells produce IL-3 thereby promoting the expansion of hematopoietic populations, in particular of the myeloid, monocytic lineage. In a controlled system attenuation of the inflammatory response requires depletion of IL-3 followed by the induction of apoptosis of inflammatory cells. Deregulated expression of pro-survival members of the Bcl-2 family such as Bcl-2 leads to the abrogation of apoptotic pathways and the generation of malignant disease as it is shown for follicular B cell lymphoma (Johnson et al 1997., Hanahan D. and Weinberg et al., 2000). In leukaemia up regulation of IL-3 is reported to trigger the expression of anti-apoptotic Bcl-2 proteins thereby neutralizing pro-apoptotic proteins ensuring enhanced survival. In this context, to investigate endogenous binding partners of Bcl-2 "in vitro" it is important to use a cellular system as close as possible to the physiological conditions.

3.1 Regulation of survival and death in factor-dependent monocytic hematopoietic progenitor cells (FDM)

FDM cells were generated (see Materials and Methods) from wild-type C57BL/6 mice as well as mice deficient for various Bcl-2 family proteins. There are several advantages to work with FDMs as compared to other cell lines like FDC-P1 and FL5.12: (i) in FDMs a large number of Bcl-2 family protein knock-out lineages are available which can be used as negative controls for our proteomics approach (ii) FDMs are suspension cells and can be mass-cultured. This is needed to produce enough protein of interest for effective immunoprecipitation.

FDMs are IL-3 dependent and therefore require recombinant IL-3 or multicolony stimulating factor (multi-CSF) in the medium to survive and proliferate. IL-3 promotes cell survival by activating the phosphatidylinositol (PI) 3-kinase/AKT signaling pathway. Depletion of IL-3 leads to activation of caspases and a commitment to cell death (Johnson et al., 1997).

Relatively late in apoptosis, the phospholipid phosphatidlyserine (PS) translocates from the inner to the outer leaflet of the plasma membrane and serves as an "eat me" signal for phagocytes (Fadok and Henson, 2003). After recognition via a specific PS receptor these phagocytes engulf the apoptotic remnants (Fadok et al., 2000, Savill and Fadok, 2000, Danial and Korsmeyer, 2004). If phagocytes are not present, which is the case for apoptotic cells in culture, the dying cell proceeds to necrosis which is characterized by cell lysis due to a fall in ATP and the disruption of ion homeostasis.

Thus, all cells in culture eventually move to necrosis at later stages. Surface exposed phosphatidylserine binds a 35-36 kDa protein, called annexin-V with high affinity in the presence of Ca^{2+}. By fluorescently marking annexin-V (for example with GFP or FITC), this property can be exploited to quantitatively determine apoptotic cells by FACS analysis. However, in necrotic cells (late phase of cell death), annexin-V can enter through the perforated plasma membrane and label PS from the inside. Therefore, a second marker is needed to distinguish between apoptotic and necrotic cells that is based on membrane permeability. Propidium iodide is a membrane impermeable DNA intercalating agent that only enters necrotic, permeabilized cells. Therefore, cells become double annexin-V/PI positive as a matter of post-apoptotic necrosis, which is hereafter referred to as dead cells. We used GFP-conjugated annexin-V (GFPAnV) and propidium iodide (PI) to perform these experiments. The number of apoptotic and living cells is quantified by flow cytometry analysis (FACS) (see chapter 2.4.1) (see Fig. 3-1)

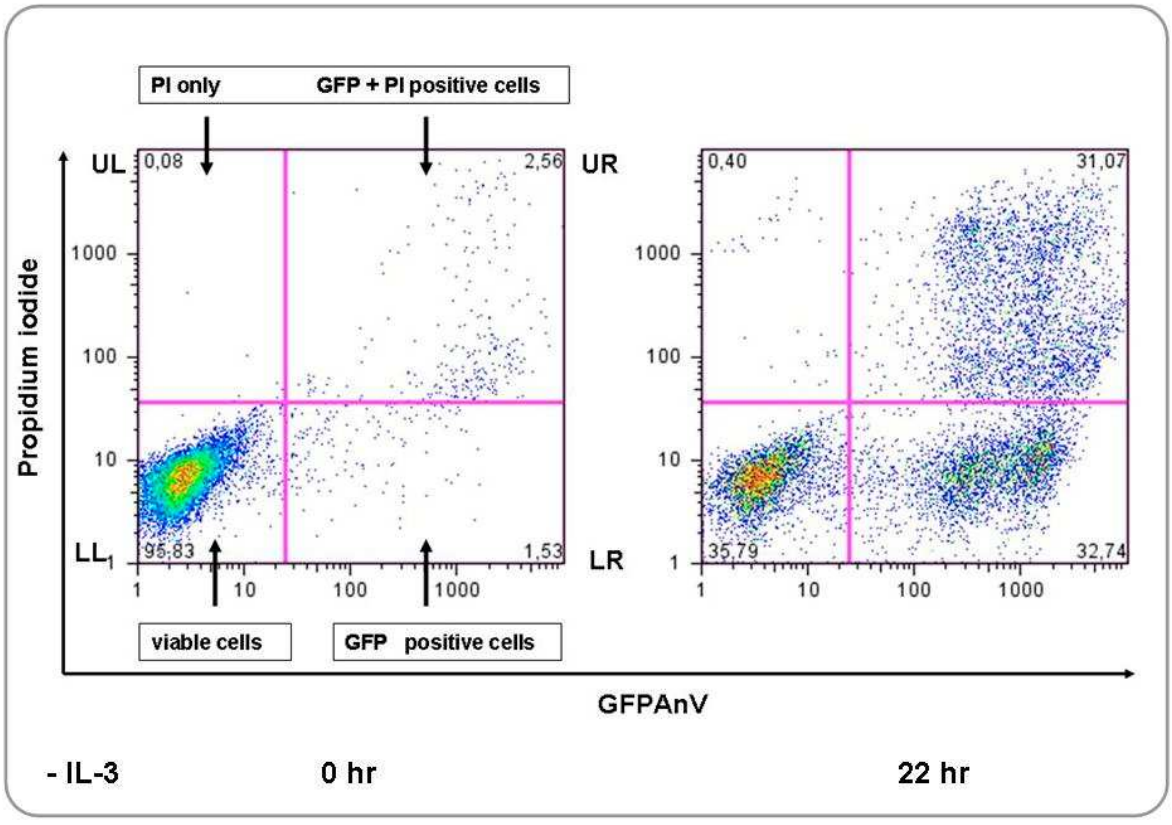

Figure 3-1: Survival or death of cells detected by flow cytometry. FACS analysis of GFPAnV/PI stained Bcl-2 $^{+/+}$ FDM cells at the indicated time points of IL-3 depletion. Dot blots represent GFPAnV stained cells along the x axis and propidium iodide staining along the y axis. Number of viable cells in the lower left (LL), apoptotic in the lower right (LR) and dead/necrotic cells in the upper right/left (UR + UL) quadrants, respectively.

3.1.2 Bcl-2 a survival factor in IL-3 dependent cells: accelerated cell death in Bcl-2 $^{-/-}$ cells

We wanted to find out how efficient FDM cells die in response to IL-3 deprivation and if this cell death was accelerated in cells deficient of the survival factor Bcl-2. Figure 3-2 shows that upon IL-3 withdrawal the number of viable wild type Bcl-2 cells (annexin-V/PI negative, lower left quadrant) gradually shifted to apoptotic (annexin-V positive/PI negative, lower right quadrant) and necrotic/dead cells (annexin-V/PI positive, upper right). While at 8 hr of IL-3 deprivation, most of the dying cells were still apoptotic, the number of necrotic cells increased until 24 h (Fig. 3-2). At 24 h, about 58 % of the cells had died (Fig. 3-3). This indicated that the cells had undergone apoptosis followed by secondary necrosis, as stated above.

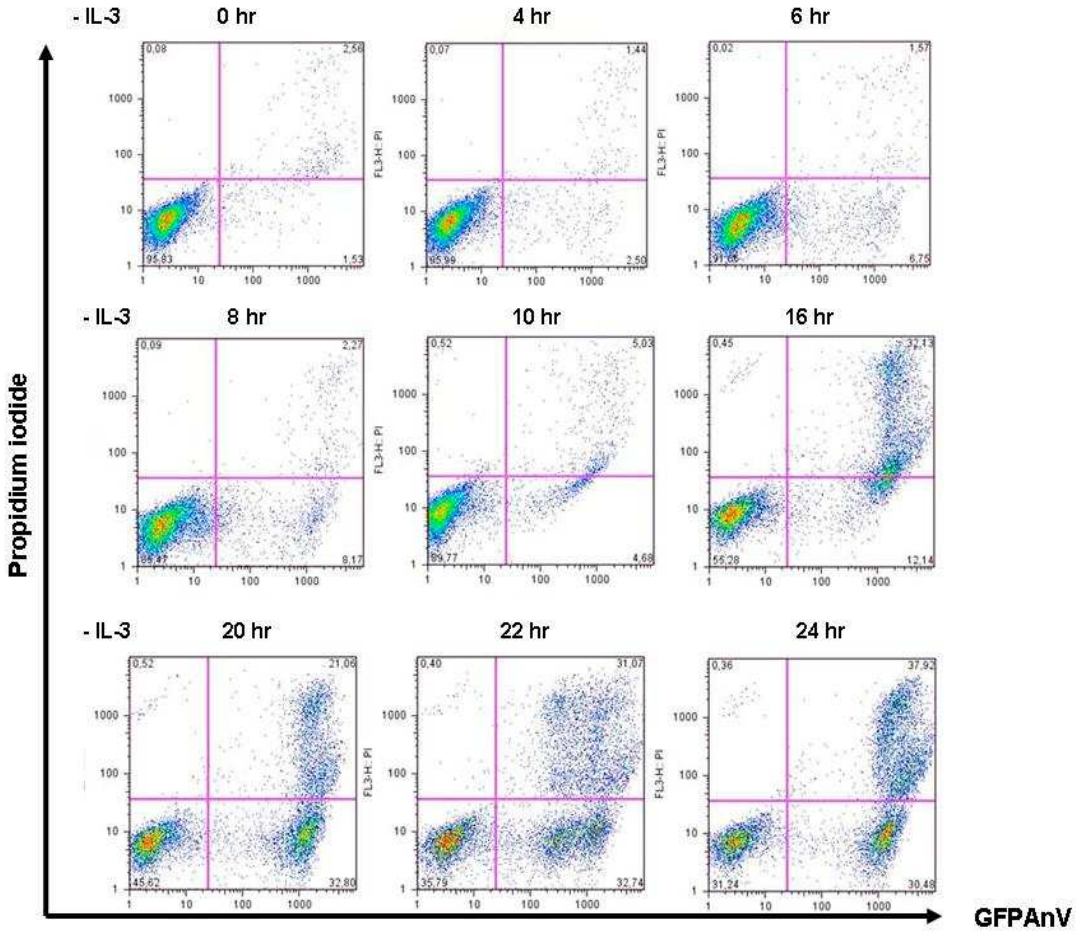

Figure 3-2: Bcl-2 $^{+/+}$ FDM cells exhibit an increase of apoptotic and secondary necrotic cells over a 24 hr time period. After withdrawing IL-3 from the growth medium Bcl-2 $^{+/+}$ FDMs were analysed at variable time points (hr – IL-3) for GFP-annexin V (GFPAnV) and propidium iodide (PI) staining. The number of fluorescent cells was quantified by using a flow cytometer. Dot blots showing the distribution of viable, apoptotic and dead cells.

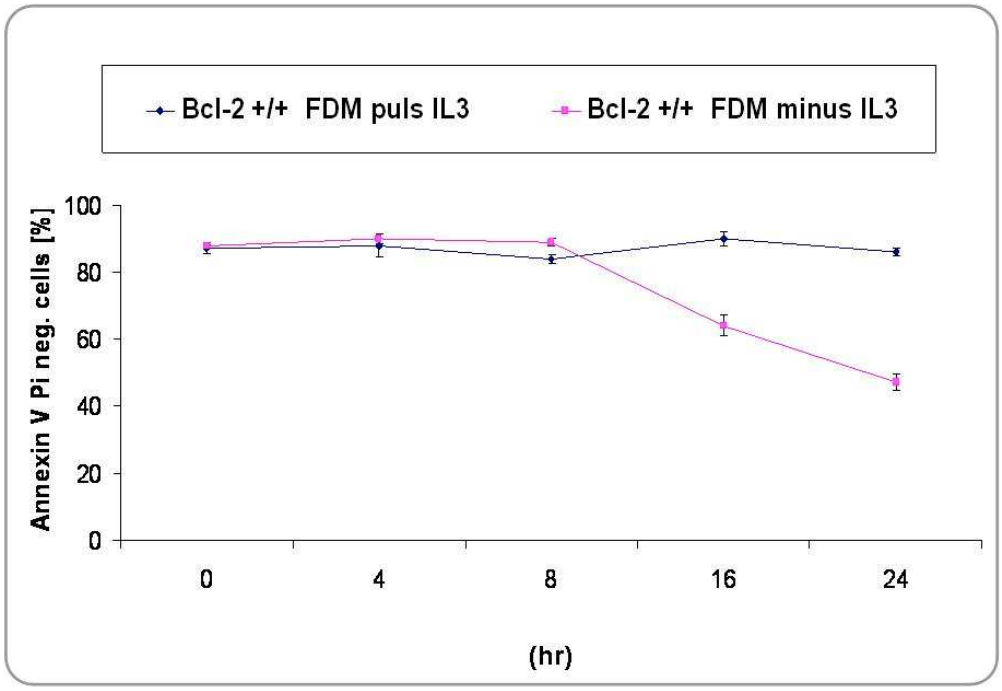

Figure 3-3: Bcl-2 $^{+/+}$ FDM cells start to die after 8 hrs. Quantitative analysis of the dot blot shown in Fig. 3-2. Annexin V/PI (GFPAnV) negative cells represent the number of "viable cells" (%). Data are mean of 3 independent experiments (n = 3) ± S.D.

We then determined apoptosis efficiency in IL-3 deprived Bcl-2 $^{-/-}$ FDMs. As expected from removing a crucial survival factor, these cells started to expose phosphatidylserine much earlier (4 hr) than Bcl-2 $^{+/+}$ FDMs (8 hr) (Fig. 3-4). At 16 h after IL-3 removal, nearly all Bcl-2 deficient cells had died whereas 68 % of the wild type cells were still alive (Fig. 3-4 and 3-5).

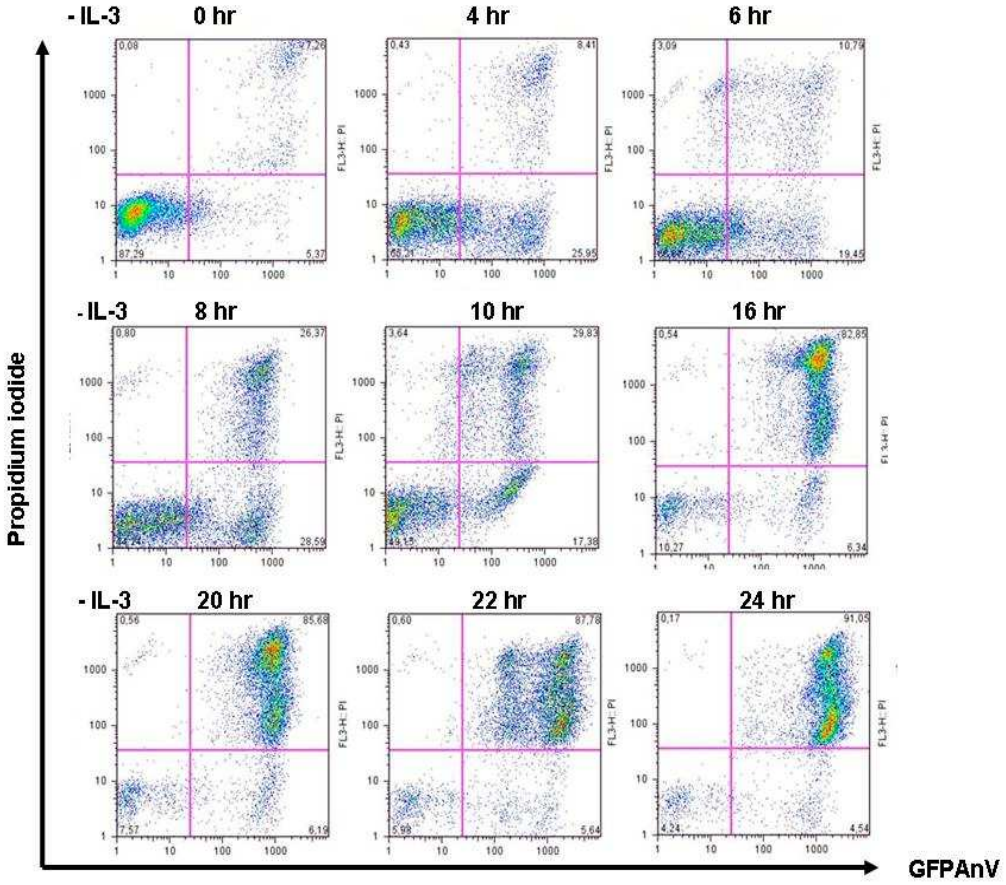

Figure 3-4: Accelerated cell death of Bcl-2 $^{-/-}$ FDM. Cell death of IL-3 depleted Bcl-2 $^{-/-}$ FDM was quantified at variable time points (up to 24 hr – IL-3) by GFP-annexin V (GFPAnV) and propidium iodide (PI) FACS analysis. Dot blots showing the distribution of viable, apoptotic and secondary necrotic cells.

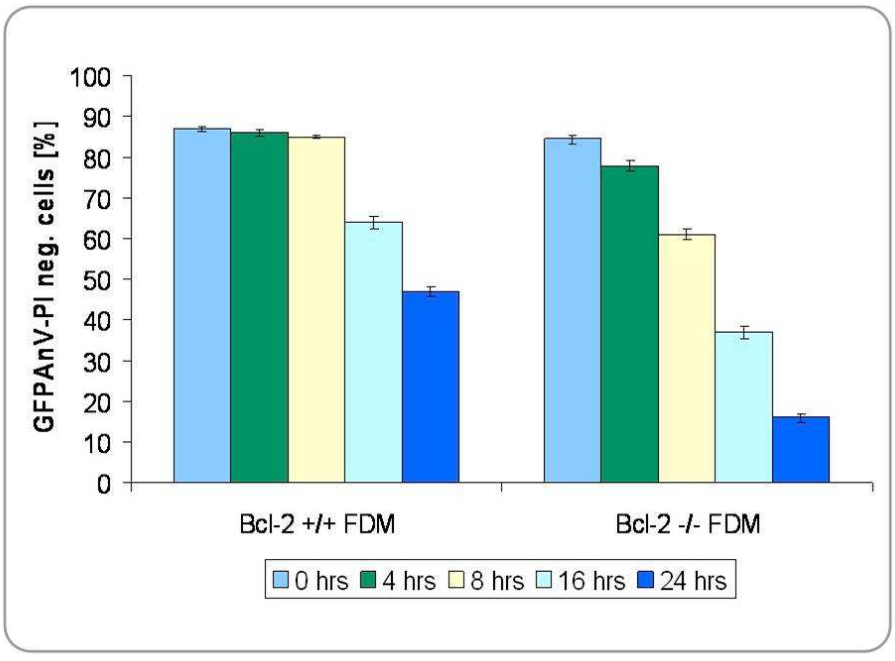

Figure 3-5: Accelerated cell death of Bcl-2 $^{-/-}$ FDM. Quantitative analysis of the dot blot shown in Fig. 3-4. Annexin V/PI (GFPAnV) negative cells represent the number of "viable cells" (%). Data are mean of 3 independent experiments (n = 3) ± S.D.

3.2 Expression and distribution of Bcl-2 family proteins in healthy and IL-3 deprived monocytes

To unravel how the expression and subcellular distribution of specific Bcl-2 family proteins is regulated during IL-3 deprivation-induced apoptosis of monocytes, we determined the levels and intracellular localization of these proteins in extracts of healthy and apoptotic FDMs.

3.2.1 Changes of Bcl-2, Bax and Bak levels in response to IL-3 deprivation

First, Bcl-2, Bak and Bax expression levels were examined by Western blot analysis in total extracts of healthy and apoptotic wild type FDMs. While the amounts of Bax and Bak did not change at all in response to IL-3 withdrawal, Bcl-2 levels slightly decreased. This was most likely due to a proteasomal degradation of Bcl-2 because the treatment of IL-3 deprived cells with the proteasome inhibitor MG132 did not show this down regulation (Fig. 3-6). Our result is consistent with previous findings that Bax and Bak are not regulated on the transcriptional or posttranscriptional level but by their changes in subcellular localization (Bax) and their propensity to change their conformation and oligomerize.

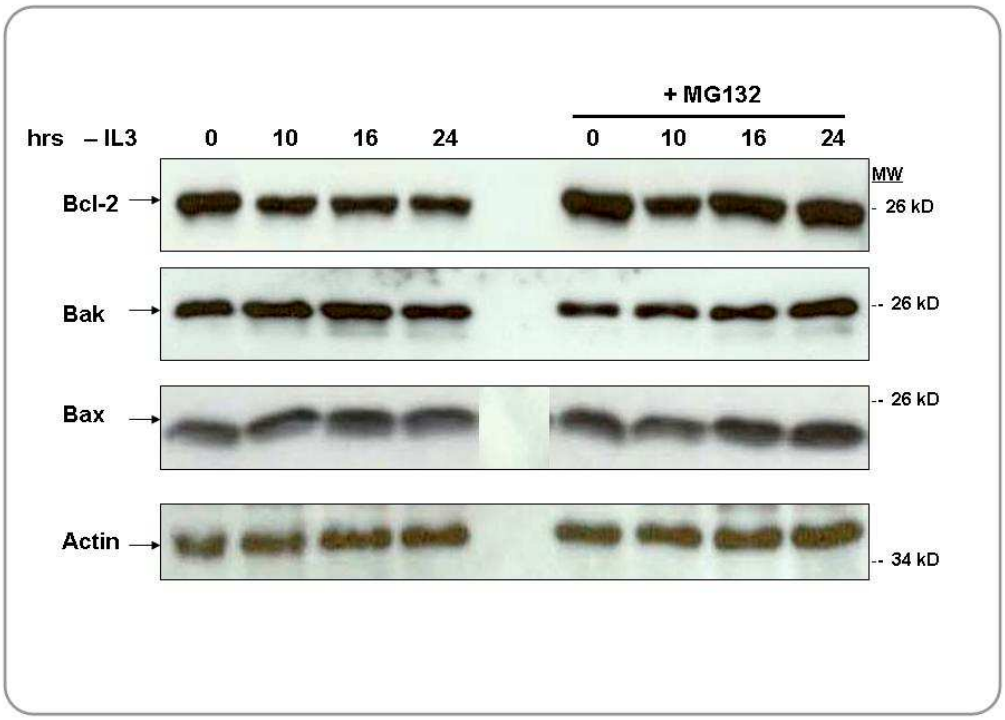

Fig. 3-6: Expression of Bax, Bak and Bcl-2 does not change. Endogenous Bcl-2, Bax and Bak were determined by Western blotting in total extracts of Bcl-2 $^{+/+}$ FDMs. Cells were incubated in IL-3 free medium for the indicated time periods. Mini PAGE 15 %, 1% CHAPS IBC Buffer, 2 x Protease Inhibitors, 4 µM MG132, 50 µg protein total samples per slot. Actin serves as a loading control.

3.2.2 Bcl-2 family members localize to different cellular fractions in healthy and IL-3 deprived mouse monocytes (FDM and FDC-P1)

Next we determined the subcellular distribution of Bcl-2 family proteins between the cytosol, and heavy (mitochondria) and light membranes (ER) in FDMs (Fig. 3-7). In these cells Bcl-2 was constitutively found on the mitochondrial membrane and did not change its localization in response to IL-3, however the level of Bcl-2 decreased in apoptotic cells. By contrast, the survival factor Mcl-1 was more or less equally distributed between the cytosol and mitochondria (on mitochondria it runs as a double band). Upon IL-3 withdrawal, this protein exhibited proteasomal degradation, preferentially on mitochondria, as previously reported (Nijhawan*, et al.*, 2003; Maurer*, et al.*, 2006). The subcellular localization did however not change.

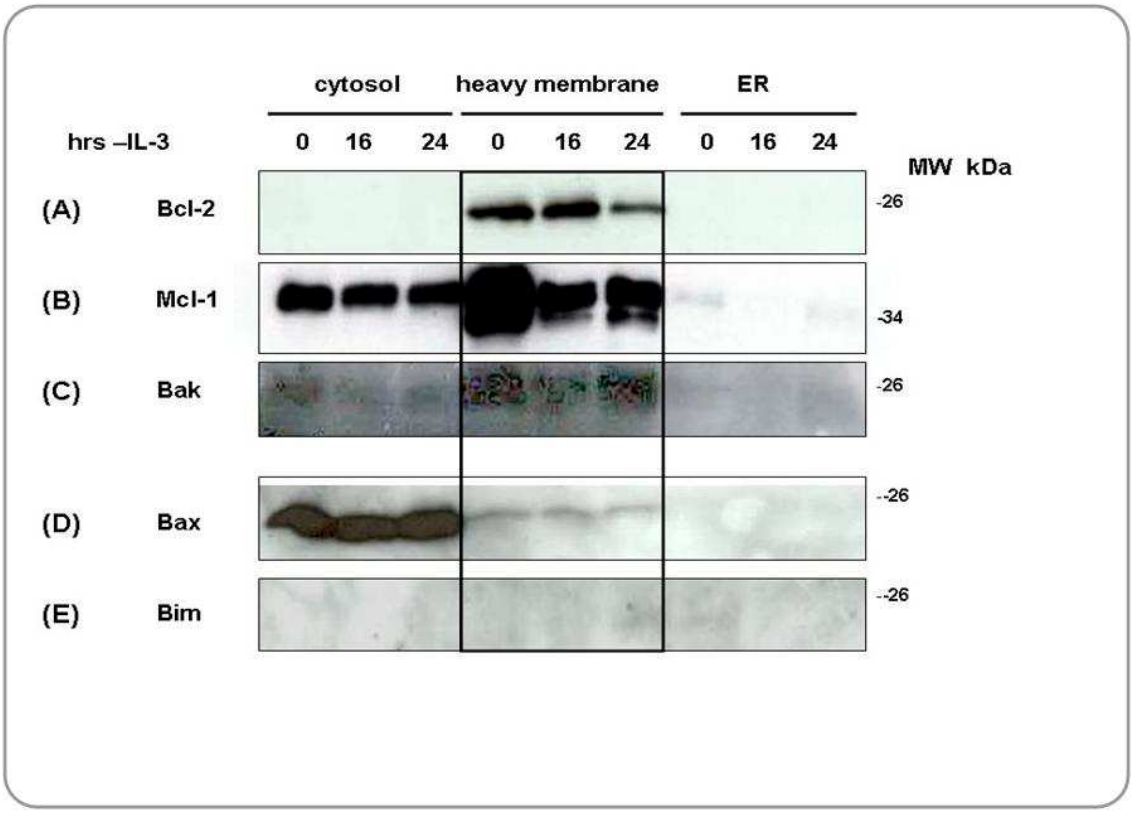

Fig. 3-7: Subcellular distribution of Bcl-2 family proteins healthy and IL-3 deprived FDMs. **(A)** Bcl-2 is permanently bound to mitochondria and its level decrease in response to IL-3 removal. **(B)** Mcl-1 is equally distributed between cytosol and heavy membranes and also gets degraded by IL-3 removal **(C)** Bak is only located on mitochondria **(D)** Bax is only found in the cytosol and did not translocate to mitochondria. **(E)** Bim could not be detected in any fraction. Cells were incubated in IL-3 free medium for the indicated time periods. Mini PAGE 15 %, **1 %** CHAPS IBC Buffer, 2 x Protease Inhibitors, 4 µM MG132, 50 µg protein total samples per slot.

The pro-apoptotic protein Bim, a BH3-only proteins majorly implicated in cytokine deprivation induced apoptosis could not be detected in the extracts of wt FDM cells (Fig. 3-7). This was

probably for two reasons. Firstly, Bim is often not expressed in healthy cells but gets transcriptionally induced in response to cytokine deprivation (Dijkers et al., 2000). Secondly, FDMs are immortalized by the Hox8b gene (see Materials and Methods) and it was been previously shown that Hox8b represses Bim transcription. Bak is already on heavy membranes of healthy FDM cells and stays more or less at similar levels after IL-3 deprivation. Bax is almost uniquely found in the cytosol fractions, and unexpectedly, it translocated only little to mitochondria in response to IL-3 deprivation. This is consistent with a previous finding that majorly Bak, but not Bax is involved in IL-3 deprivation induced apoptosis (Ekert et al., 2006).

To confirm the subcellular localization of Bcl-2 family members in another monocytic cell line, we performed similar Western blots analysis on extracts of healthy and IL-3 deprived. Like in FDMs, Bcl-2 and Bak were constitutively localized to mitochondria and did not change their localization upon IL-3 removal. Bax was again cytosolic but did not majorly move to mitochondria in apoptotic cells. Bim was this time induced on mitochondria in response to IL-3 consistent with the known transcriptional induction of this protein in cytokine-deprived cells. By contrast, the BH3-only proteins Bad and Bid mainly resided in the cytosol in healthy cells and both were proteolytic degraded in response to IL-3 deprivation. While Bid has never been implicated in this type of cells death, Bad was shown to play some role, but this initial finding has largely been disputed meanwhile. Surprisingly, Puma was already attached on heavy membranes in healthy cells and stays at equal levels throughout apoptosis after IL-3 withdrawal. This has not been found so far because, as with Bim, Puma has so far thought to be not or low expressed in healthy cells and to be transcriptionally induced in response to IL-3 deprivation. Interestingly, Puma ran as double band and the upper band was further induced after 16 h IL-3 deprivation. The nature of this band needs however to be identified.

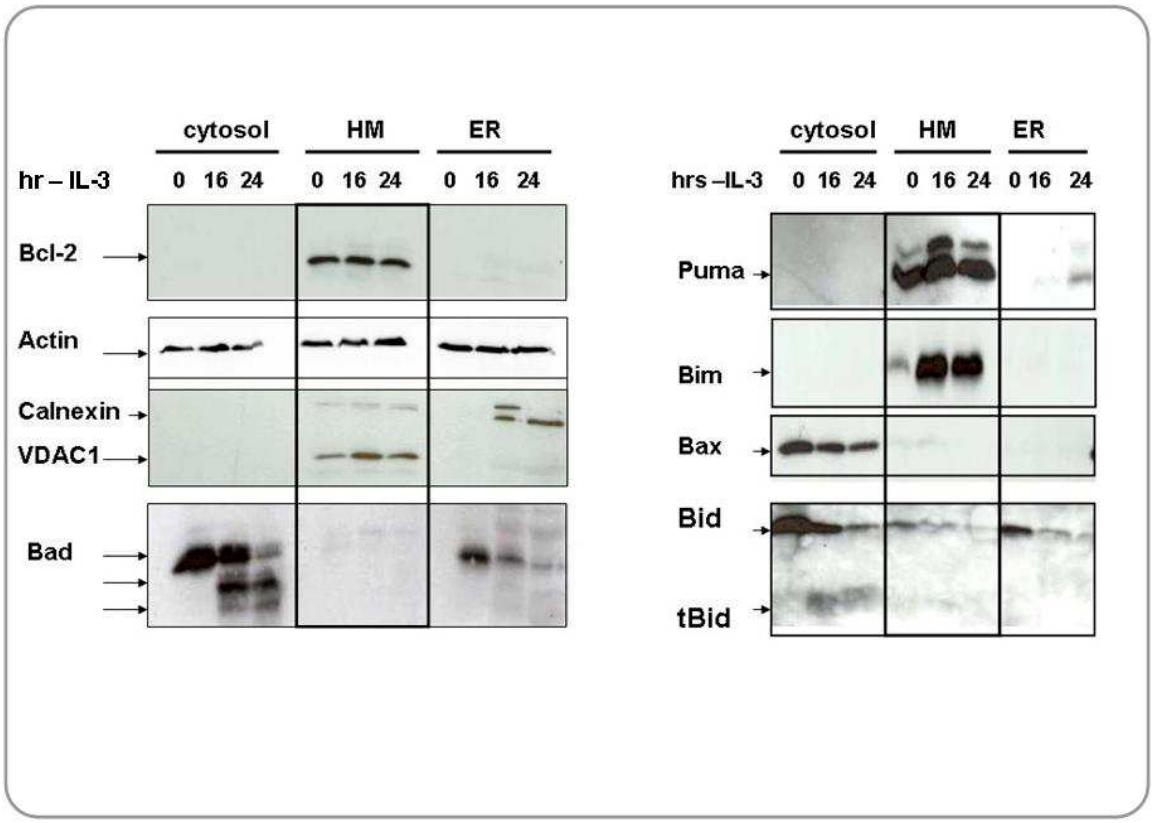

Fig. 3-8: Subcellular distribution of Bcl-2 family members in FDC-P1 cells. FDC-P1 were deprived of IL-3 for the indicated time periods and cellular fractions of cytosol, heavy and light membranes were prepared to analyse the expression of Bcl-2, Bad, Bax, Bid and Puma. Actin served a loading control for the cytosol, VDAC1 for heavy membranes and calnexin for light membranes. Mini PAGE 15 %, 1 % CHAPS IBC Buffer, 2 x Protease Inhibitors, 4 µM MG132, 50 µg protein per slot.

3.3 Investigating endogenous Bcl-2 protein complexes by blue native polyacrylamide gel electrophoresis (BN-PAGE)

To get an idea how Bcl-2 family members interact with each other in healthy and IL-3 deprived monocytes and to isolate novel Bcl-2 binding protein that may further regulate the anti-apoptotic function of Bcl-2, we started to separate Bcl-2 protein complexes by blue native (BN) polyacrylamide gel electrophoresis (BN-PAGE). The components of these complexes were then further dissected on a second dimension SDS-PAGE. To extract protein complexes of Bcl-2 form the mitochondrial membrane of FDMs, the detergent digitonin was used. We first determined the optimal concentration of digitonin to get maximal Bcl-2 solubilization from membranes.

3.3.1 Solubilization of Bcl-2 from heavy membranes of FDM cells

Firstly, the digitonin concentration was titrated against a fixed protein concentration of a mitochondria enriched fraction of wt FDMs to solubilize as much Bcl-2 protein complexes as possible out of the membrane. The solubilized samples were first separated on a BN-PAGE followed by transferring the native gel to PVDF membranes for detecting Bcl-2 complexes by anti-Bcl-2 Western blotting. As shown in Fig. 3-9, the detergent/protein ratio had a remarkable effect on Bcl-2 protein complexes because the more digitonin in relation to total mitochondrial protein, the lower the complexes.

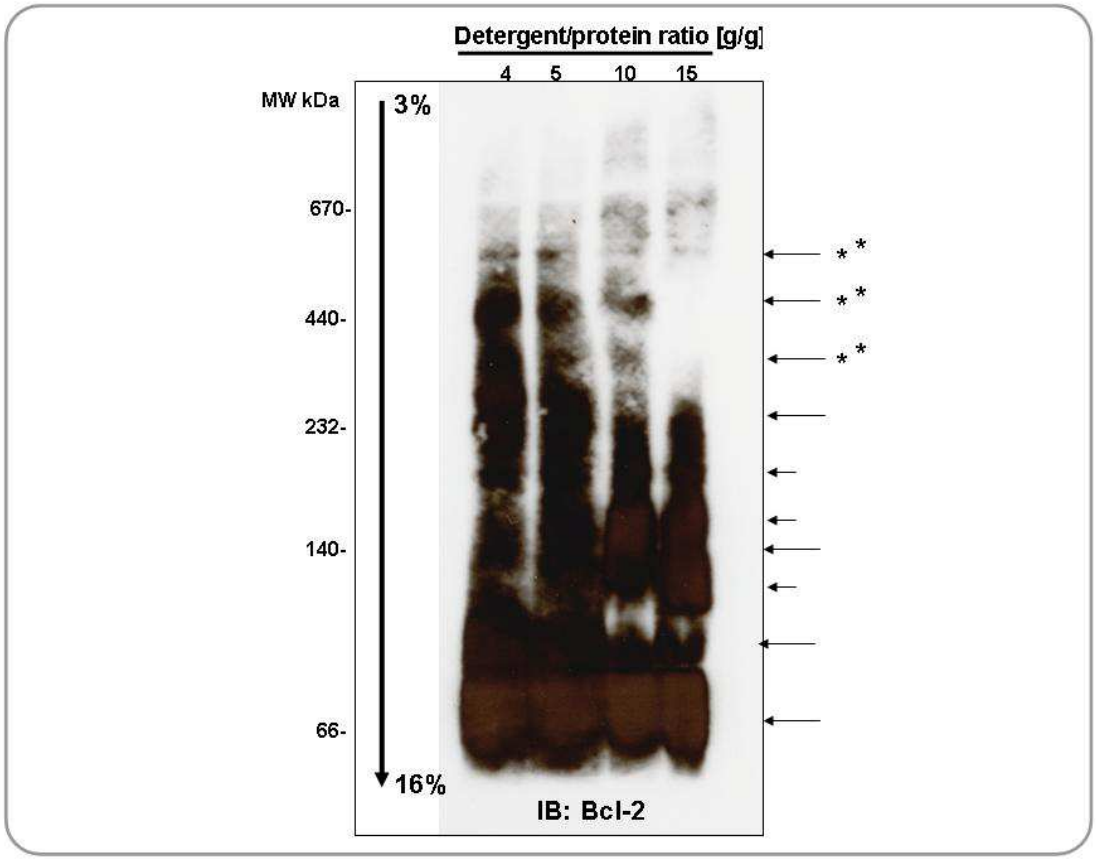

Figure 3-9: First dimension blue native PAGE (BN-PAGE) of endogenous Bcl-2 protein complexes. Arrows with asterisks: High molecular protein complexes fragment into smaller complexes by increasing concentrations of detergent. Arrows depict possible complexes containing Bcl-2; Long and short arrows depict protein sub complex composition that change by increase or decrease of digitonin/protein ratios. Samples of heavy membranes from wt FDM (150 µg/slot) were solubilized with 4, 5, 10 and 15 g digitonin/g protein and separated by BN-PAGE (3-16 %). After transfer to PVDF membranes a Western blot analysis of Bcl-2 was performed.

This was confirmed by running the blue-native strips on a second dimension SDS-PAGE separating the complexes and then probing again for Bcl-2 by Western blotting. As demonstrated in Fig. 3-10, we found that the lower the digitonin/protein ratio, the higher the Bcl-

2 complexes detected. This finding could indicate that a lower digitonin concentration insufficiently solubilizes the membranes such that big membrane pieces appear that run at high molecular masses on polyacrylamide gels. Alternatively, a high detergent concentration may disrupt part of the high molecular mass complexes so that we would lose them for further identification of their components.

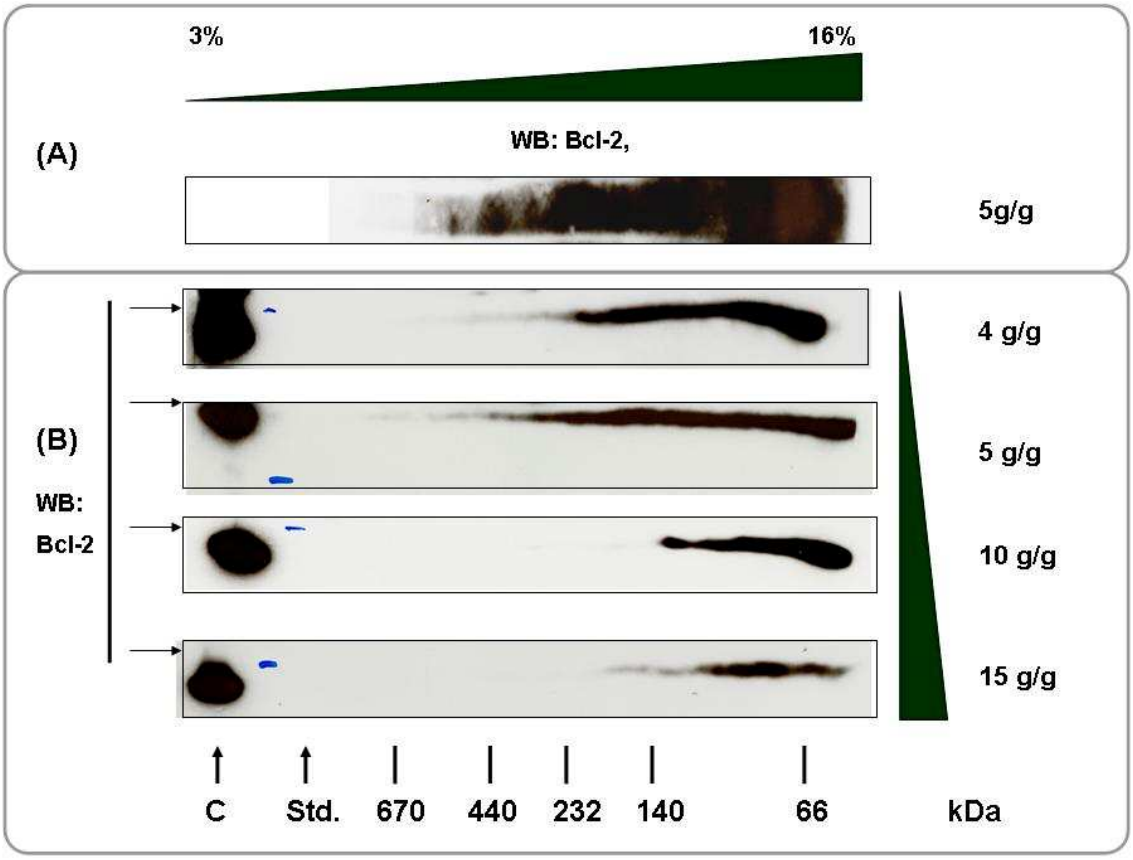

Figure 3-10: Bcl-2 is found in a trailing band (low to high molecular weight complexes) on 2D-BN-SDS-PAGE after digitonin solubilization. Anti-Bcl-2 Western blot of **(A)** first dimension BN-PAGE showing the 5g/g detergent/protein ratio **(B)** second dimension SDS-PAGE (2D-BN-SDS-PAGE) (6-16%) of the first dimension BN-PAGE equivalent of 4, 5, 10 and 15 g digitonin/g protein ratios, C=control sample, Std. = high molecular weight standard.

The detergent/protein ratio of 5 g/g showed the most reproducible band pattern after 2D-BN-SDS-PAGE. We therefore used this ratio to prepare all further solubilized heavy membrane samples to investigate the distribution of endogenous protein complexes containing Bcl-2 and other family members of the group. To increase the protein level for the isolation of Bcl-2 binding partners, 400µg solubilized heavy membrane extract were used for each sample. Figure 3-11 shows detected Bcl-2 still as a protein band that trails from the low molecular weight area (30-230 kDa) throughout to the high molecular weight area (230-700 kDa). Most of the Bcl-2 is

part of low molecular weight protein complexes (30-140 kDa), and fewer complexes containing Bcl-2 of molecular size from 230-670 kDa and more.

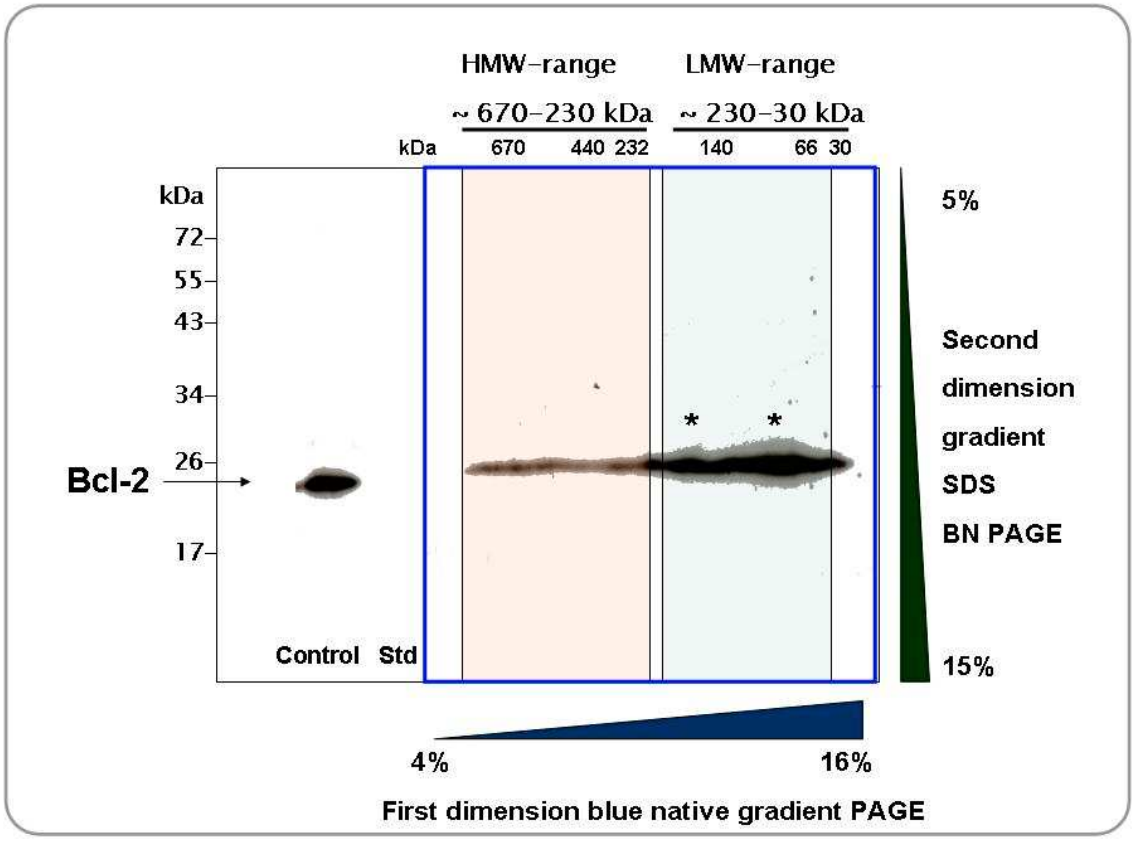

Figure 3-11: Two major Bcl-2 protein complex areas are detected by 2D-BN-SDS-PAGE. (*****) Some possible Bcl-2 sub-complexes are seen within the low molecular weight complex area from 30-230 kDa. The blue frame corresponds to the first dimension of blue native PAGE. Anti-Bcl-2 Western blot of digitonin-solubilized Bcl-2 complexes (5 g/g) from 400 ug mitochondrial protein of wt FDMs, separated by 2D-BN-SDS-PAGE (4-16 % BN-PAGE, 5-15 % 2D-SDS-PAGE gradients).

3.3.2 Co-migration of putative Bcl-2 binding partners on 2D-BN-SDS-PAGE

Since we found that Bcl-2 is a part of multiple protein complexes from 30 kDa up to 670 kDa in size, we tested the eventual co-migration of various known and putative Bcl-2 partners on 2D-BN-SDS-PAGE. Although such an analysis does not tell us anything about their physical interaction with Bcl-2, it at least gives a hint if they could bind to Bcl-2 or not. As shown in Fig. 3-12, when a heavy membrane extract of wt FDMs was analyzed by this method, VDAC-1, VDAC-1, Beclin-1 and some Bak co-migrated with Bcl-2 in the high molecular weight region between 230 – 670 kDa (pink area). By contrast, Mcl-1, Bax and most of Bak were rather present in the lower region of 30 – 230 kDa (green area). After 10 h or IL-3 deprivation, the migration of the most complexes did not majorly change. In particular, again, we did not observe any major oligomerization (up shift) of Bax. By contrast, the high molecular mass complexes of Bak clearly

increased confirming that oligomerization and activation of Bak was probably more crucial for IL-3 deprivation induced cell death that activation of Bax. Consistent with previous findings, Mcl-1 was partially degraded after IL-3 removal and found in similar molecular weight fractions of gel filtrations between 40-150 kDa (Nijhawan*, et al.*, 2003; Maurer*, et al.*, 2006). In addition, we observed a degradation of Beclin-1, which was most likely due to caspase activation and thereby inhibition of beclin-1-mediated autophagy. In general, 2D-BN-SDS-PAGE analysis revealed that Bcl-2 family proteins exhibit a distinct pattern of overlapping protein areas in healthy and IL-3 deprived monocytes. But as this method does not detect protein-protein interactions we still have to prove which co-migrating protein indeed interacts with Bcl-2. To do this, we established specific, highly efficient anti-Bcl-2 immunoprecipitations which could be analysed for known or suspected binding partners using specific antibodies on a Western blot or used to identify new binding partners by mass spectrometry analysis.

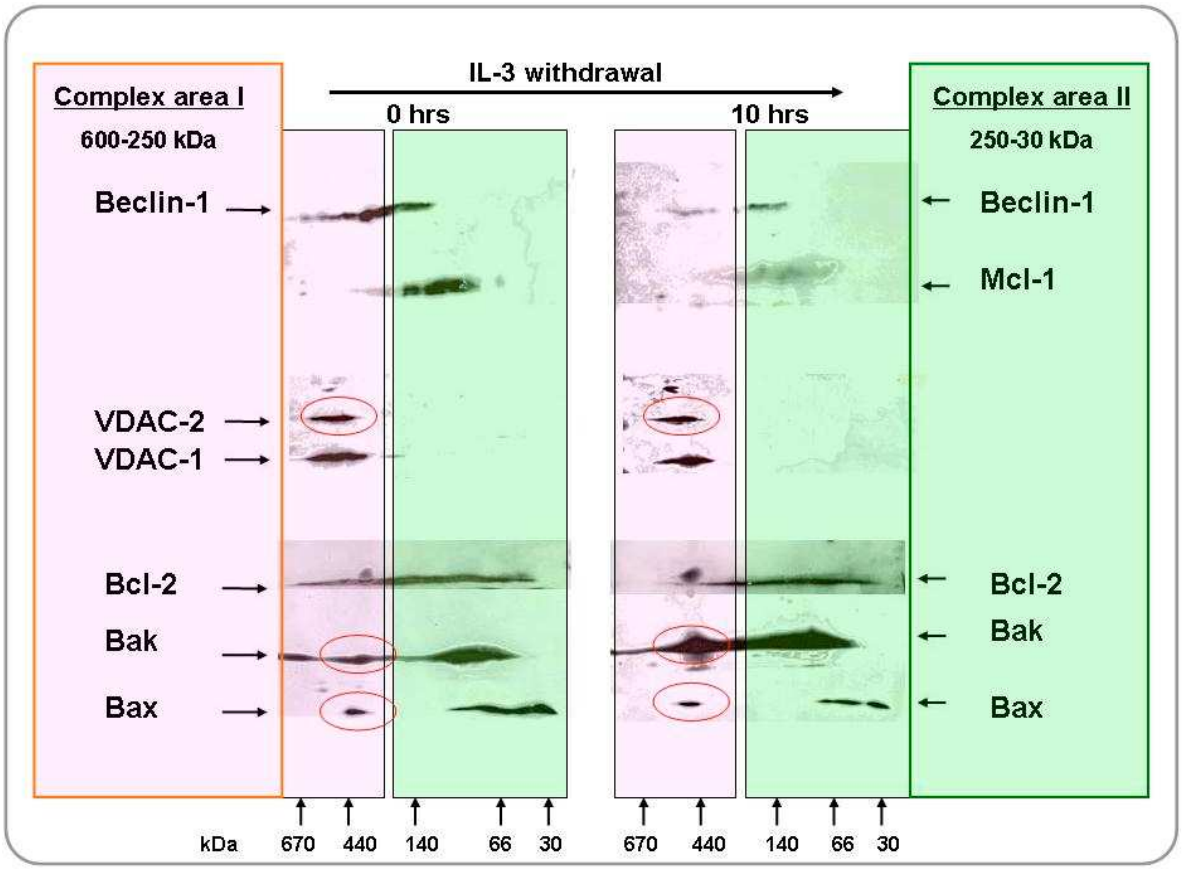

Figure 3-12: Known or putative Bcl-2 binding partner co-migrate with Bcl-2 in different complexes on 2D-BN-SDS-PAGE. Bcl-2 family proteins and others listed according their molecular weight from top, Beclin-1 (60kD), Mcl-1 (35kD), VDAC1/2 (30kD), Bcl-2 (26kD), Bak (23kD) and Bax (19kD). Detected dots in red circles of VDAC-1/2, Bak and Bax are seen in a vertical line. Note: Bak does not exist as a monomer; it is detected in a homo- or heteromeric form. Western blot analysis of 400 µg of a heavy membrane extract of healthy and IL-3 deprived (10 h) wt FDMs solubilized with digitonin (5 g/g protein), and loaded on BN gradient PAGE followed by SDS gradient PAGE. The respective antibodies are indicated. Data set represents repeated blue native PAGE experiments.

3.4 The hydrophobic pocket of Bcl-2: the most likely binding site of interaction partners

Two models of Bax/Bak activation have been proposed. In the "direct activation" model, one class of BH3-only proteins such as Bim, Puma or Bid are bound to the hydrophobic pocket of Bcl-2-like survival factors in healthy cells. In response to apoptotic stimuli, another class of BH3-only proteins, such as Noxa, Bad, Bik, etc. displace Bim, Puma and Bid from Bcl-2 and the latter can then interact with and activate Bax and/or Bak by a "hit and run" mechanism. While the on and off binding of the various BH3-only proteins to Bcl-2 should be easily measurable in co-IPs, it is certainly difficult to catch the transient interaction of Bim, Puma and Bid with Bax and Bak. The second, so called "displacement" model says that Bax and/or Bak are bound to Bcl-2-like survival factors in healthy cells and that any BH3-only protein can displace them upon apoptosis, so that they can become free to oligomerize and trigger MOMP. In this case, both the Bax/Bak binding to Bcl-2 in healthy cells and the BH3-only binding in apoptotic should be seen in anti-Bcl-2 co-IPs. To obtain a specific, highly efficient anti-Bcl-2 IP, we first had to test which anti-Bcl-2 antibody worked best for this method. Secondly, we had to define the optimal conditions (detergent, salt concentration, incubation time, etc.) to achieve a specific anti-Bcl-2 IP without contaminating the Sepharose beads with too many non-specific proteins. Thirdly, we needed proper negative controls (knock-out extracts, beads only, pre-immune or Ig serum). Lastly, we had to show, as proof of principle, that a known interaction of a protein with Bcl-2 can be detected in an anti-Bcl-2 co-IP. We chose Bak and VDAC1 as both have previously been shown by D. Grubb and A. Manoharan in our group (unpublished data) to co-IP with Bcl-2 from a heavy membrane extract of healthy wt FDC-P1 or MEFs.

3.4.1 Choosing the right anti-Bcl-2 antibody for immunoprecipitations

To examine the specificity and efficiency of anti-Bcl-2 antibodies for immunoprecipitations (IPs) we used heavy membrane extracts of three different cell lines, FDM, FDC-P1 and MEF. As shown in Fig. 3-13, the amount of endogenous Bcl-2 further increased in our IPs when 1.0 µg instead of 0.5 µg of a monoclonal anti-mouse Bcl-2 antibody (10C4) was used. However, there was no difference between 50 and 100 µg total protein suggesting that we can achieve a quite efficient IP with 100 µg protein using 1.0 µg antibody. Unfortunately, we still had substantial amounts of Bcl-2 remaining in the supernatant (SN) after the IP, but we were unable to further improve the IP, even with a higher amount of Bcl-2 antibody (up to 5.0 µg). This is consistent with the notion that immunoprecipitations are never quantitative and it is very difficult to pull down 100 % of a desired protein. When comparing the different cell line, it became apparent that FDMs express the highest amounts of Bcl-2. Thus, we chose this cell line for future IPs.

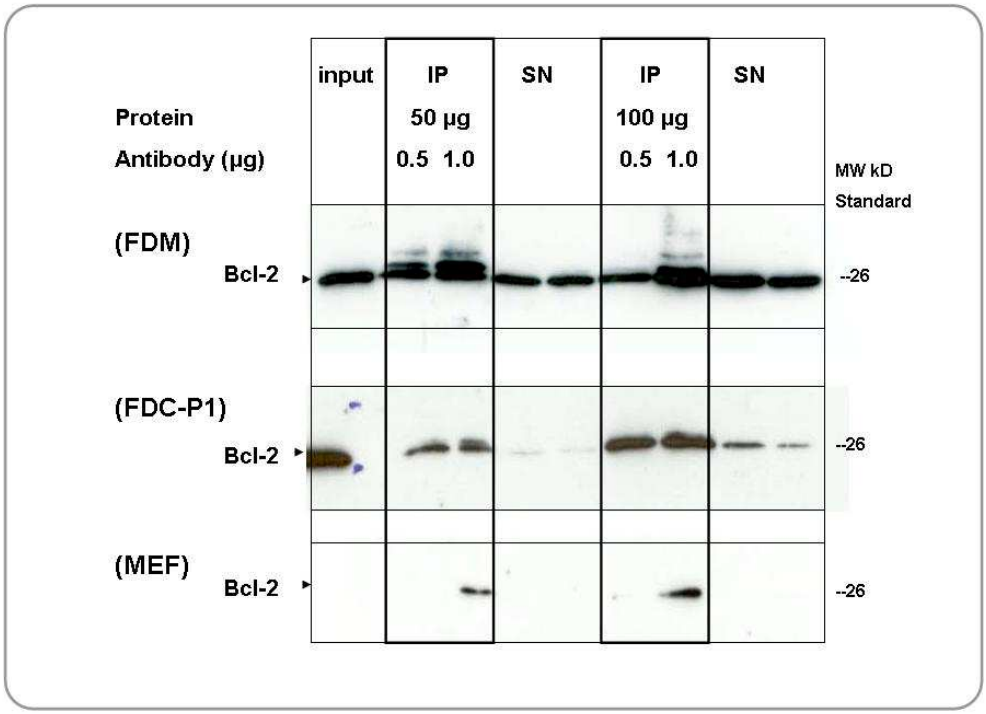

Figure 3-13: Protein and Bcl-2 antibody concentrations do not correspond. Mouse Bcl-2 10C4 antibody titration against two different protein concentrations**.** Bcl-2 Western blot analysis of immunoprecipitated (IP) endogenous Bcl-2 from heavy membrane extracts of FDM, FDC-P1 and MEF cells. Samples and antibodies were incubated for 1 h and immunocaptured for 1.5 h, Mini-PAGE 15 %, 1 % CHAPS MSH Buffer, 2 x Protease Inhibitors, reducing conditions, 300 µl IP volume and 50 µl (50 % slurry) protein A Sepharose were used. SN: supernatant after IP.

3.4.2 Choosing the right salt concentration to avoid the pull-down of non-specific proteins

Figure 3-14 summarizes the results of endogenous Bcl-2 IPs using different salt (KCL) concentrations in the buffer used to wash the immunoprecipitates. Heavy membranes fractions of healthy FDMs were solubilized in a buffer containing digitonin but no salt. The anti-Bcl-2 IPs were performed in the same buffer, but the immunoprecipitates on the protein G Sepharose beads were washed in a buffer containing different concentrations of KCL. Anti-Bcl-2 Western blot analysis of the IPs was performed under non-reducing conditions (without DTT or mercaptoethanol) in order to avoid the reduction of the antibodies and the consequent interference of light chains (ca. 25 kDa) with the detection of Bcl-2 (26 kDa) and its binding partners (often also around 20 – 40 kDa). As shown in Fig. 3-14, similar levels of Bcl-2 were pulled down independent of the stringency conditions from 50-250 mM KCL. Interestingly, Bcl-2 always runs as a triple band under non-reducing conditions (without DTT) indicating that it might be intramolecularly disulphide linked. We then analysed the anti-Bcl-2 IPs by anti-VDAC-1 and

anti-Bak Western blotting. Surprisingly, both proteins only attached to Bcl-2 under low salt conditions. Already 50 mM KCL in the washing buffer almost completely detached VDAC-1 and Bak from Bcl-2 indicating that these two proteins bound to Bcl-2 either weakly or non-specifically. To distinguish between the two possibilities, we performed two other controls, an IP with an irrelevant antibody (murine isotype IgG_1) and an anti-Bcl-2 IP from a heavy membrane extract of Bcl-2-deficient FDMs (Bcl-2-/- FDM). In both situations, VDAC-1 and Bak were pulled-down in similar amounts as in specific anti-Bcl-2 IPs if salt was omitted from the washes. Thus, our data indicate that both VDAC-1 and Bak are sticky proteins that easily bind to protein G Sepharose beads or any antibody. No specific interaction with Bcl-2 could be found, especially not at physiological salt concentrations of 150 mM KCL.

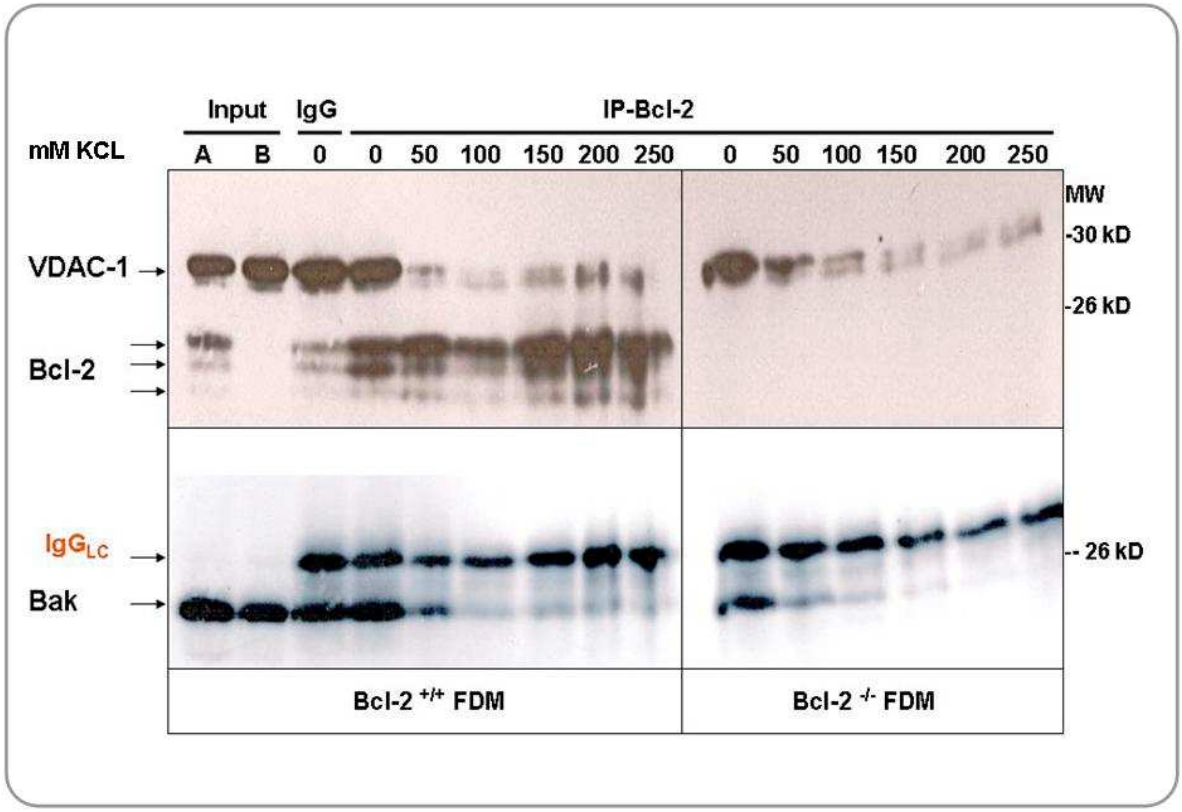

Figure 3-14: VDAC1 and Bak do not bind to Bcl-2 in co-IPs under physiological salt conditions. Heavy membrane extracts of Bcl-2 $^{+/+}$ and Bcl-2 $^{-/-}$ FDM were immunoprecipitated in a buffer containing no salt, followed by washes in buffers containing 0 – 250 mM KCL as indicated. The IPs were subjected to either anti-Bak (lower panel) or a mixture or anti-Bcl-2/VDAC-1 (upper panel) Western blotting **(A)** Input Bcl-2 $^{+/+}$ FDM, **(B)** input Bcl-2 $^{-/-}$ FDM, **(IgG_1)** isotype IP fraction, **(IP-Bcl-2)** co-immunoprecipitates of Bcl-2 probed for VDAC-1, Bcl-2 and Bak. Non-reducing conditions 1 % digitonin IBC Buffer, NO SALT FOR IPs, 2 x Protease Inhibitors, 4 µM MG132, gradient SDS-PAGE (12-19 % gradient).

We next wanted to know if Bak at least interacted with Bcl-2 under apoptotic conditions (- IL-3) as it was previously proposed. Therefore, heavy membrane extracts were taken from wt and Bcl-2 $^{-/-}$ FDMs deprived of IL-3 for 0, 16 and 24 h and subjected to anti-Bcl-2 or IgG control IP in

the absence of salt. After IP the beads were washed with buffers containing decreasing amounts of KCL (150, 100, 50 mM) and subjected to anti-Bcl-2 and anti-Bak Western blotting. As depicted in Fig. 3-15, Bcl-2 was nicely immunoprecipitated and showed a similar degradation pattern in response to IL-3 deprivation as seen above. Bak also gets degraded in response to IL-3 deprivation. However, even in the absence of IL-3, Bak did not co-IP with Bcl-2 and was only found in the supernatant after the IP. These data suggest that endogenous Bak does not bind to endogenous Bcl-2 under IL-3 deprivation conditions. Our finding is not unexpected and confirms a previous study by Willis et al. (2005). As IL-3 deprived cells die in a Bak-dependent manner, it does not make sense that Bak is captured and neutralized by Bcl-2. Rather Bak has to oligomerize and form pores to perform MOMP.

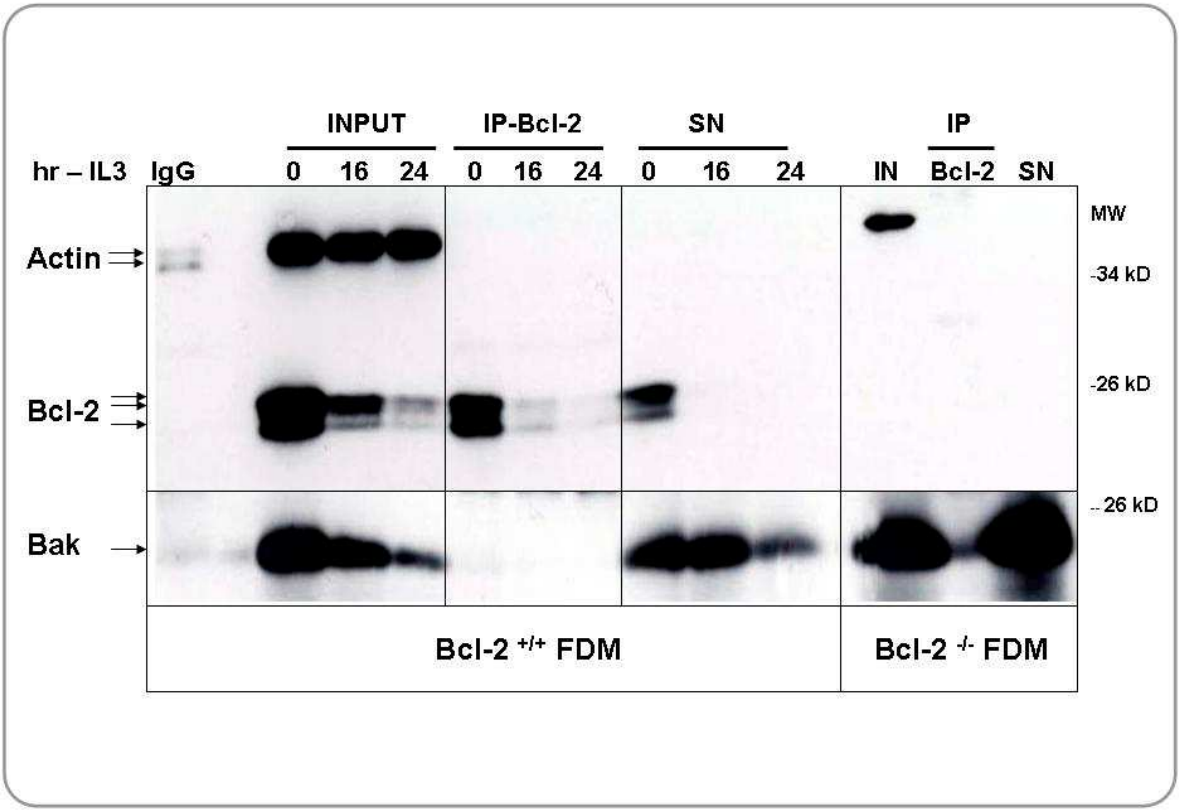

Figure 3-15: Bak does not bind to Bcl-2 in healthy and apoptotic FDM under physiological salt conditions. Anti-Bcl-2 and –Bak Western blot analysis of Bcl-2 IPs from heavy membrane extracts of wt (Bcl-2 $^{+/+}$) and Bcl-2 $^{-/-}$ FDMs. NO SALT FOR IPs, gradient SDS PAGE (12-19 %) under non reducing conditions, heavy membrane fraction, 500 µg input fraction (10 %) of IL-3 depleted FDM, 1 % Digitonin IBC Buffer, 2 x Protease Inhibitors, 4 µM MG132, repeated washing after IP in KCL gradient 150, 50, 50 mM. Data represent repeated (triple) experiments.

3.5 Isolation of Bcl-2 binding partners by co-IP and subsequent mass spectrometry analysis

3.5.1 ABT-737 assay: A concept to isolate Bcl-2 binding partners which bind to the hydrophobic pocket

In addition to verify known Bcl-2 binding partners, our second objective was to identify and characterize novel interaction partners. To make sure that we do not majorly re-isolate proteins such as BH3-onlies which predominantly bind to over expressed Bcl-2, we embarked on a strategy to pull down (IP) proteins which interacted with endogenous Bcl-2 in healthy cells. If successful, such proteins would likely be physiologically relevant binding partners and regulators of the survival activity of Bcl-2. The main problem was to develop a suitable method detecting specific interactions between endogenous, non-tagged proteins and minimizing false positive results (i.e. proteins that non-specifically bound to beads, antibodies or to regions of Bcl-2 that are not functionally relevant). Our idea was to use the recently developed BH3-mimetic ABT-737 that was designed by Oltersdorf et al. in 2005. ABT-737 is a small molecule inhibitor of the anti-apoptotic proteins Bcl-2, Bcl-xL and Bcl-w. It binds with relatively high affinity (K_i < 1 nM) to the hydrophobic pocket of these survival factors, thereby displacing previously bound factors/proteins such as Bax/Bak, BH3-onlies or other functionally relevant apoptosis regulators. Thus, our strategy was to apply ABT-737 to immunoprecipitated Bcl-2 complexes and thereby release proteins into the supernatant that are specifically bound to the hydrophobic pocket to Bcl-2 (Fig. 3-17). These proteins could then be identified by mass spectrometry analysis. Of course, we would miss proteins that are bound to other regions in Bcl-2, but at least we would get a first set of hopefully novel interaction partners in a quite specific manner. Most importantly, with this strategy we would greatly minimize contaminations of antibody fragments or proteins that stick to beads or antibodies in the IP. To further increase specificity of our approach, we set up the following controls/procedures: (i) Bcl-2 IPs were performed in salt-free buffers, but the IPs were washed with physiological salt concentrations before applying ABT-737. This ensures that we detach only proteins that were more or less strongly bound to the pocket (and under the right cellular salt conditions), (ii) to make sure that proteins did not spontaneously detach from Bcl-2 upon incubating with ABT, we used a DMSO (solvent) control (Fig. 3-17, specificity exclusion strategy), (iii) we still used beads and Bcl-2 $^{-/-}$ controls because here proteins detected in the end cannot be interactors with the hydrophobic pocket of Bcl-2 (Fig. 3-17, bait exclusion strategy). Proteins specifically released from Bcl-2 IPs by ABT, were run on a gradient SDS-PAGE, cut out of the gel and digested with trypsin. The peptides were then subjected to LC-MS/MS spectrometry. Finally the proteins were identified by Mascot

search and compared to those appearing in the negative controls (DMSO, beads, Bcl-2 $^{-/-}$ FDM) (Mass spectrometric analysis 1).

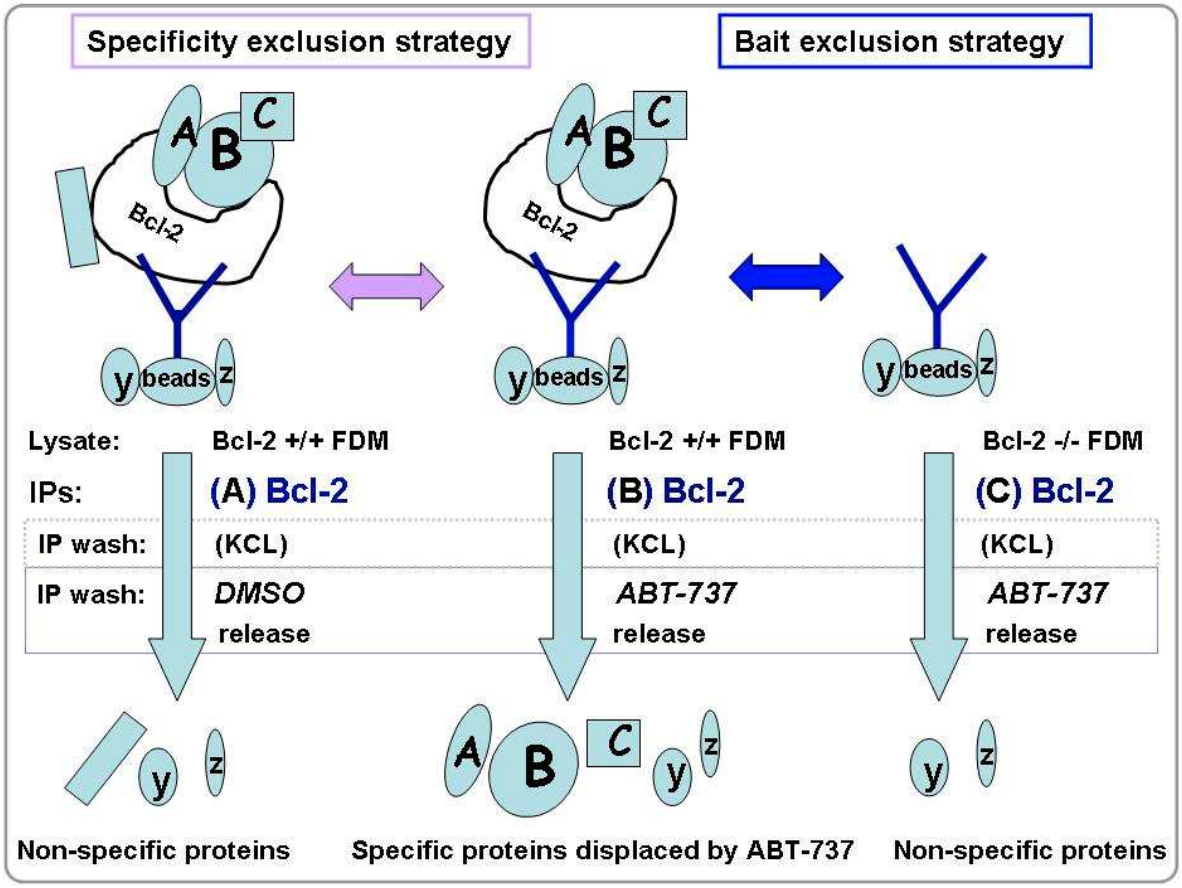

Figure 3-17: Outline of the ABT-737 strategy to enrich for "physiological" interactors bound to Bcl-2. Heavy membrane extracts of Bcl-2 $^{+/+}$ **(A, B)** or Bcl-2 $^{-/-}$ **(C).** FDM are immunoprecipitated with a monoclonal Bcl-2 antibody in a salt-free buffer. The IPs are washed with KCL and then either treated with the DMSO solvent **(A)** or the specific BH3-mimetic ABT-737 **(B, C)**. Proteins specifically released by ABT-737 from the hydrophobic pocket of Bcl-2 will be found in the supernatant along with non-specific bait and beads interactors **(B).** Some low affinity interactors may be found in the DMSO treated samples because they may detach from Bcl-2 due to the DMSO incubation procedure **(A).** In **(C)** only proteins of the bead proteome will be found.

3.5.2 A strategy to isolate the whole set of Bcl-2 interacting proteins

To identify the whole set of Bcl-2 interacting proteins, i.e. also those which do not necessarily bind to the hydrophobic pocket and get released by ABT-737, we performed a "regular" anti-Bcl-2 IP of heavy membrane extracts of FDMs, followed by physiological salt washes and detachment/denaturation in SDS to separate the whole set of IPed proteins on SDS-PAGE. By comparing the mass spectrometry data of this experiment (Mascot 2) with those from the ABT-737 assay (Mascot 1), we could uncover proteins which most likely bind to other regions of Bcl-2 than the hydrophobic pocket. To ensure specificity of this approach, we included a “beads/IgG

control" where the IP was performed with an irrelevant IgG_1 antibody instead of anti-Bcl-2 (Fig. 3-18 A, tool exclusion strategy) and an anti-Bcl-2 IP from a Bcl-2 $^{-/-}$ heavy membrane extract (Fig. 3-18 C, bait exclusion strategy). Proteins appearing in this control were considered as non-specific, because they recovered despite the absence of Bcl-2 in the IP. The full set of proteins bound to Bcl-2 independent of a BH3 domain is found by a "common" Bcl-2 IP as described above (Fig. 3-18 B).

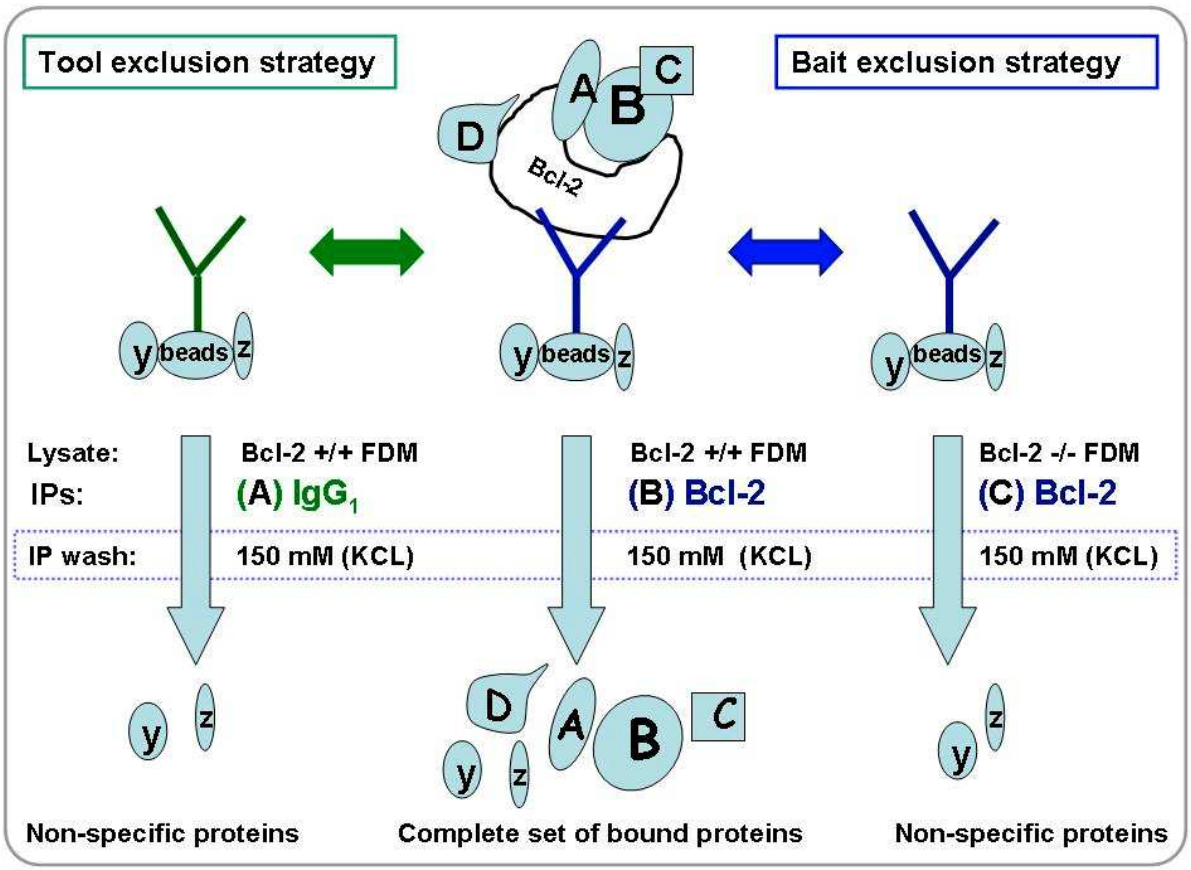

Figure 3-18: Outline of the whole set Bcl-2 strategy to isolate Bcl-2 interacting proteins. Heavy membrane extracts of Bcl-2 $^{+/+}$ **(A, B)** or Bcl-2 $^{-/-}$ **(C)** FDM are immunoprecipitated with a monoclonal Bcl-2 antibody **(B,C)** or an IgG_1 control **(A)** in a salt-free buffer. IPs were washed with KCL and then detached with SDS for SDS-PAGE and mass spectrometry analysis. In addition to the proteins A, B and C which bind to the hydrophobic pocket and released by ABT-737 (see chapter 2.9.3 Fig. 2-20 and chapter 4.5.1), a protein D should also be specifically detected in **(B)** because it binds to an other site in Bcl-2. Proteins **Y** and **Z** appear in both the IgG_1 and Bcl-2 IP because they are non-specific interactors bound to beads.

3.5.3 Elucidating the protein pattern of the ABT-737 release and the whole set Bcl-2 interactionting strategies

3.5.3.1 ABT-737 release assay

Figure 3-19 shows a silver stained gradient SDS gel containing the proteins released from anti-Bcl-2 IPs of heavy membrane extracts of Bcl-2 $^{+/+}$ and Bcl-2 $^{-/-}$ cells by DMSO, buffer of 1 µM ABT on ice or at 37 ℃ for 30 min. It appeared that most of the proteins were recovered in the Bcl-2 $^{+/+}$ IP sample treated with ABT at 37 ℃ (Fig. 3-19 B). However, an appreciable amount of proteins were also released from the ABT-treated Bcl-2 $^{-/-}$ samples and, to a lesser extent from the DMSO-treated Bcl-2 $^{+/+}$ sample, reinforcing the importance of running these negative controls in parallel.

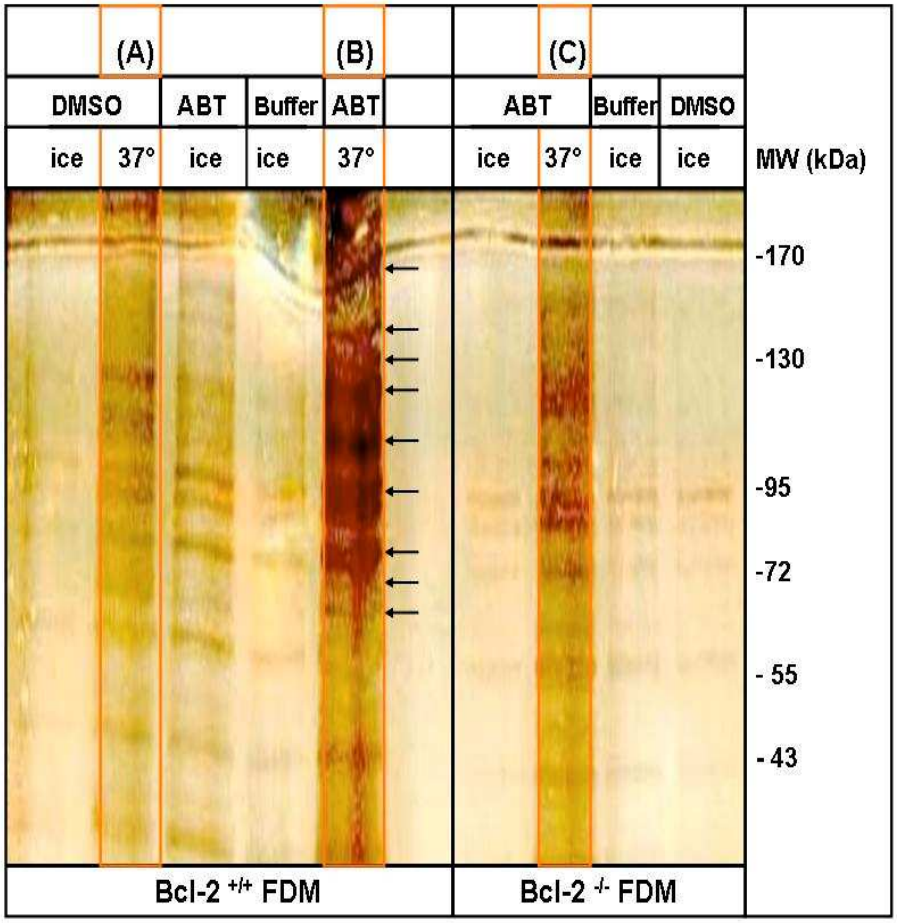

Figure 3-19: Silver stain of a SDS gel loaded with ABT-737 release samples. Heavy membrane extracts of Bcl-2 $^{+/+}$ and Bcl-2 $^{-/-}$ FDMs were incubated with murine monoclonal Bcl-2 antibody and immunocaptured. Precipitates were washed with KCL and then treated with DMSO or ABT-737 on ice or at 37 ℃ for 30 min. Samples A, B and C were treated under equal conditions. Protein eluates were electrophoretically separated by gradient PAGE (9-18 %) followed by silver staining of the gel. Gel pieces were cut along the lanes, trypsinized and subjected to mass spectrometric analysis 1 (MS 1).

3.5.3.2. Whole set Bcl-2 interactors

As shown in Fig. 3-20, the silver stain protein pattern of the various IPs, i.e. anti-Bcl-2 IP of Bcl-2 $^{+/+}$ and Bcl-2 $^{-/-}$ extracts as well as the IgG_1 control IP and a Bcl-2 IP from a FDC-P1 extract did not show any major difference. This is most likely due to the presence of the IP antibody and many non-specific and contaminating proteins that are released from the beads by SDS, despite high stringency washes in 150 mM KCL.

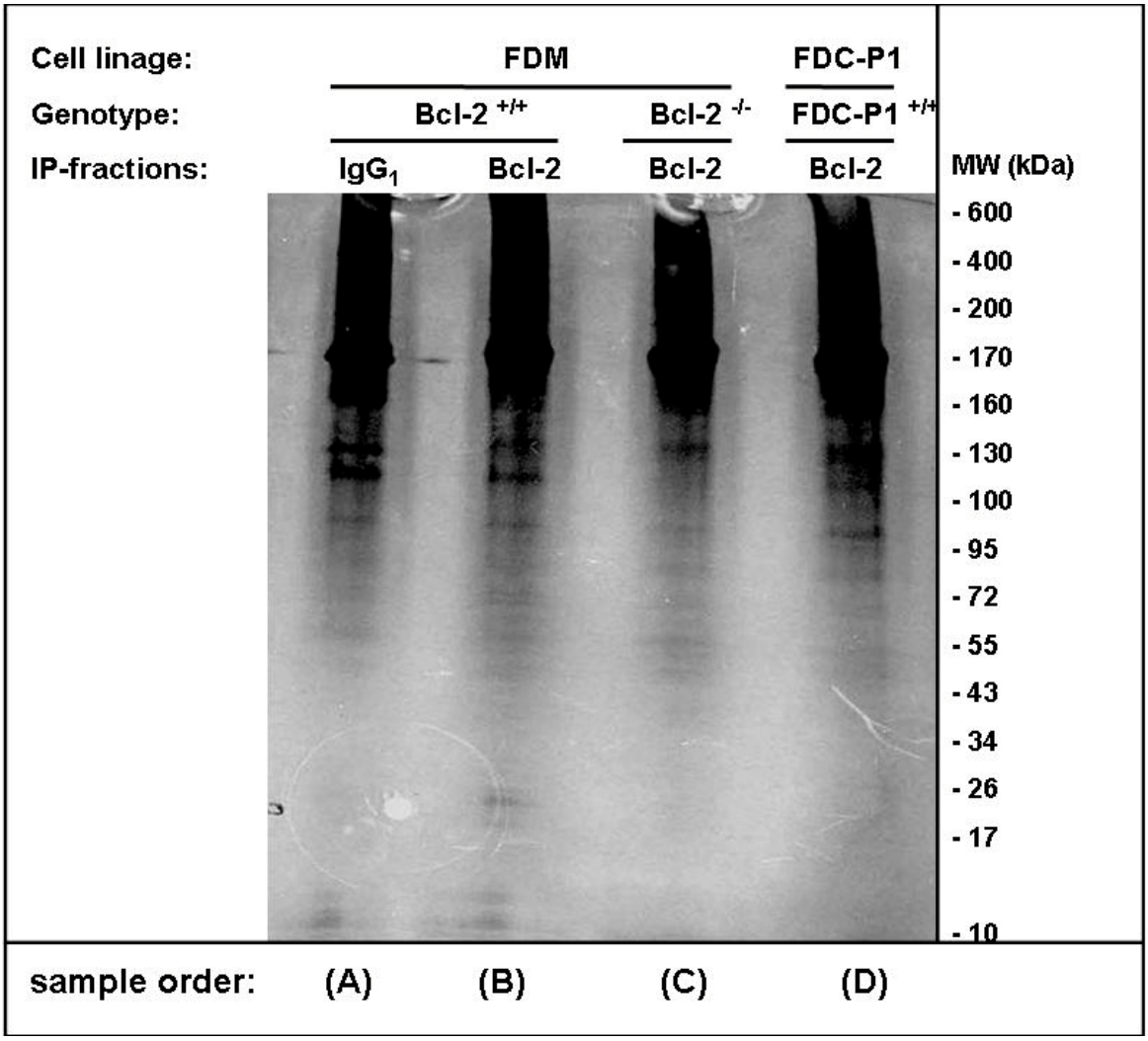

Figure 3-20: Silver stain of a SDS gel loaded with samples from the whole set Bcl-2 assay. Bcl-2 IP sample fractions exhibit an equal pattern of silver stained proteins. Heavy membrane extracts of Bcl-2 $^{+/+}$, Bcl-2 $^{-/-}$ FDM and FDC-P1 were incubated with monoclonal Bcl-2 antibody and immunocaptured. Precipitates were washed three times with KCL (150 mM, 50 mM, and 50 mM). Proteins were detached from the beads with SDS sample buffer and electrophoretically separated by a gradient gel (9-18 %) followed by silver staining of the gel. Gel pieces were cut along the lanes, trypsinized and subjected to mass spectrometric analysis 2 (MS 2).

.

3.5.4 Comparing the Bcl-2 binding partners specifically isolated by both strategies

3.5.4.1 ABT-737 assay and Mascot data from mass spectrometry analysis 1

The silver-stained lanes of probes A (DMSO), B (ABT on Bcl-2 $^{+/+}$) and C (ABT on Bcl-2 $^{-/-}$) of the ABT-737 release assay were cut into similarly sized gel pieces, digested by trypsin and subjected to LC-MS/MS mass spectrometry analysis. Importantly, for accurate comparison between the positive samples (ABT on Bcl-2 $^{+/+}$) and the negative controls, it was crucial to enumerate the gel pieces from bottom to top of each lane and always compare the same numbers. The corresponding mass spectrometry data of each gel slice were then analysed by the Mascot program.

Mascot is a software search engine that calculates the probability of the observed match between the experimental data set and each sequence database entry. Data sets obtained by Mascot software were compared between probes A, B and C of the ABT-737 assay (Fig. 3-19). Positive values were obtained by setting a threshold which was > two peptides and score values above identity. This evaluation yielded 77 specific Bcl-2 binding partners in the range of 30-200 kDa (Appendix, Table 6-4).

3.5.4.2 Whole set Bcl-2 interactor assay: Mascot data from mass spectrometry 2

Unfortunately, we had some difficulties to obtain mass spectrometry data from the approach to identify the whole set of Bcl-2 interacting partners. Below the molecular size of 50 kDa the digested protein samples were contaminated by an unknown polymer, so that these mass spectrometrical data could not be used for Mascot search and thus these important data between 10 up to 50 kDa can not be compared with the data set from the ABT-737 assay. Interestingly, samples from the upper part (50 up to 250 kDa) of the gel were free of any contamination by this polymer. As expected, the data list of this MS 2 sample analysis revealed less potential Bcl-2 binding partners (Appendix, Table 6-5). After filtering the Bcl-2 $^{+/+}$ against the negative IgG_1 and Bcl-2 $^{-/-}$ data, 8 specific potential Bcl-2 binding partners were found (excluding those ones which could not be analysed because of the contamination by a polymer of unknown origin, Fig. 3-21).

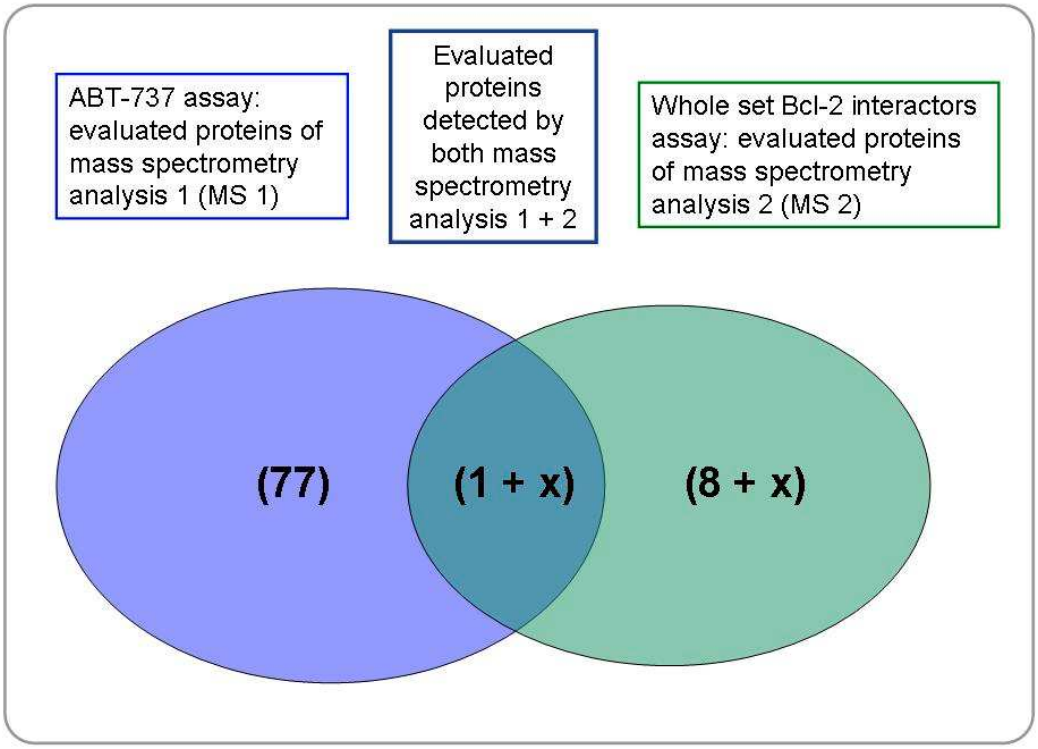

Figure 3-21: Specific Bcl-2 binding proteins found by both the ABT-737 and the whole set Bcl-2 interactor assay. Mass spectrometry analysis of the ABT-737 release assay yielded 77 specific potential Bcl-2 binding partners. Only 8 proteins of 25 were found above identity by the IP of the whole set of Bcl-2 interactors. During the latter approach, proteins < 50 kDa could not be detected due to a polymer contamination. One highly potential Bcl-2 binding protein was evaluated by both approaches. + X means the extra proteins that probably would have been detected < 50 kDa.

3.5.4.3 The non specific isotype IgG_1 and bead proteome

In order to minimize the identification of non-specific interactors, both the ABT-737 assay and the whole set Bcl-2 interaction IP assay were run in parallel with negative controls, such as the IP incubations with DMSO instead of ABT-737 and the IPs with isotype control IgG_1/beads or extracts from Bcl-2 $^{-/-}$ FDM. All these controls told us which proteins non-specifically interacted with the protein G Sepharose beads or IgG_1. A so called “bead proteome” has recently been published (Trinkle-Mulcahy et al., 2008) that showed a list of proteins which were consistently found to unspecifically stick to Sepharose beads. Some of these proteins were also found in our negative controls and they are listed in Table 3-1. Interestingly, both Bak and VDAC1-3 belong to these proteins which is consistent with our analysis above (Fig. 3-14) neither VDAC-1 nor Bak are specific, high affinity Bcl-2 interacting proteins.

Table 3-1: Non-specific protein interactors found on Sepharose beads in our assays. Extract from the list of un-specific Bcl-2 interactors. Some of them were also found on the list of the "bead proteaome" (**bold**) published by Trinkle-Mulcahy et al. (2008).

Gene	**Protein/Mus musculus**
Bak	Bcl-2 antagonist killer
Bag	**Bcl-2 associated athantogene**
BCAP29	B-cell receptor-associated protein 29 27946 kDa
CTSG	**cathepsin G preproprotein** 29077 kDa
ERZ	**Ezrin,** 69303 kDa
CANX	Calnexin, 67236 kDa
PRSS34	protease, serine, 34, 35 kDa
YWHAH	**14-3-3 eta, 28100 kDa**
Vdac1-3	**voltage-dependent anion channel 1-3, 30700 kDa**

3.5.4.4 UDP-glucose ceramide glucosyltransferase-like 1 (UGCGT1):

A specific candidate Bcl-2 interacting protein consistently identified in several IPs and/or ABT-737 release assays

We independently performed the ABT-737 release assay once and the whole set Bcl-2 interaction IPs twice and compared the mass spectrometry of three data sets to obtain overlapping proteins. Only one such protein, a 176 kDa UDP-glucose ceramide glucosyltransferase-like 1 isoform (UGCGT1), was consistently identified with more than two peptides and score values above identity in Bcl-2 $^{+/+}$ FDM and FDC-P1, but not in Bcl-2 $^{-/-}$ cells or other negative controls (Table 3-2 and Appendix 6-5). Importantly, the peptides identified differed for each assay and covered a large range of the protein pointing towards a highly significant hit (Table 3-2). As Bcl-2 protein complexes run at molecular masses between 30 – 670 kDa upon BN-PAGE (Fig. 3-11 and 3-12), UGCGT1 falls within the right molecular weight range between 30-250 kDa to account for a putative Bcl-2 binding partner.

Table 3-2: Three independent mass spectrometry analyses (an ABT-release and two whole set analysis assays) consistently revealed UGCGT1 as specific potential Bcl-2 binding partner. Significant identity score values (always more than 2 peptides) are shown in the brackets against the full set of peptides. Note that the identified peptides mostly differed between the assays (blue, red and violet colored peptides. Green peptides: three times independent, black peptides: two times independent, blue ones are single hits of each other found in MS 1 and red peptides are single hits of each other found in MS 2). The amino acid sequence of UGCGT1 combined with MS/MS identified peptide sequences are shown in the appendix (Table: 6-1).

Mass Spectrometry 1 (FDM)				
Gene	**Mass (kDa)**	**Scores (identity) and peptides**	**Protein**	**Gi Reference**
UGCGT1	**176**	**7 (4)** **44, 45, 56, 49,** **1. KANPGAWILRL** **2. RIEYQFFEDKH** **3. KQLQTLFQEEKE + Gln->pyro-Glu (N-term Q)** **4. KILETTTFFQRA** Q1083E	**UDP-glucose ceramide glucosyltransferase like 1**	**Gi |45387933** 236466498
Mass Spectrometry 2 FDM)				
UGCGT1	**180**	**10 (8)** **52, 54, 53, 58, 44, 67, 103, 97** **1. KTAVSAQLRA** **2. KANPGAWILRL** **3. KILETTTFFQRA** **4. RELYPALEGQLKE** **5. RFLSPLQQNLLKF** **6. KFLFVDADQIVRT** **7.RAIWAALQTQASSSAKN** **8. KLNIQPSETDYAVDIRS**	**UDP-glucose ceramide glucosyltransferase like 1**	**Gi |148682526**
Mass Spectrometry 2 (FDC-P1)				
UGCGT1	**180**	**3 (3)** **45, 61, 87** **1. KANPGAWILRL** **2. KFLFVDADQIVRT** **3. KLNIQPSETDYAVDIRS**	**UDP-glucose ceramide glucosyltransferase ike 1**	**Gi |148682526**

Glucosyl- and galactosyltransferases catalyse the first step in the synthesis of glycosphingolipids, i.e. the transfer of glucose or galactose to a ceramide to produce glucoslyceramide (GlcCer) or galactosylceramide (GalCer). Sphingolipids are synthesized *de novo* from serine and palmitoyl transferase (SPT) which condense to form 3-keto-dihydrosphingosine, which is reduced to dihydrosphingosine followed by acetylation by (dihydro) ceramide synthase (CerS). Ceramide is formed by the desaturation of dihydroceramide.
Ceramide is considered to be the central hub of sphingolipid metabolism, as it can be converted into other interconnected bioactive lipid species. More than 50 molecular species have been classified as ceramides and each may have its own metabolic network, resulting in increased complexities of sphingolipid signaling. Bioactive sphingolipids are hydrophobic molecules and their physiological role is restricted to biological membranes, especially the plasma membrane where they are part of the glycocalyx and so called phospholipid micro domains (rafts). A distinct and unique set of properties operates in the cell to define the subcellular distribution of diverse sphingolipid pathways across and between membranes.

There are two general mechanisms favoured for the action of lipids, (I) lipid-lipid interactions, whereby an effector lipid changes the membrane structure and/or the interaction of membrane proteins with the membrane bilayer, and (II) lipid-protein interactions, whereby a modification in the lipid modulates the function of membrane protein. How ceramides and sphingolipids in general affect apoptosis is still a matter debate. Artificial, hydrosoluble, short-chain ceramides have been shown to trigger apoptosis, presumably by migrating to the MOM and stimulating MOMP. Recently, ceramide have even been suggested to form lipid channels on the MOM that can be regulated by Bcl-2. However, without a clear picture about the exact subcellular distribution of ceramides and its glycosylated derivatives as well as their functions on membrane permeability and metabolism at their site of action, it remains only speculative what the role of these lipids might be for apoptosis.
Future work will show if UGCGT1 is indeed a crucial Bcl-2 binding partner which upon binding or release in healthy or apoptotic cells changes the lipid microenvironment of the MOM or other membranes (e.g. ER) implicated in apoptosis. It is for example possible that such a change allows a better membrane insertion, oligomerization and pore formation of Bax and Bak, so that UGCGT1 could be indirect Bax/Bak activator that is bound and neutralized by Bcl-2 (see Discussion for further informations on this topic).

Unfortunately, we found only towards the end of this work (after performing the IPs and mass spectrometry several times) that UGCGT1 was a consistent Bcl-2 binding partner under all conditions. We therefore did not have time to validate this result by performing co-IPs and gel filtration or BN-PAGE analysis or immunofluorescence studies using anti-UGCGT1

antibodies. We rather focused on another putative specific Bcl-2 binding partner that was consistently, but not always found in our assay, namely IQGAP2 (see chapter 3.6 and Table 3-3).

3.5.4.5 Other promising novel Bcl-2 binding partners specifically identified by the ABT-737 assay

Other promising Bcl-2 binding proteins aside of UGCGT1, identified with several peptides and detected as double identity scores by the ABT-737 release assay were IQGAP2, LRPPRC, MANF/ARMET and GLIPR1 but also further interesting proteins (see Appendix Table 6-4 and 6-5).

Mitochondrial specific leucine-rich PPR motif-containing protein (LRPPRC) has recently been shown to be responsible for the French Canadian variant of Leigh syndrome (LSFC), a neurodegenerative disorder caused by a tissue-specific deficiency in cytochrome *c* oxidase (COX). Mutated LRPPRC is reduced in LSFC cells resulting in decreased steady-state levels of most mitochondrial mRNAs, but not rRNAs or tRNAs. LRPPRC has a specific role for the expression of all mitochondrial DNA-encoded mRNAs. Knockdown of LRPPRC produces a generalized assembly defect in all oxidative phosphorylation complexes containing mtDNA-encoded subunits, due to a severe decrease in all mitochondrial mRNAs. LRPPRC exists in a high-molecular-weight complex (+/- 300 kDa), and it coimmunoprecipitates with SLIRP, a stem-loop RNA binding protein. The results implicate LRPPRC in posttranscriptional mitochondrial gene expression as part of a ribonucleoprotein complex that regulates the stability and handling of mature mRNAs (Sasarman et al., 2010).

A further study used RNA interference to develop an allelic series of cellular models in which LRPPRC has been stably silenced to different levels of knockdown efficiency. Than they combined these data with a genome-wide expression profiling with gene set enrichment analysis and identified cellular responses that correlate with the loss of LRPPRC. They observed a specific altered expression of genes related to hexose metabolism, prostaglandin synthesis, and glycosphingolipid biology that may either play an adaptive role in cell survival or contribute to pathogenesis (Gohil et al., 2010).

MANF or arginine-rich, mutated in early stage tumors (ARMET) is an ER stress-inducible protein and upregulated in the early stage of cerebral ischemia. ER stress agent tunicamycin induced ARMET and CHOP expression in primary cultured neurons. Treatment with recombinant human ARMET promoted neuron proliferation and prevented neuron apoptosis induced by tunicamycin suggesting that cerebral ischemia-induced ARMET expression may be protective to neurons (Yu et al., 2010).

Glioma pathogenesis-related protein 1 (GLIPR1) expression is significantly reduced in human prostate tumor tissues compared with adjacent normal prostate tissues and in multiple human cancer cell lines. Overexpression of GLIPR1 in cancer cells leads to suppression of colony growth and induction of apoptosis (Li et al., 2008).

Since we had to focus on the validation and characterization of one particular protein, we have not yet further investigated the role of LRPPRC, MANF and GLIPR1 as Bcl-2 binding partner on the MOM. Instead we started a more in-depth analysis of the putative Bcl-2 binding partner IQGAP2.

3.6 IQGAP2: a promising new Bcl-2 interaction partner identified by our screens

3.6.1 Validation of the IQGAP2/Bcl-2 interaction on the endogenous level

We identified IQ motif containing GTPase activation protein 2 (IQGAP2) as a Bcl-2 interaction partner in our ABT-737 release assay. Mass spectrometry analysis revealed 7 out of 8 different peptides with high identity score (Table 3-3).

Table 3-3: IQGAP-2 as potential binding partner of Bcl-2. Significant identity score values are shown in the brackets against the full set of peptides. Seven peptides with different sequences and high score values identified by MS/MS are shown in different colours. (see also Appendix 6-2 and 6-3).

Mass spectrometry 1				
Gene	**Mass (kDa)**	**Scores (Identity) and peptides**	**Protein/Description**	**Gi/ Reference**
IQGAP2	180416 166376	**8** (**7**) **56, 61, 49, 55, 42, 60, 55** **RYADALLSVKQ** **KQSQAVIEDARL** **RFEATTLGPALRE** **KLGIAPQIQDLLGKV** **KTLDTLLLPTANIRD** **KALVINTNPVEVYKA** **KALVGSENPPLTVIRK**	IQ motif containing GTPase activating protein 2	gi|74218637

Excitingly, this protein has also been recently pulled out as binding partner of Bcl-2, Bcl-xL and Mcl-1 in a large scale yeast-two-hybrid screen (Hybrigenomics/Servier, John Hickman, personal communication). To validate IQGAP2 as specific endogenous binding partner of Bcl-2, we performed anti-Bcl-2 and anti-IQGAP2 IPs on heavy membrane extracts of healthy FDMs and subjected these IPs to Bcl-2 and IQGAP2 Western blotting. Importantly, to avoid interference of Ig light chains with the detection of 26 kDa Bcl-2, we performed the Bcl-2 Western blot under non-reducing conditions (i.e. maintaining disulphide-linked heavy and light chains, ca. 90 kDa). Conversely, since IQGAP2 has a molecular mass of 160 – 180 kDa, anti-IQGAP2 immunoblotting was done under reducing conditions. As shown in Figure 3-22 A, the heavy membranes of wt FDMs contain appreciable amounts of both Bcl-2 and IQGAP2 (input), while no Bcl-2 was detected in the Bcl-2 KO sample. The majority of IQGAP2 runs at 180 kDa and some minor bands were detected at slightly lower molecular mass (two bands around 166-175 kDa and below 166 kDa see Fig. 3-30). Almost 90 % of Bcl-2 could be immunoprecipitated from the wt extract. A similar IP on the Bcl-2 KO sample revealed only an Ig light chain band. While the 180 kDa IQGAP2 was also slightly present in the IgG_1 control (sticking to beads), the 166 kDa form of IQGAP2 appeared only in the Bcl-2 IP. In addition, more 180 kDa IQGAP2 was pulled down together with Bcl-2. None of the IQGAP2 forms were detected in the anti-Bcl-2 IP of the Bcl-2 KO extract confirming the specificity of the IQGAP2/Bcl-2 interaction. However, for unknown reasons, the amount of IQGAP2 was lower in the Bcl-2 KO extract (see input, also see discussion below). This could have been the reason for the lower (not easily detectable) amount of IQGAP2 in the anti-Bcl-2 IP of the KO sample. To further substantiate the IQGAP2/Bcl-2 interaction, we therefore performed the inverse IPs. As depicted in Fig. 3-22 B, IQGAP2 was almost completely immunoprecipitated from a heavy membrane extract of FDMs, using a monoclonal anti-IQGAP2 antibody. The antibody mainly recognized and immunoprecipitated the 180 kDa form of IQGAP2. Lower amounts were pulled down in the Bcl-2 KO samples because less IQGAP2 protein was present (see input). To our satisfaction, the IQGAP2 IP contained appreciable amounts of the Bcl-2 triple band (seen under non-reducing conditions, see Fig. 3-22 C) of which the lower band was the most abundant. Bcl-2 KO extract showed only an IgG light chain band. These data reveal that endogenous IQGAP2 and Bcl-2 can clearly interact in a healthy mitochondria-enriched (heavy membrane) extract although not all molecules of each partner seem to be involved in this interaction (see respective remaining levels in the supernatants, SN).

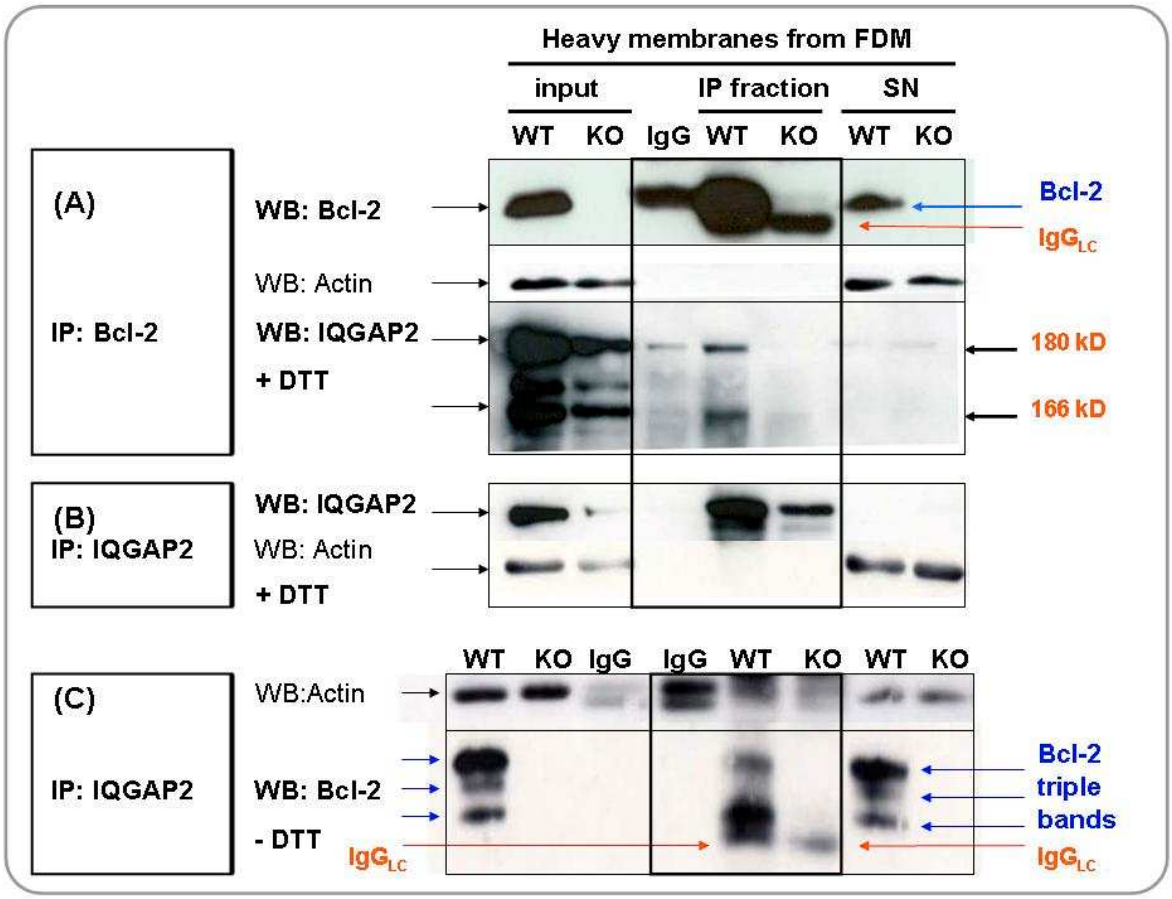

Figure 3-22: IQGAP2 binds to Bcl-2 in IP fractions of heavy membranes of healthy FDM. Heavy membrane fractions, solubilized with digitonin (1 %) of Bcl-2 $^{+/+}$ and Bcl-2 $^{-/-}$ FDMs were subjected to either anti-Bcl-2 (A) or anti-IQGAP2 (B, C) immuno-precipitation followed by anti-Bcl-2 or anti-IQGAP2 Western blotting (reducing conditions in (A, B), non-reducing in (C)). Input contains 2.5 % of the total protein used for IP (250 µg), IgG_1 was used as a control. The positions of IgG light chains are marked by an arrow. Buffer conditions: 1 % digitonin IBC Buffer, 2 x Protease Inhibitors, 4 µM MG132, no salt during IPs, repeated washing after IP in KCL low salt affinity gradient, SDS gradient PAGE 12 – 19 %.

3.6.2 Myeloid cell lymphoma-1 (Mcl-1) joins the Bcl-2/IQGAP2 protein complex on heavy membranes

Based on unpublished yeast-two-hybrid data, other survival factor of the Bcl-2 family such as Mcl-1 may also interact with IQGAP2 and hence join the Bcl-2/IQGAP2 complex. We therefore probed our anti-IQGAP IPs on an anti-Mcl-1 Western blot and found that Mcl-1 was indeed specifically pulled down from a healthy mitochondrial FDM extract with IQGAP2 (Fig. 3-23). Astonishingly, no Mcl-1 was detected in an anti-IQGAP2 IP from Bcl-2 KO cells indicating that the interaction of Mcl-1 with IQGAP2 depended on Bcl-2. Further studies in future have to be done to unravel the details of these interactions.

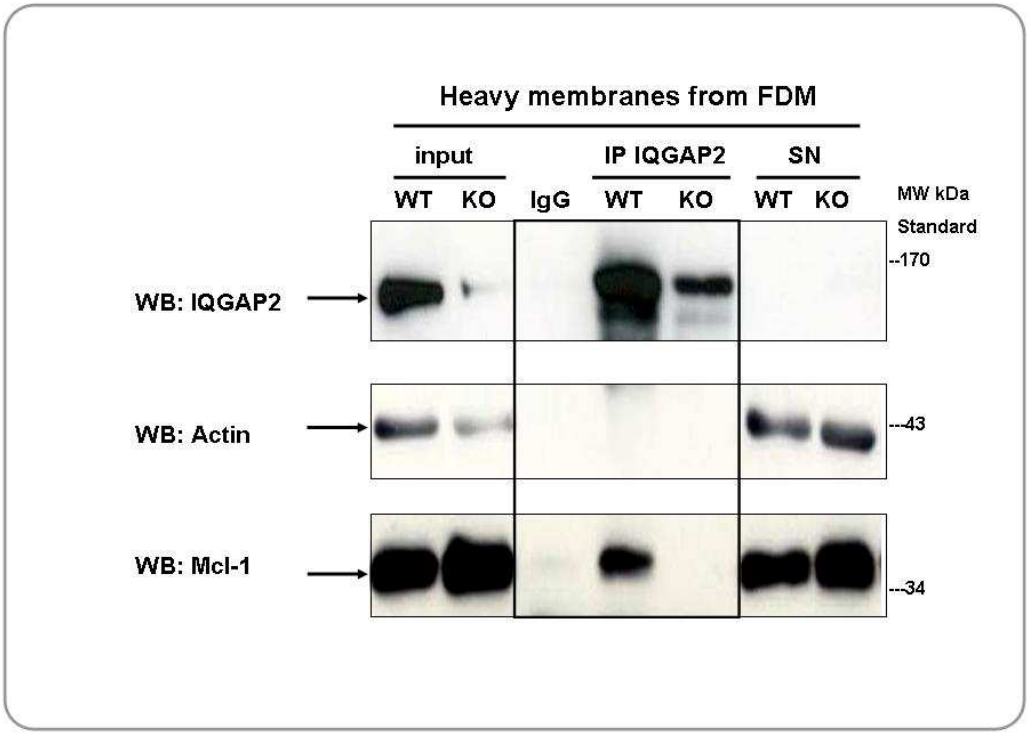

Fig. 3-23: Mcl-1 a potential endogenous binding partner of IQGAP-2. Heavy membrane extracts of Bcl-2 $^{+/+}$ (WT) and Bcl-2 $^{-/-}$ (KO) FDMs were subjected to anti-IQGAP2 IP followed by anti-IQGAP2 and anti-Mcl-1 Western blotting. Buffer conditions: (+ DTT) and SDS gradient PAGE. Input contains 2.5 % of the total protein used for IP (250 µg), IgG_1 was used as a control. Buffer conditions: 1 % digitonin IBC Buffer, 2 x Protease Inhibitors, 4 µM MG132, no salt during IPs, repeated washing after IP in KCL low salt affinity gradient, SDS gradient PAGE 12 – 19 %.

IQGAP2 is predominantly found in the cytosol and only part of the protein seems to be associated with mitochondria and the ER. Mcl-1 is also more or less evenly distributed between the cytosol and mitochondria. So, the question was where this Bcl-2-IQGAP2-Mcl-1 complex formed within the cell. As Bcl-2 is uniquely inserted into the mitochondrial and ER membranes, it was likely that the complex was possibly restricted to heavy membranes. In this case the part of Mcl-1 that is found in the cytosol would probably not bind to IQGAP2. We therefore expect that much less Mcl-1 would co-IP with IQGAP2 in a total extract because the proteins would be more diluted than in a heavy membrane extract. Indeed, as shown in Fig. 3-24, only little Mcl-1 was found in anti-IQGAP2 IPs of a total extract of FDM cells because the film had to be exposed for a long time to detect the protein. An upper band was seen as well but this is likely to be another protein cross-reacting with the Mcl-1 antibody. Again no Mcl-1 associated with IQGAP2 in the absence of Bcl-2, confirming the dependence of the Mcl-1/IQGAP2 interaction on Bcl-2.

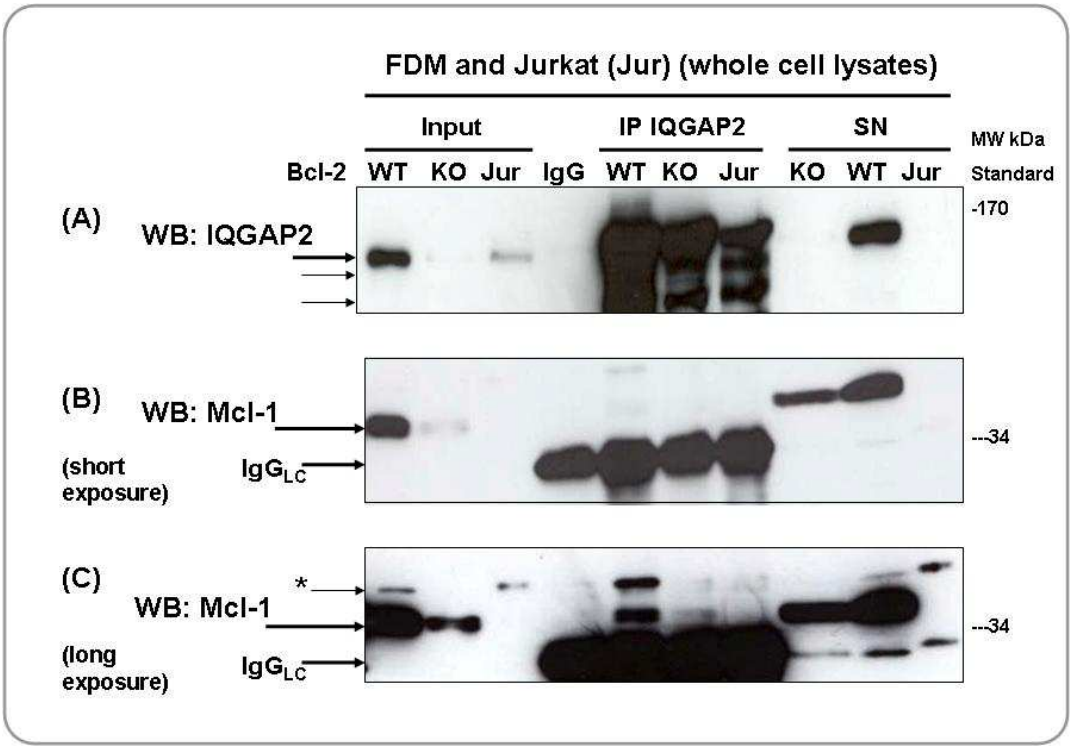

Figure 3-24: Less Mcl-1 protein associates with IQGAP2 in total extracts. Total (digitonin) 20 mg extracts of Bcl-2 $^{+/+}$ (WT) and Bcl-2 $^{-/-}$ (KO) FDMs and Jurkat (Jur) cells were subjected to anti-IQGAP2 IP followed by Western blotting of anti-IQGAP2 (**A**), anti-Mcl-1 (short exposure, **B**) and Mcl-1 in the IQGAP2 IP after exposing the film for 1 h (**C**).. Buffer conditions: (+ DTT) and SDS gradient PAGE are the same as in Figure 3-23. Note that the fat bands below 34 kDa are IgG light chains.

3.6.3 Elucidating the subcellular localization of IQGAP2 in different cell types

3.6.3.1 Localization of IQGAP2 in Bcl-2 $^{+/+}$ and Bcl-2 $^{-/-}$ FDM

We consistently observed a lower abundance of IQGAP2 in the heavy membrane samples of Bcl-2 $^{-/-}$ as compared to Bcl-2 $^{+/+}$ FDM cells (Figs 3-22, 3-23, 3-24). This could be either due to a diminished total expression/downregulation of IQGAP2 in Bcl-2-deficient cells, or alternatively, a translocation of IQGAP2 to another subcellular compartment once Bcl-2 was missing on mitochondria. If the latter was true, this would confirm that IQGAP2 interacts with Bcl-2 or even requires Bcl-2 for mitochondrial localization inside cells. On the other hand, Schmidt et al. (2008) showed that IQGAP1, another isoform of IQGAP, was more expressed in hepatocytes of two month-old Iqgap-2 $^{-/-}$ mice (as a sort of compensation mechanism). We therefore wanted to accurately determine the expression levels and subcellular distribution of IQGAP1 and IQGAP2 in wt and Bcl-2 KO FDMs by respective Western blot analysis (Fig. 3-25). In addition, we wanted to know if these parameters changed in apoptotic cells, i.e. in response to IL-3 removal

(0, 16, 24 h). For that purpose we generated cytosol, heavy membrane (mitochondria, HM) and endoplasmatic reticulum (ER) fractions of these cells (Fig. 3-25).

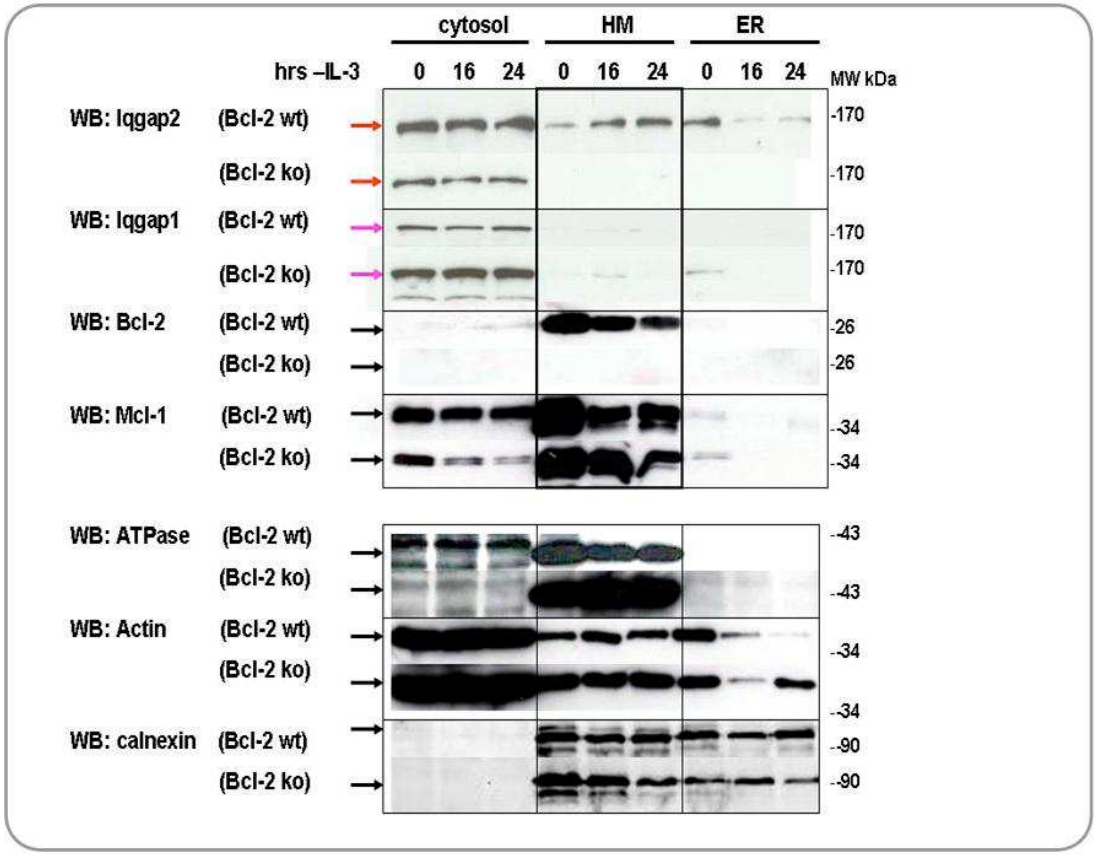

Figure 3-25: Association of IQGAP2 with mitochondria (HM) and ER fractions depends on Bcl-2. Subcellular distribution of IQGAP1, IQGAP2, Bcl-2 and Mcl-1 between the cytosol, mitochondria (heavy membranes (HM)) and ER fractions in Bcl-2 $^{+/+}$ and Bcl-2 $^{-/-}$ FDMs, in the presence (0) or absence of IL-3 for 16 or 24 h. Mini PAGE 15 %, 1 % CHAPS IBC Buffer, 2 x Protease Inhibitors, 4 µM MG132, 50 µg protein per lane. Actin as a loading control for the cytosol, ATPase for mitochondria, and calnexin for the ER. Note that the mitochondrial HM fraction also contains some ER material, whereas the ER fraction is very pure. Such a contamination is difficult to avoid, since part other ER is physically bound to mitochondria.

First of all, while Bcl-2 was predominantly found on mitochondria (HM) and never in the cytosol, part of Mcl-1 also appeared in the cytosol. As shown above, both Bcl-2 and Mcl-1 were partially downregulated in response to IL-3 deprivation. IQGAP1 was only present in the cytosol and its expression was increased in Bcl-2 KO cells. By contrast, an appreciable part of IQGAP2 localized to mitochondria and to the ER (although most of it was also cytosolic). In Bcl-2 KO cells, total IQGAP2 expression might be a bit diminished, but most importantly, there was almost no mitochondrial or ER association detected anymore. Interestingly, in response to IL-3 deprivation, mitochondrial binding of IQGAP2 increased, whereas binding to the ER decreased. These data demonstrate that mitochondrial and ER association of IQGAP2 largely depended on Bcl-2.

Moreover, during apoptosis IQGAP2 seems to move from the ER to mitochondria, maybe due to an important function of IQGAP2 during this process. This movement occurred despite the fact that Bcl-2 was partially downregulated. The result points to an important but yet unknown mechanism of the IQGAP2/Bcl-2 interaction and mitochondria during apoptosis.

The next step was to investigate the subcellular distribution of IQGAP2 and Bcl-2 in other cell lines such as MEFs, Hela and HEK293T cells. In particular, we wanted to know if the inverse condition, namely over expressed Bcl-2 would attract more IQGAP2 to mitochondrial and ER fractions. For that purpose, we used rat 6 embryo fibroblasts and HeLa cells over expressing Bcl-2.

3.6.3.2 Localization of IQGAP2 in Bcl-2 $^{+/+}$ and Bcl-2 $^{-/-}$ MEF as well as in wt and Bcl-2 over expressing Rat 6 fibroblasts

As depicted in Fig. 3-26, the subcellular distribution of IQGAP2 in Bcl-2 $^{+/+}$ and Bcl-2 $^{-/-}$ MEF is in accordance with the results obtained from Bcl-2 $^{+/+}$ and Bcl-2 $^{-/-}$ FDM cells. The only difference was that MEFs express very little IQGAP2, almost all seems to be in a nuclear membrane/nuclear fraction and the size of IQGAP2 was lower (130 kDa) than in FDMs (180 and 166 kDa) (Fig. 3-26 A, left panel). This was interesting, because Bcl-2 was not only present in the nuclear, but also in the mitochondrial (HM) and ER fractions of these cells. Thus, IQGAP2 seems to be preferentially drawn to the nuclear envelope in this case. Once Bcl-2 was deleted, this association was greatly diminished, as in Bcl-2 $^{-/-}$ FDMs. Since there was no increase of IQGAP2 elsewhere in these cells, one wonders if it gets degraded once Bcl-2 is missing. It is therefore possible that the interaction of IQGAP2 with Bcl-2 on membranes stabilizes the protein.

Consistent with MEFs, IQGAP2 also showed a low expression and unique nuclear membrane association in rat 6 embryo fibroblasts (R6 cells) (Fig. 3-26 B, right panel). Again the molecular size of the IQGAP2 was lower (ca. 130 kDa) than in FDM cells and the protein ran as double band on SDS-PAGE. Perhaps these are splice variants of IQGAP2 which are different between R6/MEF and FDMs. Stable over expression of mouse Bcl-2 in R6 cells (R6-mBcl-2) led to an increase of nuclear membrane associated IQGAP2, probably due to an increased Bcl-2 interaction and higher stabilization of the IQGAP2 protein. The extent of this increase may be even an underestimation because less protein (according to the actin control) was loaded for the Bcl-2 over expressing sample (Fig. 3-26 B). Interestingly, again, although Bcl-2 was even more over expressed on mitochondria in these cells, no IQGAP2 association/stabilization was detected in this fraction. This indicates that other cellular factors may determine the IQGAP2/Bcl-2 interaction. In addition, it will be crucial to study the change

in subcellular localization of IQGAP2 in apoptotic cells, as it was performed in FDMs (see Fig. 3-25). It is possible that IQGAP2 would then translocate from the nuclear/ER to the mitochondrial fraction.

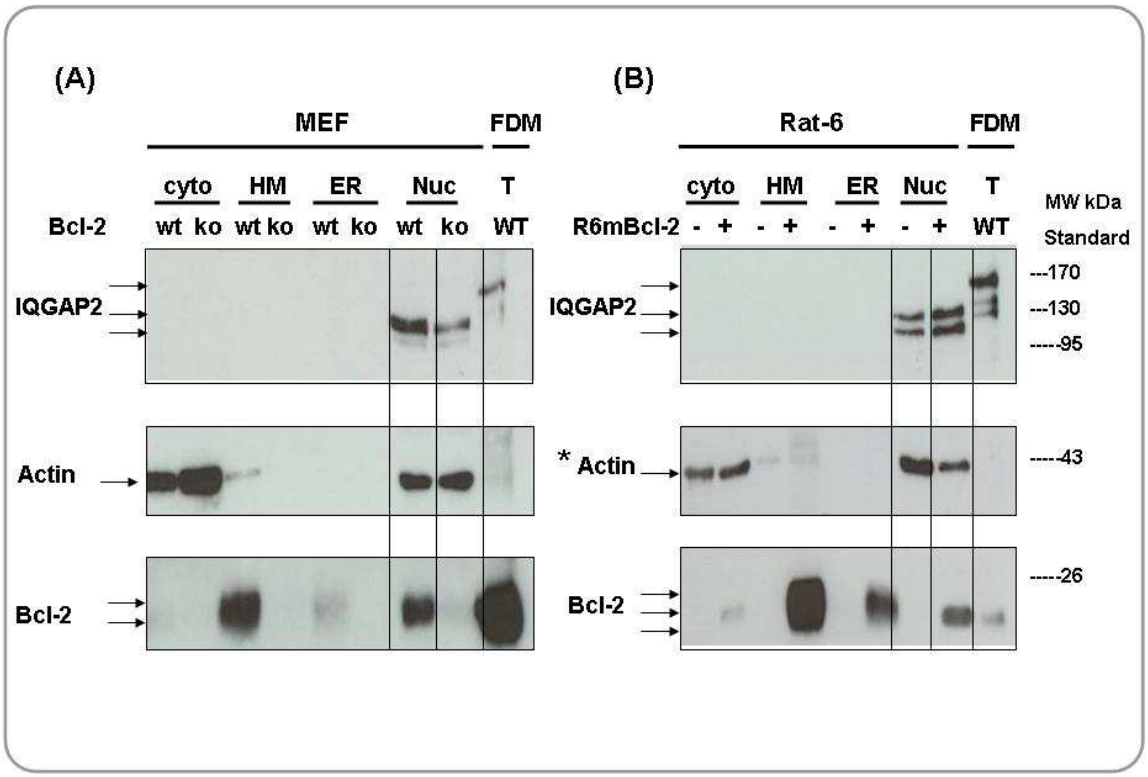

Figure 3-26: In fibroblasts, IQGAP2 is only found on the nuclear envelope as ca. 130 kDa protein (doublet), but its abundance also depends on Bcl-2. Subcellular distribution of Bcl-2 and IQGAP2 between cytosolic, mitochondrial (HM), ER and nuclear envelope fractions of Bcl-2 $^{+/+}$ and Bcl-2 $^{-/-}$ (KO) MEF **(A)** and wt and mouse Bcl-2 over expressing R6 fibroblasts (R6-mBcl-2) **(B)** Actin serves a loading control. An FDM total extract (T) is show as comparison of the IQGAP2 molecular weights. Note the reduced level of IQGAP2 in the nuclear fraction of Bcl-2 $^{-/-}$ MEFs and increased level in R6-mBcl-2 cells (*****Actin). Mini PAGE 15 %, 1 % CHAPS IBC Buffer, 2 x Protease Inhibitors, 4 µM MG132, 50 µg protein per slot.

3.6.3.3 Endogenous IQGAP2 is stabilized in HeLa cells over expressing Bcl-2

To confirm the inverse situation, namely that IQGAP2 is more efficiently bound to membranes and probably more stabilized in the presence of high levels of Bcl-2, we looked at the subcellular distribution of IQGAP2 in cytosol, total membrane (TM = heavy and light/ER), nuclear membrane/nuclear fraction (Nuc) and total extract (T) of wt and mouse Bcl-2 over expressing Hela cells. As shown in Fig. 3-27, Hela cells expressed very little IQGAP2 and it was exclusively found in the cytosol in the form of a ca. 160 kDa protein. Upon Overexpression of Bcl-2, the endogenous IQGAP2 protein was drastically upregulated in all subcellular fractions. Astonishingly, this was also the case in the cytosol, where usually only a few Bcl-2 molecules are found (Fig. 3-27). Thus, Bcl-2 had a dramatic stabilization effect on IQGAP2, maybe a

mechanism that might be important for the survival or any other function of Bcl-2 (see also below). We then treated the cells with tunicamycin, an ER stress agent which induces effective apoptosis within 24 h. Clearly, there was no major change in the subcellular distribution of either IQGAP2 or Bcl-2. It seems that the little Bcl-2 present in the cytosol was totally degraded. Concomitantly, cytosolic IQGAP2 diminished, too, showing again the interdependence of the two proteins for their stability.

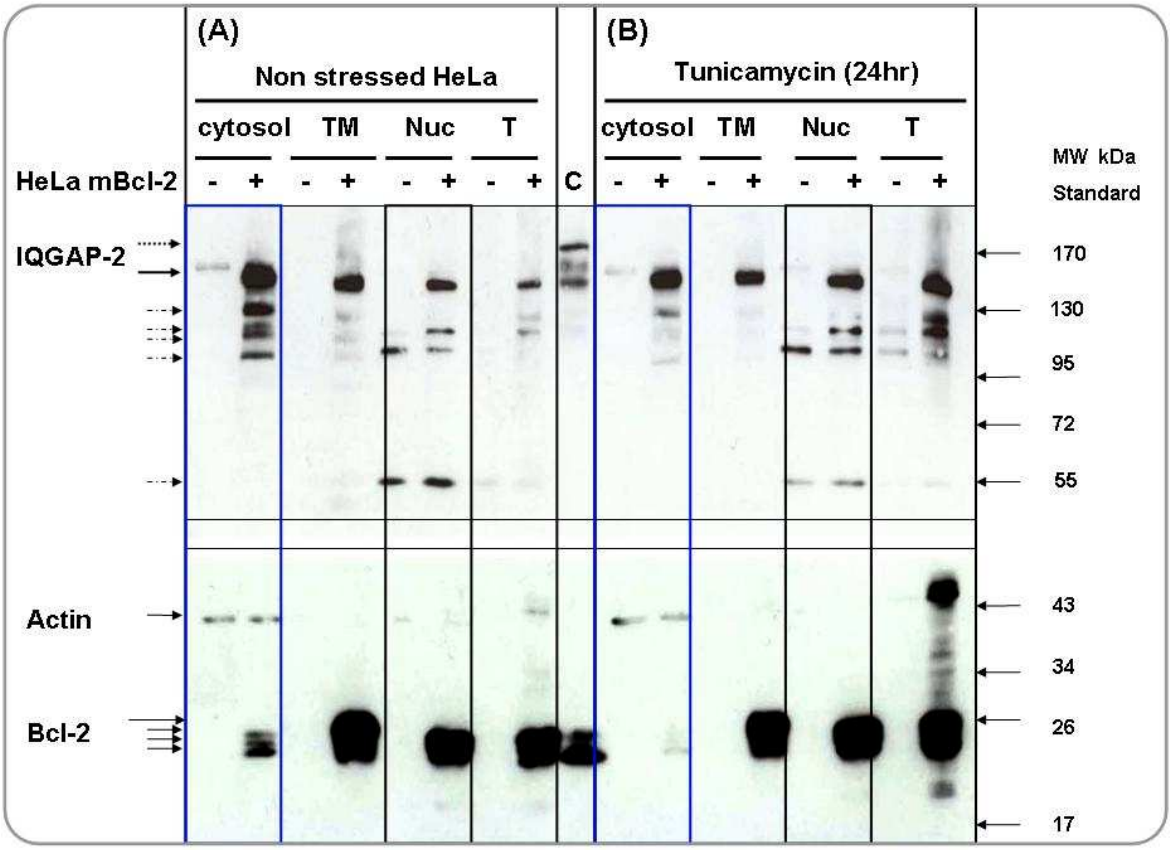

Figure 3-27: Murine Bcl-2 over expressed in HeLa stabilizes IQGAP2 in all subcellular fractions. Western blot analysis of IQGAP2 and Bcl-2. Cytosol, total membrane (TM, heavy and light/ER), nuclear membrane (Nuc) and total lysates (T) of non-stressed wt and mouse Bcl-2 over-expressing Hela cells (**A**). Cells were treated with tunicamycin (4µg/ml) for 24 hr (**B**). Actin is used as a loading control. C: total extract from FDM for comparison. Note that IQGAP2 is very low expressed in wt Hela cell, but stabilized in all fractions when Bcl-2 is over expressed. SDS gradient PAGE 12-19 %, non-reducing conditions; 1 % CHAPS IBC Buffer, 2 x Protease Inhibitors, 4 µM MG132, 50 µg protein per slot.

3.6.3.4 Subcellular distribution of Bcl-2 in IQGAP2 $^{+/+}$ and IQGAP2 $^{-/-}$ MEFs

Since we consistently found less IQGAP2 on the mitochondrial or nuclear membranes/nuclear fraction of Bcl-2 deficient cells and more IQGAP2 in Bcl-2 over expressing cells, without seeing any evidence for a higher abundance of the protein elsewhere, we thought that conversely, the levels and stability of Bcl-2 may also depend on IQGAP2. We therefore determined the expression and subcellular distribution of endogenous Bcl-2 in IQGAP2 $^{-/-}$ MEFs.

As the IQGAP2 protein was low abundant in MEFs and difficult to detect by Western blotting, except in an enriched nuclear envelope fraction (see Fig. 3-26), we determined the IQGAP2 genotype in wt and IQGAP2 $^{-/-}$ MEFs by genomic PCR. As shown in Fig. 3-28, while the PCR amplified in wt MEFs a band of 600 bp, the size of this band was 750 bp for IQGAP $^{-/-}$ MEFs. We confirmed thereby that wt MEFs contain the IQGAP-2 gene in principle able to express IQGAP2 protein (although little) and that the genotype of the IQGAP2 KO cells is correct.

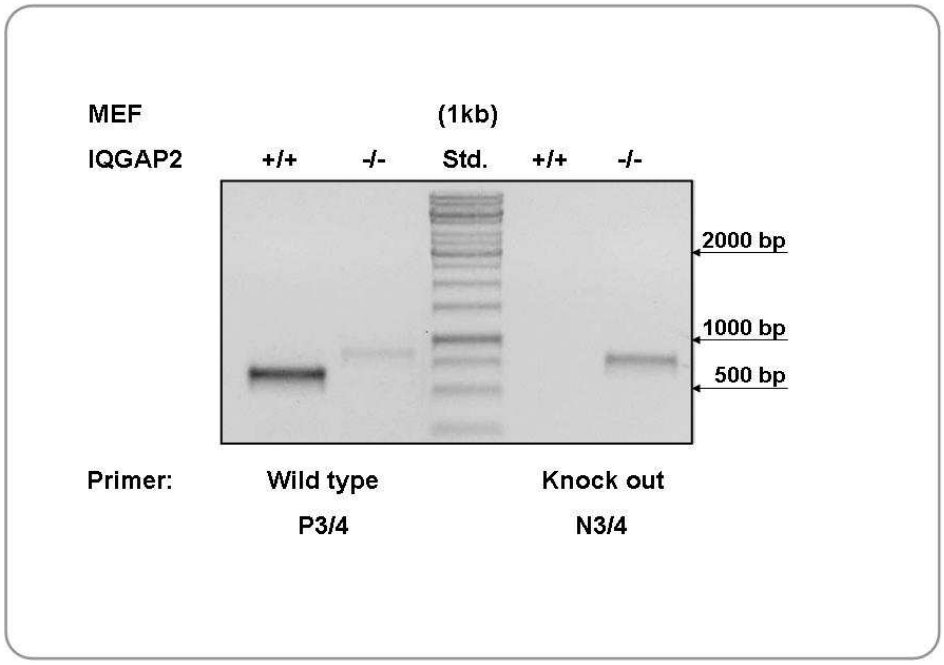

Figure 3-28: Genotyping of IQGAP2 in wt and IQGAP2-/- MEF. RT-PCR of IQGAP2 $^{+/+}$ and IQGAP2 $^{-/-}$ MEFs. The 1.0 % TAE agarose gel shows the wild type (600 bp) and the knock out (750 bp) fragments of the amplified murine DNA of IQGAP2. MEF IQGAP2 knock out primer pairs (N3/4) as well as wild type primer pairs (P3/4) were also used as a control for both, wild type and knock out RT-PCR. Standard: 1 kb Generuler.

We then compared endogenous Bcl-2 expression between wt and IQGAP2 $^{-/-}$ MEFs. For that purpose we prepared fractions of cytosol, total membranes (heavy/light membranes, TM), nuclear envelope (Nuc) and total samples (T) from both cell lines and subjected them to anti-Bcl-2 Western blotting. Indeed, as suggested, protein levels of Bcl-2 were significantly reduced in the total extract and on total membranes (but not on nuclear membranes) of IQGAP2 $^{-/-}$ as compared to wt MEFs (Fig. 3-29). This was not due to diminished protein loading as the actin Western blot showed equal protein applied to the SDS-PAGE. This indicates that a subset of IQGAP2 and Bcl-2 cooperates to stabilize each other on intracellular membranes. Furthermore, while the total membrane fraction usually contains some associated/bound actin, this was not the case in IQGAP2$^{-/-}$ cells (Fig. 3-29) indicating that IQGAP2 possibly interacts with actin or other cytoskeletal filaments (as has been previously shown, Brill et al., 1996, Korenbaum et al.,

2002, Chew et al., 2005). Thus, a lack of IQGAP2 would disrupt actin binding to membranes. Since this experiment has only been performed once, the latter finding needs to be confirmed.

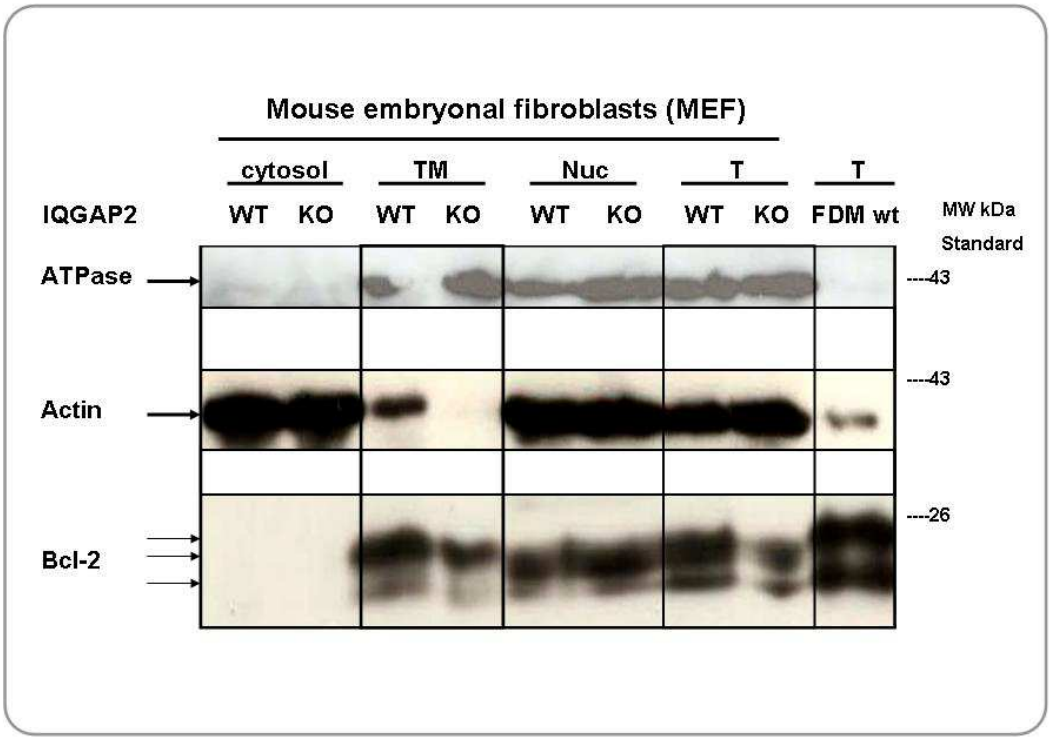

Figure 3-29: Less Bcl-2 protein was detected in the total and nuclear membrane fractions of IQGAP2 $^{-/-}$ as compared to wt MEFs. Subcellular distribution of Bcl-2 in the cytosol, total membrane (TM, heavy and light (ER), nuclear membrane/nuclear fraction (Nuc) and total lysate (T) of wt and IQGAP2 knock out (KO) MEFs. FDM total lysate (T) is used in parallel as a control. Actin is shown as cytosol and ATPase and mitochondrial (TM) loading control. However, note that some actin also appears in the TM fractions and this amount was not detected in the IQGAP2 $^{-/-}$ sample. SDS gradient PAGE 12 – 19 %, non-reducing conditions, therefore the Bcl-2 triple bands (see above), 1 % CHAPS IBC Buffer, 2 x Protease Inhibitors, 4 µM MG132, 100 µg protein per slot.

3.6.4 Comparison of the various IQGAP2 forms/bands between mouse and human cells

In Bcl-2 over expressing Hela cells, the most prominent band of stabilized IQGAP2 runs at ca. 160 kDa on SDS-PAGE. This differs from the main 180 kDa form present in FDMs (Fig. 3-27). A side-to-side analysis on SDS-PAGE reveals that the major form of IQGAP2 in HeLa-mBcl-2 cells corresponds to the lower band of the triplet seen in FDM extracts (Fig. 3-27 and 3-30 A and B). Specifically, the weakly expressed IQGAP2 protein in the cytosol of normal Hela cells seem to migrate yet differently, namely at the size of the intermediate form in FDMs (Fig. 3-30 B). Finally, in MEFs and R6 fibroblasts IQGAP2 exhibits a double band that is even smaller than the others (ca. 130 kDa). Different splice variants of IQGAP2 have been described and it is well possible that each species and/or cell type expresses another form with similar or distinct

functions (see Discussion figure 4-2). A more closer view, IQGAP2 migrates in a typical pattern of increasing charge variants that are generated by adding phosphate groups (Fig. 3-30 A and 3-30 B) as recently reported (Chew et al., 2005). Alternatively, IQGAP2 may be modified by ubiquitination and glycosylation etc, giving rise to different forms on SDS-PAGE. Importantly, from our ABT-737 release samples, we identified two forms of IQGAP2 by mass spectrometry, the 180 and the 160 kDa form. Both forms could be specifically immunoprecipitated with endogenous Bcl-2 (see Fig. 3-22) although the 160 kDa species interacted with Bcl-2 more specifically. To sort this definitely out, future work will aim at performing IQGAP2/Bcl-2 IPs in FDMs, MEFs, R6, Hela and HEK293T cells to see if all forms of IQGAP2, including phospho-IQGAP2, interact with Bcl-2. In addition, by knocking down IQGAP2 expression with a si/shRNA whose sequence we will make sure that all bands detected with our anti-IQGAP2 antibody indeed belong to various IQGAP2 proteins.

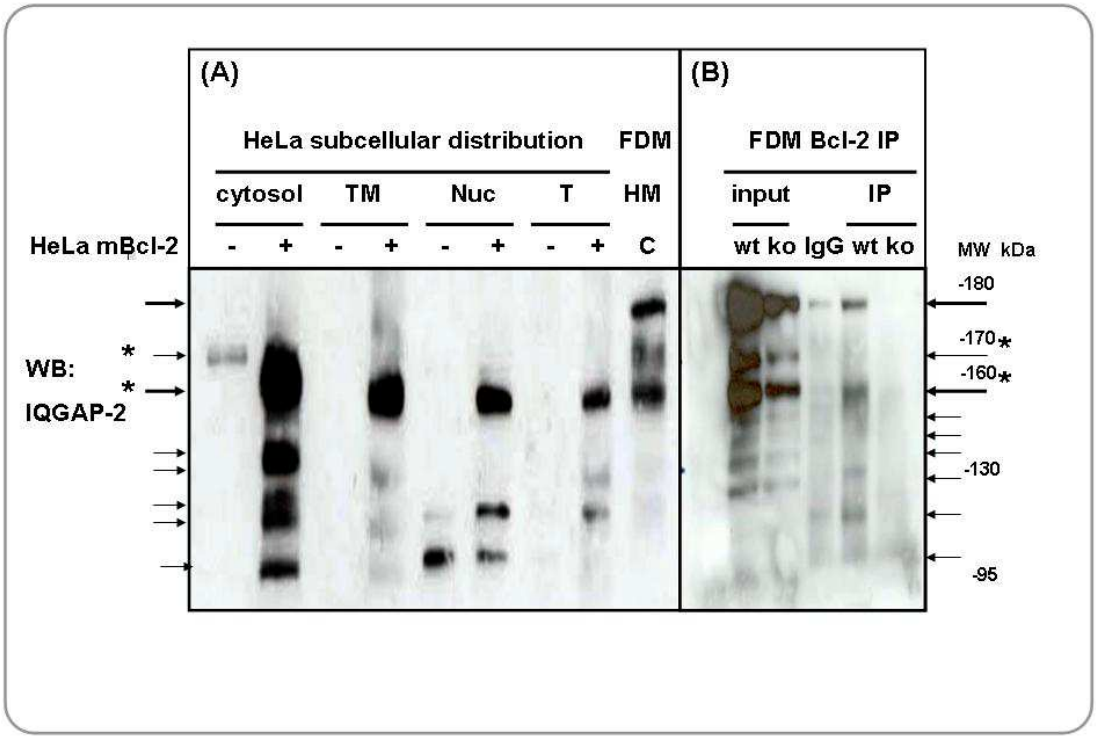

Figure 3-30: Regular pattern of migrating IQGAP2 isoforms or modifications in wt Hela, Hela-mBcl-2 and FDM cells. Western blot analysis of IQGAP2 in the cytosol, total membrane (TM), nuclear membrane (Nuc) and total lysate (T) of wild type Hela, mBcl-2 over expressing Hela (**A**) and FDM cells (**B**). It seems that from the FDM triplet, stabilized IQGAP2 in Hela-mBcl-2 corresponds to the lower band (arrow with asterisk, 160 kDa) and the faintly expressed cytosolic IQGAP2 in Hela to the middle band (arrow with asterisk, 170 kDa). Other bands appear in the lower molecular weight region, however these might be cross-reactive proteins or phosphorylated forms of IQGAP2 (arrows). The upper (180 kDa) and the lower (160 kDa) proteins of the triplet in FDMs can be specifically co-IPed with Bcl-2 (**B**). Gradient PAGE 12-18 %, non-reducing conditions.

3.6.5 Investigating the impact of Bcl-2 or IQGAP2 on the mitochondrial morphology

Schmidt et al. (2008) discovered age-dependent abnormalities in the morphology of liver and skeletal muscle mitochondria from IQGAP2 $^{-/-}$ mice. By using transmission electron micrography (TEM) they could show an edematous matrix and collapsed cristae in these mitochondria. Moreover, Altmann and Westermann (2008) identified a series of essential S. cerevisiae genes whose deletion impeded yeast survival and affected both mitochondrial morphology and the cytoskeletal network. Among them was Iqg1, the only yeast homolog of IQGAP1/2. Indeed, when Iqg1 was conditionally knocked-out in yeast, these cells showed an aberrant, clustered mitochondrial morphology, altered mitochondrial distribution within the cell and a disorganized actin cytoskeleton. The large number of yeast mutants which display both a disrupted actin cytoskeleton and an abnormal mitochondrial morphology underscores the fundamental importance of the actin cytoskeleton in determining shape, morphology and perhaps also some crucial functions of mitochondria. Obviously a variety of proteins participate in this linkage and IQGAP2 may be one of them. Several publications indicate that IQGAP proteins modify actin and regulate the actin polymerization in different cellular compartments by different localization (Bashour et al., 1997, Briggs et al., 2003). For example, Xenopus IQGAP1 accumulates at adherence junctions, whereas IQGAP2 is also significantly localized within the cell body, at the nuclear membrane or at/in the nucleus (Yamashiro et al., 2003. Chew et al., 2005 and own data Fig. 3-34 B). Indeed, by looking at the structure and domain organization of IQGAPs, it becomes apparent that they all have actin-binding and calcium/calmodulin binding regions that may be important for some aspects of cytoskeleton regulation and calcium homeostasis within the cell (for further details see discussion).

3.6.5.1 Mitochondrial morphology of MEFs deficient in Bcl-2 or (IQGAP2)

Healthy mitochondria are in a dynamic steady state of fission and fusion. Mitochondrial fission is required for the selective elimination of damaged mitochondria. This process may also be important to remove apoptotic mitochondria by a Bax/Bak mediated pore formation. Tondera et al. (2009) showed that mitochondria hyperfuse and form a highly interconnected network in cells treated with minor stress stimuli. This process requires metabolically active mitochondria that produce sufficient amounts of ATP to confer stress resistance to cells (see page 25 chapter 1.5.2.4). We accurately examined the mitochondrial morphology of wt, Bcl-2 $^{-/-}$ and IQGAP2 $^{-/-}$ MEFs in the absence and presence of 1 µg/ml of tunicamycin or 100 mM etoposide for 6 – 9 hr and monitored cytochrome c release and nuclear morphology by immunofluorescence analysis. During this time of the stress, wt cells typically showed elongated mitochondria organized in an

interconnected network without any MOMP/cytochrome c release (Fig. 3-31 A-D next page), MEFs deficient for Bcl-2 or IQGAP2 did not show such a response. Both cell types displayed punctate, clustered mitochondria that seem to be fragmented at some places (Fig. 3-32 A-B page 122 and appendix Fig. 6-1 A-B).

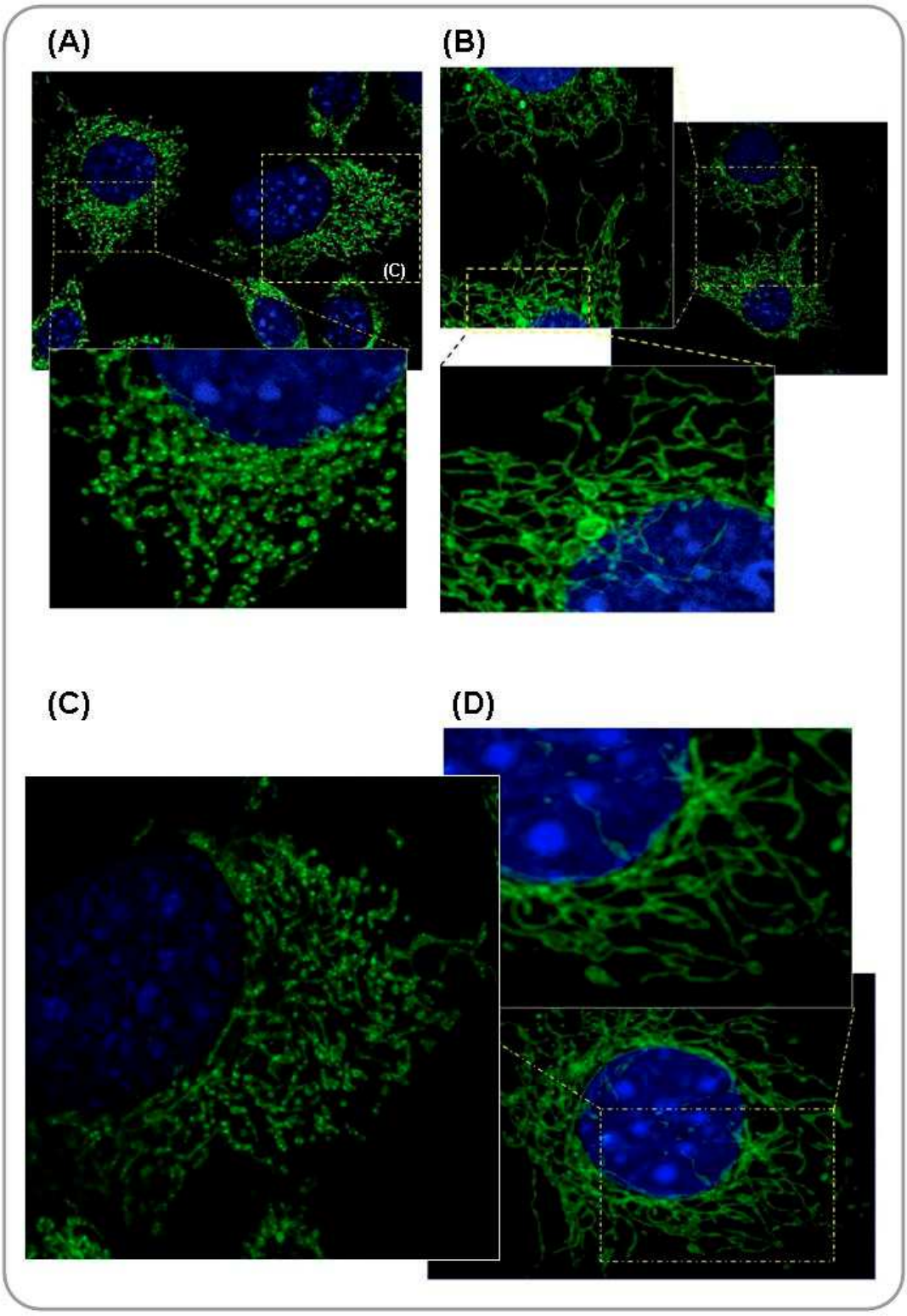

Figure 3-31 A-D: Morphology of mitochondria in healthy and etoposide treated wt MEF. Wild type mouse embryonic fibroblasts (MEFs) either untreated (**A, C**) or treated with 100 µM etoposide for 9 h (**B**) or treated with 1 µg/ml tunicamycin for 9 h (**D**), were fixed by 4 % formaldehyde and then stained with anti-cytochrome c antibodies and secondary anti-mouse Alexa 488. Nuclei are stained with Hoechst 33342. Note that while mitochondria of untreated cells (**A, C)** look more round and punctate, those of etoposide and tunicamycin treated cells exhibit an elongated, tubular structure (**B, D**). These changes occur before cytochrome c and nuclear fragmentation, i.e. at early time points of apoptosis induction. Immunofluorescence analysis was done by confocal microscopy, Leica TCS SP2 AOBS. Magnification: overviews: 630 x, zoom: 1260-1890 x

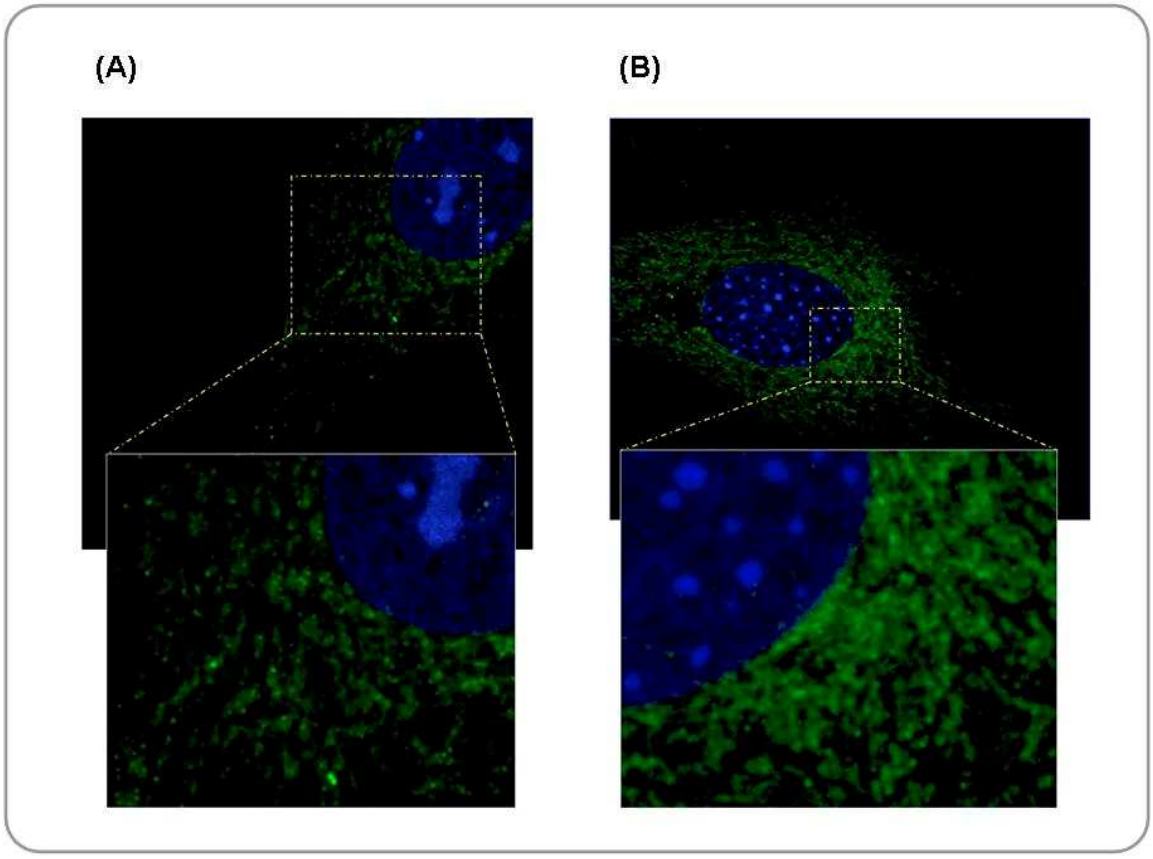

Figure 3-32 A-B: Morphology of mitochondria of healthy and treated Bcl-2 -/- MEFs. Non-treated Bcl-2 $^{-/-}$ MEF **(A)** and etoposide treated Bcl-2 $^{-/-}$ MEF after 9 hrs **(B)** were fixed by 4 % formaldehyde and then stained with anti-cytochrome c antibodies and secondary anti-mouse Alexa 488. Nuclei are stained with Hoechst 33342. Confocal microscope, Leica TCS SP2 AOBS, Magnification: overviews: 630 x, zoom: 1260-1890 x, Overview projection. Note that this genotype shows a punctated pattern of mitochondria reminiscent of wt MEF (see Fig. 3-31 A-D). For IQGAP2 $^{-/-}$ MEFs see appendix figure 3-34.

3.6.6 Elucidating co-localization of IQGAP2 and Bcl-2 inside cells by confocal microscopy

To investigate if IQGAP2 and Bcl-2 interact with each other in vivo (inside cells), we performed co-localization studies by confocal fluorescence microscopy. We identified IQGAP2 as Bcl-2 binding partner by the ABT-737 release assay and validated this interaction by co-IP of both antibodies in FDM cells. But these cells are not ideal for immunofluorescence studies because suspension cells are round, contain very little cytoplasm, hardly attach to cover slips and are difficult to transfect. We therefore chose wt and mBcl-2 over expressing Hela cells for our confocal analysis. To obtain the best signal for an IQGAP2/Bcl-2 co-localization, we thought to transiently transfect IQGAP2 into Hela-mBcl-2 cells and to score the cells with the highest

expression of both proteins for an eventual co-localization pattern. For that purpose we obtained a HA-tagged IQGAP2 cDNA from the lab of Dr. David Sacks. Unfortunately, this cDNA was very difficult to transfect and gave very little IQGAP2 expression. We found out that it was cloned under a weak SV40 promoter and also contained a mutation in the 3' part of the cDNA, which overread the stop codon leading to a longer protein. We nevertheless transfected this IQGAP2-HA cDNA into Hela-mBcl-2 cells and performed anti-Bcl-2 and anti-IQGAP2 immunofluorescence analysis after 24 h. As shown in Fig. 3-33 A, over expressed mouse Bcl-2, detected with a polyclonal anti-Bcl-2 antiserum, displayed a fluorescence staining pattern that was typical for the nuclear envelope (ring around the nucleus, red fluorescence). Of those rare cells which co-expressed IQGAP2, this pattern was also seen suggesting that IQGAP2 was at least partially recruited to the nuclear envelope by over expressed Bcl-2 (Fig. 3-33 B, green/yellow fluorescence).

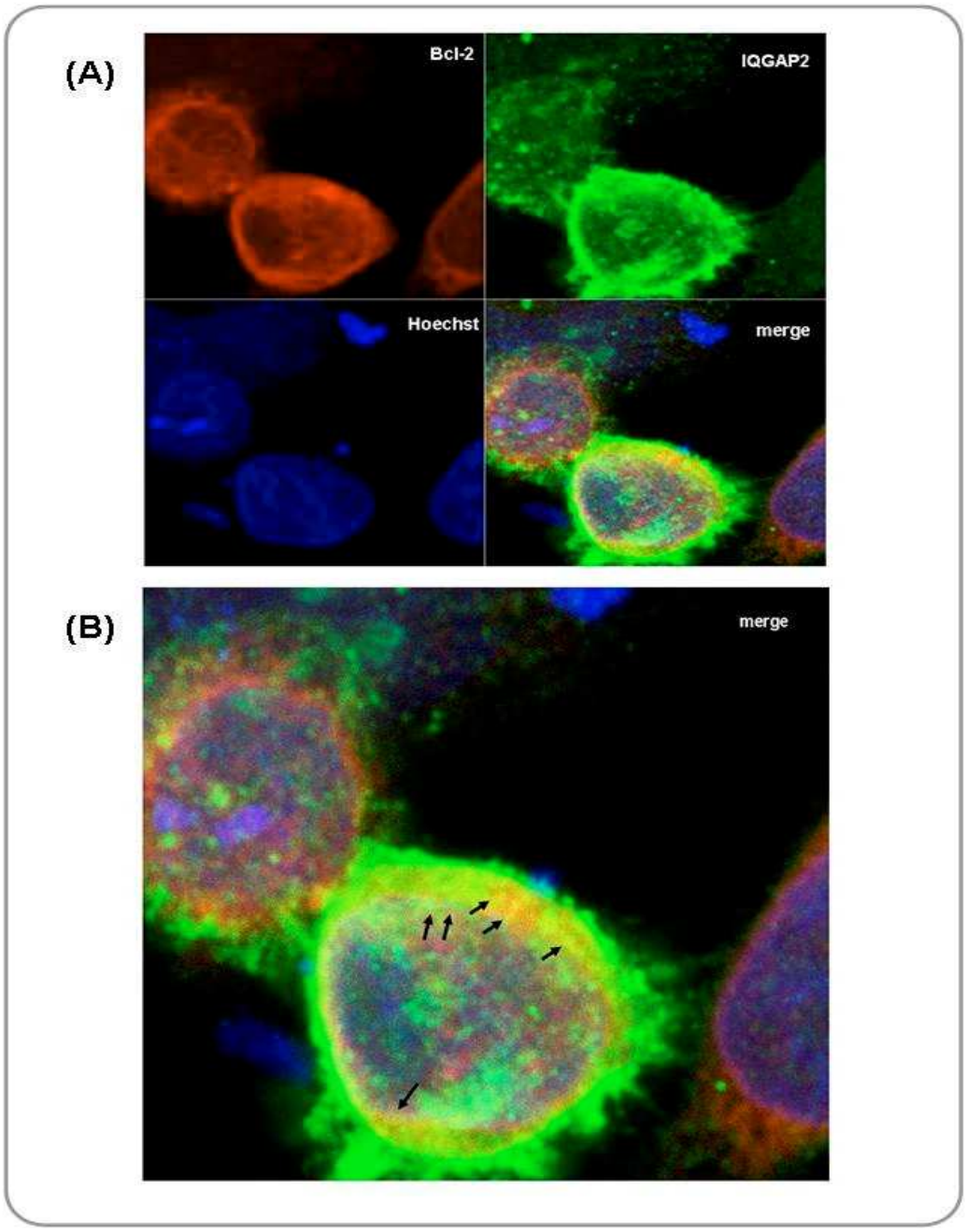

Figure 3-33 A-B: Immunofluorescence staining of co-over expressed IQGAP2 and Bcl-2. **(A)** HeLa cells over expressing mouse Bcl-2 were transiently transfected with human-IQGAP2-HA for 24 h, fixed and permeabilized and immediately stained with polyclonal rabbit α-Bcl-2 antibody (upper left, red), a monoclonal mouse α-IQGAP2 antibody (upper right, green), and Hoechst 33342 (bottom left, blue). The merge on bottom right shows that part of IQGAP2 co-localizes with Bcl-2 (yellow staining). This is especially seen in the higher magnification (**B**). Most of the IQGAP2 protein however seems to localize differently, for example to the cytosol. Confocal microscope, Leica TCS SP2 AOBS, Magnification: overviews: 630 x (**A**), zoom: 1260-1890 x (**B**)

Figure 3-34 A-C demonstrate more outspread Hela-mBcl-2 cells transiently transfected with HA-h-IQGAP-2. Mouse Bcl-2 was present (red fluorescence) on the nuclear membrane and in a network of connected dots that were reminiscent of mitochondria. IQGAP2 (green fluorescence) also formed such a network structure and partially co-localized with Bcl-2.

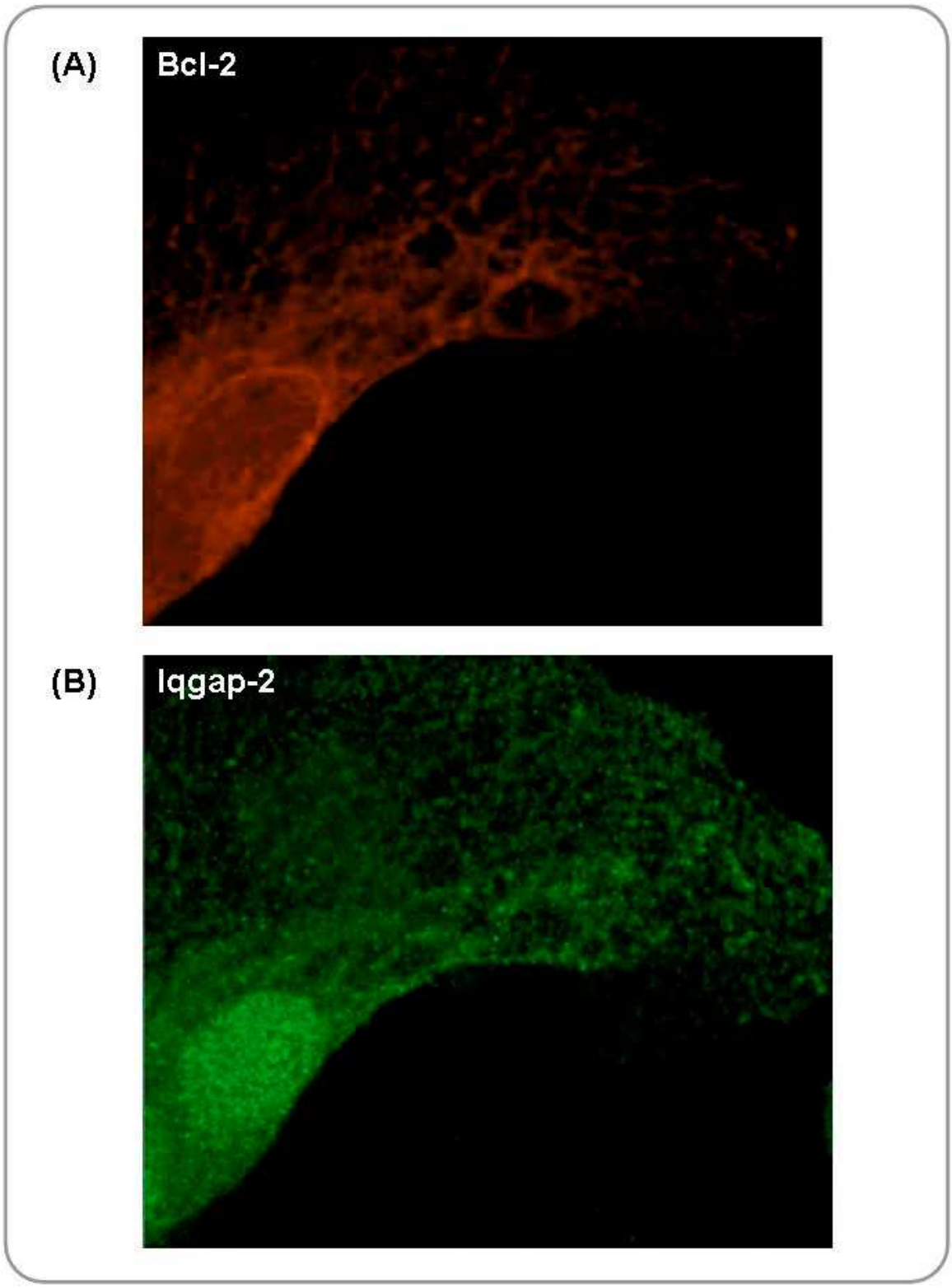

Figure 3-34 A-B: Immunofluorescence staining of co-over expressed IQGAP2 and Bcl-2. Hela cells over expressing mouse Bcl-2 were transiently transfected with human-IQGAP2-HA for 24 h, fixed and permeabilized and immediately stained with polyclonal rabbit α-Bcl-2 antibody (red fluorescence), a monoclonal mouse α-IQGAP2 antibody (green fluorescence), and Hoechst 33342 (not shown). Confocal microscope, Leica TCS SP2 AOBS. (**A**).Bcl-2 is shown as a ring around the nucleus but also within an interconnected network (**B**) IQGAP2 is concentrated at the nucleus but localizes along with Bcl-2 at similar structures within to the cytosol. Magnification: 630 x

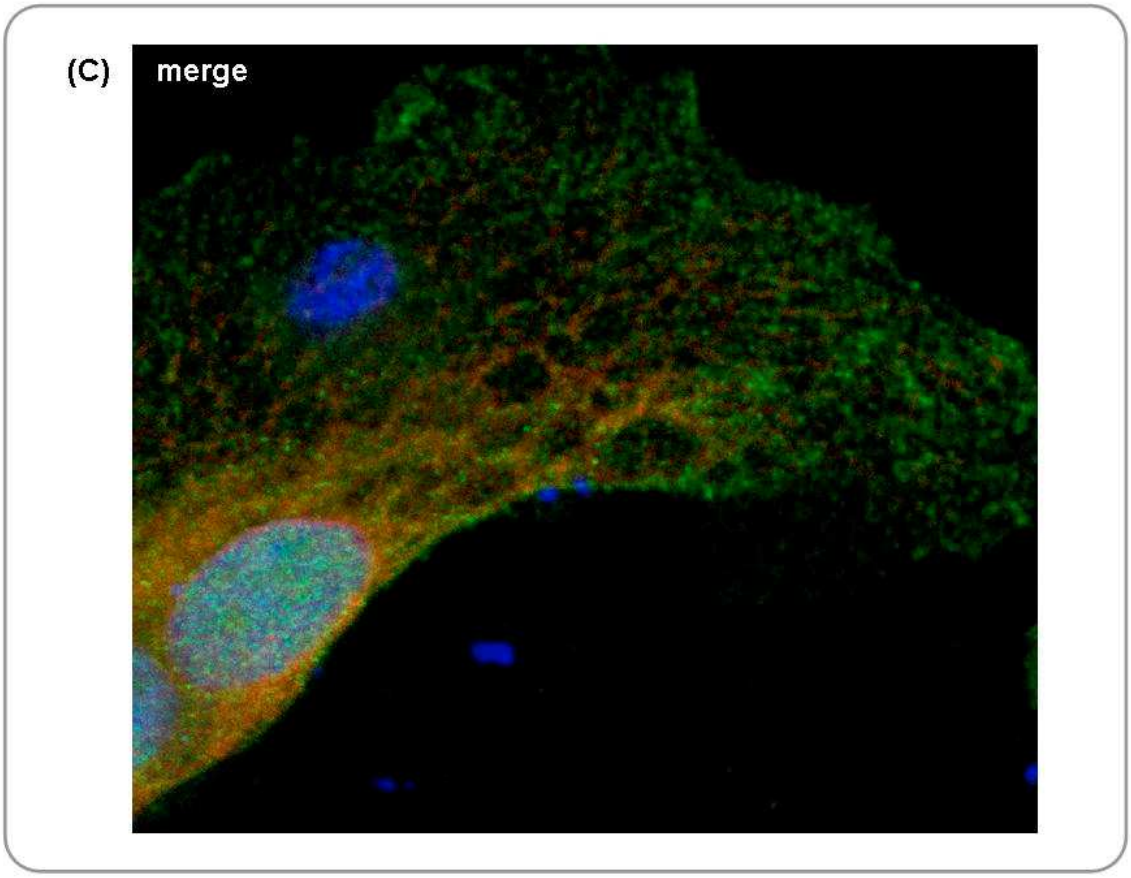

Figure 3-34 C: Immunofluorescence staining of co-over expressed IQGAP2 and Bcl-2.
Merge: IQGAP2 co-localizes partially with Bcl-2 around the nucleus and along a dotted intracellular network (green/yellow/red staining). Confocal microscope, Leica TCS SP2 AOBS, Magnification: 630 x.

3.6.7 Transiently co-expressed Flag-hBcl-2 and GFP-hIQGAP-2 do not interact

As described above in chapter 3.6.5 the IQGAP2-HA cDNA obtained from the lab of Dr. D. Sacks unfortunately transfected very badly into Hela cells and was, by consequence, low expressed. To improve transfection efficiency and intracellular expression of IQGAP2 we obtained a second, GFP-tagged human IQGAP2 cDNA from Dr. Valentina Schmidt, NY, USA. Here hIQGAP-2 expression was driven by the strong CMV promoter in the pEGFP-C1 vector. In order to investigate if IQGAP2 and Bcl-2 interact by over expression of Flag-hBcl-2 and IQGAP2 (GFP-hIQGAP-2) we transfected the plasmids either alone or together into HEK293T cells. First, we examined transfection efficiency by counting green fluorescent cells and found that while 80% of the cells were positive of the control pEGFP, about 45% showed fluorescent staining of pEGFP-h-IQGAP-2. We then prepared whole cell lysates of the transfected cells to perform anti-Bcl-2 or IQGAP2 IPs followed by Western blotting. As shown in Fig. 3-35 A, GFP-

IQGAP2 was nicely over expressed in HEK293T cells and ran at higher molecular mass than the endogenous form (ca. 166 kDa). Also Bcl-2 could be effectively over expressed. For unknown reasons, this time the co-transfection yielded much less GFP-IQGAP2 than the single IQGAP2 transfection. This was unexpected as our previous results showed that IQGAP2 gets stabilized by high levels of Bcl-2. Unfortunately, GFP-IQGAP2 could not be immunoprecipitated with Bcl-2 under these conditions. Also the inverse was not true. The weak band of Bcl-2 in anti-IQGAP2 IPs was of similar intensity as in the IgG control. This failure was not due to a lack of IPs of the respective proteins as both IQGAP2 and Bcl-2 got effectively immunoprecipitated (Fig. 3-35B). As endogenous IQGAP2 and Bcl-2 were easily IPed (Fig. 3-22), we speculated that addition of the GFP moiety to the N-terminus of IQGAP2 interfered with its binding to Bcl-2. Further studies need to be performed with untagged or small tagged versions of IQGAP2.

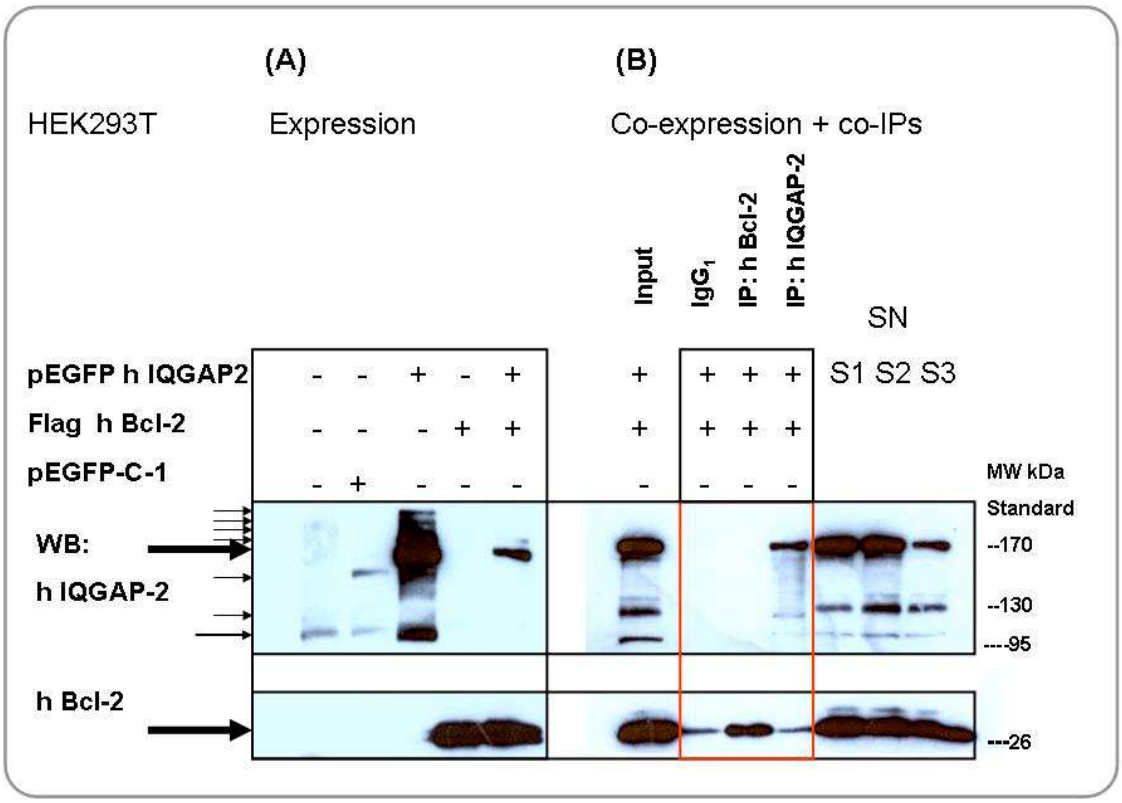

Figure 3-35 A-B: Co-over expressed GFP-h-IQGAP-2 and flag tagged h-Bcl-2 do not interact. (A+B) HEK293T were transiently transfected with either human Bcl-2 or human-IQGAP-2 or both for 24 h. **(B)** h-Bcl-2 and h-IQGAP-2 were co-transfected into HEK293T and used for the indicated immunoprecipitations (3mg, whole cell lysate) followed by Mini SDS PAGE, anti-human Bcl-2 and anti-human IQGAP2 Western blot analysis. Total cell lysates of each transfection were prepared by using IBC-buffer containing 1 % digitonin, 2 x Protease Inhibitors, 4 µM MG132, 100 µg protein per slot. (SN): supernatant, (S1) IgG1 control. (S2) Bcl-2 IP, (S3) IQGAP-2 IP

4 Discussion

Programmed cell death is regulated by the concerted interactions of the Bcl-2 family proteins. Several models have been developed to explain how anti-apoptotic and pro-apoptotic proteins regulate death and survival. It is suggested that BH3-only proteins either bind to the hydrophobic pocket of Bcl-2, Bcl-xL, Bcl-w or Mcl-1 to release Bax/Bak or an activator of Bax/Bak or that some BH3-onlies such as Bim, Puma and Bid could even interact with and directly activate Bax/Bak (Youle and Strasser, 2008). If Bcl-2-like survival factors are overexpressed they sequester and inactivate BH3-only proteins leading to cell death resistance, a state that is often reached in cancer cells. Bax and Bak are essential for apoptosis induction as cells deficient in the two proteins (Bax/Bak DKO) do not show any cytochrome c release and caspase-dependent and –independent apoptosis.

Reduction or loss of expression of survival proteins like Bcl-2 or Bcl-w supports the increase of apoptosis that may lead to neurodegenerative and immunodeficiency diseases (Mehler et al., et al., 2000, Yang and Klionsky, 2010). On the other hand, increased expression of survival proteins is often associated with the formation of tumors such as B lymphoid tumors. Furthermore, this process makes them sensitive to develop into higher transformed stages by synergistic mutations like the translocation of myc leading to more aggressive forms of follicular lymphoma (Yano et al., 1992, Mc Donnell and Korsmeyer, 1991, Strasser et al., 1993, Vaux et al., 1998, Cory et al., 2003).

Most interaction partners of Bcl-2 were found in artificial expression systems that overexpress specific Bcl-2 family proteins. Those highly enriched proteins may override sensitive cellular physiological pathways. Furthermore, co-expressed proteins favour distinct protein-protein interactions or disrupt physiologically relevant interactions. To identify "physiological" interactors of anti-apoptotic Bcl-2 proteins, it is therefore crucial to isolate binding partners under conditions where these proteins are endogenously expressed.

The focus of this thesis was to isolate unknown endogenous binding partners bound to the hydrophobic pocket or other binding sites of Bcl-2 in healthy monocytes. We found several new, putative interactions partners of Bcl-2, which may point to novel functions of Bcl-2 and/or explain how Bcl-2 regulates apoptosis through Bax/Bak.

4.1 Bcl-2 family proteins: Endogenous expression, subcellular distributions and complex formations in healthy and apoptotic cells

To find new binding partners that interact with Bcl-2 we used a physiological experimental system of IL-3 dependent, wild type and Bcl-2 $^{-/-}$ factor-dependent mouse monocytes (FDMs) isolated from the fetal liver and immortalized with the Hox8b. This cellular system has been shown to be genomically stable, even during long term culture conditions.

As expected FDMs showed stable expression levels of Bcl-2 family members. Bcl-2 and Bcl-xL mainly resided on mitochondria and the ER, although some Bcl-xL was also present in the cytosol. In response to apoptotic stimuli this subcellular localization did not change. Interestingly, Bcl-2 gets proteolytically degraded in FDM, but not in FDC-P1 cells upon IL-3 deprivation. Mcl-1 is also majorly membrane-bound and is degraded by the ubiquitin proteasome system in response to IL-3 withdrawal, as previously reported (Nijhawan*, et al.*, 2003; Maurer et al., 2006).

Bax was found in both the cytoplasm and on mitochondria. Interestingly, in apoptotic FDMs we did not observe any Bax translocation to mitochondria. Obviously, the Bax already attached to mitochondria was sufficient to drive apoptosis (together with Bak). Also, as previously reported, Bak was almost exclusively membrane bound, mostly present in mitochondria enriched fractions. The reported Bcl-2 interactor Bad was only found cytosolic and ER but not in heavy membrane (mitochondrial) fractions of healthy FDMs and FDC-P1s. As expected Bid mainly resided in the cytosol and less on heavy membranes and ER fractions. Upon apoptosis induction, neither Bad nor Bid bound to Bcl-2 survival factors or Bax/Bak. They rather got proteolytically degraded with time.

To get an idea about complex formations of Bcl-2 family members, we performed blue native gel electrophoresis and tested by Western blotting on SDS-gels at which molecular masses the respective Bcl-2 member complexes resolved. Bak was present in many complexes ranging from low (50 kDa) to high molecular masses (400 kDa) indicating that Bak was either already present in oligomers on mitochondria of healthy cells, or interacted with several inhibitors, including high molecular mass VDAC2, a reported Bak inhibitor (Cheng et al., 2003). Our results for sure indicate that Bak cannot only be bound to the survival factors Bcl-2, Bcl-xL or Mcl-1, as has been proposed in many previous reports, because these binding partners have sizes between 20 and 35 kDa and hence would never make up a complex of 400 kDa. In contrast to Bak, Bax migrated in complexes between 20 and 60 kDa, both the cytosol and on mitochondria of healthy FDMs. An extensive proteomics analysis of another PhD student in our lab revealed

that Bax was neither a dimer nor interacted with any protein in healthy cells. The molecular mass shift is most likely due to structural constraints or unknown posttranslational modifications of the Bax protein. In response to IL-3 deprivation, the range of Bak high molecular weight complexes did not change much although the tendency was that they rather decreased than increased (by communication Michael Ryan 2010). Bax complexes on the other hand clearly shifted upwards suggesting the formation of Bax oligomers crucial for MOMP in apoptotic cells.

Unexpectedly most of the BH3-only protein Puma was already found on mitochondria enriched heavy membranes in both healthy FDC-P1 and FDMs and still associated with this fraction under apoptotic conditions. Usually, Puma levels are supposed to be very low and the protein gets transcriptionally induced by either FOXO3A or p53 in response to IL-3 deprivation or genotoxic stress, respectively. After transcriptional induction, it translocates to mitochondria to either directly activate Bax/Bak or bind to Bcl-2-like survival factors to displace another BH3-only protein or a Bax/Bak activator. (Han et al., 2001, Nakano and Vousden, 2001). We however did not observe any changes in subcellular localization or amount of Puma in response to IL-3 deprivation. This is in agreement with recent studies performed in our lab by the diploma student Kai Sterz. He also found constitutive expression of Puma on mitochondria of healthy FDMs and this level did not further increase, but rather decrease (due to caspase-dependent degradation) in IL-3 deprived cells. He could further show by gel filtration analysis that Puma runs in very high molecular weight complexes both in healthy and apoptotic cells indicating that in FDMs Puma probably interacts with many inhibitory proteins (or a high mass protein) on mitochondria and activates Bax/Bak by changes in the protein complex composition. It will therefore be crucial to identify Puma binding partners in healthy and IL-3 deprived cells. Our proteomic approaches described here for Bcl-2 binding partners will help to undertake this task for Puma.

As Puma, Bim is also found in high molecular weight complexes on mitochondria of healthy FDC-P1 cells. However, it gets further induced in response to IL-3 deprivation and then maybe acts like Puma on Bax/Bak activation (Dijkers et al., 2000, Wang et al., 2007). In FDMs, Bim is rarely detected due to the fact that these cells are immortalized by Hox8b. It was been reported that the transcription factor Hox8b represses Bim expression.

4.2 Separation of endogenous Bcl-2 protein complexes

By both gel filtration (diploma work of Kai Sterz) and blue native gel analysis (chapter 3.2.2 Fig. 3-12), Bcl-2 isolated from mitochondria of healthy FDMs migrated in a trailing pattern ranging from low (30 kDa) to very high molecular weight (450 kDa) complexes. This means that Bcl-2 either binds to several cellular proteins, including those of high molecular weight, and/or the trailing is due to a lipid effect. In contrast to Bcl-xL and Mcl-1, Bcl-2 is exclusively found in membranes (never in the cytosol) and requires high concentrations of detergent to be solubilized itself and with its binding partners. This is due to many hydrophobic helices and a high affinity of lipid binding of the protein. Indeed, Mcl-1 and Bcl-xL eluted in more discrete areas between 50 and 150 kDa and also the β-barrel MOM protein VDAC-1, was detected in spots rather than a trailing band on blue native gels as shown in figure 3-12.
Due to the absence of discrete Bcl-2 spots on BN-gels, it was impossible to separately analyse various Bcl-2 complexes by subsequent SDS-PAGE. We therefore decided to determine the protein content of binding partners by mass spectrometry of the whole region. We decided to use 5 g/g digitonin for our subsequent analysis because this gave the widest range of Bcl-2 positive fractions and digitonin was the “most physiological” detergent, considering that it had been previously used to determine all components of the respiratory chain complexes (Schägger et al., 2000).
After repetitive experiments, we could define two distinct areas where Bcl-2 ran on BN-gels (see chapter 3.2.2 figure 3-12). When we probed these areas with antibodies against published Bcl-2 binding partners, we found that VDAC1 and VDAC2 co-migrated within the highest molecular weight region (260 - 600 kDa). In this region, we also found Bak, a known binding partner of VDAC2. Cheng et al. (2003) previously showed that VDAC2 is an endogenous inhibitor of Bak. Furthermore a recent publication from Ren et al. (2009) illustrates that the VDAC-2-Bak interaction is crucial for thymocyte survival. Genetic depletion of VDAC2 in thymus resulted in excessive cell death that was rescued by the co-deletion of Bak.

It is difficult to define by BN gels if Bak and Bax are Bcl-2 binding partners under endogenous conditions. As reported by Willis et al. (2007) Bcl-2 only weakly interacts with these two proteins. We found that while Bak co-migrated with Bcl-2 in the high molecular weight region (140-350 kDa), Bax stayed in the lower area. Since Bak is a small protein of 28 kD and is known to oligomerize only upon apoptotic stress, its migration in the high molecular weight region is rather unexpected, indicating that it either majorly interacts with VDAC2 which is linked to the huge PT pore or binds more proteins in addition to Bcl-2 and VDAC2. The co-migration of Bcl-2 and Bax has most likely no physiological relevance and is just by chance, as our PhD student Sandra could show that Bax does not bind Bcl-2 or any other protein in healthy FDMs.

Endogenous Beclin-1 was shown to interact with Bcl-2 in HeLa cells under nutrient rich conditions and by over expressing of both Beclin1 and Bcl-2. This points to a high molecular weight protein complex between 140-350 kDa consisting of Bcl-2/Beclin-1 and further proteins (see Fig. 3-12).

4.3 Examination of published Bcl-2 binding partners by co-immuno-precipitation

It was previously reported that Bcl-2 interacts with the VDAC1 component of the PT pore. In addition, according to the "activator" and "displacement" model it is suggested either BH3-only proteins or Bax/Bak are bound to the hydrophobic pocket of endogenous Bcl-2, Bcl-xL, Bcl-w and Mcl-1 in healthy cells (Youle and Strasser, 2008).
As shown in chapter 3.4.2, Fig. 3-14, Fig. 3-15 we could not find any interactions of Bcl-2 with VDAC-1, Bax, Bak or any BH3-only proteins in anti-Bcl-2 co-immunoprecipitations of healthy and IL-3 deprived apoptotic extracts (also see diploma thesis Kai Sterz, and own data, unpublished). Both VDAC1 and Bak turned out to be “sticky” proteins which already interacted to a certain extent with the Sepharose beads in IgG controls as well as when Bcl-2 $^{-/-}$ extracts were used for IPs. This means that interactions between Bcl-2 and VDAC1 or Bak can be wrongly viewed as real if the right controls are missing. Indeed, both VDAC1 and Bak were identified in the so called “beads proteome”, which determined the proteins sticking to beads by mass spectrometry (Trinkle-Mulcahy et al., 2008).
In summary, based on our co-IP experiments we could neither lend support to the “activator” (BH3-only proteins Bim, Puma, Bid bound to Bcl-2) nor the “derepressor” (Bax/Bak bound to Bcl-2) models of Bax/Bak activation. We therefore speculated that Bcl-2 must have other proteins bound which may act as indirect or direct Bax/Bak activators after the release from the pocket by BH3-only proteins in apoptotic cells.

4.4 Isolation of "physiological" binding partners of Bcl-2

Our rationale was that novel Bcl-2 binding proteins would most likely also bind to the hydrophobic binding pocket of Bcl-2. In addition, we thought that such proteins would not only regulate apoptosis, when released from the pocket by BH3-only proteins, but also influence other cellular processes governed by Bcl-2, such as the regulation of mitochondrial fission/fusion, cytoskeletal rearrangements, cell cycle, DNA recombination, vesicular transport, etc.

4.4.1 Co-IP strategies: A BH3-mimetic ABT-737 and a whole Bcl-2 interactome analysis

Co-immunoprecipitations from cellular fractions represent the most convincing evidence that two or more proteins will physically bind together in vivo (Ren et al., 2003, Monti et al., 2005, Phee et al., 2006). But co-IPs are not convenient to determine boundaries of a protein complex or to determine the stoichiometry of proteins that are part of the full protein complex. Precipitated protein samples consist of bait specific binding proteins and a list of non-specific protein interactors that are bound to the bait protein itself or to other surface areas. Focusing on endogenous binding partners we developed two different IP methods/strategies to reduce high levels on false-positive interactors as follows: (I) a highly specific peptide-protein interaction assay [K_i = 1 nM] using a recently developed small molecule inhibitor ABT-737 (BH3-mimetic) to displace specifically bound proteins to Bcl-2, and (II) a whole set Bcl-2 IP assay revealing all possible Bcl-2 binding partners, i.e. proteins bound to all surfaces, and not just to the hydrophobic pocket of Bcl-2. For both methods, the binding partners were identified by mass spectrometry analysis. Importantly, specificity was achieved by deducing the proteins bound to non-specific IgG or the beads or those which co-IPed from Bcl-2 $^{-/-}$ extract from the whole interactome of IPs from a Bcl-2 $^{+/+}$ extract, using Mascot analysis. For the ABT-737 assay, we included another important control. Once Bcl-2 and its binding partners were pulled-down on beads, they were incubated with ABT-737 at 37 °C. Since some proteins could have been released by the solvent and/or the high temperature only, we included a control where we incubated the beads with DMSO at 37 °C in parallel to the ABT-737 incubations.

4.4.1.1 Examination of the ABT-737 assay

Our major goal was to isolate endogenous Bcl-2 binding partners in a physiological system by blue native and co-IP techniques. To conserve the biochemical composition of protein complexes containing Bcl-2 as much as possible we used digitonin as a detergent. Digitonin cuts the full membrane containing protein-protein and protein-lipid complexes thereby preserving functionality of the complexes (Schägger and Pfeiffer, 2000). As positive control, we expected to co-IP previously reported Bcl-2 binding partners such as Bax, Bak, Puma, Bim, Bid or VDAC1. Since these proteins were found to interact with the hydrophobic pocket of Bcl-2, they should have been released by ABT-737. However, we could not detect any of these proteins, neither in the whole set, nor in the ABT-737 release IPs (see also Kai Sterz, Nina Raulf, unpublished data). As mentioned above, we found instead Bak and VDAC1 in our negative controls (IgG, beads, Bcl-2 $^{-/-}$, etc.).

We identified by mass spectrometry 77 proteins by the ABT-737 release assay which specifically bound to Bcl-2 (and not to any negative controls) and showed a high score of

identity and peptide coverage. Among them, the most promising candidates were IQGAP2 and UGCGT1 (which we will discuss further below). UGCGT1 was also found in the whole set IP, which was an independent pull-down experiment.

In addition, we found a protein called MANF or arginine-rich, mutated in early stage tumors MANF/ARMET which is localized to the ER lumen. This protein contains a perfect BH3-domain signature (and hence shows us that the ABT-737 assay worked), but MANF is a luminal ER protein and we do not know how these proteins may interact. This example tells us that probably many more cellular proteins may have BH3-domains that do not functionally act to control Bcl-2 or Bax/Bak because they are not in the right compartment and/or do not expose their BH3-domain to bind to Bcl-2.

In this context a recent publication demonstrates release of luminal ER proteins in a tBid/Bax dependent manner similar to their poreforming activities on mitochondrial membranes that may support a possible translocation of MANF from ER into the cytosol (Wang et al., 2010). And a second publication points out that MANF is upregulated by the unfolded protein response (UPS) and protects cells against various forms of endoplasmatic reticulum induced stress stimuli (Hellman et al., 2010).

Another interesting protein which we identified in our ABT-737 screen was glioma pathogenesis-related protein 1 (GLIPR1) which was shown to induce apoptosis when overexpressed. This candidate should certainly be further studied in the future.

4.5 Comparing the identified Bcl-2 binding partners between the whole set and ABT-737 release assay

Mass spectrometric data analysis of trypsinized and separated proteins from the ABT-737 assay lead to the evaluation of 77 potential interacting candidates of Bcl-2 (appendix table 6-4 and 6-5). These candidates were obtained by analysing all peptides received from the full molecular range of each specific IP-fraction. Each of these gel traces were cut into 16-18 rectangle gel pieces according to their molecular size, each of them contained between 150-250 proteins. A list of positive evaluated proteins was extracted by excluding two different negative control samples against one positive protein list. In summary, between 8100-13500 proteins of each of the IP samples were compared and 77 potential interactors of Bcl-2 were evaluated. Furthermore, to obtain a promising interaction partner of Bcl-2 we looked for proteins with many peptides plus as much as possible double identity score values. Selected proteins in this group

were: IQGAP2, UGCGT1 (GCS), LRPPRC, VARS1, ESYT1, PTPRE, AP1M1, MANF, and GLIPR1 (see also appendix Table 6-4 and 6-5).

We compared the mass spectrometry analysis from two whole set Bcl-2 IPs (1 x FDM and 1 x FDC-P1 mitochondrial extracts) with one set of ABT-737 release assay. In all conditions, the negative controls (beads, IgG, Bcl-2 $^{-/-}$, DMSO, etc.) were deduced from the total interactome sample. Unfortunately, our mass spectrometry data from to the whole set IP approach could not completely be used because the digested protein samples below 50 kDa were contaminated by an unknown polymer. However, above 50 kDa, the only protein which was consistently found under all conditions was UDP-glucose ceramide glucosyltransferase-like 1 (UGCGT1, UGCG or GCS), a specific potential Bcl-2 interacting partner with high positive double score values and multiple peptides (chapter 3.5.4.4, Table 3-2). The complete sequence of UGCGT1 and the identified peptides by MS/MS are shown in the appendix table 6-1.

4.5.1 UDP-glucose ceramide glucosyltransferase-like 1 signaling and Bcl-2

UGCGT1, glucosyl- and galactosyltransferases or glycosylceramide synthases (GCS) catalyse the first step in the synthesis of glycosphingo-lipids, i.e. the transfer of glucose or galactose to a ceramide to produce glucoslyceramide (GlcCer) or galactosylceramide (GalCer). Glycosylceramides can also be metabolized to glycosphingo-lipids (GSLs) which represent the main constituents of the outer plasma membrane in eukaryotes (see for overview chapter 1.8.3 figure 1-13). The sphingolipids ceramide and sphingosine-1-phosphate (SIP) are implicated in the regulation of apoptosis and senescence (Obeid et al., 1993, Venable et al., 1995). It is proposed that the high level of those lipids may change the membrane properties and substructure. Several proteins are shown to interact with ceramides in vitro and in vivo. As example: Ceramide-activated Ser-Thr phosphatases (CAPPs) such as PP1 and PP2A bind ceramide "in vitro" (Chalfant et al., 2004). Although sphingolipids are supposed to mainly act on the surface of plasma membranes, they are synthesized (as other phospholipids) in the ER and can also reach mitochondria via so called mitochondria-ER-associated membrane complexes, so called MAMs. Indeed, ceramides are able to form channels in the mitochondria outer membrane in response to apoptotic stimuli with a requirement for Bak and because these channels are big enough large proteins can pass through (Siskind et al., 2010). Recent reports even show that ceramide channels can be blocked by overexpression of Bcl-xL and CED-9 the Bcl-2 homolog in C. elegans (Siskind et al., 2008, see also chapter 1.6.1) Therefore, Bcl-2 would have an alternative potential role in modifying of membrane lipids as ceramides by regulating UGCGT1 thereby inhibiting cell death.

Moreover, this is in line with the found interaction of Bcl-xL, tBid and cardiolipin at "docking" sites on mitochondrial membranes which may support this interaction with ceramides (see chapter 1.5.1.1 Cardiolipin interacts with the BH3-only protein tBid, figure 1-9).
Future experiments will have to be performed on this important finding after verification of the interaction of Bcl-2 and UGCGT1 by co-immunoprecipitation experiments.

4.5.1.1 Interactions between lysosomes and mitochondria

It was shown that TNF-α induce ceramide production which in turn leads to the dephosphorylation of RB, PKCα and AKT (Lee et al., 1996, Zhou et al., 1998). Ceramides were therefore also found to activate PKCζ, AKT, the kinase KSR and cathepsin D. Activated PKCζ is also implicated in pro-apoptotic functions. It is proposed that modified ceramides from lysosomes may couple the lysosomal acid sphingomyelinase (SMase, Fig. 4-1) to the mitochondrial pathway of apoptosis (Müller et al., 1995, Zhang et al., 1997, Bourbon et al., 2002, Heinrich et al., 2004, Wang et al., 2005).

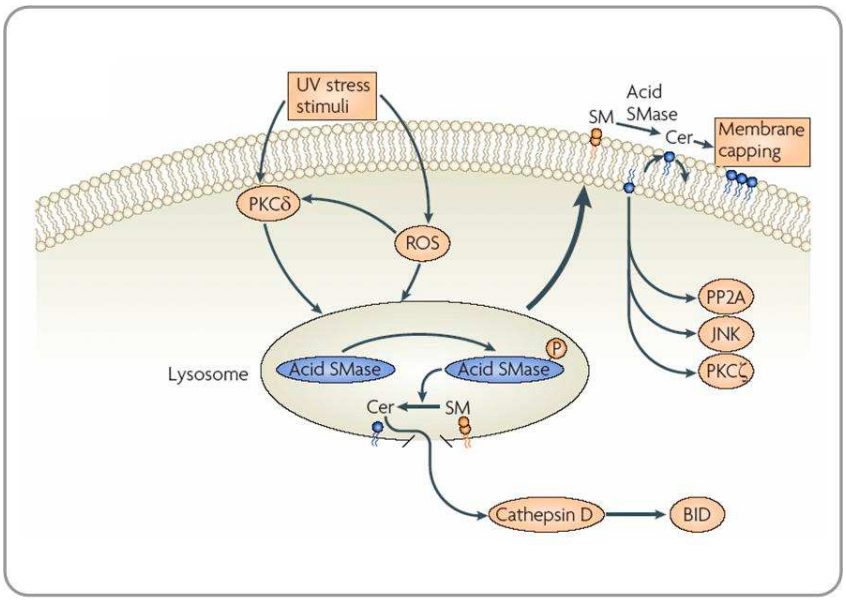

Figure 4-1: Regulation of sphingomyelinase (SMase) by PKCζ, UV and different stress stimuli. Both ROS and PKCδ have been implicated in activation of acid SMase, which may act in the lysosome to generate Cer, which in turn activates cathepsin D, leading to cleavage of the pro-apoptotic protein Bid and induction of apoptotic responses. Acid SMase may also translocate to the plasma membrane where it acts on outer leaflet sphingomyelin (SM), resulting in Cer formation. Cer can enhance the formation of membrane microdomains (capping) and/or launch signalling pathways that are mediated by protein phosphatases (for example, PP2A) and kinases (for example, c-Jun N-terminal kinase (JNK) and PKCζ), (adapted from Hannun Y, 2005)

4.5.1.2 Interactions between Bcl-2 and UGCGT1

The regulation of glycosylceramide synthase (GCS) is not clear. After its synthesis at the rough ER, it is transported to the Golgi apparatus where it is further modified. GCS is constitutively expressed in several tissues and inhibition of GCS alters growth, cell death and adhesion (Hakomori et al., 1993, Ichikawa et al., 1998, Yamashita et al., 1999). GCS may also contribute to carcinogenesis such as leukaemia or neuroepithelioma cancer (see below). It was recently reported that overexpression of the UGCGT1 (GCS) gene leads to multidrug resistance (MDR) of leukemic cells which is accompanied by higher transcription and expression of Bcl-2. Inhibition of UGCGT1 activity by a specific inhibitor (PPMP) and RNAi-mediated downregulation of UGCGT1 both were associated with decreased Bcl-2 expression and apoptosis sensitisation. This indicates that UGCGT1 may be a survival factor under certain circumstances and perform its survival action via Bcl-2, eventually leading to multidrug resistance (Liu et al., 2010).
By contrast Di Sano et al. (2003) reported that UGCGT1 inhibition by PDMP was not associated with an increased, but a decreased apoptosis in neuroepithelioma cells induced with treatment of the drug fenretinide that induces cell death independent of p53. They postulated a novel p53 independent pathway of apoptosis via the protein interactions between Golgi and ER.

A direct interaction between Bcl-2 and UGCGT1 by co-IP and a functional consequence of this interaction has not yet been described. Unfortunately, we found only towards the end of this work (after performing the IPs and mass spectrometry data evaluation several times) that UGCGT1 was a consistent Bcl-2 binding partner under all conditions. We therefore did not have any time to validate this result by performing co-IPs and gel filtration or BN-PAGE analysis or immunofluorescence studies using anti-UGCGT1 antibodies. We rather focused on another putative specific Bcl-2 binding partner that was consistently, but not always found in our assay, namely IQ motif GAP2 (IQGAP2).

4.6 Validation of IQGAP-2 as a potential new endogenous binding partner of Bcl-2

We identified IQGAP2 as a specific Bcl-2 binding partner in all our ABT-737 release assays indicating that this protein might bind to the hydrophobic pocket of Bcl-2. Unfortunately, we did not find any canonical BH3-domain in IQGAP2 that would account for such a property. However, we teamed up with the oncology group of John Hickman at Servier Pharmaceuticaly, Paris who performed a yeast-two hybrid screen with Hybrigenomics. They indeed found IQGAP2 as Bcl-2 binding partner in this system although the hit degree was only a “C”. However, excitingly the hits for IQGAP2 binding to Bcl-xL and Mcl-1 were both of the “A” degree

(best hits) (J. Hickman, personal communication). Thus, IQGAP2 seemed to be an excellent candidate for a specific, physiologically relevant Bcl-2 binding partner.

To validate the interaction of IQGAP2 with Bcl-2 on the endogenous level, we performed Bcl-2 IPs using heavy membrane extracts from healthy FDMs. Excitingly, IQGAP-2 and Bcl-2 could specifically pulled down in both anti-IQGAP2 and anti-Bcl-2 IPs. IQGAP2 was found at two molecular weight bands, one at 180 kDa and one at 166 kDa which represent two different isoforms obtained by Mascot analysis (chapter 3.6.1 table 3-3). Sometimes IQGAP2 weakly interacted with beads or the IgG_1 control indicating that the protein might be slightly sticky. However, there was always a clear increase of binding in the presence of Bcl-2. We further wanted to validate the IQGAP2/Bcl-2 interaction by co-overexpressing the two proteins in HEK293 cells. Unfortunately our first HA-tagged IQGAP2 construct under the control of a SV-40 promoter showed a very low expression, so we could not use it for any co-IP experiments. The second GFP-tagged IQGAP2, under the control of a CMV promoter produced suitable amounts of IQGAP2 for co-IPs. However, to our surprise GFP-tagged human IQGAP2 was unable to co-IP with FLAG-tagged Bcl-2. As we know from previous work that the N-terminal FLAG-tag does not affect activity and binding properties of Bcl-2, we suspect that the GFP moiety on the GFP-IQGAP2 might have interfered with binding to Bcl-2. Another explanation could be that the overexpressed form of IQGAP2 does not entirely correspond to the endogenous form. We detected only one species of GFP-IQGAP2 (the higher one) whereas endogenous IQGAP2 ran in two forms (166 and 180 kDa). Thus, future experiments will aim at performing Bcl-2/IQGAP2 IPs using a non GFP-tagged form of IQGAP2 to avoid a possible conformational change that would inhibit the interaction. In addition, we should possibly also use our monoclonal anti mouse Bcl-2 antibody that was used during the initial co-IP experiments instead of a rat polyclonal antibody.

4.6.1 Colocalization of IQGAP2 and Bcl-2 by immunofluorescence analysis

Having shown that Bcl-2 and IQGAP2 bind to each other in endogenous co-IPs we performed transient transfections of HA-tagged-IQGAP2-HA into Bcl-2 overexpressing mBcl-2 HeLa cells to test co-localization of Bcl-2 and IQGAP2 inside cells. After several attempts optimizing transient transfections of the HA-IQGAP2 plasmid we found only a few cells expressing both mBcl-2 and h-IQGAP2. Unfortunately, the transfection efficiency was not much better for the GFP-IQGAP2 plasmid. Nevertheless, we used these transfections to look for suitable cells co-expressing both mBcl-2 and h-IQGAP2. As for example shown in Fig. 3-33 and 3-34, we could partially detect a co-localization of GFP-IQGAP2 and Bcl-2 in the nuclear membrane. However, this analysis has to be further improved. Moreover, as seen with the GFP-IQGAP2/Bcl-2 co-IPs,

it is possible that the GFP fused to the N-terminus of IQGAP2 may interfere with its binding to Bcl-2.

4.6.2 IQGAP2 and Bcl-2 control each others expression

Subcellular fractionation of FDMs revealed that endogenous IQGAP2 localized to nuclear, ER, mitochondrial and cytosolic fractions. Surprisingly, its levels on mitochondria and the ER decreased in Bcl-2 $^{-/-}$ cells but without a concomitant change of expression in the cytosol. This indicated that a stable mitochondrial and ER association of IQGAP2 depended on Bcl-2, further substantiating the notion that the two proteins interacted. In apoptotic cells IQGAP2 slightly moved from the ER to mitochondrial fractions although this result has to be confirmed in further studies. We wanted to know if this interdependence between Bcl-2 and IQGAP2 also existed in other cell types. To test this we analysed the subcellular distributions of Bcl-2 and IQGAP2 in 3T9 immortalized wt and Bcl-2 $^{-/-}$ MEFs and wt and mouse Bcl-2 overexpressing R6 (R6-mBcl-2) In contrast to FDMs, MEFs and Rat-6 cells contain very low levels of endogenous IQGAP-2 because it was neither detected in cytosolic, ER or mitochondrial fractions. Instead, we found IQGAP2 in the nuclear extracts of these cells and the protein bands had different molecular masses from those of FDMs. Bcl-2 was also present in these extracts and since Bcl-2 is usually not found within the nucleus but on the nuclear membrane, we studied if the association of endogenous IQGAP2 with this membrane was regulated by Bcl-2. Indeed, whereas in Bcl-2 $^{-/-}$ MEFs, the amount of IQGAP2 bands on the nuclear membrane were diminished, their expression was increased in R6 cells overexpressing Bcl-2. This indicates that Bcl-2 controls the association and stability of IQGAP2 also in fibroblasts, with the difference that this time the interaction mainly occurred on the nuclear membrane. Interestingly, we also noticed the opposite regulation, namely that the stability of Bcl-2 was controlled by IQGAP2. When we analysed the expression levels of endogenous Bcl-2 in IQGAP2 $^{-/-}$ MEFs, we found that they were significantly reduced as compared to those in wt cells. The interdependence of Bcl-2 and IQGAP2 was also seen Hela cells. Here the levels of endogenous IQGAP2 (166 kDa) drastically increased in all membrane fractions, and even in the cytosol, when Bcl-2 was overexpressed. This stabilization/interaction did not change when the cells underwent apoptosis in response to tunicamycin.

4.6.3 Possible roles of IQGAP2 for Bcl-2 regulated cellular responses: impact on the cytoskeleton and mitochondrial fission/fusion

Stabilization of IQGAP2 at Bcl-2 sites might be important for linking mitochondria to the actin cytoskeleton. IQGAP2 is known to have a calponin/actin-binding site at its N-terminus and might bridge mitochondria to the cytoskeletal network via Bcl-2. Bcl-2 family proteins have been recently shown to regulate mitochondrial fission/fusion and motility and hence IQGAP2 may be a missing factor in this process. Indeed, when we looked at the mitochondrial morphology of MEFs lacking IQGAP2 we noticed that the organelles were more fragmented than in wt cells. This is in agreement with recent studies in yeast deficient in the IQGAP gene. These cells die due to fragmented mitochondria and a disrupted actin network (Altmann and Westermann, 2008). Moreover, liver mitochondria of IQGAP2 $^{-/-}$ mice exhibit abnormal morphologies (Schmidt et al.2008). Interestingly, while we found actin associated with heavy membrane fractions of wt MEFs, this was not the case when IQGAP2 was deleted further supporting the idea that IQGAP2 may be a scaffold for actin binding to mitochondria. A recent publication indicates that disruption of actin filaments attenuated fission and Drp1 translocation to mitochondria (DeVos et al., 2005). Therefore it would be worth to test if IQGAP2 may also be involved in the modification of cytoskeletal filaments. To resolve this future work has to aim on filaments of the cytoskeleton, Bcl-2, IQGAP2, and Drp1 by immunocytochemistry and confocal microscopy.

As shown in chapter 3.6.5 figures 3-31 A-D mitochondria from wt MEFs were able to form a highly interconnected tubular network when the cells were treated with tunicamycin and etoposide. Interestingly, after 9 hrs of treatment no sign of cytochrome c release was apparent. Not really unexpectedly, but striking, mitochondria deficient in Bcl-2 do not show a hyperfused interconnected mitochondrial network (Fig. 3-32 A-B). Already under healthy conditions Bcl-2 $^{-/-}$ mitochondria display a clumpy punctated pattern that does not change very much upon treatment with etoposide after 9 hrs (that is also seen in IQGAP2 $^{-/-}$ MEFs, but has to be verified with its corresponding wild type see appendix figure 6-1). Thus, the new finding here is, that both, Bcl-2 (and possibly IQGAP2) show a similar altered morphology of mitochondria compared to wild type MEFs. Bcl-2 and (IQGAP2) seem to be essential to maintain mitochondrial fission and fusion dynamics to support mitochondrial ATP production and survival. Further experiments on wt MEFs have to confirm the altered mitochondrial structure found in MEFs deficient for IQGAP2 (appendix figure 6-1).

4.6.4 Potential alternative signaling mechanisms of IQGAP2 during apoptosis

IQGAP2 is a multifunctional enzyme. Apart from its effect on the actin cytoskeleton, it also possesses a calcium/calmodulin binding domain that implicates that IQGAP2 may regulate calcium signalling during apoptosis (see overview figure 4-2).

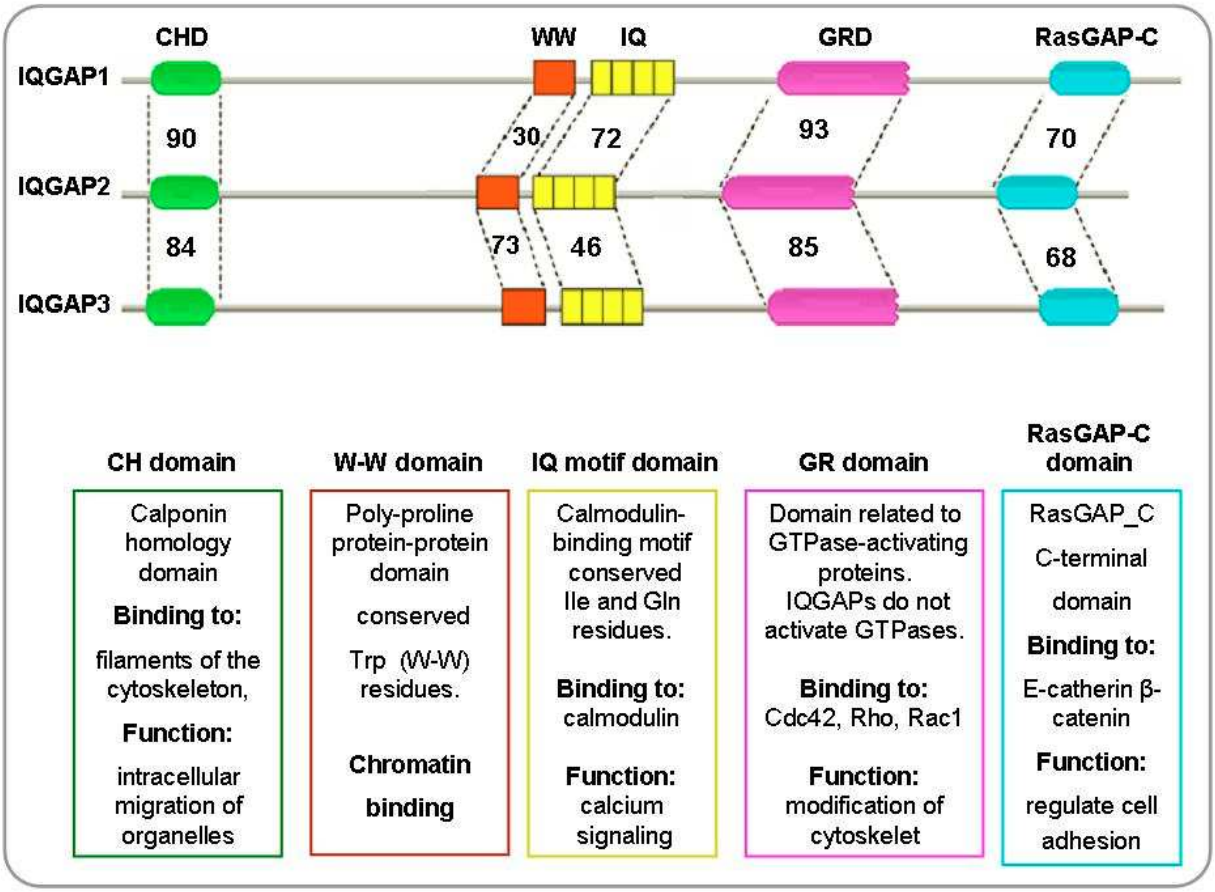

Figure 4-2: Overview of isoforms and functional domains of human IQGAPs. Three human isoforms are found at present. Percentage amino-acid identity of IQGAP1, IQGAP2 and IQGAP3 are shown. IQGAP1 is found to be associated with development of hepatocellular carcinoma (HCC) and IQGAP2 may act as tumor suppressor (Schmidt et al., 2008, White et al., 2009, 2010). In mice are different isoforms of IQGAP2 described: 180, 98 and 20 kDa and putative uncharacterized isoforms are also found at 50, 30 and 24 kDa (Uniprot), (adapted and modified from: White et al., 2009).

Its strategic localization of both the ER and mitochondria membrane may be optimally suited to control the shuttling of calcium between these two organelles through contact points, called MAMs. In addition, IQGAP2 contains domains which are homologous to those in GTPase activating proteins for the small G-proteins, Rho, Rac and Cdc42. However, although IQGAP2 was reported to interact with these G proteins, it was unable to enhance their GTPase activities.

It is therefore unknown how exactly IQGAP2 controls these proteins. Since these proteins are involved in cytoskeleton remodelling, it is conceivable to propose that IQGAP2 affects the cytoskeleton via small G proteins. Finally, IQGAP2 exhibits Pro-rich regions for protein-protein interactions and a Ras-GAP domain at its C-terminus, presumably implicated in cell adhesion. White et al. (2009) also proposed a crucial scaffolding function of the cousin of IQGAP2, IQGAP1 for component of the MAPK signalling cascade. It is possible that IQGAP2 also exerts a scaffolding function to assemble important signalling components for apoptosis regulation on the mitochondria, ER and nuclear membranes. Last, but not least IQGAP2 was found to be a phosphoprotein. Several conserved consensus PKA phosphorylation sites at S^{16}, S^{24}, S^{1455}, P^{1458}, T^{1055} and one PKC conserved site at S^{911} were identified, plus additional phosphorylation sites for p70s6 kinase, calmodulin kinase II (CAMKII), casein kinase (CK) and for CAMK/protein kinase G. Upstream of the calponin homology domain S^{16} and S^{24} belong to a region shown to enhance actin polymerization regulated by Cdc42 and Ca2+/calmodulin binding. S^{911} upstream of RasGAP domain is thought to regulate cytoskeletal dynamics. S^{1461} and $S^{1455/T1458}$ within the C-terminal RasGAP domain may regulate cell adhesion by binding to E-catherin and β-catenin which is inversely regulated by calmodulin/Cdc42. Further a domain that associates with the ends of growing microtubules, cytoplasmatic linker protein 170 (CLIP-170) was found (Fukata m et al., 1999, Briggs wm et al., 2003, Joyal h et al., 1997, Kuroda s et al., 1998).

In summary, IQGAP2 may influence apoptosis via several mechanisms involving its interaction with Bcl-2 and other Bcl-2-like survival factors. In this respect, it will also be crucial to study the binding and functional role of IQGAP2 to Bcl-xL and Mcl-1.

5 References

Abdelwahid, E., T. Yokokura, et al. (2007). "Mitochondrial disruption in Drosophila apoptosis." Dev Cell 12(5): 793-806.

Acehan, D., X. Jiang, et al. (2002). "Three-dimensional structure of the apoptosome: implications for assembly, procaspase-9 binding, and activation." Mol Cell 9(2): 423-32.

Adachi, M., X. Zhao, et al. (2005). "Nomenclature of dynein light chain-linked BH3-only protein Bim isoforms." Cell Death Differ 12(2): 192-3.

Adams, J. M., D. C. Huang, et al. (2005). "Subversion of the Bcl-2 life/death switch in cancer development and therapy." Cold Spring Harb Symp Quant Biol 70: 469-77.

Akbar AN. Borthwick NJ. Wickremasinghe RG. Panayiotidis P. Pilling D. Bofill M. Krajewski S. Reed JC. Salmon M. (1996). "Interleukin-2 receptor common *y* -chain signaling cytokines regulate activated T cell apoptosis in response to growth factor withdrawal: selective induction of anti-apoptotic *(bcl-2, bcl-x,)* but not pro-apoptotic *(bax, bcl-x,)* gene expression." Eur. J. Immunol..26: 294-99.

Lamkanfi M, Declercq W, Kalai M, Saelens X, Vandenabeele P. (2002). "Alice in caspase land. A phylogenetic analysis of caspases from worm to man." Cell Death Differ. Apr;9(4):358-61.

Altmann K. and Westermann B. (2005). "Role of Essential Genes in Mitochondrial Morphogenesis in Saccharomyces cerevisiae." Molecular Biology of the Cell Vol. 16, 5410–5417.

Antonsson, B. (2001). "Bax and other pro-apoptotic Bcl-2 family "killer-proteins" and their victim the mitochondrion." Cell Tissue Res 306(3): 347-61.

Aouacheria, A., F. Brunet, et al. (2005). "Phylogenomics of life-or-death switches in multicellular animals: Bcl-2, BH3-Only, and BNip families of apoptotic regulators." Mol Biol Evol 22(12): 2395-416.

Ardail D, Privat JP, Egret-Charlier M, Levrat C, Lerme F, Louisot P. (1990). "Mitochondrial contact sites. Lipid composition and dynamics." J Biol Chem. Nov 5;265(31):18797-802.

Arnoult D, Rismanchi N, Grodet A, Roberts RG, Seeburg DP, Estaquier J, Sheng M, Blackstone C (2005). "Bax/Bak-dependent release of DDP/TIMM8a promotes Drp1-mediated mitochondrial fission and mitoptosis during programmed cell death." Curr Biol 15:2112–2118.

Baines, C. P., C. X. Song, et al. (2003). "Protein kinase Cepsilon interacts with and inhibits the permeability transition pore in cardiac mitochondria." Circ Res 92(8): 873-80.

Baines, C. P., R. A. Kaiser, et al. (2007). "Voltage-dependent anion channels are dispensable for mitochondrial-dependent cell death." Nat Cell Biol 9(5): 550-5.

Baker, M. A., D. J. Lane, et al. (2004). "VDAC1 is a transplasma membrane NADH-ferricyanide reductase." J Biol Chem 279(6): 4811-9.

Bashour A.M. Fullerton A.T. Hart M.J. Bloom G.S. (1997). "IQGAP1, a rac- and Cdc42-binding protein, directly binds and cross-links microfilaments." J Cell Biol 137: 1555–1566.

Bassik, M. C., L. Scorrano, et al. (2004). "Phosphorylation of BCL-2 regulates ER Ca2+ homeostasis and apoptosis." Embo J 23(5): 1207-16.

Birbes H, Luberto C, Hsu YT, El Bawab S, Hannun YA, Obeid LM. (2005). "A mitochondrial pool of sphingomyelin is involved in TNFalpha-induced Bax translocation to mitochondria". Biochem J. Mar 15;386(Pt 3):445-51.

Boise, L. H., M. Gonzalez-Garcia, et al. (1993). "bcl-x, a bcl-2-related gene that functions as a dominant regulator of apoptotic cell death." Cell 74(4): 597-608.

Boldogh IR, Pon LA. (2007). "Mitochondria on the move." Trends Cell Biol. Oct;17(10):502-10.

Borner, C. (1996). "Diminished cell proliferation associated with the death-protective activity of Bcl-2." J Biol Chem 271(22): 12695-8.

Bouillet P, Metcalf D, Huang DC, Tarlinton DM, Kay TW, Köntgen F, Adams JM, Strasser A. (1999). "Proapoptotic Bcl-2 relative Bim required for certain apoptotic responses, leukocyte homeostasis, and to preclude autoimmunity." Science. Nov 26;286(5445):1735-8.

Brichese, L. and A. Valette (2002). "PP1 phosphatase is involved in Bcl-2 dephosphorylation after prolonged mitotic arrest induced by paclitaxel." Biochem Biophys Res Commun 294(2): 504-8.

Brichese, L., N. Barboule, et al. (2002). "Bcl-2 phosphorylation and proteasome-dependent degradation induced by paclitaxel treatment: consequences on sensitivity of isolated mitochondria to Bid." Exp Cell Res 278(1): 101-11.

Briggs MW, Sacks DB. (2003). "IQGAP proteins are integral components of cytoskeletal regulation." EMBO Rep. Jun;4(6):571-4.

Brill S, Li S, Lyman CW, Church DM, Wasmuth JJ, Weissbach l, Bernards A, Snijders AJ (1996). "The ras GTPase-activating-protein-related human protein IQGAP2 harbors a potential actin binding domain and interacts with calmodulin and Rho family GTPases." Mol Cell Biol 9: 4869–4878.

Brooks C, Wei Q, Feng L, Dong G, Tao Y, Mei L, Xie ZJ, Dong Z. (2007). "Bak regulates mitochondrial morphology and pathology during apoptosis by interacting with mitofusins." Proc Natl Acad Sci U S A. Jul 10;104(28):11649-54.

Brooks, R., G. M. Fuhler, et al. "SHIP1 inhibition increases immunoregulatory capacity and triggers apoptosis of hematopoietic cancer cells." J Immunol 184(7): 3582-9.

Cartron, P. F., T. Gallenne, et al. (2004). "The first alpha helix of Bax plays a necessary role in its ligand-induced activation by the BH3-only proteins Bid and PUMA." Mol Cell 16(5): 807-18.

Cassidy-Stone A, Chipuk JE, Ingerman E, Song C, Yoo C, Kuwana T, Kurth MJ, Shaw JT, Hinshaw JE, Green DR, Nunnari J (2008). "Chemical inhibition of the mitochondrial division dynamin reveals its role in Bax/Bak-dependent mitochondrial outer membrane permeabilization." Dev Cell 14:193–204.

Certo, M., V. Del Gaizo Moore, et al. (2006). "Mitochondria primed by death signals determine cellular addiction to antiapoptotic BCL-2 family members." Cancer Cell 9(5) 351-65.

Chadebech, P., L. Brichese, et al. (1999). "Phosphorylation and proteasome-dependent degradation of Bcl-2 in mitotic-arrested cells after microtubule damage." Biochem Biophys Res Commun 262(3): 823-7.

Chalfant CE, Rathman K, Pinkerman RL, Wood RE, Obeid LM, Ogretmen B, Hannun YA. (2002). " De novo ceramide regulates the alternative splicing of caspase 9 and Bcl-x in A549 lung adenocarcinoma cells. Dependence on protein phosphatase-1." J Biol Chem. Apr 12;277(15):12587-95.

Chalfant CE, Szulc Z, Roddy P, Bielawska A, Hannun YA. (2004). "The structural requirements for ceramide activation of serine-threonine protein phosphatases." J Lipid Res. Mar;45(3):496-506.

Chang, B. S., A. J. Minn, et al. (1997). "Identification of a novel regulatory domain in Bcl-X(L) and Bcl-2." Embo J 16(5): 968-77.

Chattopadhyay, A., C. W. Chiang, et al. (2001). "BAD/BCL-[X(L)] heterodimerization leads to bypass of G0/G1 arrest." Oncogene 20(33): 4507-18.

Chay CH, Cooper CC, Hellerstedt BA, Pienta KJ. (2002). "Antimetastatic drugs in prostate cancer." Clin Prostate Cancer. Jun;1(1):14-9.

Chen, C. Y. and D. V. Faller (1996). "Phosphorylation of Bcl-2 protein and association with p21Ras in Ras-induced apoptosis." J Biol Chem 271(5): 2376-9.

Chen, F. F., J. J. Yan, et al. (1996). "Immunohistochemical localization of Mcl-1 and bcl-2 proteins in thymic epithelial tumours." Histopathology 29(6): 541-7.

Cheng EH, Sheiko TV, Fisher JK, Craigen WJ, Korsmeyer SJ. (2003). "VDAC2 inhibits BAK activation and mitochondrial apoptosis." Science. Jul 25;301(5632):513-7.

Cheng, E. H., J. Nicholas, et al. (1997). "A Bcl-2 homolog encoded by Kaposi sarcoma-associated virus, human herpesvirus 8, inhibits apoptosis but does not heterodimerize with Bax or Bak." Proc Natl Acad Sci U S A 94(2): 690-4.

Chew C.S. et al., (2005). "IQGAPs are differentially expressed and regulated in polarized gastric epithelial cells." Am J Physiol Gastrointest Liver Physiol 288: G376–G387.

Chinnaiyan, A. M., D. Chaudhary, et al. (1997). "Role of CED-4 in the activation of CED-3." Nature 388(6644): 728-9.

Chinnaiyan, A. M., K. O'Rourke, et al. (1997). "Interaction of CED-4 with CED-3 and CED-9: a molecular framework for cell death." Science 275(5303): 1122-6.

Chipuk JE, Bouchier-Hayes L, Kuwana T, Newmeyer DD, Green DR. (2005). "PUMA couples the nuclear and cytoplasmic proapoptotic function of p53." Science. Sep 9;309(5741):1732-5.

Chipuk JE, Moldoveanu T, Llambi F, Parsons MJ, Green DR. (2010). "The BCL-2 family reunion." Mol Cell. Feb 12;37(3):299-310.

Chipuk, J. E. and D. R. Green (2006). "Dissecting p53-dependent apoptosis." Cell Death Differ 13(6): 994-1002.

Chipuk, J. E., L. Bouchier-Hayes, et al. (2006). "Mitochondrial outer membrane permeabilization during apoptosis: the innocent bystander scenario." Cell Death Differ 13(8): 1396-402.

Choi SY, Gonzalvez F, Jenkins GM, Slomianny C, Chretien D, Arnoult D, Petit PX, Frohman MA. (2007). "Cardiolipin deficiency releases cytochrome c from the inner mitochondrial membrane and accelerates stimuli-elicited apoptosis." Cell Death Differ. Mar;14(3):597-606.

Choi SY, Huang P, Jenkins GM, Chan DC, Schiller J, Frohman MA. (2006). "A common lipid links Mfn-mediated mitochondrial fusion and SNARE-regulated exocytosis." Nat Cell Biol. Nov;8(11):1255-62.

Choi, B. H., L. Feng, et al. (2010). "FKBP38 protects Bcl-2 from caspase-dependent degradation." J Biol Chem 285(13): 9770-9.

Conus, S., T. Kaufmann, et al. (2000). "Bcl-2 is a monomeric protein: prevention of homodimerization by structural constraints." Embo J 19(7): 1534-44.

Cory, S., D. C. Huang, et al. (2003). "The Bcl-2 family: roles in cell survival and oncogenesis." Oncogene 22(53): 8590-607.

Danial, N. N. and S. J. Korsmeyer (2004). "Cell death: critical control points." Cell 116(2): 205-19.

De Vos KJ, Allan VJ, Grierson AJ, Sheetz MP (2005). "Mitochondrial function and actin regulate dynamin-related protein 1-dependent mitochondrial fission." Curr Biol. Apr 12;15(7):678-83.

Delettre C, Griffoin JM, Kaplan J, Dollfus H, Lorenz B, Faivre L, Lenaers G, Belenguer P, Hamel CP. (2001). "Mutation spectrum and splicing variants in the OPA1 gene." Hum Genet. Dec;109(6):584-91.

Delivani, P., C. Adrain, et al. (2006). "Role for CED-9 and Egl-1 as regulators of mitochondrial fission and fusion dynamics." Mol Cell 21(6): 761-73.

Der-Fen Suen, Kristi L. Norris and Richard J. Youle. (2008). "Mitochondrial dynamics and apoptosis." Genes Dev.22: 1577-1590.

Di Sano F, Fazi B, Citro G, Lovat PE, Cesareni G, Piacentini M. (2003). "Glucosylceramide synthase and its functional interaction with RTN-1C regulate chemotherapeutic-induced apoptosis in neuroepithelioma cells." JCANCER RESEARCH July 1563_3860-3865.

Dijkers, P., Medema, R., Lammers, J., Koenderman, L. and Coffer, P. (2000). "Expression of the proapoptotic Bcl-2 family member Bim is regulated by the forkhead transcription factor FKHR-L1." Curr Biol 10(19): 1201-1204.

Diskin, T., P. Tal-Or, et al. (2005). "Closed head injury induces upregulation of Beclin 1 at the cortical site of injury." J Neurotrauma 22(7): 750-62.

Dole, M., G. Nunez, et al. (1994). "Bcl-2 inhibits chemotherapy-induced apoptosis in neuroblastoma." Cancer Res 54(12): 3253-9.

Ehrlich, P. F., W. T. McClellan, et al. (2005). "Monitoring performance: longterm impact of trauma verification and review." J Am Coll Surg 200(2): 166-72.

Ekert PG, Read SH, Silke J, Marsden VS, Kaufmann H, Hawkins CJ, Gerl R, Kumar S, Vaux DL. (2004). "Apaf-1 and caspase-9 accelerate apoptosis, but do not determine whether factor-deprived or drug-treated cells die." J Cell Biol. Jun 21;165(6):835-42.

Ekert, P. G., A. M. Jabbour, et al. (2006). "Cell death provoked by loss of interleukin-3 signaling is independent of Bad, Bim, and PI3 kinase, but depends in part on Puma." Blood 108(5): 1461-8.

Ekert, P.G., Jabbour, A.M., Manoharan, A., Heraud, J.E., Yu, J., Pakusch, M., Michalak, E.M., Kelly, P.N., Callus, B., Kiefer, T., Verhagen, A., Silke, J., Strasser, A., Borner, C. and Vaux, D.L., (2006). 'Cell death provoked by loss of interleukin-3 signaling is independent of Bad, Bim, and PI3 kinase, but depends in part on Puma'. *Blood*, 108 (5):1461-1468.

Erlacher, M., V. Labi, et al. (2006). "Puma cooperates with Bim, the rate-limiting BH3-only protein in cell death during lymphocyte development, in apoptosis induction." J Exp Med 203(13): 2939-51.

Estaquier J, Arnoult D (2007). "Inhibiting Drp1-mediated mitochondrial fission selectively prevents the release of cytochrome c during apoptosis." Cell Death Differ 14:1086–1094

Fadok, V. A. and P. M. Henson (1998). "Apoptosis: getting rid of the bodies." Curr Biol 8(19): R693-5.

Fadok, V. A., D. L. Bratton, et al. (2000). "A receptor for phosphatidylserine-specific clearance of apoptotic cells." Nature 405(6782): 85-90.

Fadok, V. A., D. R. Voelker, et al. (1992). "Exposure of phosphatidylserine on the surface of apoptotic lymphocytes triggers specific recognition and removal by macrophages." J Immunol 148(7): 2207-16.

Fadok, V.A., and Henson, P.M. (2003). "Apoptosis: giving phosphatidylserine recognition an assist–with a twist. Curr." Biol. 13, R655–R657.

Ferraro, E. and F. Cecconi (2007). "Autophagic and apoptotic response to stress signals in mammalian cells." Arch Biochem Biophys 462(2): 210-19.

Frank S, Gaume B, Bergmann-Leitner ES, Leitner WW, Robert EG, Catez F, Smith CL, Youle RJ (2001). "The role of dynaminrelated protein 1, a mediator of mitochondrial fission, in apoptosis." Dev Cell 1:515–525.

Fransson S, Ruusala A, Aspenstrom P (2006). "The atypical Rho GTPases Miro-1 and Miro-2 have essential roles in mitochondrial trafficking." Biochem Biophys Res Commun 344:500–510.

Frezza C, Cipolat S, Martins de Brito O, Micaroni M, Beznoussenko GV, Rudka T, Bartoli D, Polishuck RS, Danial NN, De Strooper B, Scorrano L. (2006). "OPA1 controls apoptotic cristae remodeling independently from mitochondrial fusion." Cell. Jul 14;126(1):177-89.

Fukata M, et al. (1999). "Cdc42 and Rac1 regulate the interaction of IQGAP1 with β-catenin." J Biol Chem;274:26044–26050.

Gallenne, T., F. Gautier, et al. (2009). "Bax activation by the BH3-only protein Puma promotes cell dependence on antiapoptotic Bcl-2 family members." J Cell Biol 185(2): 279-90.

Galluzzi, L. and G. Kroemer (2007). "Mitochondrial apoptosis without VDAC." Nat Cell Biol 9(5): 487-9.

Galluzzi, L., M. C. Maiuri, et al. (2007). "Cell death modalities: classification and pathophysiological implications." Cell Death Differ 14(7): 1237-43.

Gao S, Fu W, Dürrenberger M, De Geyter C, Zhang H. (2005). "Membrane translocation and oligomerization of hBok are triggered in response to apoptotic stimuli and Bnip3." Cell Mol Life Sci. May;62(9):1015-24.

Garcia Fernandez M, Troiano L, Moretti L, Nasi M, Pinti M, Salvioli S, Dobrucki J, Cossarizza A. (2002). "Early changes in intramitochondrial cardiolipin distribution during apoptosis." Cell Growth Differ. Sep;13(9):449-55.

García-Sáez AJ, Mingarro I, Pérez-Payá E, Salgado J. (2004). "Membrane-insertion fragments of Bcl-xL, Bax, and Bid." Biochemistry. Aug 31;43(34):10930-43.

Garrido, C., L. Galluzzi, et al. (2006). "Mechanisms of cytochrome c release from mitochondria." Cell Death Differ 13(9): 1423-33.

Gavathiotis, E., M. Suzuki, et al. (2008). "BAX activation is initiated at a novel interaction site." Nature 455(7216): 1076-81.

Gohil VM. Nilsson R. Belcher-Timme CA. Biao Luo B. Root DE. and Mootha VK. (2010). "Mitochondrial and Nuclear Genomic Responses to Loss of LRPPRC Expression." JBC Vol. 285, No. 18, pp. 13742–13747.

Gombert, W., N. J. Borthwick, et al. (1996). "Fibroblasts prevent apoptosis of IL-2-deprived T cells without inducing proliferation: a selective effect on Bcl-XL expression." Immunology 89(3): 397-404.

Gonzalvez F, Pariselli F, Dupaigne P, Budihardjo I, Lutter M, Antonsson B, Diolez P, Manon S, Martinou JC, Goubern M, Wang X, Bernard S, Petit PX. (2005). "tBid interaction with cardiolipin primarily orchestrates mitochondrial dysfunctions and subsequently activates Bax and Bak." Cell Death Differ. Jun;12(6):614-26.

Gonzalvez F. and Gottlieb E. (2008). "Cardiolipin: Setting the beat of apoptosis." Apoptosis (2007) 12:877–885.

Goping, I. S., A. Gross, et al. (1998). "Regulated targeting of BAX to mitochondria." J Cell Biol 143(1): 207-15.

Green DR, Kroemer G. (2004). "The pathophysiology of mitochondrial cell death." Science. Jul 30;305(5684):626-9.

Griffin EE, Graumann J, Chan DC. (2005). "The WD40 protein Caf4p is a component of the mitochondrial fission machinery and recruits Dnm1p to mitochondria." J Cell Biol. Jul 18;170(2):237-48.

Guan JL, Chen HC. (1996). "Signal transduction in cell-matrix interactions." Int Rev Cytol.;168:81-121.

Hacki, J., L. Egger, et al. (2000). "Apoptotic crosstalk between the endoplasmic reticulum and mitochondria controlled by Bcl-2." Oncogene 19(19): 2286-95.

Hakomori, S., and Igarashi, Y. (1993). "Gangliosides and glycosphingolipids as modulators of cell growth, adhesion, and transmembrane signaling." Adv. Lipid Res., *25:* 147–162.

Haldar S, Basu A, Croce CM. (1998). "Serine-70 is one of the critical sites for drug-induced Bcl2 phosphorylation in cancer cells." Cancer Res. Apr 15;58(8):1609-15.

Haldar, S., N. Jena, et al. (1994). "Antiapoptosis potential of bcl-2 oncogene by dephosphorylation." Biochem Cell Biol 72(11-12): 455-62.

Han BH, Gibson ME, Choi J, Knudson CM, Korsmeyer SJ, Parsadanian M, Holtzman DM. (2001). "BAX contributes to apoptotic-like death following neonatal hypoxia-ischemia: evidence for distinct apoptosis pathways." Mol Med. Sep;7(9):644-55.

Hanada, M., C. Aime-Sempe, et al. (1995). "Structure-function analysis of Bcl-2 protein. Identification of conserved domains important for homodimerization with Bcl-2 and heterodimerization with Bax." J Biol Chem 270(20): 11962-9.

Hanahan, D. and R. A. Weinberg (2000). "The hallmarks of cancer." Cell 100(1): 57-70.

Hannun Yusuf A. and Obeid Lina M. (2008). " Principles of bioactive lipid signalling: lessons from sphingolipids." Nature Reviews Vol.9 Feb 139-150.

Hedge, V. L. and G. T. Williams (2002). "Commitment to apoptosis induced by tumour necrosis factor-alpha is dependent on caspase activity." Apoptosis 7(2): 123-32.

Heinrich, M. (2004). "Cathepsin D links TNF-induced acid sphingomyelinase to Bid-mediated caspase-9 and -3 activation." *Cell Death Differ.* 11, 550–563.

Hellman M. Arumäe U. Yu L. Lindholm P. Peränen J. Saarma M. and Perttu Permi (2010). "Neurotrophic factor MANF has a unique mechanism to rescue apoptotic neurons." JBC Nov 3

Hengartner, M. O. and H. R. Horvitz (1994). "Programmed cell death in Caenorhabditis elegans." Curr Opin Genet Dev 4(4): 581-6.

Hengartner, M. O., R. E. Ellis, et al. (1992). "Caenorhabditis elegans gene ced-9 protects cells from programmed cell death." Nature 356(6369): 494-9.

Hla T. (2004). "Physiological and pathological actions of sphingosine 1-phosphate." Semin Cell Dev Biol. Oct;15(5):513-20.

Hockenbery DM, Oltvai ZN, Yin XM, Milliman CL, Korsmeyer SJ. (1993). "Bcl-2 functions in an antioxidant pathway to prevent apoptosis." Cell. Oct 22;75(2):241-51.

Hoffmann B, Stöckl A, Schlame M, Beyer K, Klingenberg M. (1994). "The reconstituted ADP/ATP carrier activity has an absolute requirement for cardiolipin as shown in cysteine mutants." J Biol Chem. Jan 21;269(3):1940-4.

Holmgreen, S. P., D. C. Huang, et al. (1999). "Survival activity of Bcl-2 homologs Bcl-w and A1 only partially correlates with their ability to bind pro-apoptotic family members." Cell Death Differ 6(6): 525-32.

Hotchkiss, R. S., A. Strasser, et al. (2009). "Cell death." N Engl J Med 361(16): 1570-83.

Hou Y., F. Gao, et al. (2007). "Bcl2 impedes DNA mismatch repair by directly regulating the hMSH2-hMSH6 heterodimeric complex." J Biol Chem 282(12): 9279-87.

Houtkooper RH, Vaz FM (2008). "Cardiolipin, the heart of mitochondrial metabolism." Cell Mol Life Sci. Aug;65(16):2493-506.

Hoyer-Hansen, M. and M. Jaattela (2007). "Connecting endoplasmic reticulum stress to autophagy by unfolded protein response and calcium." Cell Death Differ 14(9): 1576-82.

Hoyer-Hansen, M., L. Bastholm, et al. (2007). "Control of macroautophagy by calcium, calmodulin-dependent kinase kinase-beta, and Bcl-2." Mol Cell 25(2): 193-205.

Hsu Y. T. and R. J. Youle (1997). "Nonionic detergents induce dimerization among members of the Bcl-2 family." J Biol Chem 272(21): 13829-34.

Hsu Y. T., K. G. Wolter, et al. (1997). "Cytosol-to-membrane redistribution of Bax and Bcl-X(L) during apoptosis." Proc Natl Acad Sci U S A 94(8): 3668-72.

Hu Y., L. Ding, et al. (1998). "WD-40 repeat region regulates Apaf-1 self-association and procaspase-9 activation." J Biol Chem 273(50): 33489-94.

Hu Y., M. A. Benedict, et al. (1999). "Role of cytochrome c and dATP/ATP hydrolysis in Apaf-1-mediated caspase-9 activation and apoptosis." Embo J 18(13): 3586-95.

Huang C, Hales BF. (2002). "Role of caspases in murine limb bud cell death induced by 4-hydroperoxycyclophosphamide, an activated analog of cyclophosphamide."

Huang D. C. and A. Strasser (2000). "BH3-Only proteins-essential initiators of apoptotic cell death." Cell 103(6): 839-42.

Huang D. C., J. M. Adams, et al. (1998). "The conserved N-terminal BH4 domain of Bcl-2 homologues is essential for inhibition of apoptosis and interaction with CED-4." Embo J 17(4): 1029-39.

Huang D. C., J. Tschopp, et al. (2000). "Bcl-2 does not inhibit cell death induced by the physiological Fas ligand: implications for the existence of type I and type II cells." Cell Death Differ 7(8): 754-5.

Huang D. C., L. A. O'Reilly, et al. (1997). "The anti-apoptosis function of Bcl-2 can be genetically separated from its inhibitory effect on cell cycle entry." Embo J 16(15): 4628-38.

Huang D. C., S. Cory, et al. (1997). "Bcl-2, Bcl-XL and adenovirus protein E1B19kD are functionally equivalent in their ability to inhibit cell death." Oncogene 14(4): 405-14.

Huang DC, Strasser A. (2000). "BH3-Only proteins-essential initiators of apoptotic cell death." Cell. Dec 8;103(6):839-42.

Huang H. M., C. J. Huang, et al. (2000). "Mcl-1 is a common target of stem cell factor and interleukin-5 for apoptosis prevention activity via MEK/MAPK and PI-3K/Akt pathways." Blood 96(5): 1764-71.

Huang Q., A. M. Petros, et al. (2002). "Solution structure of a Bcl-2 homolog from Kaposi sarcoma virus." Proc Natl Acad Sci U S A 99(6): 3428-33.

Hunter J. J. and T. G. Parslow (1996). "A peptide sequence from Bax that converts Bcl-2 into an activator of apoptosis." J Biol Chem 271(15): 8521-4.

Ichikawa S, Hirabayashi Y. (1998). "Glucosylceramide synthase and glycosphingolipid synthesis." Trends Cell Biol. May;8(5):198-202.

Innes K. M., S. J. Szilvassy, et al. (1999). "Retroviral transduction of enriched hematopoietic stem cells allows lifelong Bcl-2 expression in multiple lineages but does not perturb hematopoiesis." Exp Hematol 27(1): 75-87.

Inohara N., D. Ekhterae, et al. (1998). "Mtd, a novel Bcl-2 family member activates apoptosis in the absence of heterodimerization with Bcl-2 and Bcl-XL." J Biol Chem 273(15): 8705-10.

Jabbour A. M., C. P. Daunt, et al. (2010). "Myeloid progenitor cells lacking p53 exhibit delayed up-regulation of Puma and prolonged survival after cytokine deprivation." Blood 115(2): 344-52.

Jabbour A. M., M. A. Puryer, et al. (2006). "Human Bcl-2 cannot directly inhibit the Caenorhabditis elegans Apaf-1 homologue CED-4, but can interact with EGL-1." J Cell Sci 119(Pt 12): 2572-82.

Jagasia R., Grote, P., Westermann, B. & Conradt, B. (2005). "DRP-1-mediated mitochondrial fragmentation during EGL-1-induced cell death in C. elegans." Nature 433, 754–760.

Jeffers J. R., E. Parganas, et al. (2003). "Puma is an essential mediator of p53-dependent and -independent apoptotic pathways." Cancer Cell 4(4): 321-8.

Jiang F, Ryan MT, Schlame M, Zhao M, Gu Z, Klingenberg M, Pfanner N, Greenberg ML. (2000). " Absence of cardiolipin in the crd1 null mutant results in decreased mitochondrial membrane potential and reduced mitochondrial function." J Biol Chem. Jul 21;275(29):22387-94.

Johnson DE. (1998). "Regulation of survival pathways by IL-3 and induction of apoptosis following IL-3 withdrawal." Front Biosci.Mar 15;3:d313-24.

Jourdan M., J. L. Veyrune, et al. (2003). "A major role for Mcl-1 antiapoptotic protein in the IL-6-induced survival of human myeloma cells." Oncogene 22(19): 2950-9.

Joyal JL, Annan RS, Ho YD, Huddleston ME, Carr SA, Hart MJ, Sacks DB. Calmodulin modulates the interaction between IQGAP1 and Cdc42. (1997). "Identification of IQGAP1 by nanoelectrospray tandem mass spectrometry." J Biol Chem 272:15419–25.

Kagan VE, Tyurin VA, Jiang J, Tyurina YY, Ritov VB, Amoscato AA, Osipov AN, Belikova NA, Kapralov AA, Kini V, Vlasova II, Zhao Q, Zou M, Di P, Svistunenko DA, Kurnikov IV, Borisenko GG. (2005). "Cytochrome c acts as a cardiolipin oxygenase required for release of proapoptotic factors." Nat Chem Biol. Sep;1(4):223-32.

Kang, C. B., L. Feng, et al. (2005). "Molecular characterization of FK-506 binding protein 38 and its potential regulatory role on the anti-apoptotic protein Bcl-2." Biochem Biophys Res Commun 337(1): 30-8.

Karbowski M, Lee YJ, Gaume B, Jeong SY, Frank S, Nechushtan A, Santel A, Fuller M, Smith CL, Youle RJ (2002). "Spatial and temporal association of Bax with mitochondrial fission sites, Drp1, and Mfn2 during apoptosis." J Cell Biol 159:931–938.

Karbowski M., Norris, K., Cleland, M., Jeong, S., and Youle, R. (2006). "Role of Bax and Bak in mitochondrial morphogenesis." Nature 443, 658–662.

Kerr J. F., A. H. Wyllie, et al. (1972). "Apoptosis: a basic biological phenomenon with wide-ranging implications in tissue kinetics." Br J Cancer 26(4): 239-57.

Kim H., M. Rafiuddin-Shah, et al. (2006). "Hierarchical regulation of mitochondrion-dependent apoptosis by BCL-2 subfamilies." Nat Cell Biol 8(12): 1348-58.

Kim R., M. Emi, et al. (2006). "Regulation and interplay of apoptotic and non-apoptotic cell death." J Pathol 208(3): 319-26.

Kim R., M. Emi, et al. (2006). "Role of mitochondria as the gardens of cell death." Cancer Chemother Pharmacol 57(5): 545-53.

Knudson C. M., K. S. Tung, et al. (1995). "Bax-deficient mice with lymphoid hyperplasia and male germ cell death." Science 270(5233): 96-9.

Korenbaum E, Rivero F. (2002). "Calponin homology domains at a glance". J Cell Sci. Sep 15;115(Pt 18):3543-5.

Korsmeyer S. J., M. C. Wei, et al. (2000). "Pro-apoptotic cascade activates BID, which oligomerizes BAK or BAX into pores that result in the release of cytochrome c." Cell Death Differ 7(12): 1166-73.

Koshkin V, Greenberg ML. (2000). "Oxidative phosphorylation in cardiolipin-lacking yeast mitochondria." Biochem J. May 1;347 Pt 3:687-91.

Krieser R. J. and K. White (2002). "Engulfment mechanism of apoptotic cells." Curr Opin Cell Biol 14(6): 734-8.

Krieser R. J. and K. White (2009). "Inside an enigma: do mitochondria contribute to cell death in Drosophila?" Apoptosis 14(8): 961-8.

Krieser, R. J., F. E. Moore, et al. (2007). "The Drosophila homolog of the putative phosphatidylserine receptor functions to inhibit apoptosis." Development 134(13): 2407-14.

Kroemer, G., L. Galluzzi, et al. (2007). "Mitochondrial membrane permeabilization in cell death." Physiol Rev 87(1): 99-163.

Kukat A. (2007). " Mitochondriale Fusions- und Fissionsvorgänge am Modellsystem von Mega-Mitochondrien einer ρ0-Zelllinie." Dissertation zur Erlangung des Naturwissen-schaftlichen Doktorgrades der Bayerischen Julius-Maximilians-Universität Würzburg

Kumar S, Gupta RK, Bhake AS, Samal N. (1992). "Cardiotoxic effects of high doses of cyclophosphamide in albino rats." Arch Int Pharmacodyn Ther. Sep-Oct;319:58-65.

Kumar S. (2000). "Cell death in the fly comes of age." Cell Death Differ. Nov;7(11):1021-4.

Kumar S. (2007). "Caspase function in programmed cell death." Cell Death Differ 14(1): 32-43.

Kuroda S, et al.(1998). "Role of IQGAP1, a target of the small GTPases Cdc42 and Rac1, in regulation of Ecadherin-mediated cell-cell adhesion." Science 1998;281:832–5.

Kuwana T., M. R. Mackey, et al. (2002). "Bid, Bax, and lipids cooperate to form supramolecular openings in the outer mitochondrial membrane." Cell 111(3): 331-42.

Laster S. M., J. G. Wood, et al. (1988). "Tumor necrosis factor can induce both apoptic and necrotic forms of cell lysis." J Immunol 141(8): 2629-34.

Le Gouill S., K. Podar, et al. (2004). "Mcl-1 regulation and its role in multiple myeloma." Cell Cycle 3(10): 1259-62.

Le Gouill S., K. Podar, et al. (2004). "VEGF induces Mcl-1 up-regulation and protects multiple myeloma cells against apoptosis." Blood 104(9): 2886-92.

Lee JY, Hannun YA, Obeid LM. (1996). "Ceramide inactivates cellular protein kinase Calpha." J Biol Chem. May 31;271(22):13169-74.

Lee YJ, Jeong SY, Karbowski M, Smith CL, Youle RJ. (2004). "Roles of the mammalian mitochondrial fission and fusion mediators Fis1, Drp1, and Opa1 in apoptosis." Mol Biol Cell. Nov;15(11):5001-11.

Leist, M. and P. Nicotera (1997). "The shape of cell death." Biochem Biophys Res Commun 236(1): 1-9.

Letai, A., M. C. Bassik, et al. (2002). "Distinct BH3 domains either sensitize or activate mitochondrial apoptosis, serving as prototype cancer therapeutics." Cancer Cell 2(3): 183-92.

Lettre, G. and M. O. Hengartner (2006). "Developmental apoptosis in C. elegans: a complex CEDnario." Nat Rev Mol Cell Biol 7(2): 97-108.

Levine, B. (2005). "Eating oneself and uninvited guests: autophagy-related pathways in cellular defense." Cell 120(2): 159-62.

Levine, B. and J. Yuan (2005). "Autophagy in cell death: an innocent convict?" J Clin Invest 115(10): 2679-88.

Ley, R., K. E. Ewings, et al. (2005). "Regulatory phosphorylation of Bim: sorting out the ERK from the JNK." Cell Death Differ 12(8): 1008-14.

Li Likun, ElMoataz Abdel Fattah Cao G. Ren C. Yang G. Goltsov AA. Chinault AC. Cai WW. Terry L. Timme TL. and Thompson TC. (2008). "Glioma Pathogenesis-Related Protein 1 Exerts Tumor Suppressor Activities through Proapoptotic Reactive Oxygen Species–c-Jun–NH2 Kinase Signaling." Cancer Res 68: (2). 434-43.

Li, H., H. Zhu, et al. (1998). "Cleavage of BID by caspase 8 mediates the mitochondrial damage in the Fas pathway of apoptosis." Cell 94(4): 491-501.

Liang XH, Kleeman LK, Jiang HH, Gordon G, Goldman JE, Berry G, Herman B, Levine B. (1998). " Protection against fatal Sindbis virus encephalitis by beclin, a novel Bcl-2-interacting protein." J Virol. Nov;72(11):8586-96.

Liang, X. H., J. Yu, et al. (2001). "Beclin 1 contains a leucine-rich nuclear export signal that is required for its autophagy and tumor suppressor function." Cancer Res 61(8): 3443-9.

Liang, X. H., S. Jackson, et al. (1999). "Induction of autophagy and inhibition of tumorigenesis by beclin 1." Nature 402(6762): 672-6.

Lindsten, T., A. J. Ross, et al. (2000). "The combined functions of proapoptotic Bcl-2 family members bak and bax are essential for normal development of multiple tissues." Mol Cell 6(6): 1389-99.

Ling, Y. H., C. Tornos, et al. (1998). "Phosphorylation of Bcl-2 is a marker of M phase events and not a determinant of apoptosis." J Biol Chem 273(30): 18984-91.

Liu Y, Xie KM, Yang GQ, Bai XM, Shi YP, Mu HJ, Qiao WZ, Zhang B, Xie P. (2010). "GCS induces multidrug resistance by regulating apoptosis-related genes in K562/AO2 cell line." Cancer Chemother Pharmacol. Aug;66(3):433-9.

Lockshin, R. A. and Z. Zakeri (2004). "Caspase-independent cell death?" Oncogene 23(16): 2766-73.

Lockshin, R. A., C. O. Facey, et al. (2001). "Cell death in the heart." Cardiol Clin 19(1): 1-11.

Lotze, M. T. and K. J. Tracey (2005). "High-mobility group box 1 protein (HMGB1): nuclear weapon in the immune arsenal." Nat Rev Immunol 5(4): 331-42.

Lovell, J. F., L. P. Billen, et al. (2008). "Membrane binding by tBid initiates an ordered series of events culminating in membrane permeabilization by Bax." Cell 135(6): 1074-84.

Lum, J. J., D. E. Bauer, et al. (2005). "Growth factor regulation of autophagy and cell survival in the absence of apoptosis." Cell 120(2): 237-48.

Lum, J. J., R. J. DeBerardinis, et al. (2005). "Autophagy in metazoans: cell survival in the land of plenty." Nat Rev Mol Cell Biol 6(6): 439-48.

Lutter, M., G. A. Perkins, et al. (2001). "The pro-apoptotic Bcl-2 family member tBid localizes to mitochondrial contact sites." BMC Cell Biol 2: 22.

Lutter, M., M. Fang, et al. (2000). "Cardiolipin provides specificity for targeting of tBid to mitochondria." Nat Cell Biol 2(10): 754-61.

Macaskill AF, Rinholm JE, Twelvetrees AE, Arancibia-Carcamo IL, Muir J, Fransson A, Aspenstrom P, Attwell D, Kittler JT (2009). "Miro1 is a calcium sensor for glutamate receptor-dependent localization of mitochondria at synapses." Neuron 61:541–555.

Martinou, J.C., and Youle, R.J. (2006). "Which came first, the cytochrome c release or the mitochondrial fission?" Cell Death Differ. 13, 1291–1295.

Martins, L. M., I. Iaccarino, et al. (2002). "The serine protease Omi/HtrA2 regulates apoptosis by binding XIAP through a reaper-like motif." J Biol Chem 277(1): 439-44.

Maurer, U., C. Charvet, et al. (2006). "Glycogen synthase kinase-3 regulates mitochondrial outer membrane permeabilization and apoptosis by destabilization of MCL-1." Mol Cell 21(6): 749-60.

May, W. S., P. G. Tyler, et al. (1994). "Interleukin-3 and bryostatin-1 mediate hyperphosphorylation of BCL2 alpha in association with suppression of apoptosis." J Biol Chem 269(43): 26865-70.

Mazel, S., D. Burtrum, et al. (1996). "Regulation of cell division cycle progression by bcl-2 expression: a potential mechanism for inhibition of programmed cell death." J Exp Med 183(5): 2219-26.

McCormick AL, Smith VL, Chow D, Mocarski ES. (2003). "Disruption of mitochondrial networks by the human cytomegalovirus UL37 gene product viral mitochondrion-localized inhibitor of apoptosis." J Virol. Jan;77(1):631-41.

McDonnell TJ, Korsmeyer SJ. (1991). "Progression from lymphoid hyperplasia to high-grade malignant lymphoma in mice transgenic for the t(14; 18)." Nature. Jan 17;349(6306):254-6.
McKinstry, W. J., C. L. Li, et al. (1997). "Cytokine receptor expression on hematopoietic stem and progenitor cells." Blood 89(1): 65-71.

Meeusen S, DeVay R, Block J, Cassidy-Stone A, Wayson S, McCaffery JM, Nunnari J. (2006). "Mitochondrial inner-membrane fusion and crista maintenance requires the dynamin-related GTPase Mgm1." Cell. Oct 20;127(2):383-95.

Meeusen S, McCaffery JM, Nunnari J. (2004). "Mitochondrial fusion intermediates revealed in vitro." Science. Sep 17;305(5691):1747-52.

Mehler M. F. and Gokhan S. (2000). "Mechanisms underlying neural cell death in neurodegenerative diseases: alterations of a developmentally-mediated cellular rheostat." Trends Neurosci. 23, 599–605.

Meier, P., A. Finch, et al. (2000). "Apoptosis in development." Nature 407(6805): 796-801.

Meier, P., J. Silke, et al. (2000). "The Drosophila caspase DRONC is regulated by DIAP1." Embo J 19(4): 598-611.

Merker HJ, Herbst R, Kloss K. (1968). "Electron microscopical studies on the mitochondria of the human uterus epithelium during the secretive phase." Z Zellforsch Mikrosk Anat. 1968;86(1):139-52.

Mikhailov V. Mikhailova M. (2003). "Association of Bax and Bak homo-oligomers in mitochondria. Bax requirement for Bak reorganization and cytochrome c release." J Biol Chem 278(7): 5367-76.

Mirkes PE, Little SA, Umpierre CC. (2001). "Co-localization of active caspase-3 and DNA fragmentation (TUNEL) in normal and hyperthermia-induced abnormal mouse development." Teratology. Mar;63(3):134-43.

Monney, L., I. Otter, et al. (1996). "Bcl-2 overexpression blocks activation of the death protease CPP32/Yama/apopain." Biochem Biophys Res Commun 221(2): 340-5.

Montessuit S, Somasekharan SP, Terrones O, Lucken-Ardjomande S, Herzig S, Schwarzenbacher R, Manstein DJ, Bossy-Wetzel E, Basañez G, Meda P, Martinou JC. (2010). "Membrane remodeling induced by the dynamin-related protein Drp1 stimulates Bax oligomerization." Cell. Sep 17;142(6):889-901.

Monti M, Orrù S, Pagnozzi D, Pucci P. (2005). "Interaction proteomics." Biosci Rep. Feb-Apr;25(1-2):45-56.

Morgenstern JP, Land H. (1990). "A series of mammalian expression vectors and characterisation of their expression of a reporter gene in stably and transiently transfected cells." Nucleic Acids Res. Feb 25;18(4):1068.

Mozdy AD, McCaffery JM, Shaw JM.J. (2000). "Dnm1p GTPase-mediated mitochondrial fission is a multi-step process requiring the novel integral membrane component Fis1p." Cell Biol. Oct 16;151(2):367-80.

Muchmore, S. W., M. Sattler, et al. (1996). "X-ray and NMR structure of human Bcl-xL, an inhibitor of programmed cell death." Nature 381(6580): 335-41.

Müller G, Ayoub M, Storz P, Rennecke J, Fabbro D, Pfizenmaier K. (1995). "PKC zeta is a molecular switch in signal transduction of TNF-alpha, bifunctionally regulated by ceramide and arachidonic acid." EMBO J. May 1;14(9):1961-9.

Nakano, K. and K. H. Vousden (2001). "PUMA, a novel proapoptotic gene, is induced by p53." Mol Cell 7(3): 683-94.

Negrini M, Silini E, Kozak C, Tsujimoto Y, Croce CM. (1987). "Molecular analysis of mbcl-2: structure and expression of the murine gene homologous to the human gene involved in follicular lymphoma." Cell. May 22;49(4):455-63.

Neuspiel M, Zunino R, Gangaraju S, Rippstein P, McBride H (2005). "Activated mitofusin 2 signals mitochondrial fusion, interferes with Bax activation, and reduces susceptibility to radical induced depolarization." J Biol Chem 280:25060–25070.

Nijhawan, D., Fang, M., Traer, E., Zhong, Q., Gao, W., Du, F. and Wang, X. (2003). "Elimination of Mcl-1 is required for the initiation of apoptosis following ultraviolet irradiation." Genes Dev **17**(12):1475-1486.

Obeid LM, Linardic CM, Karolak LA, Hannun YA. (1993). "Programmed cell death induced by ceramide." Science. Mar 19;259(5102):1769-71.

Oberst A, Bender C, Green DR. (2008). "Living with death: the evolution of the mitochondrial pathway of apoptosis in animals." Cell Death Differ. Jul;15(7):1139-46.

Oh KJ, Barbuto S, Pitter K, Morash J, Walensky LD, Korsmeyer SJ. (2006). "A membrane-targeted BID BCL-2 homology 3 peptide is sufficient for high potency activation of BAX in vitro." J Biol Chem. Dec 1;281(48):36999-7008.

Olichon A, Baricault L, Gas N, Guillou E, Valette A, Belenguer P, Lenaers G. (2003). "Loss of OPA1 perturbates the mitochondrial inner membrane structure and integrity, leading to cytochrome c release and apoptosis." J Biol Chem. Mar 7;278(10):7743-6.

Olichon A, Elachouri G, Baricault L, Delettre C, Belenguer P, Lenaers G. (2007). "OPA1 alternate splicing uncouples an evolutionary conserved function in mitochondrial fusion from a vertebrate restricted function in apoptosis." Cell Death Differ. Apr;14(4):682-92.

Olichon A, Emorine LJ, Descoins E, Pelloquin L, Brichese L, Gas N, Guillou E, Delettre C, Valette A, Hamel CP, Ducommun B, Lenaers G, Belenguer P. (2002). "The human dynamin-related protein OPA1 is anchored to the mitochondrial inner membrane facing the inter-membrane space." FEBS Lett. Jul 17;523(1-3):171-6.

Oltersdorf T, Elmore SW, Shoemaker AR, Armstrong RC, Augeri DJ, Belli BA, Bruncko M, Deckwerth TL, Dinges J, Hajduk PJ, Joseph MK, Kitada S, Korsmeyer SJ, Kunzer AR, Letai A, Li C, Mitten MJ, Nettesheim DG, Ng S, Nimmer PM, O'Connor JM, Oleksijew A, Petros AM, Reed JC, Shen W, Tahir SK, Thompson CB, Tomaselli KJ, Wang B, Wendt MD, Zhang H, Fesik SW, Rosenberg SH. (2005). "An inhibitor of Bcl-2 family proteins induces regression of solid tumours." Nature.Jun 2;435(7042):677-81.

Oltvai ZN, Milliman CL, Korsmeyer SJ. (1993). "Bcl-2 heterodimerizes in vivo with a conserved homolog, Bax, that accelerates programmed cell death." Cell. Aug 27;74(4):609-19.

O'Reilly LA, Huang DC, Strasser A. (1996). "The cell death inhibitor Bcl-2 and its homologues influence control of cell cycle entry." EMBO J. Dec 16;15(24):6979-90.

Ott, M., Norberg, E., Walter, K.M., Schreiner, P., Kemper, C., Rapaport, D., Zhivotovsky, B. and Orrenius, S., (2007). 'The mitochondrial TOM complex is required for tBid/Bax-induced cytochrome c release'. J Biol Chem, 282 (38):27633-9.

Otter I, Conus S, Ravn U, Rager M, Olivier R, Monney L, Fabbro D, Borner C. (1998). "The binding properties and biological activities of Bcl-2 and Bax in cells exposed to apoptotic stimuli." J Biol Chem. Mar 13;273(11):6110-20.

Pardo, J., Urban, C., Galvez, E.M., Ekert, P.G., Muller, U., Kwon-Chung, J., Lobigs, M., Mullbacher, A., Wallich, R., Borner, C. and Simon, M.M., (2006). 'The mitochondrial protein Bak is pivotal for gliotoxin-induced apoptosis and a critical host factor of Aspergillus fumigatus virulence in mice'. J Cell Biol, 174 (4):509-519.

Parone PA, James DI, Da Cruz S, Mattenberger Y, Donze O, Barja F, Martinou JC (2006). "Inhibiting the mitochondrial fission machinery does not prevent Bax/Bak-dependent apoptosis." Mol Cell Biol 26:7397–7408.

Pattingre, S. and B. Levine (2006). "Bcl-2 inhibition of autophagy: a new route to cancer?" Cancer Res 66(6): 2885-8.

Pavlov, E.V., Priault, M., Pietkiewicz, D., Cheng, E.H., Antonsson, B., Manon, S., Korsmeyer, S.J., Mannella, C.A. and Kinnally, K.W., (2001). 'A novel, high conductance channel of mitochondria linked to apoptosis in mammalian cells and Bax expression in yeast'. *J Cell Biol*, 155 (5):725-731.

Petlickovski A, Laurenti L, Li X, Marietti S, Chiusolo P, Sica S, Leone G, Efremov DG. (2005). "Sustained signaling through the B-cell receptor induces Mcl-1 and promotes survival of chronic lymphocytic leukemia B cells." Blood. Jun 15;105(12):4820-7.

Petros AM, Medek A, Nettesheim DG, Kim DH, Yoon HS, Swift K, Matayoshi ED, Oltersdorf T, Fesik SW. (2001). "Solution structure of the antiapoptotic protein bcl-2." Proc Natl Acad Sci U S A. Mar 13;98(6):3012-7.

Phee BK, Shin DH, Cho JH, Kim SH, Kim JI, Lee YH, Jeon JS, Bhoo SH, Hahn TR. (2006). "Identification of phytochrome-interacting protein candidates in Arabidopsis thaliana by co-immunoprecipitation coupled with MALDI-TOF MS." Proteomics. Jun;6(12):3671-80.

Polster BM, Pevsner J, Hardwick JM. (2004). "Viral Bcl-2 homologs and their role in virus replication and associated diseases." Biochim Biophys Acta. Mar 1;1644(2-3):211-27.

Poommipanit, P. B., B. Chen, et al. (1999). "Interleukin-3 induces the phosphorylation of a distinct fraction of bcl-2." J Biol Chem 274(2): 1033-9.

Puthalakath H, Strasser A. (2002). "Keeping killers on a tight leash: transcriptional and post-translational control of the pro-apoptotic activity of BH3-only proteins." Cell Death Differ. May;9(5):505-12.

Puthalakath H, Villunger A, O'Reilly LA, Beaumont JG, Coultas L, Cheney RE, Huang DC, Strasser A. (2001). "Bmf: a proapoptotic BH3-only protein regulated by interaction with the myosin V actin motor complex, activated by anoikis." Science. Sep 7;293(5536):1829-32.

Ramjaun AR, Tomlinson S, Eddaoudi A, Downward J. (2007). "Upregulation of two BH3-only proteins, Bmf and Bim, during TGF beta-induced apoptosis." Oncogene. Feb 15;26(7):970-81.

Rathmell, J.C. and Thompson, C.B., (2002). 'Pathways of apoptosis in lymphocyte development, homeostasis, and disease'. Cell, 109 Suppl:S97-107.

Reed, J. C. (2006). "Proapoptotic multidomain Bcl-2/Bax-family proteins: mechanisms, physiological roles, and therapeutic opportunities." Cell Death Differ 13(8): 1378-86.

Ren D. Hyungjin Kim, Ho-Chou Tu, Todd D. Westergard, Jill K. Fisher, Jeff A. Rubens, Stanley J. Korsmeyer, James J.-D. Hsieh and Emily H.-Y. Cheng (2009)."The VDAC2-BAK Rheostat Controls Thymocyte Survival." Science Signaling (85).

Ren L, Emery D, Kaboord B, Chang E, Qoronfleh MW. (2003). "Improved immunomatrix methods to detect protein:protein interactions." J Biochem Biophys Methods. Aug 29;57(2):143-57.

Riccio P, Schägger H, Engel WD, Von Jagow G. (1977). "bc1-Complex from beef heart. One-step purification by hydroxyapatite chromatography in Triton X-100, polypeptide pattern and respiratory chain characteristics." Biochim Biophys Acta. Feb 7;459(2):250-62.

Rodriguez, A., H. Oliver, et al. (1999). "Dark is a Drosophila homologue of Apaf-1/CED-4 and functions in an evolutionarily conserved death pathway." Nat Cell Biol 1(5): 272-9.

Rodriguez, J. and Y. Lazebnik (1999). "Caspase-9 and APAF-1 form an active holoenzyme." Genes Dev 13(24): 3179-84.

Rong, Y. and C. W. Distelhorst (2008). "Bcl-2 protein family members: versatile regulators of calcium signaling in cell survival and apoptosis." Annu Rev Physiol 70: 73-91.

Rong, Y. P., A. S. Aromolaran, et al. (2008). "Targeting Bcl-2-IP3 receptor interaction to reverse Bcl-2's inhibition of apoptotic calcium signals." Mol Cell 31(2): 255-65.

Rong, Y. P., G. Bultynck, et al. (2009). "The BH4 domain of Bcl-2 inhibits ER calcium release and apoptosis by binding the regulatory and coupling domain of the IP3 receptor." Proc Natl Acad Sci U S A 106(34): 14397-402.

Rosse, T., R. Olivier, et al. (1998). "Bcl-2 prolongs cell survival after Bax-induced release of cytochrome c." Nature 391(6666): 496-9.

Roux A, Uyhazi K, Frost A, De Camilli P. (2006). "GTP-dependent twisting of dynamin implicates constriction and tension in membrane fission." Nature. May 25;441(7092):528-31.

Ruffolo, S. C. and G. C. Shore (2003). "BCL-2 selectively interacts with the BID-induced open conformer of BAK, inhibiting BAK auto-oligomerization." J Biol Chem 278(27): 25039-45.

Ruffolo, S. C., D. G. Breckenridge, et al. (2000). "BID-dependent and BID-independent pathways for BAX insertion into mitochondria." Cell Death Differ 7(11): 1101-8.

Ruvolo, P. P., X. Deng, et al. (1998). "A functional role for mitochondrial protein kinase Calpha in Bcl2 phosphorylation and suppression of apoptosis." J Biol Chem 273(39): 25436-42.

Santel A, Fuller MT. (2001). "Control of mitochondrial morphology by a human mitofusin." J Cell Sci. Mar;114(Pt 5):867-74.

Saotome M, Safiulina D, Szabadkai G, Das S, Fransson A, Aspenstrom P, Rizzuto R, Hajnoczky G (2008). "Bidirectional Ca2?-dependent control of mitochondrial dynamics by the Miro GTPase." Proc Natl Acad Sci USA 105:20728–20733.

Sasarman F, Brunel-Guitton C, Antonicka H, Wai T, Shoubridge EA; LSFC Consortium. (2010). " LRPPRC and SLIRP interact in a ribonucleoprotein complex that regulates posttranscriptional gene expression in mitochondria." Mol Biol Cell. Apr;21(8):1315-23.

Sato, T., M. Hanada, et al. (1994). "Interactions among members of the Bcl-2 protein family analyzed with a yeast two-hybrid system." Proc Natl Acad Sci U S A 91(20): 9238-42.

Sattler, M., H. Liang, et al. (1997). "Structure of Bcl-xL-Bak peptide complex: recognition between regulators of apoptosis." Science 275(5302): 983-6.

Savill, J. and V. Fadok (2000). "Corpse clearance defines the meaning of cell death." Nature 407(6805): 784-8.

Scatena, C. D., Z. A. Stewart, et al. (1998). "Mitotic phosphorylation of Bcl-2 during normal cell cycle progression and Taxol-induced growth arrest." J Biol Chem 273(46): 30777-84.

Schägger H, Pfeiffer K. (2000). " Supercomplexes in the respiratory chains of yeast and mammalian mitochondria." EMBO J. Apr 17;19(8):1777-83.

Schendel, S. L., M. Montal, et al. (1998). "Bcl-2 family proteins as ion-channels." Cell Death Differ 5(5): 372-80.

Scherer, W.F., Syverton, J.T. and Gey, G.O., (1953). 'Studies on the propagation in vitro of poliomyelitis viruses. IV. Viral multiplication in a stable strain of human malignant epithelial cells (strain HeLa) derived from an epidermoid carcinoma of the cervix'. J Exp Med, 97 (5):695-710.

Schinzel, A., T. Kaufmann, et al. (2004). "Conformational control of Bax localization and apoptotic activity by Pro168." J Cell Biol 164(7): 1021-32.

Schmelzle, T., A. A. Mailleux, et al. (2007). "Functional role and oncogene-regulated expression of the BH3-only factor Bmf in mammary epithelial anoikis and morphogenesis." Proc Natl Acad Sci U S A 104(10): 3787-92.

Schmidt VA, Chiariello CS, Capilla E, Miller F, Bahou WF. (2008). "Development of hepatocellular carcinoma in Iqgap2-deficient mice is IQGAP1 dependent." Mol Cell Biol. Mar;28(5):1489-502.

Scorrano L, Ashiya M, Buttle K, Weiler S, Oakes SA, Mannella CA, Korsmeyer SJ. (2002). "A distinct pathway remodels mitochondrial cristae and mobilizes cytochrome c during apoptosis." Dev Cell. Jan;2(1):55-67.

Sedlak, T. W., Z. N. Oltvai, et al. (1995). "Multiple Bcl-2 family members demonstrate selective dimerizations with Bax." Proc Natl Acad Sci U S A 92(17): 7834-8.

Sheridan C, Delivani P, Cullen SP, Martin SJ. (2008). "Bax- or Bak-induced mitochondrial fission can be uncoupled from cytochrome C release." Mol Cell. Aug 22;31(4):570-85.

Shimizu, S. and Y. Tsujimoto (2000). "Proapoptotic BH3-only Bcl-2 family members induce cytochrome c release, but not mitochondrial membrane potential loss, and do not directly modulate voltage-dependent anion channel activity." Proc Natl Acad Sci U S A 97(2): 577-82.

Shimizu, S., A. Konishi, et al. (2000). "BH4 domain of antiapoptotic Bcl-2 family members closes voltage-dependent anion channel and inhibits apoptotic mitochondrial changes and cell death." Proc Natl Acad Sci U S A 97(7): 3100-5.

Shimizu, S., M. Narita, et al. (1999). "Bcl-2 family proteins regulate the release of apoptogenic cytochrome c by the mitochondrial channel VDAC." Nature 399(6735): 483-7.

Shimizu, S., Y. Matsuoka, et al. (2001). "Essential role of voltage-dependent anion channel in various forms of apoptosis in mammalian cells." J Cell Biol 152(2): 237-50.

Shirane, M. and K. I. Nakayama (2003). "Inherent calcineurin inhibitor FKBP38 targets Bcl-2 to mitochondria and inhibits apoptosis." Nat Cell Biol 5(1): 28-37.

Siskind LJ, Feinstein L, Yu T, Davis JS, Jones D, Choi J, Zuckerman JE, Tan W, Hill RB, Hardwick JM, Colombini M. (2008). "Anti-apoptotic Bcl-2 Family Proteins Disassemble Ceramide Channels." J Biol Chem. Mar 14;283(11):6622-30.

Siskind LJ, Fluss S, Bui M, Colombini M. (2005). "Sphingosine forms channels in membranes that differ greatly from those formed by ceramide." J Bioenerg Biomembr. Aug;37(4):227-36.

Siskind LJ, Mullen TD, Romero Rosales K, Clarke CJ, Hernandez-Corbacho MJ, Edinger AL, Obeid LM. (2010). "The BCL-2 protein BAK is required for long-chain ceramide generation during apoptosis." J Biol Chem. Apr 16;285(16):11818-26.
Siskind LJ. (2005). "Mitochondrial ceramide and the induction of apoptosis." J Bioenerg Biomembr. Jun;37(3):143-53.

Smirnova E, Griparic L, Shurland DL, van der Bliek AM. (2001). "Dynamin-related protein Drp1 is required for mitochondrial division in mammalian cells." Mol Biol Cell. Aug;12(8):2245-56.

Snyder, S. H., M. M. Lai, et al. (1998). "Immunophilins in the nervous system." Neuron 21(2): 283-94.

Srivastava, R. K., A. R. Srivastava, et al. (1999). "Growth arrest and induction of apoptosis in breast cancer cells by antisense depletion of protein kinase A-RI alpha subunit: p53-independent mechanism of action." Mol Cell Biochem 195(1-2): 25-36.

Srivastava, R. K., C. Y. Sasaki, et al. (1999). "Bcl-2-mediated drug resistance: inhibition of apoptosis by blocking nuclear factor of activated T lymphocytes (NFAT)-induced Fas ligand transcription." J Exp Med 190(2): 253-65.

Srivastava, R. K., Q. S. Mi, et al. (1999). "Deletion of the loop region of Bcl-2 completely blocks paclitaxel-induced apoptosis." Proc Natl Acad Sci U S A 96(7): 3775-80.

Srivastava, R. K., S. J. Sollott, et al. (1999). "Bcl-2 and Bcl-X(L) block thapsigargin-induced nitric oxide generation, c-Jun NH(2)-terminal kinase activity, and apoptosis." Mol Cell Biol 19(8): 5659-74.

Strasser A, Harris AW, Cory S. (1993). "Eμ-mu-bcl-2 transgene facilitates spontaneous transformation of early pre-B and immunoglobulin-secreting cells but not T cells." Oncogene. Jan;8(1):1-9.

Strasser, A., L. O'Connor, et al. (1996). "Lessons from bcl-2 transgenic mice for immunology, cancer biology and cell death research." Behring Inst Mitt(97): 101-17.

Suzuki, M., R. J. Youle, et al. (2000). "Structure of Bax: coregulation of dimer formation and intracellular localization." Cell 103(4): 645-5.

Takacs-Vellai K, Vellai T, Puoti A, Passannante M, Wicky C, Streit A, Kovacs AL, Müller F. (2005). "Inactivation of the autophagy gene bec-1 triggers apoptotic cell death in C. elegans" Curr Biol. Aug 23;15(16):1513-7.

Takacs-Vellai, K., A. Bayci, et al. (2006). "Autophagy in neuronal cell loss: a road to death." Bioessays 28(11): 1126-31.

Takacs-Vellai, K., T. Vellai, et al. (2005). "Inactivation of the autophagy gene bec-1 triggers apoptotic cell death in C. elegans." Curr Biol 15(16): 1513-7.

Tamura, A. and K. Yui (1995). "Age-dependent reduction of Bcl-2 expression in peripheral T cells of lpr and gld mutant mice." J Immunol 155(1): 499-507.

Tamura, Y., S. Simizu, et al. (2004). "The phosphorylation status and anti-apoptotic activity of Bcl-2 are regulated by ERK and protein phosphatase 2A on the mitochondria." FEBS Lett 569(1-3): 249-55.

Tang, H. L., H. L. Lung, et al. (2008). "Vimentin supports mitochondrial morphology and organization." Biochem J 410(1): 141-6.

Tieu Q, Nunnari J. (2000). "Mdv1p is a WD repeat protein that interacts with the dynamin-related GTPase, Dnm1p, to trigger mitochondrial division." J Cell Biol. Oct 16;151(2):353-66.

Tondera D, Grandemange S, Jourdain A, Karbowski M, Mattenberger Y, Herzig S, Da Cruz S, Clerc P, Raschke I, Merkwirth C, Ehses S, Krause F, Chan DC, Alexander C, Bauer C, Youle R, Langer T, Martinou JC. (2009). "SLP-2 is required for stress-induced mitochondrial hyperfusion." EMBO J. Jun 3;28(11):1589-600.

Tooze, S. A. and T. Yoshimori (2010). "The origin of the autophagosomal membrane." Nat Cell Biol 12(9): 831-5.

Trinkle-Mulcahy L, Boulon S, Lam YW, Urcia R, Boisvert FM, Vandermoere F, Morrice NA, Swift S, Rothbauer U, Leonhardt H, Lamond A. (2008). "Identifying specific protein interaction partners using quantitative mass spectrometry and bead proteomes." J Cell Biol. Oct 20;183(2):223-39.

Tsujimoto Frank G. Haluska, Sheldon Finver, Yoshihide Tsujimoto & Carlo M. Croce (1986). "The t(8; 14) chromosomal translocation occurring in B-cell malignancies results from mistakes in V−D−J joining." Nature 324, 158 – 161.

Tsujimoto, Y. and S. Shimizu (2007). "Role of the mitochondrial membrane permeability transition in cell death." Apoptosis 12(5): 835-40.

Valentijn, A. J., J. P. Upton, et al. (2008). "Bax targeting to mitochondria occurs via both tail anchor-dependent and -independent mechanisms." Cell Death Differ 15(8): 1243-54.

Van Cruchten, S. and W. Van Den Broeck (2002). "Morphological and biochemical aspects of apoptosis, oncosis and necrosis." Anat Histol Embryol 31(4): 214-23.

Van der Bliek AM. (2009). " Fussy mitochondria fuse in response to stress." The EMBO Journal (2009) 28, 1533–1534.

Van Venetië R, Verkleij AJ. (1982). "Possible role of non-bilayer lipids in the structure of mitochondria. A freeze-fracture electron microscopy study." Biochim Biophys Acta. Nov 22;692(3):397-405.

VanBrocklin MW, Verhaegen M, Soengas MS, Holmen SL. (2009). "Mitogen-activated protein kinase inhibition induces translocation of Bmf to promote apoptosis in melanoma." Cancer Res. Mar 1;69(5):1985-94. Epub 2009 Feb 24.

VanBrocklin, M. W., M. Verhaegen, et al. (2009). "Mitogen-activated protein kinase inhibition induces translocation of Bmf to promote apoptosis in melanoma." Cancer Res 69(5): 1985-94.

Varadi A, Johnson-Cadwell LI, Cirulli V, Yoon Y, Allan VJ, Rutter GA. (2004). "Cytoplasmic dynein regulates the subcellular distribution of mitochondria by controlling the recruitment of the fission factor dynamin-related protein-1." J Cell Sci. Sep 1;117(Pt 19):4389-400.

Vaux David L. (1998). "Immunopathology of apoptosis - introduction and overview." Springer Semin Immunopathol (1998) 19 : 271-278.

Vaux, D. L. and J. Silke (2005). "IAPs, RINGs and ubiquitylation." Nat Rev Mol Cell Biol 6(4): 287-97.

Vaux, D. L. and J. Silke (2005). "IAPs--the ubiquitin connection." Cell Death Differ 12(9): 1205-7.

Vaux, D.L., Cory, S. and Adams, J.M., (1988). 'Bcl-2 gene promotes haemopoietic cell survival and cooperates with c-myc to immortalize pre-B cells'. *Nature*, 335 (6189):440-442.

Veis DJ, Sorenson CM, Shutter JR, Korsmeyer SJ. (1993). "Bcl-2-deficient mice demonstrate fulminant lymphoid apoptosis, polycystic kidneys, and hypopigmented hair." Cell. Oct 22;75(2):229-40.

Venable ME, Lee JY, Smyth MJ, Bielawska A, Obeid LM. (1995). "Role of ceramide in cellular senescence." J Biol Chem. Dec 22;270(51):30701-8.

Villunger, A., C. Scott, et al. (2003). "Essential role for the BH3-only protein Bim but redundant roles for Bax, Bcl-2, and Bcl-w in the control of granulocyte survival." Blood 101(6): 2393-400.

Villunger, A., E. M. Michalak, et al. (2003). "p53- and drug-induced apoptotic responses mediated by BH3-only proteins puma and noxa." Science 302(5647): 1036-8.

Vyssokikh, M. Y. and D. Brdiczka (2003). "The function of complexes between the outer mitochondrial membrane pore (VDAC) and the adenine nucleotide translocase in regulation of energy metabolism and apoptosis." Acta Biochim Pol 50(2): 389-404.

Vyssokikh, M. Y., L. Zorova, et al. (2002). "Bax releases cytochrome c preferentially from a complex between porin and adenine nucleotide translocator. Hexokinase activity suppresses this effect." Mol Biol Rep 29(1-2): 93-6.

Vyssokikh, M., L. Zorova, et al. (2004). "The intra-mitochondrial cytochrome c distribution varies correlated to the formation of a complex between VDAC and the adenine nucleotide translocase: this affects Bax-dependent cytochrome c release." Biochim Biophys Acta 1644(1): 27-36.

Walensky, L. D., K. Pitter, et al. (2006). "A stapled BID BH3 helix directly binds and activates BAX." Mol Cell 24(2): 199-210.

Wang Q, Gao F, May WS, Zhang Y, Flagg T, Deng X. (2008). "Bcl2 negatively regulates DNA double-strand-break repair through a nonhomologous end-joining pathway." Mol Cell. 29;29(4):488-98.

Wang SW, Denny TA, Steinbrecher UP, Duronio V. (2005). "Phosphorylation of Bad is not essential for PKB-mediated survival signaling in hemopoietic cells." Apoptosis. Mar;10(2):341-8.

Wang X, Schwarz TL (2009). "The mechanism of Ca2?-dependent regulation of kinesin-mediated mitochondrial motility." Cell 136:163–174.

Wang X. Olberding KE. White C. Li C. (2011). "Bcl-2 proteins regulate ER membrane permeability to luminal proteins during ER stress-induced apoptosis."
Cell Death and Differentiation 18, 38–47

Wang YF, Jiang CC, Kiejda KA, Gillespie S, Zhang XD, Hersey P. (2007). "Apoptosis induction in human melanoma cells by inhibition of MEK is caspase-independent and mediated by the Bcl-2 family members PUMA, Bim, and Mcl-1." Clin Cancer Res. Aug 15;13(16):4934-42.

Wang, J. M., J. R. Chao, et al. (1999). "The antiapoptotic gene mcl-1 is up-regulated by the phosphatidylinositol 3-kinase/Akt signaling pathway through a transcription factor complex containing CREB." Mol Cell Biol 19(9): 6195-206.

Wang, K., X. M. Yin, et al. (1996). "BID: a novel BH3 domain-only death agonist." Genes Dev 10(22): 2859-69.

Wang, T. H. and H. S. Wang (1996). "p53, apoptosis and human cancers." J Formos Med Assoc 95(7): 509-22.

Wasiak S, Zunino R, McBride HM. (2007). "Bax/Bak promote sumoylation of DRP1 and its stable association with mitochondria during apoptotic cell death." J Cell Biol. May 7;177(3):439-50.

Wei, M. C., T. Lindsten, et al. (2000). "tBID, a membrane-targeted death ligand, oligomerizes BAK to release cytochrome c." Genes Dev 14(16): 2060-71.

Wei, M. C., W. X. Zong, et al. (2001). "Proapoptotic BAX and BAK: a requisite gateway to mitochondrial dysfunction and death." Science 292(5517): 727-30.

Welch, C., M. K. Santra, et al. (2009). "Identification of a protein, G0S2, that lacks Bcl-2 homology domains and interacts with and antagonizes Bcl-2." Cancer Res 69(17): 6782-9.

White CD, Brown MD, Sacks DB. (2009)."IQGAPs in cancer: a family of scaffold proteins underlying tumorigenesis." FEBS Lett. Jun 18;583(12):1817-24.

White CD, Khurana H, Gnatenko DV, Li Z, Odze RD, Sacks DB, Schmidt VA. (2010). "IQGAP1 and IQGAP2 are Reciprocally Altered in Hepatocellular Carcinoma." BMC Gastroenterol. Oct 26;10:125.

Wiens, M., A. Krasko, et al. (2000). "Molecular evolution of apoptotic pathways: cloning of key domains from sponges (Bcl-2 homology domains and death domains) and their phylogenetic relationships." J Mol Evol 50(6): 520-31.

Willis SN, Chen L, Dewson G, Wei A, Naik E, Fletcher JI, Adams JM, Huang DC. (2005). "Proapoptotic Bak is sequestered by Mcl-1 and Bcl-xL, but not Bcl-2, until displaced by BH3-only proteins." Genes Dev. Jun 1;19(11):1294-305.

Willis, S. N. and J. M. Adams (2005). "Life in the balance: how BH3-only proteins induce apoptosis." Curr Opin Cell Biol 17(6): 617-25.

Willis, S. N., J. I. Fletcher, et al. (2007). "Apoptosis initiated when BH3 ligands engage multiple Bcl-2 homologs, not Bax or Bak." Science 315(5813): 856-9.

Willis, S. N., L. Chen, et al. (2005). "Proapoptotic Bak is sequestered by Mcl-1 and Bcl-xL, but not Bcl-2, until displaced by BH3-only proteins." Genes Dev 19(11): 1294-305.

Yamamoto, K., H. Ichijo, et al. (1999). "BCL-2 is phosphorylated and inactivated by an ASK1/Jun N-terminal protein kinase pathway normally activated at G(2)/M." Mol Cell Biol 19(12): 8469-78.

Yamashiro S. et al., (2003). "Localization of Two IQGAPs in Cultured Cells and Early Embryos of Xenopus laevis." Cell Motility and the Cytoskeleton 55:36–50.

Yamashita, T., Wada, R., Sasaki, T., Deng, C., Bierfreund, U., Sandhoff, K., and Proia, R. L. A vital role for glycosphingolipid synthesis during development and differentiation. Proc. Natl. Acad. Sci. USA, *96:* 9142–9147, 1999.

Yang Z, Klionsky DJ. (2010). "Mammalian autophagy: core molecular machinery and signaling regulation." Curr Opin Cell Biol. Apr;22(2):124-31.

Yang, E., J. Zha, et al. (1995). "Bad, a heterodimeric partner for Bcl-XL and Bcl-2, displaces Bax and promotes cell death." Cell 80(2): 285-91.

Yano T, Jaffe ES, Longo DL, Raffeld M. (1992). "MYC rearrangements in histologically progressed follicular lymphomas." Blood. Aug 1;80(3):758-67.

Yin, X. M., Z. N. Oltvai, et al. (1994). "BH1 and BH2 domains of Bcl-2 are required for inhibition of apoptosis and heterodimerization with Bax." Nature 369(6478): 321-3.

YONG-YU LIU, TIE-YAN HAN, ARMANDO E. GIULIANO and MYLES C. CABOT (2001). "Ceramide glycosylation potentiates cellular multidrug resistance." The FASEB Journal. 15:719-730.

Youle RJ, Strasser A. (2008). " The BCL-2 protein family: opposing activities that mediate cell death." Nat Rev Mol Cell Biol. Jan;9(1):47-59.

Youle, R. J. and A. Strasser (2008). "The BCL-2 protein family: opposing activities that mediate cell death." Nat Rev Mol Cell Biol 9(1): 47-59.

Yu Yong-Qiang, Liu LC. Wang FC. Liang Y. Cha DQ. Jing-Jing Zhang JJ. Shen YJ. Wang HP. Fang S. and Shen YX. (2010). "Induction profile of MANF/ARMET by cerebral ischemia and its implication for neuron protection." Journal of Cerebral Blood Flow & Metabolism 30, 79–91.

Zalk, R., A. Israelson, et al. (2005). "Oligomeric states of the voltage-dependent anion channel and cytochrome c release from mitochondria." Biochem J 386(Pt 1): 73-83.

Zha J, Harada H, Yang E, Jockel J, Korsmeyer SJ. (1996). "Serine phosphorylation of death agonist BAD in response to survival factor results in binding to 14-3-3 not BCL-X(L)." Cell. Nov 15;87(4):619-28.

Zha, J., H. Harada, et al. (1996). "Serine phosphorylation of death agonist BAD in response to survival factor results in binding to 14-3-3 not BCL-X(L)." Cell 87(4): 619-28.

Zhang Y, Yao B, Delikat S, Bayoumy S, Lin XH, Basu S, McGinley M, Chan-Hui PY, Lichenstein H, Kolesnick R. (1997). "Kinase suppressor of Ras is ceramide-activated protein kinase." Cell. Apr 4;89(1):63-72.

Zhang, J., N. Alter, et al. (1996). "Bcl-2 interrupts the ceramide-mediated pathway of cell death." Proc Natl Acad Sci U S A 93(11): 5325-8.

Zhang, Y., M. Adachi, et al. (2006). "Bmf contributes to histone deacetylase inhibitor-mediated enhancing effects on apoptosis after ionizing radiation." Apoptosis 11(8): 1349-57.

Zhang, Z., S. M. Lapolla, et al. (2004). "Bcl-2 homodimerization involves two distinct binding surfaces, a topographic arrangement that provides an effective mechanism for Bcl-2 to capture activated Bax." J Biol Chem 279(42): 43920-8.

Zhou H, Summers SA, Birnbaum MJ, Pittman RN. (1998). "Inhibition of Akt kinase by cell-permeable ceramide and its implications for ceramide-induced apoptosis." J Biol Chem. Jun 26;273(26):16568-75.

6 Appendix

6.1 Mitochondrial morphology of MEFs deficient in IQGAP2

Unfortunately, wild type IQGAP2 MEFs died by infection before we were able to seed them on cover slips. As described in chapter 3.6.5.1 and shown in figure 3-32 A-B Bcl-2 $^{-/-}$ MEFs originating from C75BL/6 mice display a similar mitochondrial morphology corresponding to their wild type form. IQGAP2 $^{-/-}$ MEFs and their parental wild type derived from 129J mice could not be compared with the Bcl-2 $^{-/-}$ MEFs because of the different genotype. So we are not able to compare and discuss the mitochondrial phenotype of IQGAP $^{-/-}$ and Bcl-2 $^{-/-}$ MEFs. We are only able to compare and describe those mitochondria from healthy IQGAP2 $^{-/-}$ MEFs and etoposide treated IQGAP2 $^{-/-}$ mitochondria. Both, healthy and stressed mitochondria show a similar punctated and disorganized clumped structure. However, because of the missing 129 J wild type phenotype we do not know if this mitochondrial morphology is due to the deficiency in IQGAP2 (Fig. 6-1 A-B).

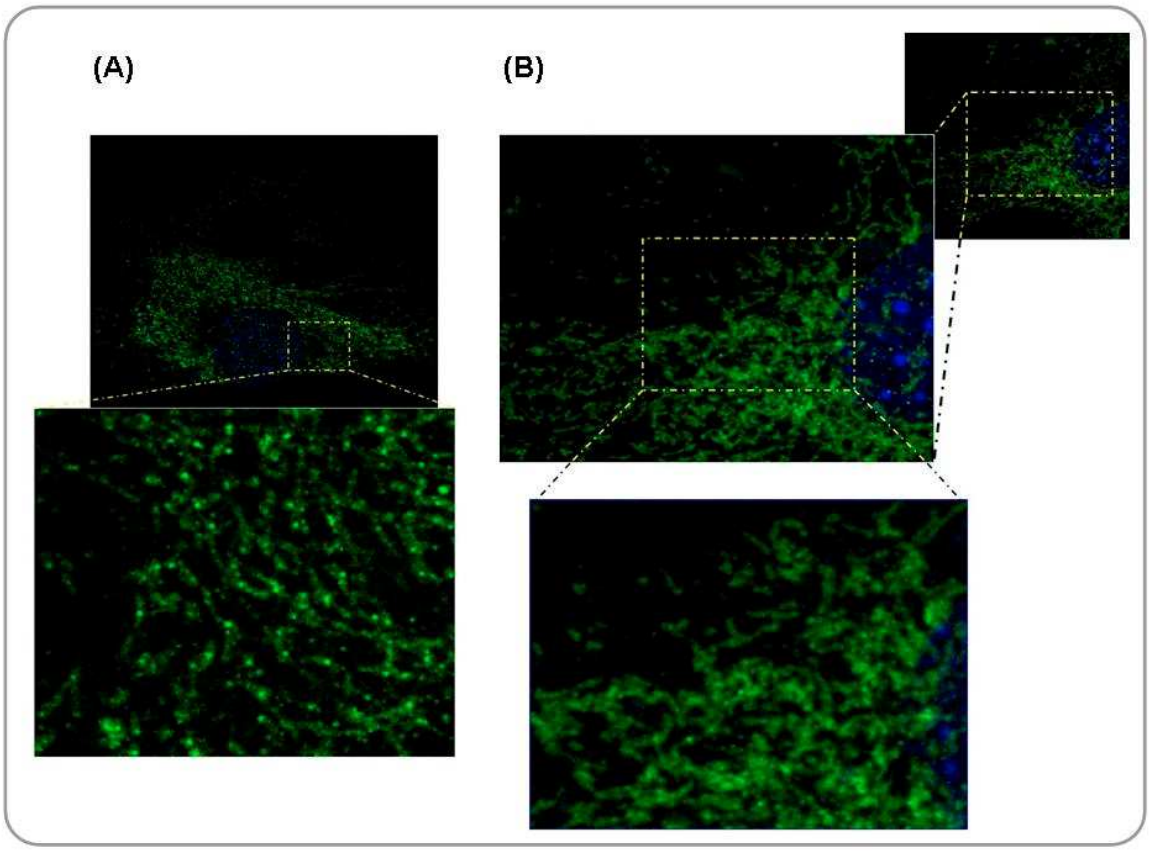

Figure 6-1: Morphology of mitochondria of IQGAP2 $^{-/-}$ MEFs. (A) Non-treated IQGAP2 $^{-/-}$ and **(B)** etoposide (100 µM, 9 hrs) treated IQGAP2 $^{-/-}$ MEFs. Fixed by 4% formaldehyde and stained with anti-cytochrome c antibodies and secondary anti-mouse Alexa 488. Nuclei are stained with Hoechst 33342. Immunofluorescence analysis was done by confocal laser scanning microscopy, Leica TCS SP2 AOBS, Magnification: overviews: 630 x zoom: 1260-1890 x. Note a while non-treated mitochondria show a fragile punctated pattern, apoptotic IQGAP2 $^{-/-}$ MEFs show a largely dotted and clumped structure.

6.2 Mass Spectrometry

Table 6-1: UGCGT1 a glucosyl ceramide synthase: Amino acid sequence of UGCGT1 and identified peptide sequences by MS/MS analysis. Peptides found by ABT-737 release and two whole set analysis assays. UGCGT1 (1551 aa). Peptide sequences: blue, red and violet colored peptides found only once; green peptides: found three times independently and black peptides: found two times independently in all three mass spectrometry analysis.

MCSRGDANTADAAAARRVTGLRYNMRLLIALALPCLFSLAEANSKAITTSLTTKWFSAPLLLEASEFLAED
SQEKFWSFVEATQNIGSSDHHDTDHSYYDAVLEAAF**RFLSPLQQNLLKF**CLSLRSYSASIQAFQQIAVD
EPPPEGCKSFLSVHGKQTCDLDTLESLLLTAADRPKPLLFKGDHRYPSSNPESPVVILYSEIGHEEFSNIH
HQLISKSNEGKINYVFRHYISNPSKEPVYLSGYGVELAIKSTEYKAKDDTQVKGTEVNATVIGESDPIDEV
QGFLFGKL**RELYPALEGQLKE**FRKHLVESTNEMAPLKVWQLQDLSFQTAARILAASGALSLVVMKDISQ
NFPTKARAIT**KTAVSAQLRA**EVEENQKYFKGTIGLQPGDSALFINGLHIDLDTQDIFSLFDTLRNEARVME
GLHRLGIEGLSLHNIL**KLNIQPSETDYAVDIRS**PAISWVNNLEVDSRYNSWPSSLQELLRPTFPGVIRQIR
KNLHNMVFIIDPVHETTAELISIAEMFLSNHIPLRIGFIFVVNDSEDVDGMQDAGVAVLRAYNYVAQEVDG
YHAFQTLTQIYNKVRTGETVKVEHVVSVLEKKYPYVEVNSILGIDSAYDQNRKEARGYYEQTGVGPLPV
VLFNGMPFEKEQLDPDELETITMH**KILETTTFFQRA**VYLGELSHDQDVVEYIMNQPNVVPRINSRILTAKR
EYLDLTASNNFYVDDFARFSALDSRGKTAAIANSMNYLTKKGMSSKEIYDDSFIRPVTFWIVGDFDSPSG
RQLLYDAIKHQKTSNNVRISMINNPSQEISDSSTPIF**RAIWAALQTQASSSAKN**FITKMAKEETAEALAAG
VDIAEFSVGGMDVSLFKEVFESSRMDFILSHALYCRDVLKLKKGQRVVISNGRIIGPLEDNELFNQDDFHL
LENIILKTSGQKIKSHIQQLRVEEDVASDLVMKVDALLSAQPKGEA**RIEYQFFEDKH**SAIKLKPKEGETYY
DVVAVVDPVTREAQRLAPLLLVLTQLINMNLRVFMNCQSKLSDMPLKSFYRYVLEPEISFTADSSFAKGPI
AKFLDMPQSPLFTLNLNTPESWMVQSVRTPYDLDNIYLEEVDSIVAAEYELEYLLLEGHCYDITTGQPPR
GLQFTLGTSANPTIVDTIVMANLGYFQL**KANPGAWILRL**RKGRSDDIYRIYSHDGTDSPPDANDVVVILN
NFKSKIIKVKVQKKADMANEDLLSDGTNENESGFWDSFKWGFSGQKAEEVKQDKDDIINIFSVASGHLY
ERFLRIMMLSVLKNTKTPVKFWFLKNYLSPTFKEFIPYMAKKYNFQYELVQYKWPRWLHQQTEKQRIIW
GYKILFLDVLFPLVVD**KFLFVDADQIVRT**DLKELRDFNLDGAPYGYTPFCDSRREMDGYRFWKSGYWAS
HLAGRKYHISALYVVDLKKFRKIAAGDRLRGQYQGLSQDPNSLSNLDQDLPNNMIHQVPIKSLPQEWLW
CETWCDDASKKRAKTIDLCNNPMTKEPKLEAAVRIVPEWQDYDQEI**KQLQTLFQEEKE**LGTLHTEETQE
GSQKHEEL

green: peptides consistently found in three independent MS samples (FDM+FDM+FDC-P1)
black: peptides consistently found in two independent MS samples (FDM+FDC-P1)
blue: peptides found in MS1 FDM
red: peptides found in MS2 FDM

Table 6-2: Amino acid sequence of IQGAP2 and seven identified peptide sequences by MS/MS from the ABT-737 assay. IQGAP-2 amino acid sequence (1575 aa). Note that found peptide sequences are distributed over the full sequence. Data were obtained by specific interaction with ABT-737.

MPHEELPSLQRPRYGSIVDDERLSAEEMDERRRQNIAYEYLCHLEEAKRWMEVCLVEELPP
TTELEEGLRNGVYLAKLAKFFAPKMVSEKKIYDVEQTRYKKSGLHFRHTDNTVQWLRAMEAI
GLPKIFYPETTDVYDRKNIPRMIYCIHALSLYLF**KLGIAPQIQDLLGKV**DFTEEEISNMRKELEK
YGIQMPAFSKIGGILANELSVDEAALHAAVIAINEAIEKGVAKQTIITLRNPNAVLTCVDDSLSQ
EYQKELWEAKKKKEESAKLKNSCISEEERDAYEELLTQAEIQSNISTVNRMAAVDHINAVLQE
GDPENTLLALKKPEAQLPAVYPFAAVMYQNELFNLQKQNTSNYLAHEELLIAVEMLSAVALLN
QALESSDLVAVQNQLRSPTIGFNNLDEAHVD**RYADALLSVKQ**EALSQGQDTLSWNEIQNCI
DMINNQIQEENDRMVVLGYINEAIDAGNPL**KTLDTLLLPTANIRD**VDPDCAQHYQDVLFYTKS
QKLGDPKNVSKVLWLDEIQQAINEANVDENRAKQWVTLVVDVNECLDRKQSDHILTALKSSP
SNIHNILPECANKYYDTLVKAKESKTDNESSEGSWVTLNVQEKYNYYYNTDSKEGSWVPPE
LCLSKESWLTGEEIEDIVEEVTSDYIREKLWSASEDLLV**RFEATTLGPALRE**EFEARKAFLYE
QTESVVKIQAFWKGFKQRQEYLHRQQVFAGNVDSVVKIQSWFRMVTARKSYLSRLRYFED
HKNEIVKIQSLLRASKARDDY**KALVGSENPPLTVIRK**FVYLLDQSDLDFQEELEVARLREEVV
TKIRANQQLEKDLNLMDIKIGLLVKNRITLEDVISHRKKLNKKKGGEIEILNNTDNKGIKSLSKER
RKTLETYQQLFYLLQTKPSYLAKLIFQMPQNKSTKFMDTVIFTLYNYASNQREEYLLLKLFKTA
LEEEIKSKVDQVQDIVTGNPTVIKMVVSFNRGARGQNTLRQLLAPVVKEIIED**KALVINTNPVE**
VYKAWVNQLETQTGEASKLPYDVTTEQALTYPEVKNKLEASIENLRKVTDKVLGSIISSLDLL
PYGLRYIAKVLKNSIREKFPDATEEELLKIVGNLLYYRYMNPAIVAPDGFDIIDMTAGGQINSN
QRRNLGSVAKVLQHAASNKLFEGENEHLSSMNNYLSETYQEFRKYFQEACDVPEPEEKFN
MDKYTDLVTVSKPVIYISIEEIINTHLLLLEHQDAIATEKSDLLNELLESLGEVPTVESFLGEGAV
DPNDPNKENTLNQLSKTEISLSLTSKYDVKDGEAVDGRSLMIKTKKLIIDVTRNQPGSTLTEIL
ETPATGQQELEHAKDMESRAVVDSRTPEEG**KQSQAVIEDARL**PLEQKKRKIQRNLRTLEQT
GHVSSKNKYQDILNEIAKDIRNQRIHRKLRKAELSKLQQTLNALNKKAAFYEDQINYYDTYIKT
CVDNLKRKNSRRSIKLDGKAEPKGTKRVKPVRYTAAKLHDKGVLLGIDDLQTNQFKNVMFDII
ATEDMGIFDVRSKFLGVEMEKVQLNIQDLLQMQYEGVAVMKMFDKVKVNVNLLIYLLNKKFY
GK

Table 6-3: Gene tree of IQGAP2.

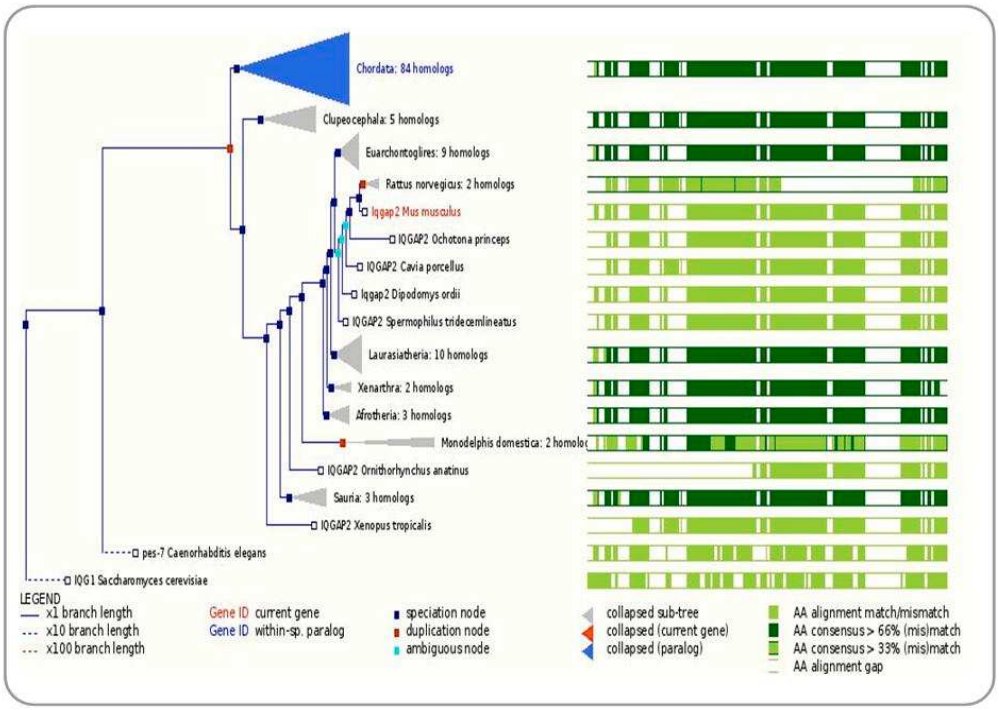

Table 6-4: Potential Bcl-2 binding proteins evaluated from Mascot data of the ABT-737 assay: Data obtained from mass spectrometric analysis 1. Proteins were evaluated by filtering the positive fractions (ABT-737 treated samples of Bcl-2 $^{+/+}$ FDM and Bcl-2 $^{-/-}$ FDM) against the control fractions (DMSO treated and Bcl-2$^{-/-}$ FDM samples). Scores (Identity): Complete amount of found peptides against peptides with significant scores; more than two peptides with score values above identity are shown in the brackets (bold) against the full set of peptides. Only score values above identity of each peptide are shown.

Mass spectrometry 1				
Mouse Gene	**Mass (kDa)**	**Identity Scores (>2)**	**Protein/Description**	**Gi/ Reference**
Dock10	249.4	**3(3)** **43, 72, 69**	Dedicator of cytokinesis 10	gi|190194393
IQGAP2	180.4 166.3	**8** (**7**) **56, 61, 49, 55, 42, 60, 55**	**IQ motif containing GTPase activating protein 2**	gi|74218637
UGCGT1 GCS	176.3	**7** (**4**) **44, 45, 56, 49**,	**UDP-glucose ceramide glucosyltransferase-like 1**	gi|45387933
LRPPRC mLRP130	147.3	**6 (4**) **45, 44, 50, 82**	**Leucine rich protein mLRP130]**	gi|21165513
VARS1	140.2	**5** (**4**) **64, 95, 66, 42**	Valyl-tRNA synthetase	gi|4590328
INPPL1 SHIP2	133.3	**3 (2)** **50, 52**	**SH2-containing inositol-phosphatase**	gi|1209068

Gene	**Mass (kDa)**	**Identity Scores (>2))**	**Protein/Description**	**Gi/ Reference**
ESYT1	121.4	**5 (4)** **47, 51, 104, 73**	**Membrane bound C2 domain containing protein**	gi|33859650
ACLY	119.6	**4(3)** **60, 106, 76**	**ATP citrate lyase**	gi|29293809
NRP-1	102.9	**2(2)** **48, 70**	Neuropilin 1	gi|6679134
KPNB1	97.1	**4 (3)** **52, 42, 89**	**Importin subunit beta-1**	gi|30931411
FNRB ITGB1	88.1	**4(3)** **66, 51, 43**	Fn receptor beta prechain	gi|762977
PTPRE	80.6	**8 (5)** **71, 79, 46, 80, 71,**	**Protein tyrosine phosphatase epsilon**	gi|1199933
LCP-2 (SLP-76)	70.1	**3(2)** **56**, **43**	**Lymphocyte cytosolic protein (SH2 domain containing leukocyte protein)**	gi|31543113
PLD4	56.1	**2(2)**	**Phospholipase D family, member 4**	gi|30725764

		43, 41		
Gene	**Mass (kDa)**	**Identity Scores (>2))**	**Protein/Description**	**Gi/ Reference**
VIM	53.6	**4(2)** **55, 60**	**Vimentin**	gi|55408
CAP1	53.0	**3 (3)** **48, 48, 50**	CAP, adenylate cyclase-associated protein 1	gi|148698451
GDI2	52.9	**4(2)** **71, 42**	Guanosine diphosphate (GDP) dissociation inhibitor 2, isoform CRA_b	gi|148700276
CDC10 SEPT7	50.6	**2(2)** **36, 57**	Cell division cycle 10 homolog	gi|28173550
MRPS30	49.9	**2(2)** **43, 66**	Mrps30 protein	gi|20988722
CCM2	49.8	2(2) **43, 59**	Cerebral cavernous malformation 2 homolog	gi|22122481
TUBA1C	49.8	**3(2)** **50, 81**	Tubulin,alpha 1C	gi|6678469
SEPT11	48.9	**3(2)** **37, 58**	Sept11 protein	gi|38328220

Gene	Mass (kDa)	Identity Scores (>2))	Protein/Description	Gi/ Reference
AP1M1	48.5	**7 (4)** **46, 50, 55,** , **50**	**Adaptor-related protein complex** AP-1, mu subunit 1	gi|6671557
FLOT1	47.4	**3(2)** **43, 87**	Flotillin 1	gi|6679809
***PSMC4**	47.3	**2(2)** **45, 39**	**Proteasome** (prosome, macropain) **26S subunit, ATPase, 4**	gi|62201535
SNX5	46.7	**5 (2)** **76**, **48**	Sorting nexin 5	gi|18034769
ACTR2	44.6	**9 (2)** **44, 63**	Actr2 protein	gi|29126784
TSG101	44.0	**2(2)** **47, 54**	**Tumor susceptibility gene 101 protein**	gi|11230780
ND	40.6	**3(2)** **52**, **63**	**Calcium binding protein 39, isoform CRA_b**	gi|148708308
ALDOC	39.3	**3(3)** **64, (71), 108**	Zebrin II; Aldolase C fructose- Bis phosphate	gi|619373

Gene	Mass (kDa)	Identity Scores (>2)	Protein/Description	Gi/ Reference
HNRNPDa	38.3	**3(3)** **43, 48, 84**	Heterogeneous nuclear ribonucleoprotein D isoform a	gi|116256512
GNAI2	38.1	**3(3)** **64, 49 (46)**	G protein Gi2 alpha	gi|9489054
***mCBP**	36.8	**3(3)** **55, 53, 82**	Nuclear poly(C)-binding protein, splice variant E	gi|1360003
***PSMD7**	36.5	**2(2)** **43, 75**	**Proteasome** (prosome, macropain **26S subunit, non-ATPase, 7**	gi|6754724
HNRNPDb	36.1	**2(2)** **97, 48**	Heterogeneous nuclear ribonucleoprotein D isoform b	gi|116256518
MDH2	35.589 35.574	**4(3)** **55, 46, 105**	Malate dehydrogenase Malate dehydrogenase 2, NAD (mitochondrial)	gi|1200100 gi|31982186
		3(3) 36kD **55, 53, 82**	mCBP	gi|495128

***mCBP**	34.994	**2(2) 18kD 54, 48**		
Gene	**Mass (kDa)**	**Identity Scores (>2)**	**Protein/Description**	**Gi/ Reference**
STX4	34.144	**2(2) 72, 52**	Syntaxin 4A (placental)	gi|6678177
HNRPAB	33.795	**2(2) 41, 48**	Hnrpab protein	gi|27695334
MLEC	33.614 32.322 32.264	**4(3) 57**, (**46**), **98**	MKIAA0152 protein Malectin Unnamed protein product	gi|37359796 gi|188497650 gi|26327381
CDK5	**33.267**	**2(2) 49, 57**	Cyclin-dependent kinase 5	gi|6680908
RSU1	31.442	**2(2) 51, 42**	**Ras suppressor protein 1**	gi|31982028
STX7	29.718	**4(3)**	Syntaxin 7	gi|31560462

		77, 44, 77		
Gene	**Mass (kDa)**	**Identity Scores (>2)**	**Protein/Description**	**Gi/ Reference**
CLIC1		**3(3) 34kD 41, 46. 70**	**Chloride intracellular channel 1**	gi|15617203
CLIC1	26.996	**4(3) 26kD 43, 92, 73**	**"Independent of each other found" Chloride intracellular channel 1**	gi|15617203
HMG	24.892	**2(2) 73, 49**	**High mobility group protein HMG**	gi|620098
ND	24.663	**2(2) 53, 77**	**Component C5 of proteasome**	gi|1165123
RGS19	24662	**3(2) 57, 68**	Regulator of G-protein signaling 19	gi|13385944
ND	24.379	**2(2) 24kD 62, 81**	Hypothetical protein LOC70564	gi|27229101
ND	24.379	**3(2) 20kD 57, 65**	Hypothetical protein LOC70564	gi|27229101
PILRP		**2(2)**	Cell surface receptor FDFACT	gi|11932937

	23.962	**44, 43**		
Gene	**Mass (kDa)**	**Identity Scores (>2)**	**Protein/Description**	**Gi/ Reference**
RAB4B	23.710	**6(6)** **51, 66, 58, 82, 46, (78)**	**Ras-related GTP-binding protein 4b**	gi|57524538
RANBP1	23.582	**2(2)** **43, 43**	**RAN / TC-4 binding protein** **RAN binding protein 1**	gi|431422 gi|153792001
SM22 **TAGLN**	23.582	**6(3)** **45,61, 58**	Transgelin	gi|5007032
ATP5A1	23.349	**3(2)** **52, 65**	ATP synthase, H+ transporting, mitochondrial F1 complex,	gi|20070412
ND	23.032	**3(3)** **60, 77, 60**	**Proteasome subunit MC13**	gi|673450
TCL10	22656	**5(3)** **53, 44, (46)**	**TC10-like Rho GTPase**	gi|9968513
ND	22.319 22.358	**8(4)** **66, 58, 66, (62)**	**Ras-related protein ORAB-1** **RAB1, member RAS oncogene**	gi|131785 gi|56205120

			family	
Gene	**Mass (kDa)**	**Identity Scores (>2)**	**Protein/Description**	**Gi/ Reference**
GAIP/ RGS19	22.240	**3(2)** **57, 68**	GAIP/RGS19 short isoform	gi|27461941
RAB22A	21.788	**3(2)** **43, 42, 35**	**RAB22A, member RAS oncogene family**	gi|148747177
CIB1	21.750	5(2) 57, 57	**Calcium and integrin binding 1**	gi|6755154
MRPL12	21.695	4(4) 46,57,47,63	**Mitochondrial ribosomal protein L12**	gi|22164792
ND	21.532	**5(4)** **69,43,70, 89**	unnamed protein product	gi|26341846
REEP5	21.116 21.476	**4(2)** **47, 46**	**Receptor accessory protein 5** **Receptor expression enhancing P5**	gi|15341776 gi|50234914
ND	21.323 21.450	**8(4)** **59, 71, 66, 58**	**Ras-like protein** **unnamed protein product**	gi|190875 gi|12842616
		6(4)	**Histone cluster 1, H1c**	

HIST1H1C	21.254	66, 60, 76, 49		gi|9845257
Gene	**Mass (kDa)**	**Identity Scores (>2)**	**Protein/Description**	**Gi/ Reference**
MRPS28	20.534	**2(2)** **76, 70**	**Mitochondrial ribosomal protein S28**	gi|31981288
PDAP1	20.523	**2(2)** **42, 41**	**PDGF associated protein** **Pdap1 protein**	gi|1136586 gi|77415381 gi|90652001
MRPL49	19.121	**2(2)** **64, 71**	**Mitochondrial ribosomal protein L49**	gi|13385752
MANF	19.000	**4(3)** **43, 69, 58**	**Armet protein Mesencephalic astrocyte-derived neurotrophic factor**	gi|28913725
SSR4	18.924	**3(2)** **62, 48**	Signal sequence receptor, delta	gi|6678145
GLIPR1	17.080	**3(2)** **103, 65**	**GLI pathogenesis-related**	gi|47059151
MYL3	16.920	**7(5)** **47, 60, 50, 63, 64**,	**Myosin light chain 3**	gi|188590
ND (fragment)	16.818	**2(2)**	Iintegrin alpha-6 chain, melanoma cell - mouse (fragment)	gi|110578

		70, 108		
Gene	**Mass (kDa)**	**Identity Scores (>2)**	**Protein/Description**	**Gi/ Reference**
ND **HNRPDL 46kDa**	16.521	**2(2)** **57, 48**	unnamed protein product (heterogeneous nuclear ribonucleoprotein D-like)	gi|12847801
ND	14.167	**5(4)** **55, 53, 79, 51**	TI-225	gi|1167510
HIST1 H2AA	14.048	**8(6)** **41, 70, 54, 75, (58), (60)**	**Histone cluster 1, H2aa**	gi| 28316756
ND	13.502	**3(3)** **41, 61, 66**	unnamed protein product	gi| 74207672

Table 6-5: Potential binding proteins of the whole set Bcl-2 IP assay found in FDM and FDC-P1. Data obtained from mass spectrometric analysis 2 (MS2). Proteins were evaluated by filtering the positive Bcl-2 IP fractions of Bcl-2 $^{+/+}$ FDM against the control IgG_1 IP of Bcl-2 $^{+/+}$ FDM fraction and Bcl-2 IP fraction of Bcl-2 $^{-/-}$ FDM. The Bcl-2 IP fraction of FDC-P1 was additional filtered against the controls. Significant scores: more than two peptides with score values above identity of each are shown in the brackets (bold) against the full set of peptides found. Only proteins with more than two peptides and score values above identity are shown.

Gene	Mass (kDa)	Identity Scores (>2)	Protein/Description	Gi/ Reference
UGCGL1 **UGGT1**	180.0 176.0	**"FDM"** **10 (8)** **52, 54, 53, 58, 44, 67, 103, 97** **"FDC-P1"** **3 (3)** **45, 61, 87**	**UDP-glucose ceramide glucosyltransferase-like** **Endoplasmatic reticulum multi-pass membrane protein** **Lipid metabolism; sphingolipid metabolism.**	**Gi |148682526**
	161.0	**FDM** **13 (7)** **39, 50, 47, 58, 73, 93, 41** **FDC-P1** **18 (10)** **47, 53, 51, 54, 51, 64, 86, 81, 52, 60**	**p162 protein,** eukaryotic translation initiation factor subunit 10 (theta)	**gi| 146219837**
ND	166.4	**FDM** **3 (3)**	EPRS protein	**gi| 66267550**

		43, 52, 116		
Gene	**Mass (kDa)**	**Identity Scores (>2)**	**Protein/Description**	**Gi/ Reference**
VCP	89.2	**FDM** **3(3)** **53, 51, 46**	**Valosin-containing protein** VCP Is a target of Akt signaling required for cell survival (activation of caspase activity)	**gi| 55217**
SEC23A	86.1	**FDCP1** **4 (3)** **39, 55, 76**	**SEC23A** Component of the COPII coat, that covers ER-derived vesicles involved in transport from the endoplasmic reticulum to the Golgi apparatus.	**gi|67906177**
DLAT	67.9	**FDM** 3**(2)** **22, 68, 51**	**Dihydrolipoamide S-acetyltransferase** This gene encodes component E2 of the multi-enzyme pyruvate dehydrogenase complex (PDC). PDC resides in the inner mitochondrial membrane and catalyzes the conversion of pyruvate to acetyl coenzyme A.	**gi| 2159464**
eIF3 p66	63.5	**FDM** **2(2)** **88, 62** **FDC-P1** **2(2)** **76, 58**	**eIF3, p66** Component of the eukaryotic translation initiation factor 3 (eIF-3) complex, which is required for several steps in the initiation of protein synthesis.	**gi| 2992164**

Gene	**Mass (kDa)**	**Identity Scores (>2)**	**Protein/Description**	**Gi/ Reference**
ND	60.5	**FDM** **4(2)** **78, 64** **FDC-P1** **5(5)** **78, 84, 54, 102, 49**	Chaperonin isoform 5	**gi| 114582376**
ND			**N**ot **D**etermined: gene not specified	

6.3 Abbreviations

mg	milligram	10^{-3} gram
µg	microgram	10^{-6} gram
ng	nanogram	10^{-9} gram
pg	picogram	10^{-12} gram
fg	femptogram	10^{-15} gram

A	A	Ampere
	Aa	Amino acid
	Ab	Antibody
	ADP	Adenosine diphosphate
	AIF	Apoptosis-inducing factor
	Akt	Protein kinase B
	Apaf-1	Apoptosis-protein-associated-factor 1
	APS	Ammonium peroxide sulfate
	ARK	Apaf-1 related killer
	Asp	Aspartic acid
	ATP	Adenosine diphosphate
B	Bad	Bcl-2 antagonist
	Bak	Bcl-2-associated antagonist/killer
	Bax	Bcl-2-associated protein x
	Bcl-2	B-cell lymphoma gene 2α
	Bcl-xL	B-cell lymphoma gene x (long form)
	BH	Bcl-2 homology
	Bid	BH-3 interacting death agonist
	Bim	Bcl-2 interacting mediator of cell death
	BIR	Baculoviral IAP repeat
	Bmf	Bcl-2 modifying factor
	Bok	Bcl-2-related ovarian killer
	bp	base pair
	BSA	Bovine serum albumin

C	℃	Degrees centrigrade
	C.	*Caenorhabditis*
	CAD	Caspase-activated DNase
	CARD	Caspase activation and recruitment domain
	cDNA	Copy deoxyribonucleic acid
	CED	*C.elegans* death genes
	CHAPS	3-[(3-cholamidopropyl)-dimethylammonio]-1-propane-sulphonate
	cIAP	cellular inhibitor of apoptosis protein
	CK1	Casein kinase1
	C-terminus	Carboxy terminus
	ctrl	control
D	*D.*	*Drosophila*
	Dark	*Drosophila* Apaf-1-related killer
	DcR	Decoy receptor
	DD	Death domain
	DED	Death effector domain
	Diablo	Direct IAP binding protein with low pI
	DIAP	*Drosophila* inhibitor of apoptosis
	DISC	Death-inducing signaling complex
	DKO	Double knockout
	DMEM	Dulbecco´s Modified Eagles Medium
	DMSO	Dimethylsulfoxid
	DNA	Deoxyribonucleid acid
	dNTP	Deoxyribonucleosid triphosphate
	Drice	*Drosophila* ICE
	Dronc	*Drosophila* Nedd2-like caspase
	DTT	Dithiothreitol
E	*E.*	*Escherichia*
	ECL	Enhanced chemiluminescence
	EDTA	Ethylendiaminetetraaceticacid
	e.g.	exempli gratia (for example)
	EGFP	Enhanced green fluorescent protein
	Egl-1	Egg-laying defective-1
	Endo G	Endonuclease G

	ER	Endoplasmatic reticulum
	EtBr	Ethidium bromide
	et al.	*et alii (and others)*
F	FACS	Fluorescence activated cell sorting
	FADD	Fas-associated death domain protein
	Fas	
	FasL	Fas Ligand
	FCS	Fetal calf serum
	Fig.	Figure
	FLIP	FLICE inhibiting protein
	FOXO3A	Forkhead transcription factor 3 A
	FSC	Forward scatter
G	g	gravitational constant
	GFP	Green fluorescent protein
	GSK-3β	Glycogen synthase kinase-3β
H	h	hora (hour)
	HEPES	N-2-Hydroxyethylpiperazine-N'-2-Ethanesulfonic Acid
	HRP	Horseradish peroxidase
	HtrA2	High temperature requirement A
I	IAP	Inhibitor of apoptosis protein
	ICAD	Inhibitor of caspase-activated DNAse
	ICE	Interleukin-1*ß*-converting enzyme
	i.e.	id est (that is)
	Ig	Immunoglobulin
	IL	Interleukin
	ILK	Integrin-linked kinase
	IP	Immunoprecipitation
J	JNK	c-Jun N-terminal kinase
K	kDa	kilodalton
	KO	Knockout
L	L	Ligand
	LB-medium	Luria-Bertani-medium
	LC-MS/MS	
	LMU	Luminescence units
M	M	Molar
	mA	milliampere
	MAPK	Mitogen-activated protein kinase

	Mcl-1	Myeloid cell leukemia sequence-1
	MEF	Mouse embryonic fibroblast
	MG-132	Carbobenzoxy-leucyl-leucyl-leucinal (Z-LLL-CHO)
	MIM	Mitochondrial inner membrane
	Min.	Minute
	mM	millimolar
	MMP	Mitochondrial membrane permeabilization
	MOM	Mitochondrial outer membrane
	MOMP	Mitochondrial outer membrane permeabilization
	mRNA	Messenger ribonucleic acid
N	Noxa	Latin word for “damage”
	NMR	Nuclear magnetic resonance
	NP-40	Nonidet P-40
	N-terminus	Amino terminus
O	Omi/HtrA2	Omi/High temperature requirement A2, mitochondrial serine protease, antagonist of IAPs
	OMM	Outer mitochondrial membrane
P	PAGE	Polyacrylamide gel electrophoresis
	PARP	Poly ADP-ribose polymerase
	PBS	Phosphate buffered saline
	PC	Phosphatidylcholin
	PCD	Programmed cell death
	PCR	Polymerase chain reaction
	PDB	Protein Data Base
	PE	Phosphatidylethanolamin
	PFA	Paraformaldehyde
	pH	potentia hydrogenii
	PI	Propidiumiodide
	PI-3	Phosphatidylinositol-3
	PMSF	Phenylmethansulfonylfluorid
	PMT	Photo mulitplier tube
	P/S	Penicillin and Streptomycin
	PS	Phosphatidylserine
	PVDF	Polyvinylidenfluorid
	POD	Peroxidase
	Puma	p53-upregulated modulator of apoptosis

R	Rcf	Relative centrifugal force
	RFU	Relative fluorescence units
	RIP	Receptor interacting protein
	RNA	Ribonucleic acid
	ROCK1	Rho-associated, coiled-coil containing protein kinase1
	ROS	Reactive oxygen species
	RPMI	Roswell Park Memoriel Institute (Moore et al., 1967)
	rpm	Rounds per minute
	RT	room temperature
S	SDS	Sodium dodecyl sulfate
	SDS-PAGE	Sodium dodecyl sulfate-Polyacrylamide gel electrophoresis
	shRNA	short hairpin RNA
	siRNA	short inhibitory RNA
	Smac	Second mitochondria-derived activator of caspase
	SN	Supernatant
	SOP	Standard Operating Procedure
	SSC	Side scatter
	SV 40	Simian virus 40
T	tBid	truncated BH-3 interacting domain
	TNF	Tumor necrosis factor
	TRADD	TNF-receptor associated death domain
	TRAF	TNF-receptor associated factor
	TRAIL	TNF-related apoptosis-inducing ligand
	Tris	Tris (hydroxymethyl)-methylamine
	TX-100	Triton X-100
U	U	Unit
	UV	Ultraviolet
V	V	Voltage
	VDAC	Voltage-dependent anion channel
W	Wt	Wildtype
X	XIAP	X-linked inhibitor of apoptosis

6.4 List of figures and tables

6.4.1 List of Figures

6.4.2 List of Tables

6.5 List of Publications

Vogel S, **Kiefer T**,_Raulf N, Sterz K, Manoharan A, Borner C. (2009). **"Mechanisms of Bax/Bak activation: Is there any light at the end of the tunnel?"**
Gastroenterology and Hepatology From Bed to Bench.;2:S11-S18

Manoharan A, **Kiefer T**, Leist S, Schrader K, Urban C, Walter D, Maurer U, Borner C. (2006). **"Identification of a 'genuine' mammalian homolog of nematodal CED-4: is the hunt over or do we need better guns?"** Cell Death and Differentiation 13, 1310–1317.

Ekert PG, Jabbour AM, Anand Manoharan A, Heraud JE, Yu J, Pakusch M, Michalak EM, Kelly PN, Callus B, **Kiefer T**, Verhagen A, John Silke J, Strasser A, Borner C, Vaux DL. (2006). **"Cell death provoked by loss of interleukin-3 signaling is independent of Bad, Bim, and PI3 kinase, but depends in part on Puma."** BLOOD SEPT 108, NUMBER 5

6.6 Conferences

6.6.1 Oral-Presentations

6th Tuscany Retreat on Cancer Research 2009
Palazzo di Piero, Sarteano-Siena, Tuscany, 2009, Italy
"Bcl-2: in search of its partners"

Retreat: Obergurgl
Bcl-2 binding partners on mitochondria: How many protein complexes exist?!
Obergurgl, March 2008, Austria

6.6.2 Poster Presentation

4th Swiss Apoptosis Meeting
Analysis of known and new Bcl-2 binding proteins by co-immunoprecipitation and Blue Native/SDS 2-D electrophoresis: evidence for an endogenous Bcl-2/VDAC-1-/Bak complex
Bern, Switzerland, August 2006